TECHNICKÁ UNIVERZITA V LIBERCI

FAKULTA STROJNÍ

KATEDRA MATERIÁLU

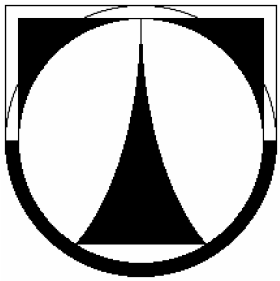

DIZERTAČNÍ PRÁCE

Ing. Tran Doan Hung

2010

TECHNICKÁ UNIVERZITA V LIBERCI

FAKULTA STROJNÍ

KATEDRA MATERIÁLU

STUDIJNÍ OBOR: 2303V002

STROJÍRENSKÁ TECHNOLOGIE

ZAMĚŘENÍ: MATERIÁLOVÉ INŽENÝRSTVÍ

GEOPOLYMERNÍ KOMPOZITNÍ SYSTÉMY NA BÁZI TERMÁLNÍ SILIKY: STUDIE POSTUPU PŘÍPRAVY A MECHANICKÝCH VLASTNOSTÍ

THERMAL SILICA-BASED GEOPOLYMER COMPOSITE SYSTEM: STUDY OF PROCESSING AND MECHANICAL PROPERTIES

ŠKOLITEL: **prof. Ing. Petr Louda, CSc.**.

ROZSAH PRÁCE

POČET STRAN	160
POČET OBRÁZKŮ	79
POČET TABULEK	35
POČET PŘÍLOH	5

ANOTACE

Geopolymery jsou anorganické polymerní materiály s chemickým složením podobným zeolitům bez definované krystalové struktury, které se svým chováním blíží keramice. Geopolymery jsou stále považovány za nové materiály pro přípravu povrchových vrstev, lepidel a pojiv pro vláknové kompozity stejně jako materiály pro přípravu betonů. Obecně lze říci, že jakékoli minerální jíly s vysokým obsahem oxidu křemičitého a oxidu hlinitého mohou být rozpuštěny v alkalickém prostředí za exotermické reakce – polykondenzačního procesu geopolymerizace, při kterém se utváří geopolymer. Konvenční geopolymerní pryskyřice, na bázi metakaolínu a jemu podobných surovinách, obsahují příliš velké částice a vykazují značnou viskozitu, aby mohly být efektivně použity pro impregnaci vláken. Pro impregnaci vláken vyztužujících geopolymerní kompozity byla v této studii použita geopolymerní pryskyřice na bázi termální siliky, která je charakteristická přítomností částic amorfního oxidu křemičitého o velikostech pohybujících se v nanorozměrech. Byly studovány vlastnosti dvou geopolymerních pojiv, zde označených jako M1 a M2, na bázi termální siliky, hydroxidu draselného a funkčních aditiv – boritanů pro typ M1 a fosforečnanů pro typ M2. Vzorky geopolymerních pryskyřic s hustotou 2,2 kg/m^3 vykazují mechanické vlastnosti pohybující se kolem 20 MPa pro mez pevnosti v ohybu, 100 MPa pro mez pevnosti v tlaku a 25 GPa pro modul pružnosti v ohybu a 120 GPa pro modul pružnosti v tlaku. Pro přípravu kompozitních vzorků bylo navrženo laboratorní impregnační zařízení simulující technologii pultruze zajišťující konstantní obsah geopolymerní pryskyřice v prepregu. Pro šest typů vláken použitých pro přípravu vyztužených kompozitů byly definovány optimální podmínky vytvrzování pro dosažení konečných mechanických parametrů a to jak pro případ konstantně se zvyšující teploty tak pro případ vytvrzování za laboratorních podmínek. Byla sledována zbytková pevnost geokompozitů po vystavení vysokým teplotám a odolnost těchto materiálů vůči hoření. Dále byla provedena úvodní studie k hodnocení mechanických parametrů geokompozitů vytvořených z vyztužujících tkanin. Je prezentován i úspěšný experiment s výrobou geopolymerních kompozitních tyčí na bázi čedičové výztuže provedený technologií pultruze. Systematická studie podává přehled o geopolymerech a geokompozitech na bázi termální siliky a možnostech jejich potenciálních aplikací v průmyslu.

Klíčová slova: *geopolymer na bázi oxidu křemičitého, jednosměrné vlákna, geokompozit, podmínky vytvrzování, mechanické vlastnosti, mikrostruktura, odolnost vůči hoření.*

ANNOTATION

Geopolymers are inorganic polymeric materials with a chemical composition similar to zeolites but without defined crystalline structure and possessing ceramic-like features. They are still considered as a new material for coatings and adhesives, a new binder for fiber composites, and a new cement for concrete. Generally, any mineral clays that contain high concentration of silica and alumina can be diluted into alkaline medium to make an exthermal reaction – polycondensation process of geopolymerization to form geopolymers. However, a conventional geopolymer resin based on classical metakaoline and similar raw materials, containing rather large particle and remarkable high viscosity, hardly used effectively for fiber impregnation. In our study, recommended application of thermal silica-based geopolymer with nanosized amorphous silica as a main component for fiber reinforced composites are investigated. Properties of two geopolymer binders, here abbrivated as M1 and M2 consisted of thermal silica, potassium hydroxide solution and functional additives: alkalin borate addition to M1 and alkalin phosphate addtition to M2, are determined. With the density is around 2.2 $Mg.m^{-3}$, the bare geopolymers exhibit mechanical properties at the top range, approximately 20 MPa and 100 MPa of flexural and compressive strength, and 25 GPa and over 120 GPa of flexural and compressive modulus respectively. Effective home-made impregantion machine is designed based on the simulation of real pultrusion technique for good pre-pregs with constant proportion resin in the reinforcements. The optimal curing conditions, both at elevated temperature or at ambient conditions, for achieving good mechaniacl properties of six fiber reinforced geocomposites are defined. Fire-resistant properties, especially the residual strength of the geocomposites are investigated. In addition, preliminary study about mechanical properties of woven fabric reinforced geocomposites are carried out. Successful experiment of continuous basalt reinforced composite rods on real pultrusion system is also presented. Systematic study shows us an overal view of thermal silica based geopolymer and composites thereof, last but never least reveals potential applications in industries.

Key words: *silica-based geopolymer, unidirectional fiber, geocomposite, curing conditions, mechanical property, microstructure, fire-resistant property.*

MÍSTOPŘÍSEŽNÉ PROHLÁŠENÍ

Prohlašuji, že:

Obsah disertační práce je mým vlastním dílem a neosahuje žádné informace, které by byly publikovány jinými autory než autory, kteří jsou uvedeni v odkazech. Žádná část práce nebyla využita pro jinou než tuto disertační práci.

Beru na vědomí, že Technická univerzita v Liberci (TUL) nezasahuje do mých autorských práv užitím mé disertační práce pro vnitřní potřebu TUL.

Užiji-li disertační práci nebo poskytnu-li licenci k jejímu využití, jsem si vědom povinnosti informovat o této skutečnosti TUL. V tomto případě má TUL právo ode mne požadovat úhradu nákladů, které vynaložila na vytvoření díla až do jejich skutečné výše.

Byl jsem seznámen s tím, že na mou disertační práci se plně vztahuje zákon č. 121/2000 Sb., o právu autorském, zejména §60 – školní dílo.

Datum: 20/11/2010

Ing. Tran Doan Hung

DECLARATION

I hereby declare that:

To the best of my knowledge, the content of the thesis is original in my own work and contains no material which has been previously published by other people, except references that are stated. No part of this work has been submitted for the award of any other degree or diploma in any universities.

It is totally no problems in my copyright when this PhD-thesis work is used for internal purposes of Technical University of Liberec.

The thesis text, exclusive of tables, figures and appendices are applied to my PhD-dissertation in full with the notification of Copyright Act. No. 121/2000 Coll. and satisfied the Section 60, Shool Work.

Date: 20/11/2010

Signature

Ing. Tran Doan Hung

ACKNOWLEDGEMENTS

I would not have finished this PhD. dissertation without the guidance, support and assistance of not only many respectable professors, generous colleagues, patient relatives and close friends but also funding projects. So, in no particular order:

I would like to express my respectful gratitude to my principal supervisor, Prof. Petr Louda for his interest and dedication to see me completing this thesis. I have personally been inspired by Louda's leadership, intelligence, generosity and his passion for knowledge and business.

My sincere gratitude also extends to my another supervisor associate professor Dora Kroisová. Without her, the thesis would not have been completed in time. Additionally, I would like to thank Kroisová for not only her endless works of revising, editing and giving valuable feedback for my dissertation but also her emotional support, while having had to manage the Geopolymers Group and her other busy schedules.

I would like to thank Ing. Oleg Bortnovsky, PhD and Ing. Petr Bezucha from Research Institute of Inorganic Chemistry, Inc., Ústí nad Labem for their valuable discussion, revision, and they help with the raw materials, macro file code and co-develope method to calculate the virtual material properties when assuming that the outer support span-to-depth ratios forward to infinitive. They never minded answering any of my silly questions.

I would like to respect associate professor Ing. Karel Daďourek, CSc. for his helpful advice about testing standards, structure of the dissertation and a lot of knowledgement.

I am grateful to Ing. Pavel Kejzlar for co-working to coat a lot of samples and SEM technique. Moreover, I also would like to be thankful to RNDr. Věra Vodičková, Ing. Petra Prokopčáková, Ph.D, Ing. Vladimír Nosek, Ing. Adam Hotař, Ph.D., Ing. Pavel Hanus, Ph.D., Ing. David Pospíšil and Mr. Milan Vyvlečka for many supports during not only finish my dissertation but also for all the time I study here.

I would like to acknowledge the general support provided by head, vice-head and all members of the Departmet of Material Science, Faculty of Mechanical Engineering,

Technical University of Liberec and Research Institute of Inorganic Chemistry, Inc., Ústí nad Labem, Czech Republic. The financial contributions from the Ministry of Industry and Trade of Czech Republic under the project FT-TA4/068 and from the Ministry of Education and Youth of Czech Republic under project MSMT 4674788501, Departmet of Material Science, Faculty of Mechanical Engineering, Technical University of Liberec and and Research Institute of Inorganic Chemistry, Inc. are all duly acknowledged for supporting the work in the thesis.

I also wish to extend to my thanks to Mrs. Hana Šiftová for not only her excellent job in setting everything in order and efficient secretarial work but also emotional encouraging smiles every morning.

In addition, I would like to thank my colleagues from Nha Trang University, especially to rector Dr. Vu Van Xung, who always persuage and give me emotional supports during the time of my study in Czech Republic.

Last but definitely not least, I am indebted to my family who nudged me when I needed it, and celebrated with me when I was done. These include my parents and parents-in-law: Tran Doan Hong, Luong Thi Hien, Vu Duy Trinh and Dang Thi Huong for their caring and patience. My wife, Vu Dang Ha Quyen, for her immeasurable love and endless support. She has been a constant source of strength and a brilliant helper throughout times of adversity while trying to fulfill my goal. My son, Tran Vu Dung, for cheering me up at the weekend after hard working days in the laboratory, you always in my heart and the aspiration for my hard work.

I am greatly indebted to you all for your kindness, support and helps. You will be in my heart, my soul forever.

TABLE OF CONTENTS

ANOTACE / ANNOTATION.....ii
MÍSTOPŘÍSEŽNÉ PROHLÁŠENÍ / DECLARATION.....iv
ACKNOWLEDGEMENTS.....v
TABLE OF CONTENTS.....vii
LIST OF FIGURES.....x
LIST OF TABLES..... xiv

1. INTRODUCTION **1**
1.1 GENERAL 1
1.2 GEOPOLYMER BASED COMPOSITE 3
1.3 AIMS OF THE RESEARCH 4
2. LITERATURE REVIEW **6**
2.1 INTRODUCTION 6
2.2 GEOPOLYMER 6
2.2.1 GEOPOLYMER TERMINOLOGY 6
2.2.2 GEOPOLYMERIZATION 9
2.2.3 PROPERTIES OF GEOPOLYMERS AND COMPOSITES THEREOF 13
2.2.4 POTENTIAL APPLICATIONS OF GEOPOLYMER MATERIALS 39
3. EXPERIMENTAL AND RESEARCH METHODOLOGIES **44**
3.1 RAW MATERIALS 44
3.1.1 GEOPOLYMER RESIN 45
3.1.2 REINFORCEMENT 46
3.1.2.1 UNIDIRECTIONAL FIBERS 46
3.1.2.2 FABRIC FIBERS 48
3.2 FABRICATION OF GEOPOLYMER COMPOSITES 49
3.2.1 PULTRUSION TECHNIQUE 49
3.2.2 PREPARATION OF GEOCOMPOSITE SAMPLES 51
3.3 CHARACTERIZATION OF GEOPOLYMER COMPOSITES 53
3.3.1 TESTING OF MECHANICAL PROPERTIES 53
3.3.2 EVALUATION METHOD 55
3.3.2.1 THEORY OF NEW OPTIONAL CALCULATION METHOD 56
3.3.3 MICROSTRUCTURE OF GEOCOMPOSITES 62

4. PROPERTIES OF INITIAL MATERIALS OF GEOCOMPOSITES 63
4.1 INTROCDUCTION 63
4.2 PROPERTIES OF GEOPOLYMER MATRIX 63
4.2.1 MICROSTRUCTURE OF GEOPOLYMER 63
4.2.2 MECHANICAL PROPERTIES 65
4.3 PROPERTIES OF FIBER REINFORCEMENT 69
5. EFFECTS OF CURING TEMPERATURE ON MECHANICAL PROPERTIES 73
5.1 INTRODUCTION 73
5.2 EXPERIMENTAL 73
5.2.1 PREPARATION OF COMPOSITE SPECIMENS 73
5.2.2 TESTING OF FLEXURAL PROPERTIES AND DATA TREATMENT 74
5.2.3 POROSITY OF COMPOSITES 75
5.2.4 MICROSTRUCTURE AND VOLUME FRACTION OF FIBERS 75
5.3 RESULTS AND DISCUSSION 75
5.3.1 GENERAL PICTURE 75
5.3.2 ROLE OF POROSITY 86
5.3.3 MICROSTRUCTURE AND VOLUME FRACTION OF FIBERS 90
5.4 CONCLUSIONS 94
6. EFFECTS OF CURING TIME ON MECHANICAL PROPERTIES 95
6.1 INTRODUCTION 95
6.2 EXPERIMENTAL 95
6.2.1 PREPARATION OF COMPOSITE SPECIMENS 95
6.2.2 MECHANICAL TESTING SETUP AND DATA TREATMENT 96
6.3 RESULTS AND DISCUSSION 97
6.3.1. EFFECTS OF CURING TIME AT ELEVATED TEMPERATURE 97
6.3.2 EFFECTS OF CURING TIME AT AMBIENT CONDITIONS 102
6.4 FAILURE BEHAVIOUR OF THE GEOCOMPOSITE 110
6.5 MICROSTRUCTURE OF GEOCOMPOSITE CURED AT AMBIENT CONDITIONS 114
6.6 CONCLUSIONS 117
7. FIRE-RESISTANT PROPERTIES OF GEOCOMPOSITES 118
7.1 INTRODUCTION 118
7.2 EXPERIMENTAL DESIGN 119

7.2.1 FABRICATION PROCEDURES 119
7.2.2 TESTING SETUP 119
7.2.3 MECHANICAL MEASUREMENT 120
7.3 RESULTS AND DISCUSSION 120
7.4 CONCLUSIONS 138
8. FABRIC REINFORCED GEOCOMPOSITES AND REAL PULTRUDED GEOCOMPOSITE RODS 139
8.1 GEOCOMPOSITES REINFORCED BY WOVEN FABRICS 139
8.1.1 FLEXURAL PROPERTIES OF WOVEN FABRIC GEOCOMPOSITES 139
8.2.2 MICROSTRUCTURE OF FABRIC REINFORCED GEOCOMPOSITES 142
8.2 MECHANICAL PROPERTIES OF GEOCOMPOSITE RODS 144
8.3 CONCLUSIONS 146
9. CONCLUSIONS AND RECOMMENDATIONS 147
9.1 REMARKABLE CONCLUSIONS 147
9.2 LIMITATIONS AND RECOMMENDATIONS 152
REFERENCES 154
APPENDIX A 161
APPENDIX B 168
APPENDIX C 171
APPENDIX D 173
APPENDIX E 174

LIST OF FIGURES

Fig. 2.1 Tetrahedral configuration of sialate Si-O-Al-O [22]. 7

Fig. 2.2 Davidovits's proposed geopolymer designations [7, 8, 10, 27, 30]. 8

Fig. 2.3 Conceptual model for geopolymerization [13]..... 11

Fig. 2.4 Density (a) and Fusion temperature (b) of geopolymers (pure matrix) [7, 68]. 22

Fig. 2.5 CTE of geopolymer materials [7, 68]. 23

Fig. 2.6 Three-point flexural strength of geopolymer composites in function of the use-temperature [7, 68]. 23

Fig. 2.7 Predicted time to flashover of materials in accordant with ISO 9705 corner/room fire test [10, 12]. 25

Fig. 2.8 Comparative percentage of strength retention at high temperature [14]. 29

Fig. 2.9 RHR spectra of (a) DGEBA (b) 20% Geopolymer-DGEBA and (c) 20% kaolin-DGEBA variation with time [78]. 31

Fig. 2.10 SEA spectra of (a) DGEBA (b) 20% Geopolymer-DGEBA and (c) 20% kaolin-DGEBA variation with time [78]. 32

Fig. 2.11 SEM images of geopolymer–stainless steel mesh composites after 80 ^{o}C curing (a, b), 800 ^{o}C/30 min exposure (c, d), 1050 ^{o}C/2 hours (e, f) exposure and then tested under flexure conditions (left column shows the composite structure and right column shows the surface of steel mesh [79]. 34

Fig. 2.12 Compression stress vs strain curve of composite with M/S = 1/2 consisting 80% size 0.25-0.50 mm and 20% size 0.50-1.50 mm of ceramic spheres [80]. ... 35

Fig. 2.13 Heat release rate versus time for OSU test specimens [50]. 37

Fig. 2.14 Specific optical smoke density versus time for NBS smoke tests [50]. 37

Fig. 2.15 High-early strength of (K,Ca)-poly(sialate-siloxo) cement [10]. 41

Fig. 2.16 Geopolymers and potential applications [7, 8, 30, 68]. 43

Fig. 3.1 Mounting tab for single filament fiber testing [93] 47

Fig. 3.2 Tensile testing machine Instron LaborTech 2.050, TUL. 48

Fig. 3.3 Schematic representation of a pultrusion machine [96] 49

Fig. 3.4 Simplified illustration of a pultrusion machine. 50

Fig. 3.5 Home-made pultrusion machine, TUL-KMT. 51

Fig. 3.6 Rubber silicon mould for sample making. 52

Fig. 3.7 Vacuum bagging technique [4, 97]. 53

Fig. 3.8 Universal Testing Machine - Instron Model 4202, TUL-KMT. 54

Fig. 3.9 Ratio of the effective value E to the virtual value E^{*}; ratios E^{*}/G in the legend. 59

Fig. 3.10 Dependences of R^*_{mo}/R_{mo} ratios at different E^*/G (in the legend). 61

Fig. 3.11 TESCAN VEGA 3XM Microscope, TUL. 62

Fig. 4.1 SEM images of unpolished surface of geopolymer composite matrix M1 at magnification a) 13170x and b) 200x. 64

Fig. 4.2 SEM images of polished surface of geopolymer composite matrix M2 at magnification a) 7190x, b) 200x. 64

Fig. 4.3 Typical stress vs strain curve in flexure of M2 system at span 80 mm. 66

Fig. 4.4 Typical load vs displacement curve of comperessive test of M1 system. 67

Fig. 4.5 Reciprocal effective flexural properties vs. $(H/L)^2$ ratio a) elasticity modulus, b) flexural strength. 68

Fig. 4.6 Effect of temperature on tensile strength of commercial fibers. 71

Fig. 5.1 Effects of temperature of curing on flexural strength and modulus of geopolymer composite M0-Carbon. 76

Fig. 5.2 Effects of temperature of curing on flexural strength of geopolymer composite M1 system at outer support span-to-depth ration L/H = 20 to 1 78

Fig. 5.3 Effects of temperature of curing on flexural modulus of geopolymer composite M1 system at outer support span-to-depth ration L/H = 20 to 1 78

Fig. 5.4 Effects of temperature of curing on flexural strength of geopolymer composite M2 system at outer support span-to-depth ration L/H = 20 to 1 80

Fig. 5.5 Effects of temperature of curing on flexural modulus of geopolymer composite M2 system at outer support span-to-depth ration L/H = 20 to 1 80

Fig. 5.6 Examples of elementary treatment of results by means of linear regression (curing temperatures: basalt 85 °C, carbon 95 °C, glass 55 °C). 82

Fig. 5.7 Survey on dependences of main mechanical properties on curing temperature in accordance with size-independent method. 84

Fig. 5.8 Effects of curing temperature on porosities of geocomposites. 87

Fig. 5.9 Relationship between flexural strength, modulus and porosity; grey points: temperature of curing >100 °C or < 60 °C. 89

Fig. 5.10 SEM of geopolymer composite M0/Carbon (a) at 55 ^oC, (b) at 75 ^oC and (c) at 115 ^oC curing temperature with magnification 9800x. 90

Fig. 5.11 SEM of geopolymer composite M0/Carbon (a) at 75 ^oC and (b) at 115 ^oC curing temperature with magnification 200x. 90

Fig. 5.12 Typical SEM images of M1/Carbon curing at 65 ^oC on sections perpendicular to fibers a) 10000x, b) 1000x and surfaces of composite c) 1880x and d) 301x. 92

Fig. 5.13 Typical SEM images for volume fraction of fibers a) M1-C, b) M2-C, c) M1-B, d) M2-B, e) M1-E glass and f) M2-E glass with magnation around 2000x..... 93

Fig. 6.1 Effects of curing time on flexural strength of geopolymer composite M1 system in accordance with DIN EN 658-3:2002 (L/H = 20 to 1). 97

Fig. 6.2 Effects of curing time on flexural modulus of geopolymer composite M1 system in accordance with DIN EN 658-3:2002 (L/H = 20 to 1). 98

Fig. 6.3 Effects of curing time on flexural strength of geopolymer composite M2 system at ratio L/H = 20 to 1. 100

Fig. 6.4 Effects of curing time on flexural modulus of geopolymer composite M2 system at ratio L/H = 20 to 1. 100

Fig. 6.5 Linear regression of reciprocal effective values 1/E and $1/R_{mo}$ vs $(H/L)^2$ of geocomposites M1 system for curing time 1:01:05 at 80 ^oC. 101

Fig. 6.6 Effects of curing time on mechanical properties of geopolymer composites curing at ambient conditions at ratio L/H = 20 to 1. 104

Fig. 6.7 Rotary oil vacuum pump. 107

Fig. 6.8 Linear regression of reciprocal effective values 1/E and $1/R_{mo}$ vs $(H/L)^2$ of geocomposites M1 system cured at ambient condition for over 40 days. 109

Fig. 6.9 Typical stress – strain relationships of unidirectional geocomposites based on M1 geopolymer matrix tested in flexure at L/H = 20 to 1, a) M1/C, c) M1/B and e) M1/E-glass cured at time 1:1:5 hours at 80 ^oC and b) M1/C, d) M1/B and f) M1/E-glass cured at ambient conditions for over 40 days. 111

Fig. 6.10 Typical delamination failure pattern of the composite samples. 112

Fig. 6.11 Typical compressive failure pattern in the outer fiber surfaces of the composite samples. 113

Fig. 6.12 Stress – strain relationships of unidirectional geocomposites M1/Basalt cured at ambient conditions for over 40 days and tested in flexure at L/H = 40 to 1... 113

Fig. 6.13 SEM images of perpendicular sections of geopolymer composite matrix M1 with a) E-glass (700x), b) basalt (8.000x), c) carbon (10.000x) and d) carbon (1000x). 115

Fig. 6.14 SEM surface images of geopolymer composite matrix M1 and a) E-glass (300x), b) basalt (300x), c) carbon (1.880x) and d) typical micro-crack of M1/C composite curing at elevated temperature 65 ^oC for 5 hours (1880x). 116

Fig. 7.1 Residual mechanical properties of geocomposites M1/Carbon fibers. 122

Fig. 7.2 Residual mechanical properties of geocomposites M1/Basalt fibers. 123

Fig. 7.3 Residual mechanical properties of geocomposites M1/E-glass fiber. 123

Fig. 7.4 Residual mechanical properties of geocomposites M2/Carbon fiber. 125

Fig. 7.5 Residual mechanical properties of geocomposites M2/Carbon fiber. 126

Fig. 7.6 Residual mechanical properties of geocomposites M2/E-glass fiber. 126

Fig. 7.7 Outer calcinated layer of composite M1 after exposing up to 800 ^oC at macro structure (a) and micro-structure (b at 500x). 128

Fig. 7.8 SEM images of M1/carbon after exposing up to 600 ^oC on sections perpendicular to fibers a) 10kx and b) 1.0 kx and surfaces of composite c) 2.0 kx and d) 500x. 129

Fig. 7.9 SEM of M1/carbon after exposing up to 800 ^{o}C a) 5.0kx and b) 500x and 1000 ^{o}C c) 2.0kx and d) 500x on sections perpendicular to fibers. 130

Fig. 7.10 SEM of M1/carbon after exposing up to 800 ^{o}C (a) and 1000 ^{o}C (b) on the surfaces of composite at magnification 500x. 131

Fig. 7.11 SEM of M2/carbon after exposing up to 600 ^{o}C a) 5.0kx and b) 1.0kx and 1000 ^{o}C c) 20.0kx and d) 200x on sections perpendicular to fibers and surfaces of composite. 132

Fig. 7.12 SEM of M2/carbon after exposing up to 600 ^{o}C (a) and 1000 ^{o}C (b) on the surfaces of composite at 500x. 133

Fig. 7.13 EDX of line profiles through cross-section of filament fiber in the composite M1-carbon after calcination at a) room temperature, b) 800 ^{o}C , c) 1000 ^{o}C and d) SEM after exposing up to 800 ^{o}C (at 20kx). 134

Fig. 7.14 Residual flexural strength of some commercial composites after fire exposure at a 25 kW/m^2 radiant heat source for 20 minutes [12, 125]. 135

Fig. 7.15 Reciprocal effective flexural properties vs. $(H/L)^2$ ratio a) elasticity modulus, b) flexural strength of M1/Carbon after thermal exposure. 137

Fig. 8.1 Reciprocal effective flexural properties of M1 and M2 reinforced by F1 and F2 vs. $(H/L)^2$ ratio. 141

Fig. 8.2 SEM images on polished sections of geopolymer composite matrix M1 and carbon HTS twill a) 10.0kx and b) 1.0kx and S-glass twill c) 8.0kx and d) 400x. 143

Fig. 8.3 SEM images on polished sections of geopolymer composite matrix M2 and carbon HTS twill a) 10.0kx and b) 228x and S-glass twill c) 8.0kx and d) 200x. 144

Fig. 8.4 Schematic representation of machine for basalt fiber composite rod. 145

LIST OF TABLES

Table 2.1 Comparison between SiC fibre/K-PSS GEOPOLYMITE Composite and SiC fibre/Ceramic Matrix composites [7, 9] 18

Table 2.2 Coefficient of thermal expansion (CTE) of geopolymers 22

Table 2.3 Fire performance index of unmodified DGEBA and modified DGEBA system 32

Table 3.1 Chemical composition of geopolymer matrices M0, M1 and M2 expressed as main principle elements atomic ratios 45

Table 3.2 Kinds of used fabric fibers 48

Table 4.1 Some physical properties of pure geopolymer matrix 65

Table 4.2 Flexural properties of pure geopolymer matrix at different spans 66

Table 4.3 Compressive properties of geopolymer matrix 67

Table 4.4 Flexural properties of pure matrix M1 and M2 when $(H/L)^2 \rightarrow 0$ 68

Table 4.5 Main properties of selected fibers from producers or suppliers 69

Table 4.6. Mechanical properties of filaments in accordance with Japanese Industrial Standard (JIS R 7601) 70

Table 5.1 Flexural properties of geocomposite with matrix M0 and the carbon fibers at different temperature of curing at L/H = 20 to 1 76

Table 5.2 Flexural properties of geopolymer composites M1 system at outer support span-to-depth ration L/H = 20 to 1. 77

Table 5.3 Flexural properties of geopolymer com posites M2 system at outer support span-to-depth ration L/H = 20 to 1. 79

Table 5.4 Survey of estimation of basic virtual flexural properties of geocomposites reinforced with unidirectional fibers at different curing temperature 83

Table 5.5 Flexural properties of geocomposites cured in optimal range of elevated temperature from 65 to 85 ^{o}C in accordance with size-independent testing method 85

Table 5.6 Effects of porosities (vol.%) of geocomposites on curing temperature 88

Table 5.7 Volume percentage of fibers [vol.%] in geocomposites via SEM images ... 91

Table 6.1 Flexural properties of geocomposites M1 system at L/H = 20 to 1 99

Table 6.2 Flexural properties of geocomposites M2 system at different curing time at outer support span-to-depth ratios L/H = 20 to 1. 99

Table 6.3 Virtual flexural properties of geopolymer composites cured at time 1:01:05 hours in accordance with size-independent method 102

Table 6.4 Flexural properties of composites based on M1 system at ratio L/H = 20 to 1 103

Table 6.5 Flexural properties of composites based on M2 system at ratio L/H = 20 to 1 103

Table 6.6 Flexural properties of geocomposites cured at ambient conditions for over 40 days for M1 and 50 days for M2 at various outer support span-to-depth ratios. 106

Table 6.7 Virtual flexural properties of geocomposites cured at ambient conditions in accordance with novel size-independent method 108

Table 7.1 Flexural properties of geocomposites M1 reinforced by Carbon fibers cured at 80 ^{o}C after thermal exposure for 60 minutes at different L/H ratios 121

Table 7.2 Flexural properties of geocomposites M1 reinforced by Basalt fibers cured at 80 ^{o}C after thermal exposure for 60 minutes at different L/H ratios 121

Table 7.3 Flexural properties of geocomposites M1 reinforced by E-glass fibers cured at 80 ^{o}C after thermal exposure for 60 minutes at different L/H ratios 122

Table 7.4 Flexural properties of geocomposites M2 reinforced by Carbon fibers cured at 85 ^{o}C after thermal exposure for 60 minutes at different L/H ratios 124

Table 7.5 Flexural properties of geocomposites M2 reinforced by Basalt fibers cured at 85 ^{o}C after thermal exposure for 60 minutes at different L/H ratios 124

Table 7.6 Flexural properties of geocomposites M2 reinforced by E-glass fibers cured at 85 ^{o}C after thermal exposure for 60 minutes at different L/H ratios 125

Table 7.7 Typical properties of structural materials [12] 136

Table 8.1 Flexural properties of geocomposites reinforced by woven fabrics at various outer support span-to-depth ratios 140

Table 8.2 Flexural strength of M1 and M2 reinforced by F1 and F2 in accordance with Size-independent method..... 142

Table 8.3 Flexural properties of unidirectional basalt fiber reinforced geocomposite rod by real pultruded machine at various outer support span-to-depth ratios 146

1. INTRODUCTION

1.1 GENERAL

Composite materials had been known in various forms throughout the history of mankind, just as it was in 1500 B.C. when the Egyptians and Israelites were using straw to reinforce mud bricks and the history of modern composites probably began in 1937 when salesmen from the Owens Corning Fiberglass Company began to sell fiberglass to interested parties around the United States [1]. Until now, however, these materials scientists are always arguing about such definitions. The name implies that the material is composed of dissimilar constituents, and that is not true of all materials. Even a material as simple as pure hydrogen has a composite chemical constitution of protons and electrons, which in turn are composed of still smaller and dissimilar entities. A certain degree of arbitrariness is required in settling on a working definition for most materials classes, and certainly for composites. The state of art definition *"Composite materials are multiphase materials obtained through the artificial combination of different materials in order to attain properties that the individual components by themselves cannot attain. They are not multiphase materials in which the different phases are formed naturally by reactions, phase transformations, or other phenomena"* [2].

In this work of dissertation, we will follow a common notion that "composites" to be materials in which a homogeneous "matrix" component is "reinforced" by a stronger and stiffer constituents that are fibrous but may have a particulate form. Typically fibers are impregnated by a matrix material that acts to transfer loads to the fibers and protects the fibers from abrasion and environmental attack as well.

In general, composites bring many attractive advantages to the designer of structural devices, among which we can list [2-4]:

- ✓ Composites possess high stiffness, strength, and toughness, which can be comparable with structural metal alloys. Moreover, they usually provide the properties at substantially less weight than metals: their "specific" modulus and

strength, very strong and stiff structures can be designed, with substantial weight savings.

- ✓ The ability to align the fiber orientation with the direction of principle stresses, anisotropic structure can be made and therefore achieve high structural efficiency.
- ✓ Very good environmental degradation and corrosion resistance properties, involving sliding friction, with tribological ("wear") properties approaching those of lubricated steel.
- ✓ Very low coefficient of thermal expansion, also giving the possibility of designing the material to give desired thermal expansion in a particular direction.
- ✓ Excellent fatigue resistance in comparison with metal alloys, and often show evidence of accumulating fatigue damage, so that the damage can be detected and the part replaced before a catastrophic failure occurs, even fatigue free for carbon fiber composites.
- ✓ Improved vibration damping properties and energy absorbing safety structures.
- ✓ Easy to repair the damaged structures.
- ✓ Ability to manufacture complex shapes at lower costs compared with fabricated or machined metallic alloys.
- ✓ Time and cost reductions on tooling and manufacturing of one-offs, prototypes and short length production runs.

On the contrary, composites are not perfect for all applications, and the designer needs to be aware of their drawbacks. Among these cautionary notes we can list [2-4]:

- ✓ Not all applications are weight-critical. If weight-adjusted properties not relevant, steel and other traditional materials may work fine at lower cost.
- ✓ Anisotropy and other "special" features are advantageous in that they provide a great deal of design flexibility. The well-known tools of stress analysis used in isotropic linear elastic design must be extended to include anisotropy, not all designers are comfortable with these more advanced tools.

- ✓ Even after several years, economies of scale of composites are still not well developed. As a result, composites are almost always more expensive – often much more expensive than traditional materials, so the designer must look to composites' various advantages to offset the extra cost.
- ✓ Although composites have been used extensively in demanding structural applications for a half-century, the long-term durability of these materials is much less certain than that of steel or other traditional structural materials.

1.2 GEOPOLYMER BASED COMPOSITE

Materials are selected for a given application based principally on the properties of materials. Most engineering structures are required to bear loads, so the material property of greatest interest is very often its strength. Strength alone is not always enough, however, in some cases stiffness is high demanded or many other structures a great penalty accompanies weight, aircraft is an example.

In 1978, Joseph Davidovits proposed that binders could be produced by a polymeric reaction of alkaline liquids with the silicon and the aluminum in source materials of geological origin or by-product materials such as fly ash and rice husk ash [5]. These binders have been coined as term geopolymers since 1979; they are inorganic polymeric materials with a chemical composition similar to zeolites but without defined crystalline structure and possessing ceramic-like features in their structures and properties. The amorphous to semi-crystalline three dimensional of sialate network consists of SiO_4 and AlO_4 tetrahedra which are linked alternately by sharing all the oxygens to create polymeric Si-O-Al bonds [6, 7]. Geopolymers are still considered as a new material for coatings and adhesives, a new binder for fiber reinforced composites, and a new cement for concrete [8].

Fiber-reinforced composites based on geopolymer matrix (geocomposite) have been well-known for over 20 years, since the first Davidovits' patent was filed [9]. These new materials can be fabricated and cured at room temperature or thermoset in a simple autoclave. After approximately several hours of curing, these materials exhibit excellent features such as lightweight and high strength but are also ideally fire resistant, with non toxic fumes and smokes, and resist all organic solvents [8, 10-13].

These special properties permit us to use geopolymer matrix composites more efficiently in high-tech technologies such as aerospace, naval architecture, ground transportation or automotive industry, especially for those applications that require high temperature resistance [8, 10, 12, 14]. Geopolymer composites can efficiently replace lightweight, high strength composites which are made from carbon or glass fibers and ceramic matrices or organic matrices due to high costs associated with special ceramic processing requirements and impossibility of the application of most organic matrix composites at temperatures above 200 °C [14, 15]. In addition, wide scale of reinforcement fibers can be used, and special matrices can protect carbon from oxidation [14, 16].

In general, any mineral clay that contain high concentration of silicon oxide (silica) and aluminum oxide (alumina) can be diluted into alkaline medium to make an exthermal reaction – polycondensation process of geopolymerization to form geopolymer material. From literatures we can find that the raw materials for geopolymers are kaoline, metakaoline, fly-ash, furnace blast and so on... However, some big drawbacks are generated when geopolymer resins is used as a matrix for composites reinforced by fibers. For effective impregnation of fabric or fiber rovings containing single filaments of diameter ranging about 7 to 25 μm, resin with low viscosity and maximum particle size lower than the fiber filament diameter should be used and preferred size is of order of 5 μm [9, 17]. Therefore a conventional geopolymer resin based on classical metakaoline and similar raw materials, containing rather large particle and remarkable high viscosity, can be hardly used effectively for fiber impregnation, or very high pressure must be applied to penetrate the resin into the spaces between single filament fibers [18]. Recommended application of thermal silica-based geopolymer with nanosized amorphous silica as a main component could solve these obstacles [17].

1.3 AIMS OF THE RESEARCH

The presented study dealts with the manufacturing procedure of thermal silica based geopolymer composites reinforced by selected commercial fibers. Effects of curing conditions, temperature and time at elevated or ambient conditions, on mechanical properties of the composites with appropriate method of fabrication. Finding adjusted

methods for calculation properties of resulting composites and evaluation the mechanical properties of composites after thermal exposing up to high temperature.

Experiments will be conducted to study systematically the main properties of reinforced geocomposite system, including:

1. Microstructure and mechanical properties of selected geopolymer matrices.
2. Properties of commercial reinforcements: carbon, glass and basalt fiber in the real conditions and after different temperature of treatment.
3. Develop new appropriate method for calculation the mechanical properties of geopolymer composite systems.
4. Optimal temperature of curing condition for fiber reinforced geocomposite system.
5. Optimal time of curing under vacuum technique at elevated curing temperature in the oven for reinforced geocomposite system.
6. Mechanical properties of the geocomposites cured at ambient conditions
7. Mechanical property retention of geopolymer composite system at high temperature.
8. Mechanical properties of geopolymer reinforced by selected fabric fibers.
9. Preliminary survey of real pultrusion system and recommend the potential application geocomposites into industries.

2. LITERATURE REVIEW

2.1 INTRODUCTION

This Chapter provides a brief overview of history of geopolymer, geopolymer chemistry and synthesis, the properties of geopolymer binders based on various raw materials without the use of aggregates, the recent development of thereof composites. In addition, the effects of choice of initial raw materials alkaline medium activators and conditions of curing on the final properties are summerized. Last but never least, the potential applications of geopolymer are presented as well. The aim is to provide background knowledge of geopolymer research in a relative chronological and systematic designation.

2.2 GEOPOLYMER

2.2.1 GEOPOLYMER TERMINOLOGY

The first and foremost desire for the research of geopolymer science and technology is a need to find alternative materials to substitute common organic plastic which involved in the aftermath of various catastrophic fires in France between 1970-1973 [10] and commercialization of this kind of material is motivated by the demand to find alternative cleaner materials which can substitute Ordinary Portland cement (OPC) as a construction material [7, 19, 20].

The term geopolymer has been first coirned since 1979 by a French professor Joseph Davidovits [7], they are inorganic polymeric materials with a chemical composition similar to zeolites but containing an amorphous structure and possessing ceramic-like in their structures and properties. Moreover these materials can polycondense at low temperature as 100 ^{o}C. To discuss the chemical structure of gepolymers, the term poly(sialate) was suggested as a descriptor of silico-aluminate structure of the type of material [7, 21]. The amorphous to semi-crystalline three dimensional of sialate network consists of SiO_4 and AlO_4 tetrahedra which are linked alternately by sharing all the oxygens to create basic polymeric Si-O-Al bonds (Fig. 2.1) [22].

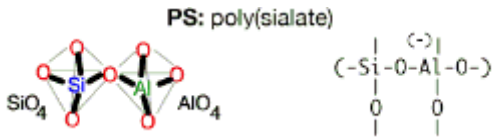

Fig. 2.1 Tetrahedral configuration of sialate Si-O-Al-O [22].

The negative charge of Al^{3+} in IV-fold coordination becomes a network forming and requires extra positives ions to compensate and balance the electricity of the geopolymer framework. Commonly, either cation such as sodium (Na^{+}), potassium (K^{+}) or calcium (Ca^{++}) are chosen for this electrical balance. Other possitive ions such as lithium (Li^{+}), barium (Ba^{++}), ammonium (NH_4^{+}) or hydronium (H_3O^{+}), however, may can be used as well [7].

In order to describe the possible combinations, Tossell has cited the forms in which the alumina and silica can be combined to create the geopolymer binder that causes differences in properties and naming conventions. While Al-O-Al linkages have been shown to be possible in high energy disordered systems, the nature of geopolymerization makes such linkages unable [23]. The Loewenstien's aluminum avoidance principle, which states that aluminum cannot be bonded together by an oxygen, is generally accepted when modeling geopolymeric materials because Al-O-Al bonding is more energetically unfavorable. Utilizing Gibbs free energy minimization calculation, based on the preferred energy the linkages Al-O-Al is demonstrated in geopolymers derived from metakaolin and activated with sodium. However, this combination has been shown to take place in case the molar ratios Si:Al below 1.15 and represented just a very small proportion of the bonding in this structure [24].

Being negligent the bonding Al-O-Al the remaining possible combination linkages allowed are Si-O-Si (siloxo) and Si-O-Al (sialate). Based on the chemical designations of these molecules, the terminology "poly(sialate)" is suggested for geopolymers based on silico-aluminate; Sialate is an abbreviation for silicon-oxo-aluminate [7, 21, 25].

Poly(sialates) are chain and ring polymers with Si^{4+} and Al^{3+} in IV-fold coordination with oxygen and range from amorphous to semi-crystalline with the empirical formula:

$$M_n \{-(SiO_2)_z–AlO_2\}_n \cdot wH_2O \qquad (2\text{-}1)$$

where “z” is 1, 2, 3 or higher up to 32; M is a monovalent cation such as potassium or sodium, and “n” is a degree of polycondensation. Davidovits has also distinguished 3 types of polysialates, namely the Poly(sialate) type (-Si-O-Al-O), the Poly(sialate-siloxo) type (-Si-O-Al-O-Si-O) and the Poly(sialate-disiloxo) type (-Si-O-Al-O-Si-O) as repeating units [5-8, 26-29]. The structures of these polysialates can be schematized as in Figure 2.2 [7, 8, 10, 27, 30]

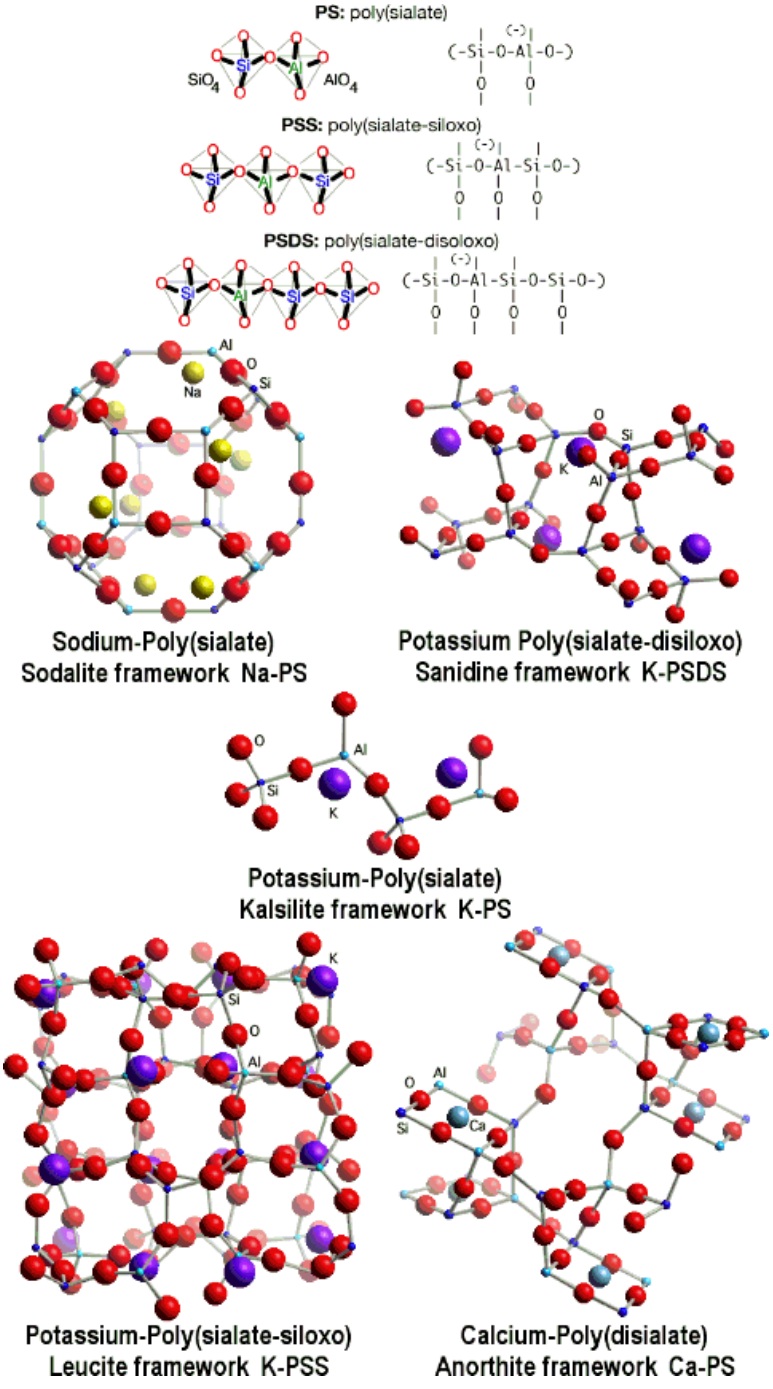

Fig. 2.2 Davidovits’s proposed geopolymer designations [7, 8, 10, 27, 30].

2.2.2 GEOPOLYMERIZATION

In a generic manner, the term ‘geopolymer’ is used to describe the amorphous to semi crystalline reaction products from synthesis of alkali aluminosilicates from reaction with alkali hydroxide/alkali silicate solution, however, geopolymeric gels and composites are also commonly referred to as “geocement” [31], “low-temperature inorganic polymer glass” (LTIPG or IPG) [32], “alkali-activated fly ash cement” [33, 34], “hydroceramic” [35], “alkali-bonded ceramic” [36], “inorganic polymer concrete” [37] or “alkali-activated aluminosilicate systems” [38]. Although this variety of nomenclature of geopolymers, these terms all describe materials which are synthesized utilizing the same chemical designations, that can be described as a complex system of coupled alkali mediated dissolution and precipitation reactions in an aqueous reaction substrate [13].

Geopolymerization is a reaction that chemically integrates minerals or geosynthesis that involves naturally occurring silico-aluminates [39]. Any pozzolanic compound or source of silica and alumina, which is readily dissolved in the alkaline medium, acts as a source of geopolymer precursor species and thus lends itself to geopolymerization [40]. The alkali medium as an activator is a compound from the element of first group in the periodic table, so this material is also called as alkali activated aluminosilicate binders or alkali activated cementitious material [40]. Silicon and aluminum atoms react to form molecules that are chemically and structurally comparable to those building natural rocks [39]. The resulting inorganic polymeric material can be considered as an amorphous equivalent of geological feldspars, but synthesized in a manner same as thermosetting organic polymers. For this reason, these materials are also termed as ‘‘geopolymers’’, in recognition of being inorganic polymer analogues to traditional organic systems of polymers [41].

Aluminosilicate oxide materials containing aluminum Al^{3+} in IV-fold coordination are necessary for the alkali activating process of geopolymerization. Should other coordinations of aluminum be present in the source materials for geopolymerization, the IV-fold aluminum will dominate the reaction and will be completely exhausted while aluminum (V) and aluminum (VI) remain unreacted unless converted to the less stable formation [42]. Aluminosilicates that are naturally occurring in the crust of the earth are

the main sources of these materials, such as kaolinite, feldspars, mine tailings, volcanic ashes, as well as numerous other forms of minerals and clays [43]. Other sources of materials that are rich in aluminum and silicon which can be used for geopolymerization include byproducts of industrial processes such as fly ash, which is the waste product of coal combustion plants, furnace slag, and construction residuals [43].

Pozzolanic compound or source of silica and alumina that is readily dissolved in alkaline solution will suffice as a source of geopolymer precursor species and thus lend itself to geopolymerisation. Conceptually, the formation of geopolymers follow much the same route as that for most zeolites and containing three main steps: (1) Dissolution, with the formation of mobile precursors through the complexing action of hydroxide ions, (2) Partial orientation of mobile precursors as well as the partial internal restructuring of the alkali polysilicates and (3) Reprecipitation where the whole system hardens into an inorganic polymeric structure [29]. These processes were first recommended by Glukhovsky in the 1950s, general mechanism for the alkali activation of materials primarily comprising silica and reactive alumina were divided into three stages: (a) destruction-coagulation; (b) coagulation-condensation; (c) condensation-crystallization [13]. There are, however, some significant differences between zeolite formation and geopolymerisation and most of these are related to the composition of the initial reaction mixture of raw materials [29].

Fig. 2.3 displays a highly simplified reaction mechanism for geopolymerization [13]. The reaction mechanism shown in the figure outlines the key processes occurring in the transformation of a solid aluminosilicate source into a synthetic alkali aluminosilicate. It should be noted that the essential requirement for processing of initial raw materials is fine grinding, heat treatment etc. to vary the reactivity of aluminum in the system is not shown for the sake of simplicity. Though presented linearly, these processes are largely coupled and occur concurrently. Dissolution of the aluminosilicate solid source by alkaline hydrolysis (consuming water) produces aluminate and silicate species. The volume of data available in the field of aluminosilicate dissolution and weathering represents a whole field of scientific endeavor in itself [44-46]. It is important to note that the dissolution of solid particles at the surface resulting in the liberation of aluminate and silicate (most likely in monomeric form) into solution has always been assumed to be the mechanism

responsible for conversion of the solid particles during geopolymerization. This assumption does have almost overwhelming scientific merit based on the literature describing alkaline dissolution, and so is shown in Fig. 2.3. Despite this, the actual process of particle-to-gel conversion has never been confirmed in the highly alkaline and poorly solvated conditions prevailing during geopolymer synthesis. Without the benefit of conclusive mechanistic understanding of solid particle conversion, surface dissolution will be assumed in the simplistic mechanistic model described here [13]

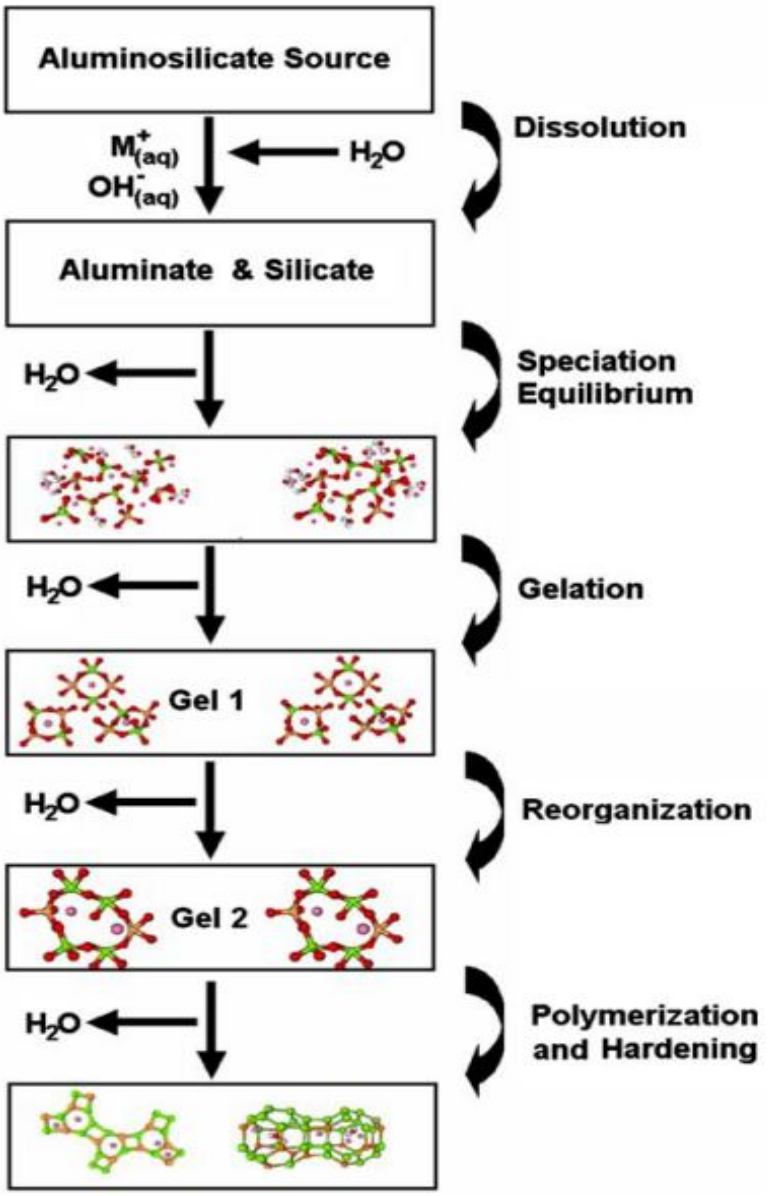

Fig. 2.3 Conceptual model for geopolymerization [13]

The hardening mechanism among others involves the chemical reaction of geopolymeric precursors such as alumino-silicate oxides (Al^{3+} in IV-fold coordination) with alkali polysilicates yielding polymeric Si-O-Al bonds. The IV-fold coordination of Al is emphasized by written (Si_2O_5,Al_2O_2) for these particular aluminosilicate oxides instead of [28]. The most commonly applied method of obtaining these materials involves calcining aluminosilicate hydroxides (Si_2O_5,$Al_2(OH)_4$) such as kaolinite according to the reaction below [7].

(a) $2(Si_2O_5,Al_2(OH)_4) \rightarrow (Si_2O_5,Al_2O_2)_n + 4H_2O$ (2-2)

or by condensation process of and Al_2O vapors:

(b) $4SiO\ (vapor) + 2Al_2O\ (vapor) + 4O_2 \rightarrow (Si_2O_5,Al_2O_2)_n$ (2-3)

with also production of:

$2SiO + O_2 \rightarrow 2SiO_2$ (Condensed Silica Fume) (2-4)

$Al_2O + O_2 \rightarrow Al_2O_3$ (Corundum) (2-5)

Studies have shown that the calcination of kaolinite process can complete itself at 600 ^oC for 6 hours [47]; between 600 and 750 ^oC for 10 hours [48] or even more quickly in only two hours and requires temperature up to 750 °C [49] dependence on source of materials. The geopolymerization process itself is an exothermic polycondensation reaction involving alkali activation by a cation in solution. The reaction leading to the formation of a polysialate geopolymer is described below [7, 27, 29] and usually at room temperature to less than 150 ^oC [8, 14, 16, 27, 50].

$$(Si_2O_5,Al_2O_2)n + 3nH_2O \xrightarrow{NaOH/KOH} \underset{\text{Geopolymeric precursor}}{n(OH)_3\text{-Si-O-Al-}\overset{(-)|}{(OH)_3}} \quad (2\text{-}6)$$

$$\underset{\text{Orthosialate}}{n\overset{(-)|}{(OH)_3}\text{-Si-O-Al-}(OH)_3} \xrightarrow{NaOH/KOH} \underset{\text{(Na,K)-Poly(sialate)}}{(Na^+/K^+)(\text{-Si-O-Al-O-})_n\ \overset{|\quad(-)|}{\underset{|\quad\ |}{O\quad O}}} + 3nH_2O \quad (2\text{-}7)$$

Additional amounts of amorphous silica must be present in order to form either the polysialate-siloxo or polysialate-disiloxo structures of geopolymers. The reaction for the polysialate-siloxo formation is also provided as an illustration of how the two reactions differ [7, 29, 31].

$$(Si_2O_5,Al_2O_2)n + nSiO_2 + 3nH_2O \xrightarrow{NaOH/KOH} n(OH)_3\text{-Si-O-Al(-O-Si-(OH)}_3\text{)-O-Si-(OH)}_3 \quad (2\text{-}8)$$

Geopolymeric precursor

$$n(OH)_3\text{-Si-O-Al(-O-Si-(OH)}_3\text{)-O-Si-(OH)}_3 \xrightarrow{NaOH/KOH} (Na/K)(\text{-Si-O-Al-O-Si-O})_n + nH_2O \quad (2\text{-}9)$$

Ortho(sialate-siloxo) (Na,K)-Poly(sialate-siloxo)

It has been assumed that these syntheses are taken place through oligomers (including dimer and trimer) which provide the particular unit structures of three dimensional macromolecule of geopolymer edifice [7, 31].

The last term in Equation (2-7) and (2-9) reveals that water is released during the chemical reaction which occurs in the formation of geopolymers. This water, expelled from the geopolymer matrix during the curing and further drying periods, leaves behind discontinuous nano-pores in the matrix, which provide benefits to the performance of geopolymers. The water in a geopolymer mixture, therefore, plays no role in the chemical reaction that takes place; it merely provides the workability to the mixture during handling [51, 52]

2.2.3 PROPERTIES OF GEOPOLYMERS AND COMPOSITES THEREOF

In order to use geopolymers as an engineering material, knowledge of their chemical, physical, and mechanical properties and so on must be fully understood. While the earlier researches were conducted through industry and kept as proprietary knowledge [7], there have been recently numerous studies attempting to clarify the properties of these materials.

Specifications of geopolymer materials have often been explained in terms of their microstructural properties. These include both the porosity of the materials and extent to which the geopolymerization takes place. Using Nuclear Magnetic Resonance (NMR), a presence of aqueous $Al(OH)_4^-$ was discovered to be trapped inside pores within the geopolymeric binders [42]. This implies that not only is a portion of the aluminum not being reacted, but this inability to completely react creates porosities [42]. In addition, this research shown that the presence of this aqueous phase was also correlated to the silicon to aluminum ratio used to prepare the sample and found that geopolymers with Si:Al $\leq$ 1.40 cannot be accurately characterized by their Si:Al ratio because the degree of unreacted aluminum is too great. In fact, when curing conditions and source materials are held constant, the Si:Al ratio directly affects the nature of the porosity with higher Si:Al ratios having larger overall pore volumes but lower average pore diameter [53]. The same effect was also analyzed in another study in an attempt to tailor porosity to meet specific properties. It was discovered that choosing an appropriate alkali activator and curing conditions would enable the ability to control the geopolymerization process and obtain desired porosities [54]. Other studies have also presented that Si:Al ratios directly affect the rate and extent of geopolymerization and thereof production. It has also been shown that incomplete geopolymerization can lead to pockets of unreacted metakaolin which act as structural point defects within the material [55]. In order to study the effect of the chemical composition on this phase, Singh and his colleagues determined that when the SiO_2:Al_2O_3 ratio is increased, the percent of unreacted metakaolin will be decreased. The unreacted phase, however, was still present even with SiO_2:Al_2O_3 ratios as high as 15 [55]. The process of the geopolymerization is carried out more fully, in case additional silica is added to the sample until an equilibrium point is reached, at which the excess silica begins to hinder the alkali cations ability to react with the aluminum. Controlling the SiO_2:M_2O ratio (M = Na or K) is another factor that influences the reactivity. It was determined that around SiO_2:M_2O = 2.00 the maximum amount of geopolymerization occurs with a decreasing amount of reactivity as SiO_2:M_2O ratios deviate from that point [56]. Other research discovered that the geopolymerization reactions only occur at the surfaces of the particles of source materials, which theorize that the source materials themselves are responsible for the extent of unreacted materials [57]. Therefore, the particle size of

the source materials will be the most important parameter in determining the extent of geopolymerization where initial materials with higher specific surface area will react more homogeneously due to the higher availability of surface molecules which can interact in the process of geopolymerization [58].

The geopolymeric materials are "polymer", thus they transform, polycondense and adopt a shape rapidly at low temperature (a few hours at 30 ^{o}C, a few minutes at 85 ^{o}C and could be a few seconds with microwaves); but also "geopolymers", thus they are mineral materials which are hard, weather resistant and withstand high temperature [7]. In order to effectively apply geopolymers as an engineering material, especially construction material, many researchers have tried to determine the mechanical and elastic properties of geopolymers such as Young's modulus, compressive strength, and flexural strength. Recently, the physical and chemical properties, however, have been clarified in many researches.

The two most commonly used aluminosilicates are metakaoline and fly-ash, they are quite much available in nature and forms as a byproduct of industrial process; for example, in China and India, the two countries that consume large amounts of cement, together with producing over 300 million tons of fly ash per year [59]. Many studies have been performed to determine the compressive strength and flexural strength of the derived geopolymers. A quite large range of the compressive strengths from around 10 MPa to 100 MPa has been evaluated for geopolymers based on kaolin without aggregates [48, 53, 57, 58, 60] meanwhile fly-ash based geopolymers without aggregates have been shown to range between 20 MPa and 100 MPa [33, 59, 61-64]. Oleg Botnovsky and his colleagues have determined that the flexural strength of geopolymers based on metakaolin without the use of aggregates varies from 9 MPa to 16 MPa [48]; when 4 MPa of compression is used in the molds, however, the bending strength of pure geopolymer could reach at approximately 50 MPa [57]. Fly ash based geopolymers without aggregates, however, have been recorded as having a flexural strength ranging in a quite range from 2.0 MPa to 14.2 MPa [61, 65].

In company with strength, additionally, Young's modulus or elastic modulus of the material is also very important parameter to be investigated for engineering applications. Because the geopolymer materials are porous naturally, complicated

fracture mechanics lead to wide ranges of uncertainties when strengths are experimentally evaluated due to the destructive nature of these tests; therefore, it has been suggested that Young's modulus but not the compressive strength is the most effective mean of rating the physical nature of geopolymeric materials [53]. Throughout the literature, the typical values of compressive Young's modulus reported for metakaolin based geopolymers without aggregates range from 1.5 GPa to 6 GPa [53, 60]. Concerning about the Young's modulus of geopolymers based on fly ash without aggregates, however, we found no studies evaluated this value up to now.

The development of composite concept based on geopolymer matrix was just started in 1982 by professor Joseph Davidovits, a chemical, physical and material scientist from nonprofit Geopolymer Institute in Saint-Quentin, France [7]. Fiber-reinforced composites based on geopolymer matrix have been well-known for over 20 years, however, since the first Nicolas Davidovits and his coleagues' patent, no. 4,888,311, was filed in United State Patent [9]. According to this invention, a composite named ceramic-ceramic material is disclosed having a fibrous reinforcing ceramic and a ceramic matrix made of a geopolymeric compound containing one of these: a poly(sialate) geopolymer $M_n(\text{-Si-O-Al-O-})_n$ and/or poly(sialate-siloxo) $M_n(\text{-Si-O-Al-O-Si-O-})_n$, and an oriented or randomly disposed fibrous reinforcement such as ultrafine silicious and/or aluminous and/or silico-aluminous constituents, of size smaller than 5 μm, preferably lower than 2 μm; M representing at least one alkaline cation (Na^+, K^+, and/or Ca^{2+}), and n is the degree of polymerization. The geopolymeric compound was obtained by polycondensation at a temperature between 20 °C and 120 °C, with the same technologies as for organic plastics, from an alkaline alumino-silicate reaction mixture which expressed in terms of mole ratios of the oxides being between or equal values: M_2O/SiO_2 = 0.10 to 0.95; SiO_2/Al_2O_3 = 2.50 to 6.00 and M_2O/Al_2O_3 = 0.25 to 5.70. The fibrous reinforcement consists of ceramic fibers such as SiC, Al_2O_3, SiO_2, glass, carbon. The addition of alkaline sulphides and alkaline sulphites enables glass fibers to be protected against chemical attack due to the alkalinity of the matrix. Five important illustrations were taken in range of two series of oxide mole rations.

Example 1, a reaction mixture is prepared, containing 17.33 moles of H_2O, 1.630 moles of K_2O, 4.46 moles of SiO_2 and 1.081 moles of Al_2O_3. Where Al_2O_3 comes from

an alumino-silicate oxide $(Si_2O_5,Al_2O_2)_n$ in which the Al cation is in 4-fold coordination with oxygens, SiO_2 comes from this alumino-silicate oxide, and from a solution of potassium silicate; K_2O comes from the potassium silicate and anhydrous KOH. The mole ratios of reactive oxides are: $M_2O/SiO_2 = 0.36$, $SiO_2/Al_2O_3 = 4.12$, $H_2O/Al_2O_3 = 16.03$, $M_2O/Al_2O_3 = 1.51$. The pH of this mixture is about 14, a carbon fibre cloth, stable in alkaline medium, is impregnated; the cloth is then covered with a plastic sheet to prevent evaporation, then placed in an oven at 85 °C for 90 minutes. It is then removed from the mould, and after drying at 85 °C, a board is obtained, however, whose matrix is completely cracked, crazed and having no coherence. To solve these problems, 5 to 95 parts by weight of filler must be added, generally 50 part by weight, of granulometry higher than 50 µm [66]. In the examples given here, only 20 parts by weight of silico-aluminous fillers, of the fire clay type, of granulometry lower than 200 µm are added to the reaction mixture. A carbon fibre cloth is impregnated and scraped, then a multi-layer board is made up containing several layers of this impregnated cloth. It is covered with a plastic sheet, placed beneath a weight to ensure cohesion, and polycondensed in an oven at 85 °C for 90 minutes. It is removed from the mould, and after drying at 85 °C, a board is obtained and their flexural strength is quite low, only about 65 MPa was recorded. Impregnation does not really take place to within the bulk of the material, and the composite material breaks very easily into separate sheets. There is no cohesion between the fibres.

It is expected that adding sodium sulphite, or more generally alkaline and alkaline earth sulphides and sulphites can protect the glass fibre against corrosion due to the high alkalinity of the reaction medium (pH = 14). 0.80 moles of sodium sulphite Na_2SO_3, and 0.50 moles of SiO_2 from silica dust, of dimensions lower than 1 µm is added to the reaction mixture of example 1. The mole ratios of resuting reactive oxides are now: $(Na_2O,K_2O)/SiO_2 = 0.48$, $SiO_2/Al_2O_3 = 4.60$, $H_2O/Al_2O_3 = 16.03$, $(Na_2O,K_2O)/Al_2O_3 = 2.25$, $SO_2/Al_2O_3 = 0.74$ and $SO_2/SiO_2 = 0.16$. This mixture is very fluid and used to impregnate a cloth of a silicon type of glass fiber E, a carbon fiber taffeta and a SiC fiber taffeta. After hardening and shaping under a metal plate at 70 °C for 15 minutes, the boards are dried at 120 °C. The flexural strength is evaluated as 140 MPa for the glass E, 175 MPa for the carbon and 210 MPa for the SiC fibers. The flexural strength of reinforced SiC fiber geocomposite stays practically unchanged

up to 800 °C. An important comment is any ceramic fibres are usable for reinforcing geopolymer, though they give slightly lower bending strengths, silicon carbide fibre, such as the proprietary brand Nicalon, is the preferred in this case. The choice of ceramic fibre is made according to the thermal or chemical environment in which the composite material of the invention is placed during its particular industrial use.

Another example is taken place as a method to fabricate composite multi-layer materials combining fibre reinforcement with sheet materials or aluminium foil, like a honeycomb. The reaction mixture like of above example is settled on an alumium sheet, simple contact of the aluminium with the reaction mixture causes immediate appearance of a large quantity of gas, and attacking of the aluminium. If there is no attack, there is nevertheless sticking between the sulfo-silico-aluminate matrix and the aluminum.

Table 2.1 Comparison between SiC Fibre/K-PSS GEOPOLYMITE Composite and SiC Fibre/Ceramic Matrix composites [7, 9]

Composite (fiber/matrix)	**Processing temp., [^{o}C]**	**Mean Strength, [MPa]**
Uncoated SiC/SiC	ca.1400	135
Coated SiC/SiC	ca.1400	170
SiC/Li Alum. Silicate	ca.1400	860
SiC/cordierite	ca.1400	170
SiC/ZrO	ca.1400	180
SiC/mullite	ca.1400	80
SiC/mullite-30% SiC/BN	ca.1500	140
SiC/Vycor Glass	ca.1500	440
SiC/VPS + 50% BN	ca.1500	320
SiC/K-PSS GEOPOLYMITE	70	380

Last but never least, it can be seen from this invention is an opportunity to compare the mechanical properties of composite based on geopolymer matrix and reinforced by SiC fiber with the mechanical properties of composites obtained by traditional ceramic techniques. As shown in Table 2.1, composite ceramic-ceramic materials cured at

70 ^{o}C possessing the same characteristics as those made at temperatures up to 1500 °C, these results were republished in Journal of Thermal Analysis Vol. 37 in 1991. It is obvious that these high temperatures greatly limit technological applications of these materials, whereas the very low fabrication temperature for composites according to the invention enable the simple huge mass production of any object of any shape.

Bill E. Laney et al. continued the development of advanced geopolymer composites, a self-hardened, high temperature-resistant, foamed composite based on an alkali metal silicate matrix devoid of chemical water has dispersed therein inorganic particulates, organic particulates, or a mixture of inorganic and organic particulates to benefit from the advantages of organic fibers, foam fillers, etc., while enjoying the assurance of limited combustibility, non-toxicity, and energy conservation, and is produced at ambient temperature by activating the silicates of an aqueous, air-entrained gel containing matrix-forming silicate, particulates, flyash, surfactant, and a pH-lowering (around 11) and buffering agent [67]. According to this invention a broad class of high temperature composite materials that combinate, essentially, of two distinct phases - one of many different silicate-based geopolymers like a ceramic matrix and a homogeneous dispersion of organic/inorganic additives of various shapes and dimensions. Individually, these two phases are generally unsuitable for high temperature applications, however, they combine in the composite form to produce a wide spectrum of refractory materials. Moreover, these materials can be cured at ambient condition, controlled density, and tailored for specific applications, over significant temperature ranges, by judicious specifications of dispersed phase components and selective chemical modifications to pre-gelled geopolymer resins. Without being limited by theory, it is believed that the geopolymer matrix material surrounds the filler particles and, even when internal organic particles melt or decompose due to intense heat conduction from external high temperature surfaces, the geopolymer matrix material retains its structural integrity and other performance qualities when geopolymer matrix must be present in sufficient amounts to coat and support the filler particles. Accordingly, even flammable organic particles as expanded polystyrene (EPS) beads are added to the advanced geopolymer composite, overall fire resistance of resulting material is improved. In this manner, the inorganic geopolymer matrix material, when bonded to organic fiber particles in accordance with the present

invention, prevents excessive surface burning, flame spread, and smoke generation while maintaining adequate dimensional stability and low density thermal insulation. When the composition is cast into boards or panels of appropriate thicknesses, such a material can serve as its own fire safe thermal barrier.

Another useful organic particle is used here is polyethylene terephthalate (PET) polyester chopped staple fibers. An amount over 150g of PET can be employed 450g of cured geopolymer matrix material and still meet one of the criteria for limited combustibility, because PET has a heat of combustion of about 9,600 btu/lb. (22.51 KJ/g) and in accordance with ASTM E-84 "Surface Burning Characteristics of Building Materials", a "limited combustible" material has a potential heat of combustion which is less than 3500 btu/lb. (8.2 KJ/g) of material and demonstrates a flame spread rating of less than 25 places. Smoke generated ratings are compared with a same class as incombustible inorganics, e.g., calcium silicate board. Compositions of the present invention which incorporate PET filler particles in the form of short fibers or laminated blankets have achieved all three criteria for limited combustibility. Although advanced geopolymer composites which employ EPS materials have not been tested in accordance with ASTM E-84; qualitatively, they have been observed to perform in a manner similar to the PET compositions, and, accordingly, they are expected to achieve similar quantitative ratings.

A reaction mixture is made containing 3-6 kg of English kaolin is added to 9-18 kg of sodium silicate solution, SiO_2:Na_2O weight ratio of 3.22, and 90-160g of dissolved flake $MgCl_2.6H_2O$ in 3-6 kg of tap water. Additionally, 60-100 g sodium lauryl sulfate, $CH_3(CH_2)_{11}OSO_3Na$, in dry form. After mixing for 45 minutes at Hobart Model L-800 mixer at speed 3, foamed geopolymer resin densities are approximately 0.8 $g.cm^{-3}$. Chemical modification could be taken place from this mixture to produce advanced geopolymer composites with a variety of macroscopic physical properties. For example, powdered relay steel or ferrite particles are dispersed in geopolymer resins to produce castable, high magnetic permeability, refractory materials, or 2% by weight addition of calcium chromate to the solution inhibits long-term corrosion. Similarly, the electrical conductivity of geopolymer resins can be altered by adding 1-5% by weight of acetylene black, and these modified geopolymer resins, in combination with "spherical close packed" dispersions of EPS beads or other non-conducting "spacer"

particles, provide a high temperature material which is electromagnetically equivalent to low temperature "reticulated foam" microwave absorbers.

Advanced geopolymer composites fabricated from these raw materials, by category, include: waste materials - flyash, sludges, slags, confetti, rice husks, bagasse, saw dust, etc; volcanic aggregates - expanded perlite, pumice, scoria, and obsidian; mineral forms - expanded mica (vermiculite), borosilicates, clays, metal oxides, etc.; plant and animal remains - distomaceous earth, sea shells, coral, excreta, hemp fibers, etc.; and manufactured fillers - silica microspheres, mineral fibers and mats, chopped/woven fiberglass, metal wools, turnings, or shavings, and synthetic microspheres, fibers, or mats typically exhibit the following characteristics: low combustibility; high melting points (similar to ceramics and refractories); low thermal and electrical conductivity; high acoustic absorptivity; low toxicity; low solubility in water; moderate acid/base resistance; mildew-, rot-, and vermin-proof; and insensitivity to infrared, ultraviolet, neutron, and charged particle radiation.

In 1991, Joseph Davidovits and Michel Davidovics presented properties of the Poly(sialate-disiloxo) geopolymer type (-Si-O-Al-Si-O-Si-O-), M-PSDS and derived thereof, at the 36th SAMPE Symposium and published by Journal of Thermal Analysis. The binder showed very-low viscosity inorganic resins, harden like thermosetting organic resins as low at 65 ^{o}C for very short cure-cycle, but possess ceramic-like in their properties and have use-temperature range up to 1000 – 1200 °C. These geopolymers provide faithful reproduction of mold or die surface and allow for precision and fineness of products [7, 68]. The geopolymers which were used in these studies are the inorganic countertype of organic resins, were developed by the Geopolymere group (with Michel Davidovics and Nicolas Davidovits), GEOPOLYMITE® binders under United State Patents no. 4,349,386; 4,472,199; 4,888,311; 5,342,595; 5,352,427 [9, 28, 66, 69, 70] and supplied by Neuschäffer & al., Randel & al., at the licensed German Company Dynamit Nobel (later Hüls Troisdorf AG, now sublicensed to Willig GmbH, binders TROLIT® and WILLIT®). The most promising resins for advanced composites with organic matrices, result from the conjunction of two advanced techniques: geopolymerization and sol-gel technology, fluoro-poly(sialate-disiloxo), F,M-PSDS Geopolymite resins [70]. F,M-PSDS is a combination of a geopolymeric network made of poly(sialate-disiloxo) and molecular

silicon oxide SiO_2 embedded within the matrix. The trapped molecular SiO_2 yields a low-porosity, highly-packed microstructure, with higher density (Fig. 2.4a). Fig. 2.4b, Fig. 2.5 and Table 2.2 present the physical properties of geopolymers such as fusion temperature and coefficient of thermal expansion CTE, they are a function of the Si/Al ratio. Fig. 2.5 displays a comparison between the coefficient of thermal expansion CTE for traditional materials and for geopolymers. CTE values measured for geopolymers are those of commercially available Geopolymite resins, without any additional filler. In the case of F,M - PSDS formulations, CTE values increase with the amount of molecular silicon oxide SiO_2 packed inside the geopolymeric tri-dimensional network (type 1,2, 3) [7, 68].

Table 2.2 Coefficient of thermal expansion (CTE) of geopolymers

Geopolymers	**Si/Al [1]**	**CTE.10^{-6} [1/^{o}C]**
K-PSS	2	4
K-PSDS	3	6
F,M-PSDS 1	3.5	10
F,M-PSDS 2	5	15
F,M-PSDS 3	20	25

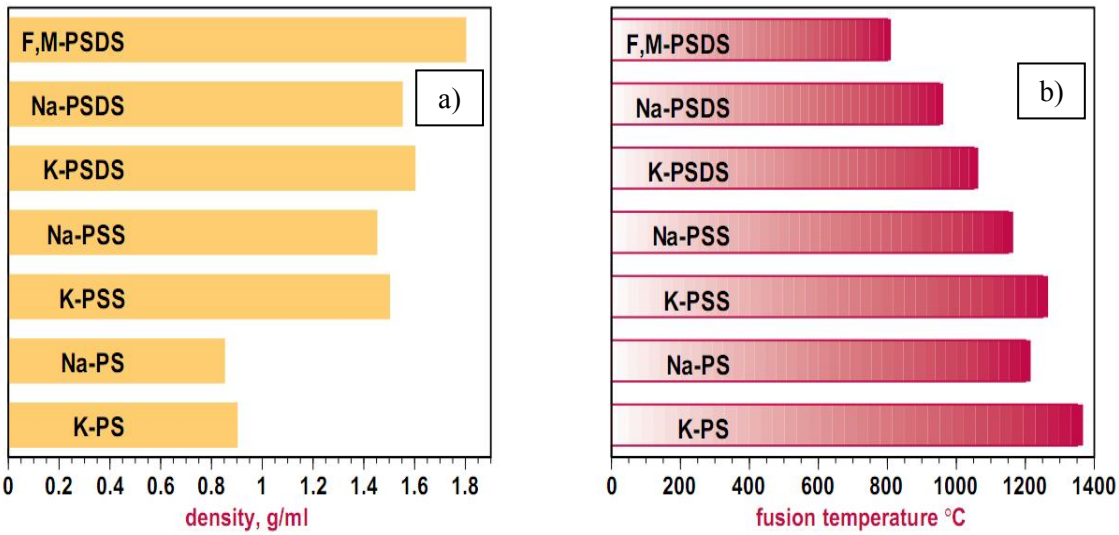

Fig. 2.4 Density (a) and Fusion temperature (b) of geopolymers (pure matrix) [7, 68].

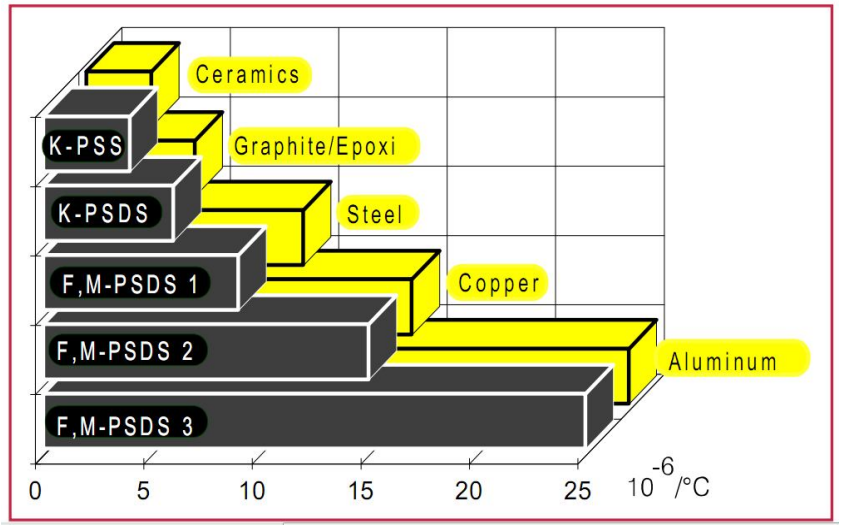

Fig. 2.5 CTE of geopolymer materials [7, 68].

A wide range of alkaline resistant inorganic reinforcements has been used to combine with geopolymer matrices. The relationship between operating temperature, flexural strength and fiber types, is presented in Table 2.1. Fig. 2.6 shows retention of the flexural strength of geopolymer matrix F,M-PSDL or K-PSDS reinforced by Carbon, E-glass or SiC fabrics at high use-temperature in three-point bending mode. E-glass and Carbon fabrics should be used up to 450 °C with the F,M-PSDS matrix. Higher temperatures require ceramic fibers such as SiC, Nicalon fabrics, or Safil aluminum oxide fibers. In all cases, a use-temperature higher than 700 °C implies a M-PSDS matrix. A successful combination of SiC fiber with skills of reinforced plastics/composites industry showed non-burning, non-smoking, non-toxic benefits [7, 68].

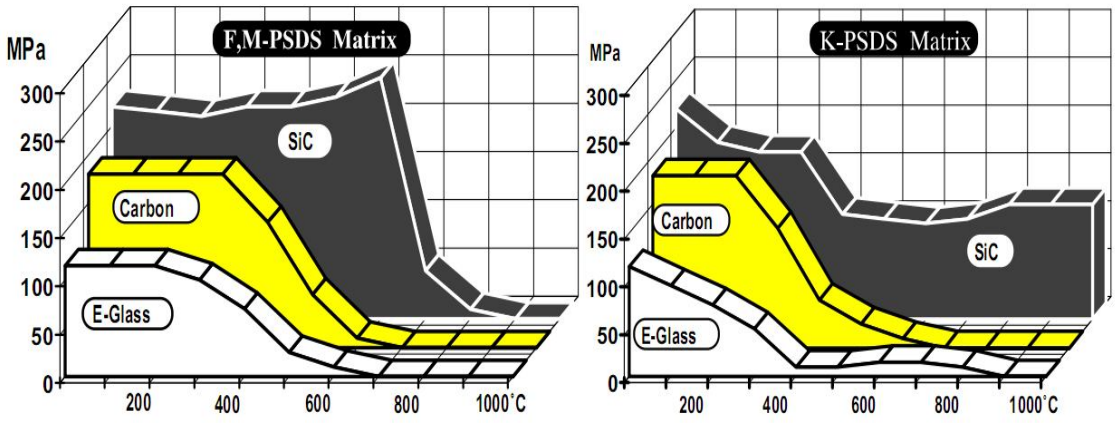

Fig. 2.6 Three-point flexural strength of geopolymer composites in function of the use-temperature [7, 68].

Richard E. Lyon and his partners, 1997, used carbon fiber to reinforce potassium aluminosilicate geopolymer matrix and compare the fire response of resulting material to commercial organic matrix composites which being used for transportation, military, and infrastructure applications, such as glass- or carbon-reinforced polyester, vinylester, epoxy, bismaleimde, cyanate ester, polyimide, phenolic, and engineering thermoplastic. A potassium aluminosilicate, or poly(sialate-siloxo), with the empirical formula: $Si_{32}O_{99}H_{24}K_7Al$. This particular resin hardens to an amorphous or glassy material at moderate temperatures with a density of about 2.14 g/cm^3 and is one of a family of inorganic Geopolymer materials described previously [7, 68]. Cross-ply fabric laminates were made by hand rolling to impregnate potassium aluminosilicate geopolymer liquid resin, SiO_2/AlO_2 in a mole ratio of 27/1, into 25 layers of 3K plain weave carbon fabric (Amoco T-300, 193 g/m^2), and air drying 30 seconds at 80 ^oC to remove residual moisture and develop tack. Unidirectional tape was used to fabricate cross-ply laminates for off-axis tensile testing of inplane shear properties. In all cases hand-impregnated plies were cut, stacked, and cured in a vacuum bag at 80 ^oC in a heated press with 0.3 MPa pressure for 3 hours. The panels were then removed from the vacuum bag and dried for an additional 24 hours at 100 ^oC for until constant weight was achieved. About 22% of the as-mixed liquid resin is water, about half of which is removed during the curing and drying process. The thickness of final laminate was about 5.6 mm, fiber volume fraction of approximately 50–55% and density was 1.85 g/cm^3. While, organic matrix cross-ply laminates of polyester (PE), vinylester (VE), epoxy (EP), cyanate ester (CE), bismaleimide (BMI), PMR-15 polyimide (PI), and phenolic (PH), thermoset resins as well as thermoplastic polyphenylene sulside (PPS), polyetheretherketone (PEEK), polyetherketoneketone (PEKK), polyarylsulfone (PAS), and polyethersulfone (PES) resin matrices were prepared from commercial S-glass, E-glass or carbon fabric prep-regs (not details of fabrication procedure were described in this study). The density of these cured laminates ranged from about 1.55 to about 1.98 g/cm^3 at the nominal 60% volume carbon and glass fiber loading, respectively. Ignitability - heat release and smoke, Flame spread index, Residual flexural strength, Tensile properties, Inplane shear properties, Interlaminar shear properties were evaluated in accordance with ASTM E-1354, ASTM E-162-83, ASTM D-790, ASTM D3039-76, ASTM D3518-76, ASTM D3846 respectively. From the results, important

conclusions should be noted: At irradiance levels of 50 kW/m^2 typical of the heat flux in a well-developed fire the laminates of glass or carbon reinforced commercial organic matrices listed above ignited readily and released appreciable heat and smoke, meanwhile carbon-fiber reinforced geopolymer composites did not ignite, burn, or release any smoke at all even after extended heat flux exposure (Fig. 2.7). The Geopolymer matrix carbon fiber composite retains 67%, 154 MPa after exposure up to 800 ^{o}C for 1 hour in comparison with 245 MPa at 22 ^{o}C after curing, of its original flexural strength after a simulated large fire exposure, this is also indicated that the geopolymer matrix can protect carbon fiber from oxidation [12].

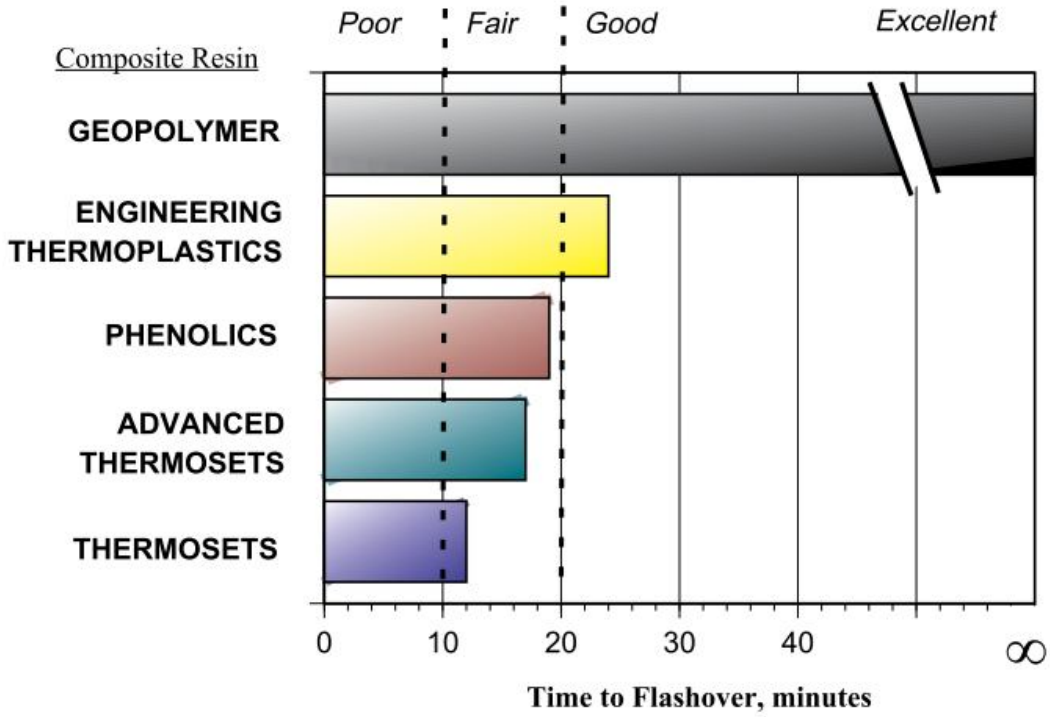

Fig. 2.7 Predicted time to flashover of materials in accordant with ISO 9705 corner/room fire test [10, 12].

The influence of reinforcement types on the flexural properties of geopolymer composites was investigated by Hammell James and cooperators, this study published by SAMPE International Symposium and Exhibition in 1998 and represented in the 2nd International Conference, Géopolymère '99 [71, 72]. The ingredient of used geopolymer resin was same as previous works by Richard E. Lyon (1997); the reinforcement consisted of:

- Woven carbon fabrics with 1, 3, 12, and 50k tows

- Unidirectional carbon made using 3k tows
- Woven E and S glass fabrics
- Combinations of carbon and E-glass stacked 1 to 1
- Two stainless steel 20 and 40 wire meshes in combination with E-glass fabric stacked 2 E-glass layers to 1 steel mesh layer

Geopolymer resin was penetrated into the fabrics manually, stacked together and placed into a plastic bag, standard vacuum bagging technique was used. The bag was placed in a heated press at 80 °C and 3 MPa for 3 hours. The laminates were then removed from the press and inserted into a furnace for final curing at 80 °C for 24 hours or until a constant mass was achieved. The number of layers had to be altered to obtain a reasonable thickness of composite and the volume fraction of reinforcement was approximately 50%. The plates, approximately 175 x 175mm in plan dimension, were cut from the sample using a diamond blade. The samples were tested on MTS Teststar system over a simply supported span of 100 mm with a center-point load deflection rate of 2.8 mm/min in accordance with ASTM D790. The specimens were 1.6 to 6.5 mm thick depending on the reinforcement that was used. The performances of resulting composites were evaluated by using classical bending theory.

The lowest density (≈1.9 g/cm^3) is for the carbon composite plates. Addition of E-glass fabric increased the density to approximately 2.4 g/cm^3, and the density increased to about 3.4 g/cm^3 for the plates made with steel wire mesh. The strength of the carbon fabric plates increased as the tow size decreased, because larger tow size causes more significant tow bending during weaving and difficulties to penetrate resin into fabrics, not transfer force between composite layers at higher strains. So, it could be preferred to have non woven fabrics, the unidirectional carbon fabric provided the highest flexural strength of about 525 MPa. These specimens also had the highest flexural modulus about 85 GPa. When the E-glass is combined with carbon, the strength of the composites reduced. Geopolymer reinforced by unidirectional E-glass and carbon fiber, however, showed approximately the same strength as plain of continuous carbon fiber only. So, carbon-glass combinations can be a potential utilization to improve economic value. The current study showed many limitations that steel wire meshes can not be used competitively due to the high density. In applications where ductility is

essential and weight is not critical, it may provide an alternative. Also, if a steel fabric is to be used, it should be a finer mesh so that there is adequate bond.

In point of view of water stability under wet-dry conditions, an investigation was taken place by Hammell et al. in 2000. The study showed that when the inorganic matrix, a potassium aluminosilicate, or poly(sialate-siloxo) with high molar ratio SiO_2/AlO_2=27, composites embedded by 3K plain weave carbon fabric (Amoco T-300, 193 g/m^2) as the research of Richard E. Lyon and his partners (1997) were subjected to wet–dry cycles, the flexural strengths were found to deteriorate rapidly. Though carbon fibers do not degrade in water, the matrix was assumed to contribute entirely to the degradation of the composite strength. This experimental investigation was undertaken to improve the matrix performance. In order to eliminate the contribution of strength from the carbon fabric, meanwhile maintain the fiber–matrix interaction, it was decided that interlaminar shear strength of the composite would be used as a response variable for the study of degradation. In this mode of loading, the shear strength of the matrix is measured, but at the same time there is interaction between the fiber and the matrix. Based on the chemistry of dissolution in water, it was expected that lowering the silica/alumina ratio in the matrix would improve its stability in water. Five sample designations with different Silica/Alumina ratios as 27.0, 18.2, 19.7, 19.7 and 27.0 of the reaction geopolymer mixtures which reinforced by 8 layers of the 3k PAN based carbon fabric. The vacuum bagging technique was setup, the stacked fabric was covered with a teflon release ply and a breathing layer to allow for the removal of entrained air. Next, the bag was placed into a heated press at 80 ^oC and 3 MPa. The temperature was ramped from 80 to 150 ^oC over 1 hour. The sample was maintained at 150 ^oC for 1 hour, and then cooled to room temperature for approximately 4 hours. The specimens were soaked in water at temperature of 50 ^oC in a chamber for 2 hours. After this, s drying cycle time of 3 hour was chosen to assure complete drying of all specimens. 50 wet-dry cycles were applied for each sample. Finally, all tests were conducted in accordance with ASTM D-3518 using a 50 kN MTS Sintech test frame at a control load displacement rate of 2.5 mm/min. Based on the shear strength from this investigation, it is obvious that the silica/alumina ratio has a significant effect on both the strength and water stability of geopolymer matrices. Reduction of the silica/alumina ratio of the inorganic matrix increases the shear strength by as much as

53% (20.3 MPa with SiO_2/AlO_2 = 18.2/1 in comparison with 13.3 MPa with SiO_2/AlO_2 = 27/1). Another observation is that reduction in the silica/alumina ratio results in consistent improvement in the residual strength after 50 wet–dry cycles condition and that the optimum ratio is 18.2 [73].

In comparative study of high temperature composites, Papakonstantinou et al. (2001) used composites based on popular geopolymer resin and 3K plain weave carbon fabric (Amoco T-300, 193 g/m^2) as reinforcements (opened in all most previous publication) to compare to properties of commercial ceramic/ceramic composites which were fabricated at high temperature (see more Davidovits et al. 1989; Davidovits 1991). In point of view of strength retention at high temperature, it can be seen from Fig. 2.8 that the SiC/SiC composites retained 80% of the room temperature at 800 ^oC dropping almost linearly to 55% at 1200 ^oC. The SiC/zircon as well as the SiC/BN/zircon remained appoximately 50% of the strength at 1200^oC. The SNF/SNC composite retained almost 94% of room temperature strength after exposing up to 1200 ^oC, and the BMAS/SiC exhibited even higher strength at 1100 and 1200 ^oC, about 14 and 28% increase, respectively. At 600 ^oC the strength of Nicalon/LAS composite also showed slightly higher. On the contrary the strength of Saphkon/Al_2O_3 composite remained only 58% at 800 ^oC and 46% at 1200 ^oC. Alumina/glass and alumina/tin/glass exhibited the same behavior and comparably well up to 400 ^oC with around 75% of their strength, at 600 ^oC, however, the glass matrix softens.

In general, when the environment is not oxidizing, the carbon/carbon composites do not lose their strength at elevated temperatures and under particular conditions, the composites can be used at temperature in excess of 3000 ^oC [74]. Typicaly carbon/carbon composite, however, oxidizes at 400 ^oC [75]; in oxidization environment at 1000 ^oC, carbon/carbon composites retain only 20% of the room temperature strength [76]. Lou et al. reported that the initial oxidation temperature can increase to 657 ^oC when composites fabricated by rapid CVD with anti-oxidation additives [75] and with the use of anti-oxidative fillers ($MoSi_2$) the retained strength of the composites can increase up to 41% ater exposing to 1000 ^oC [76]. On the contrary, the polysilate composites, although reinforced by carbon fibers, could retain up to 63% of their original strength at 800 ^oC. This is also means polysialate geopolymer matrix protects the carbon fiber from oxidation [14].

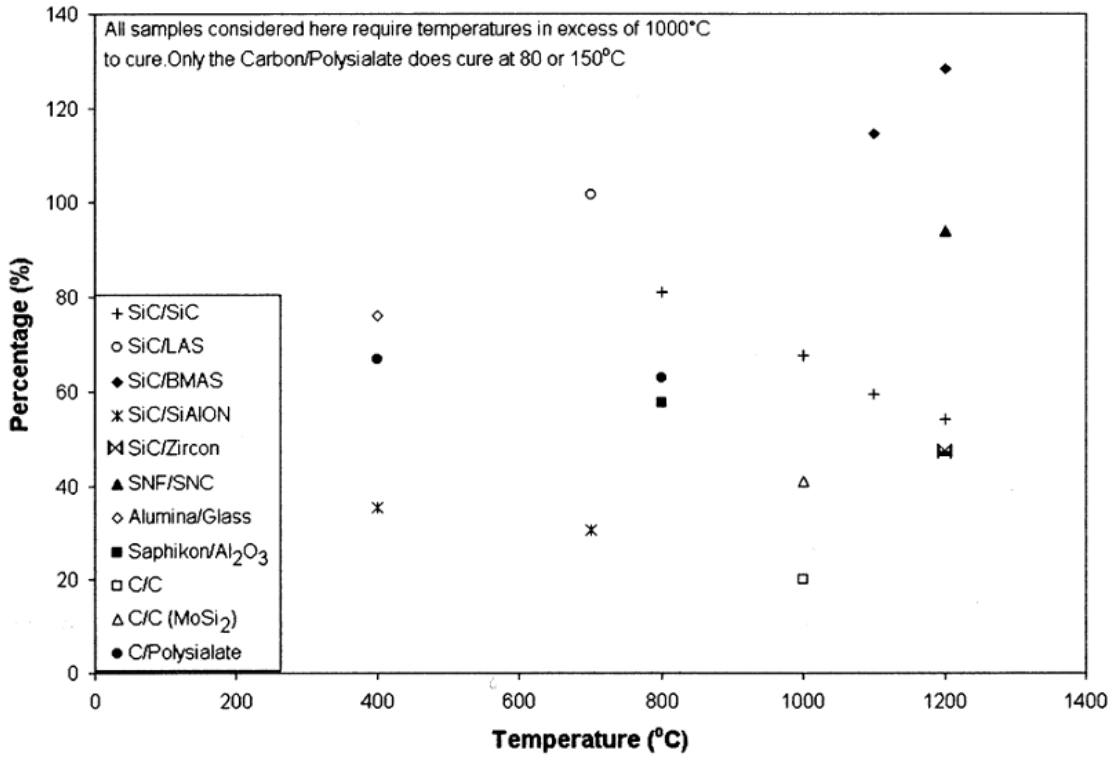

Fig. 2.8 Comparative percentage of strength retention at high temperature [14].

In 2003, Waltraud M. Kriven et al. studied the microstructure and microchemistry of fully-rected geopolymers and geopolymer matrix composites. In this research, the processing, intrinsic microstructure and properties of geopolymer materials and geopolymer composites have been investigated. Curing of geopolymers was achieved by one of three routes: pressureless curing, warm pressing, and curing in a high-pressure autoclave. The materials were fabricated at ambient temperatures up to 80 °C. The work has focused on elimination of entrapped air, increased degree of reactivity, improvement in dissolution chemistry and attainment of adequate workability. Composites have been made and tested using basalt fiber weaves and chopped basalt fibers. Using fiber reinforcement, the bending strength and work of fracture of geopolymer materials have been increased from an average of 2.8 MPa to 10.3 MPa and from 0.05 kJ/m^2 to 21.8 kJ/m^2, respectively. Electron microscopy techniques (SEM, TEM/EDS, in situ hot stage TEM) were used to study the effect of processing variables on microstructure. The microstructure of fully reacted geopolymers was sponge-like and consisted of nanoparticulates separated by nanopores whose features are of the order of ≤10 nm. The local microchemistry of

fully reacted geopolymer frequently observed corresponded to a silica (SiO_2) to alumina (Al_2O_3) ratio of 4:1. This is sometimes called the polysialate siloxo (PSS) composition. In situ, hot-stage TEM observations made during heating for 4 hours up to 1000 °C showed that the nanosized microstructure was stable, although continuous evolution of (presumably) H_2O was noticed upon heating in the hot stage TEM [77].

Hussain et al. (2004) investigated about thermal and fire performance of novel hybrid geopolymer composites [78], In this study synthesized geopolymer is incorporated into the cross-linked polymeric structure systems by manipulating the chemical composition of the geopolymer and hence compatibility, rather than physical blending. In so doing, they make use of the processability and properties of the cross-linked epoxy resin, in combination with the geopolymers to produce inorganic organic hybrid materials, which have excellent mechanical properties such as stiffness and strength, and in particular are more fire resistant. Thus the first system reported involves the choice of a standard, bi-functional epoxy resin, diglycidyl ether of bisphenol A (DEGEBA) to be incorporated with the geopolymers. The results are also compared with a physically blended epoxy–kaolin blend to investigate any synergistic effect of producing a more homogeneously dispersed network on the fire performance.

Inorganic geopolymer was synthesized by the reaction of kaolin (HR1-F grade, particle size of 38.2 μm, Astralia), potassium silicate (SiO_2/K_2O = 2.0, SiO_2 = 29.3 wt.% and K_2O = 14.5 wt.%) and potassium hydroxide solution (5M KOH, Bdh Merck Pty. Ltd)) at room temperature. Initially, the desired amount of potassium silicate was mixed with 5M KOH and then 20 g kaolin was added and mixed for 5–30 minutes. The viscous mix was then added to a mixture of DGEBA epoxy resin and the curing agent with constant stirring for 15 min. The mixture was then placed in the Teflon coated mold and was cured at 60 ^oC for 6 hous followed by post curing at 180 ^oC for 2 hours. To fabricate filler dispersed composites, 20 g of pure kaolin was mixed with the mixture of DGEBA epoxy resin and the curing agent for 1 hour. The mix was then placed in a Teflon coated mold and was then cured at 80 ^oC for 6 hours followed by post curing at 180 ^oC for 2 hours. The sample was then cut, ground and polished for thermal, cone calorimetry and microstructure analysis. Fire performance tests including time to ignition (TTI), rate of heat release (RHR), time to reach maximum RHR, smoke density, carbon monoxide and carbon dioxide evolution and the sample mass loss were

determined by cone. The heat flux produced was 50 kW/m^2 on the specimen, which had an exposed surface of 100 × 100 mm.

The cone calorimeter provides important information on the combustion behavior of a material under ventilated conditions. Fig. 2.9 presents the rate of heat release (RHR) of unmodified DGEBA and modified DGEBA variation with time at a heat flux of 50 kW/m^2. The peak rate of heat release for DGEBA is high at around 1400 kW/m^2 after 150 seconds. However, 20% kaolin modified DGEBA has a lower peak rate of release at 1100 kW/m^2, which is significantly reduced to 21.5% compared to unmodified DGEBA. In contrast, DGEBA modified with 20% geopolymer showed a peak release rate at 702 kW/m^2, which is 47% lower than that of unmodified DGEBA. The significant rate of heat release reduction is attributed to incorporation of geopolymer.

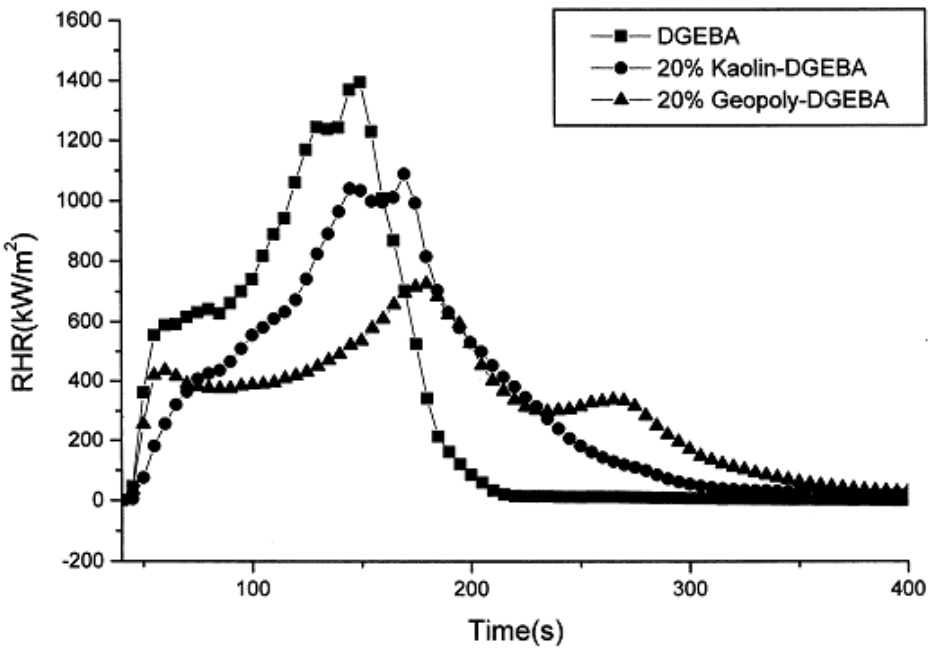

Fig. 2.9 RHR spectra of (a) DGEBA (b) 20% Geopolymer-DGEBA and (c) 20% kaolin-DGEBA variation with time [78].

Fig. 2.10 shows the smoke generation at specific extinction area (SEA) of resulting composites as a function of time. SEA measures the total obscuration area of smoke produced, divided by the totalmass loss during burning, thus measuring efficiency of a given mass of flammable volatiles converted when it burns.

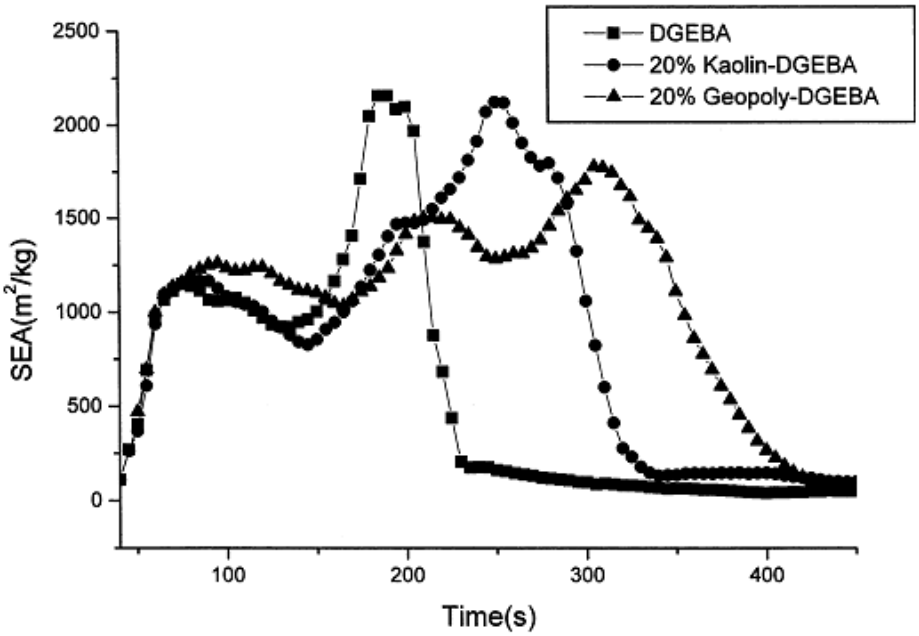

Fig. 2.10 SEA spectra of (a) DGEBA (b) 20% Geopolymer-DGEBA and (c) 20% kaolin-DGEBA variation with time [78].

The fire performance of a material can also be calculated from the fire performance index, (FPI), which is the ratio between the time of ignition (time) and the peak rate heat release (RHR). The results of fire performance of the composites are summerized in Table 2.3.

Table 2.3 Fire performance index of unmodified DGEBA and modified DGEBA system

DGEBA system	RHR	Time to ignition	FPI	Av. CO2 yield	Mass loss
	[kW/m^2]	[s]	[sm^2/kW]	[kg/kg]	[%]
DGEBA	1396	65	0.046	1.48	82.8
20% Kaolin-DGEBA	1100	69	0.062	1.99	73.9
20% Geo- polyDGEBA	735	60	0.081	1.955	74.7

In order to meet an important requirement for structural applications where a catastrophic failure during service can result in significant loss of life in, Zhao and his colleagues (2007) tried to overcome the limitations of previous works from Hammell, Balaguru et al. 1998 and 1999 by infiltrating fine stainless steel mesh with geopolymer resin. Geopolymer matrix used here has a similar composition in the open literature published by Richard E. Lyon et al. (1997) with molar ratios Si/Al = 32:1, K/Al = 7:1. Six stainless steel mesh layers (9 x 50 mm^2) were impregnated with the geopolymer resin and laid on top of each other. Vacuum-bagging technique was used and the lamination structure was pressed at ~3 MPa for 1 hour, followed by curing for overnight at room-temperature and for an additional 2 days at 80 ^oC. In some cases, 10 vol.% of Nextel 610 chopped alumina fibers was added to the geopolymer resin before casting into bars or making composites in order to improve the strength of materials. The geopolymer resin itself showed typically brittle behavior of ceramics and fractured at a flexure strain of 0.1% and a flexure strength of about 25 ±2 MPa. The resulting materials, however, show superior ductility, the steel mesh reinforced geopolymer composite yielded at the stress level of 41 ±5 MPa instead of fast fracture typical of ceramics. After yielding, the sample continued to deform but the stress only increased slowly. None of composite samples were determined to fracture lower than 1% of flexure strain. When about 10 vol.% of chopped alumina fiber, Nextel 610, was mixed into the geopolymer resin, the strength of the resulting composites reached at 56 ± 8 MPa. Moreover, the geopolymer–steel mesh composites were calcinated up to 800 ^oC for 30 minutes and 1050 ^oC for 2 hours, ‘‘yielding strength’’ of the high temperature exposed composite samples decreased to 24 ±2 MPa and 18 ±4 MPa at 800 ^oC and 1050 ^oC respectively. But the ductile behavior of composite samples maintained after high temperature treatment [79].

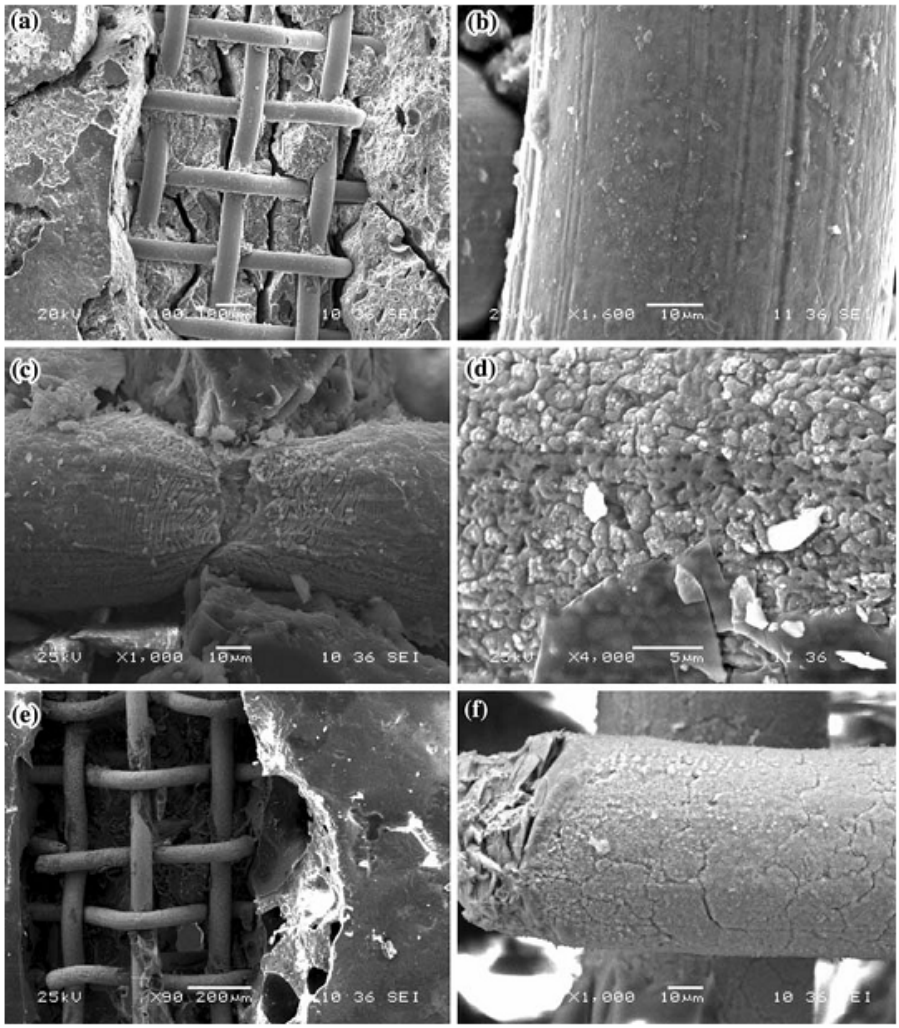

Fig. 2.11 SEM images of geopolymer–stainless steel mesh composites after 80 ^{o}C curing (a, b), 800 ^{o}C/30 min exposure (c, d), 1050 ^{o}C/2 hours (e, f) exposure and then tested under flexure conditions (left column shows the composite structure and right column shows the surface of steel mesh [79].

Christos G. Papakonstantinou et al. (2008) evaluated the compressive strength and the fire performance of two different types of syntactic foams made by embedding randomly dispersed spheres in fire-resistant polysialate matrix which was well-known in the previous publications with high ratio SiO_2/Al_2O_3 = 27/1 (Davidovits 1991; Davidovits and Davidovics 1991). The first type of foam utilized ceramic spheres with three diameter ranging: 0.25-0.50 mm, 0.50-1.50 mm, 0.50-2.80 mm and densities from 0.40 to 0.48 g/cm^3, while the second type incorporated expanded polystyrene beads (commercial name Polys Beto) with a density of 0.025 g/cm^3 and the average diameter of the beads ranged from 1 to 3 mm. These syntactic foams (cylinders) were

made with different combinations of spheres and varying matrix-to-sphere ratios (M/S) ratios and tested in uniaxial compression in the first stage. Secondly, they were subjected to the Ohio State University (OSU) heat release rate test and the NBS smoke burner test as specified by the Federal Aviation Administration (FAA). The maximum compressive stress was 6.3 MPa when the composite was fabricated with M/S ratio of 1/1.5, 80% ceramic spheres size 0.25-0.50 mm and 20% ceramic spheres size 0.50-1.50 mm , the density of this composite was about 801 kg/m^3. When the Polystyrene spheres were added to geopolymmer, the strength reduced remarkably, composite made of M/S ratio of 1/2 and 80% polystyrene spheres and 20% ceramic sphere size 0.50-2.80 mm had compression stress of 0.79 MPa and density of 333 kg/m^3. Fig 2.12 shows the typical compression stress vs strain curve of composite with M/S = 1/2 consisting 80% size 0.25-0.50 mm and 20% size 0.50-1.50 mm of ceramic spheres.

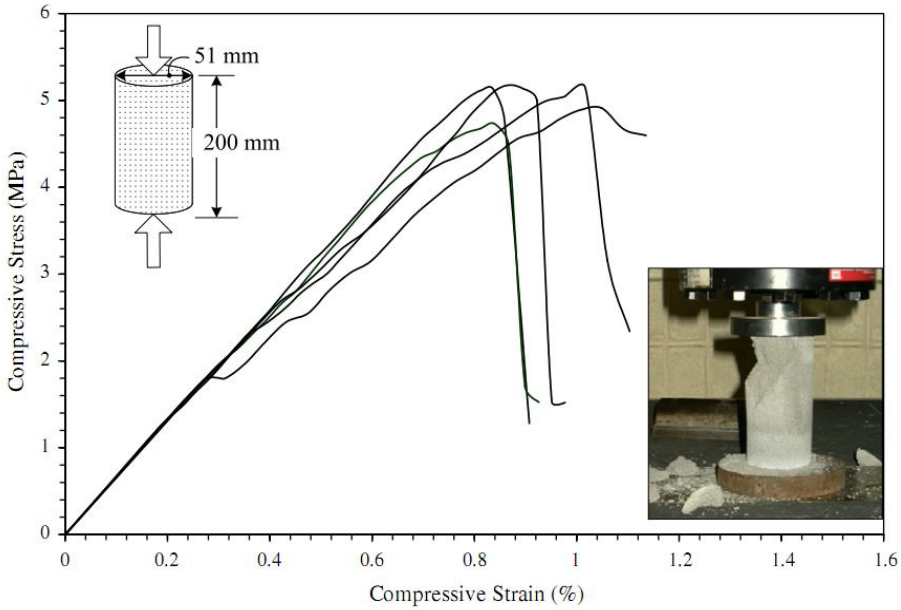

Fig 2.12 Compression stress vs strain curve of composite with M/S = 1/2 consisting 80% size 0.25-0.50 mm and 20% size 0.50-1.50 mm of ceramic spheres [80].

In term of fire behavior, the study reported that the syntactic foam specimens manufactured from the ceramic spheres were not affected by fire exposure during the tests. They exhibited remarkable stability and passed the FAA requirements for both heat release and smoke emission. The ceramic syntactic foams did not ignite when subjected to both the OSU and NBS fire tests and did not show any appreciable heat

release. Moreover, the specimens actually absorbed heat during testing. It is believed that this heat absorption phenomenon can be explained by the heat sink effect. The absorbed heat was likely used to convert the free water in the inorganic, polysialate matrix into steam. The syntactic foam, however, manufactured from the expanded polystyrene spheres exhibited flaming combustion during the OSU test, but the heat release remained below the acceptable FAA levels. It is believed that the polysialate matrix serves as an insulator, limiting the heat release and smoke emission to acceptable FAA levels.

Concerning about the mechanical behavior and fire resistance of inorganic biocomposite, Giancaspro et al. using waste sawdust as filler and reinforcement for inorganic potassium aluminosilicate binder. A very low percentage of high strength glass and carbon fiber were used to improve the strength of sawdust – geopolymer boards [50, 81]. The two major variables investigated in this study were sawdust content, 29 and 34% based on workability and compressing strength, used in the biocomposite mix and type of reinforcement, woven carbon and glass fabric 3k Woven C&G or 3k unidirectial carbon tape, used on the exterior faces of the sandwich plate. The two primary response variables included heat release rate and optical smoke density, which were measured experimentally using the Ohio State University (OSU) in accordance with ASTM test method E906 and National Bureau of Standards (NBS) Smoke Chamber test methods, respectively. The heat release rate, HRR, was calculated as a function of time, t, from the thermopile output reading, the total heat released during the first 2 and 5 min was integrated and shown on Fig 2.13. Fig 2.14 presents the specific optical smoke density versus time for NBS smoke test specimens. All specimens passed the Federal Aviation Administration requirements for heat release and smoke emission, the criteria used for evaluation of the test results in these studies. Relative to 15 other wood plastic composites that utilize organic polymers, the inorganic biocomposite showed superior heat release rates during 5 min of fire exposure [50].

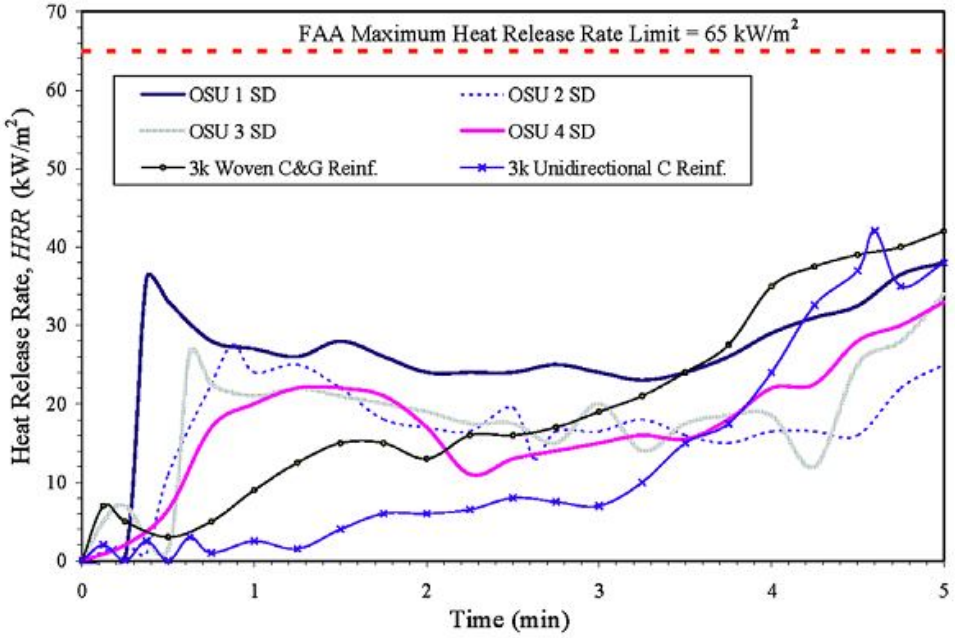

Fig. 2.13 Heat release rate versus time for OSU test specimens [50].

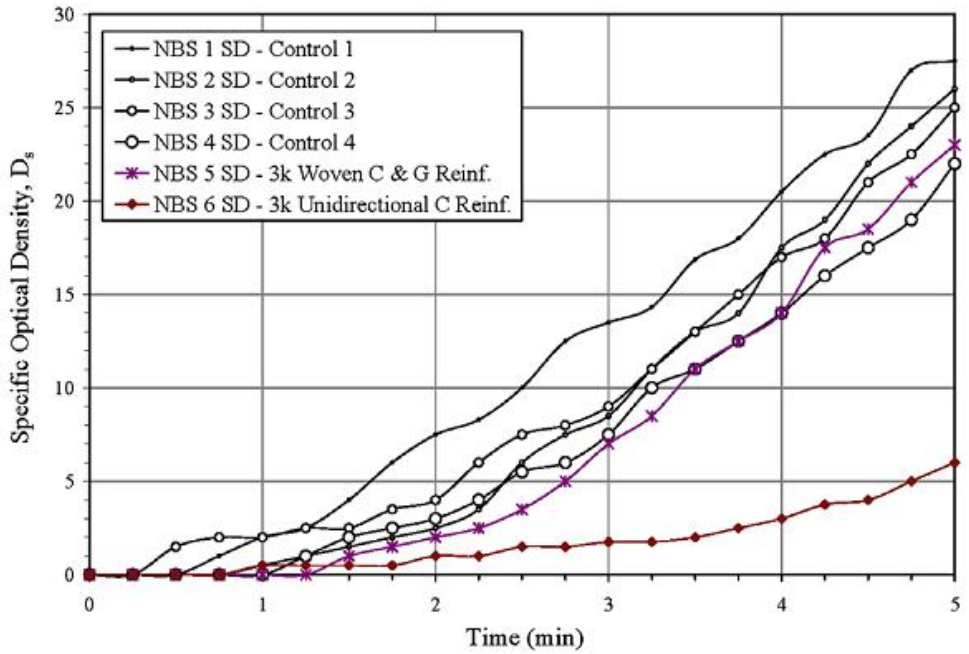

Fig. 2.14 Specific optical smoke density versus time for NBS smoke tests [50].

In the second study, the biocomposite boards were made using various proportions of sawdust ranging from about 11% to 38% by mass and two layer of fiber reinforcements utilized to strengthen these boards. The primary variables for the reinforcements were listed below:

- woven carbon and glass fabric with 3k carbon tows in the warp direction (‘‘3k Woven C&G”); reinforcements were 3k carbon tows (3000 filaments) of 234 GPa modulus;
- 3k unidirectional carbon tape (‘‘3k Uni C tape”); reinforcements were 3k carbon tows (3000 filaments) and the modulus of elasticity was 230 GPa;
- 12k high-modulus carbon tows (‘‘12k HMC tow”) consisting of 12,000 filaments per tow with a modulus of 640 GPa;
- 2k alkali-resistant glass roving (‘‘2k AR-glass roving”) consisting of 1566 filaments with a modulus of 72 GPa;
- 4k standard glass roving (‘‘4k E-glass roving”) consisting of 4000 filaments with a modulus of 72 GPa.

Both compressive and flexural specimens were prepared in a similar manner. First, the waste sawdust used for the fabrication was screened for large wood fragments (greater than 10 mm) and non-cellulose material. Once this debris was removed, the sawdust was then mixed with the appropriate amount of inorganic matrix in a high-shear mixer for one minute. The resulting mixture was then poured into wooden molds lined with one layer of non-porous Teflon fabric to facilitate easy removal of the specimen. The matrix cures in about 24 h at 20 ^{o}C but they were kept in the mold for 4 days to avoid variability in strength gain. Each test was conducted using a constant mid-span deflection rate of 2 mm/min. The load versus deflection behavior was recorded until failure was reached. From a processing standpoint, the maximum sawdust content could be increased up to 29% (with 71% inorganic matrix binder) without compromising workability and the composite has a compressive strength and modulus of 6.8 MPa and 0.64 GPa. The best flexural stiffness could be archived when 2 layer of 3k Woven C&G were used [81].

2.2.4 POTENTIAL APPLICATIONS OF GEOPOLYMER MATERIALS

Geopolymers and geocomposites thereof with outstanding properties such as quick setting, going well with all most commercial reinforcements, quite low permeability, acid resistant, high early strength, fire resistant, and fabricated at low temperature with reasonable costs have promised numerous possibilities for industrial applications. At the first stage when Davidovits and Davidovics started the development of a geopolymer matrix concept of composites. The ojective was to fabricate molding tools and patterns to replace metal tooling for small production processes in the plastic processing industry and the foundry industry; and the targeted working temperatures were in the range of 200-350 ^{o}C [8]. Later on, the demand for higher operational temperatures required better perfomances up to 800 ^{o}C from the problems of fire resistance panels for aircraft cabin interiors was addressed in the 1990's when we started the development or fire resistant, initiated by Lyon in 1994 and 1995 at the American Federal Aviation Administration (FFA) [8]. Fire resistance was considered as original application of geopolymeric materials [7]. Geopolymers are ideal for high temperature applications because, they are mineral polymers and the essence of all mineral polymers is never burn [82]. In addition, for pure matrix, fusion temperature ranging of over 800 and 1400 ^{o}C; the coefficient of thermal expansion (CTE) as low as that of ceramics (approximately $4.10^{-6}/^{o}$C) [7, 68]; time to flashover forwards to infinity [12]; thermal conductivity as low as industrial insulator material Bakelite, ranging from 0.4 to 0.6 W/(m.K); specific heat is 1.5 time higher than that of brick and as high as asbestos Bakelite, ranging 1000 to 1600 J/kg.K [3] and unpublished data from the report of the project FT-TA4/068, Departement of Material Science, Technical University of Liberec. For more examples, geopolymer composites reinforced by carbon fibers can be fabricated at low tempareture, has cost less than traditional and advanced carbon/organic and inorganic materials and perform better without any ignition, burning, or smoke and retain 63% of its initial flexuarl strength at 800 ^{o}C [12, 14].

The second potential of geopolymer is as a green cement. Ordinary Portland cement (OPC) is highest volume engineering material in used and the second human consumption after water in the world, but its production contributes 5% of anthropogenic carbon dioxide emissions [83]. OPC, used in the aggregates industries,

results from the calcination of limestone (calcium carbonate) and silica at temperature up to 1450^{o}C according to the reaction:

$$5CaCO_3 + 2SiO_2 \rightarrow (3CaO,SiO_2)(2CaO,SiO_2) + 5CO_2 \quad (2.10)$$

The production of one tone of cement directly generates 0.55 tonnes of chemical CO_2 and requires the combustion of carbon-fuel to yield an additional 0.40 tonnes of CO_2. To simplify: 1 tonne of cement = 1 tonne of CO_2 [84]. In order to combat this pollution source, geopolymers have been used either as replacements to or as additives to cement because of the similar nature and properties of these materials. About 20-30% minor reduction of CO_2 emissions may be achieved through the blending of Portland cement with replacement materials such as coal-fly ash and iron blast furnace slag [84]; The production of one ton of kaolin based-geopolymeric cement generates 0.180 tonnes of CO_2, from combustion carbon-fuel at temperature only up to about 750 ^{o}C, compared with 1 tonne of CO_2 for Portland cement, i.e. six times less. Fly ash based-geopolymeric cement emits even less CO_2, up to nine times less than Portland cement. This simply means that, in newly industrializating countries, six to nine times more cement for infrastructure and building applications might be manufactured, for the same emission of green house gas CO_2 [85, 86]. In addition, unlike conventional Portland cement, geopolymeric cements do not rely on lime and are not dissolved by acidic solutions. Portland based cements (plain and slag blended) are destroyed in acidic environment. Calcium aluminate cement is expensive to produce, and does not behave satisfactorily, having 30 to 60% of weight loss (destruction). Geopolymeric cements, Potassium-Poly(sialate-siloxo) type, Geopolymite®, remain stable with a loss in the 5-8 % range. This acid-resistant cement hardens rapidly at room temperature and provides compressive strength in the range of 20 MPa, after only 4 hours at 20 °C, when tested in accordance with the standards applied to hydraulic binder mortars (Fig. 2.15). The final 28-day compressive strength is in the range of 70-100 MPa [10].

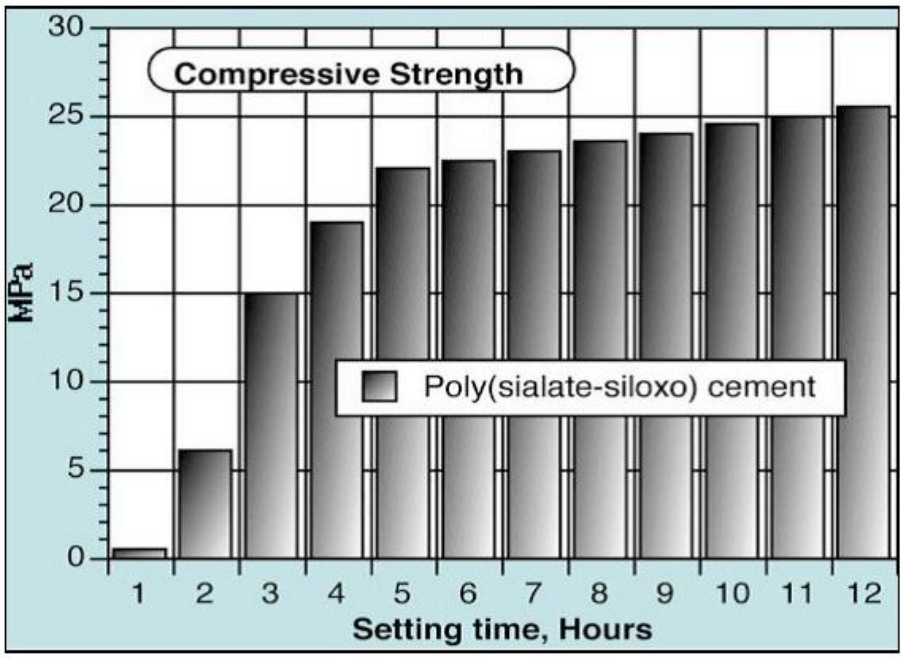

Fig 2.15 High-early strength of (K,Ca)-poly(sialate-siloxo) cement [10].

A third environmental application of geopolymers is in toxic waste management. In order to prevent interation of the hazardous contaminants from toxic wastes, such as arsenic, mercury, and lead along with other heavy metals, asbestos, and radioactive wastes, some of which are often thrown into landfills where they pose a risk to local bodies of water and agriculture [29], they must be solidified or contained within an impermeable material that will last for thousands of years. Such a product has been developed – a technology that could solve the problems of reactor entombment and some of the stubborn environmental pollutants that bother modern civilization [8]. One of the new technology is the chemistry of geopolymerization [87]. In this invention, a method for solidifying and disposing of waste is described. The waste is combined and mixed with a silico-aluminate geopolymer binder. The resulting mixture is bound together with a geopolymeric matrix. When allowed to set, it forms a hard, monolithic solid. The mixture is subjected to a suitable engineering process, such as casting or pressing, to produce a waste disposal product having superior long term stability. Several years later Van Jaarsveld et al. strongly favored the geopolymer technology for immobilising toxic metals. They determined that geopolymers are an excellent choice of construction materials whenever landfills and waste sites are being constructed and can be used as a solid basis to prevent leakages and erosions, an effective cap to

prevent rain water contamination and provide a safe cover for the purpose of building, and as interior structures to prevent wastes layers from contacting each other or dangerously shifting [29, 62].

Li et al. 2006 developed adsorbents from coal fly ash treated by a solid-state fusion method using NaOH at 250 – 350 ^{o}C. These fly ash-derived inorganic polymers, amorphous aluminosilicate geopolymers, assessed as potential adsorbents for removal of some basic dyes, methylene blue and crystal violet, from aqueous solution. The synthesised materials exhibit much higher adsorption capacity than fly ash itself and natural zeolite. The adsorption isotherm can be fitted by Langmuir and Freundlich models while the two-site Langmuir model producing the best results. It was also found that the fly ash derived geopolymeric adsorbents show higher adsorption capacity for crystal violet than methylene blue and the adsorption temperature influences the adsorption capacity and the adsorption process follows the pseudo second-order kinetics [88].

Hanzlicek et al., 2009, stated that it is possible to use the geopolymer binder as fixing and joining material in restoration of the valuable historical objects. Particular geopolymer composite was created to match the structure and color for reinforcement of the terracotta Baroque statue. The application in the cavity of the sculpture creates system of consolidating rims and ribs. Only on the unseen part of the statue, however, was used the geopolymer technique, which ensured the stability and durability of the object without disrupting the aesthetics for the viewer. The exterior modulation and final restoration was carried out using classic technologies, specifically calcite-bonding agents [89].

In conclusion, the potential application of geopolymers and composites thereof are summerized in Fig. 2.16 [7, 8, 30, 68]. The atomic ratio Si:Al in the poly(sialate) structure determines the properties and application fields. A low Si:Al ratio (1,2,3) initiates a 3D-Network that is very rigid. A high Si:Al ratio confers linear polymeric character on the geopolymeric materials.

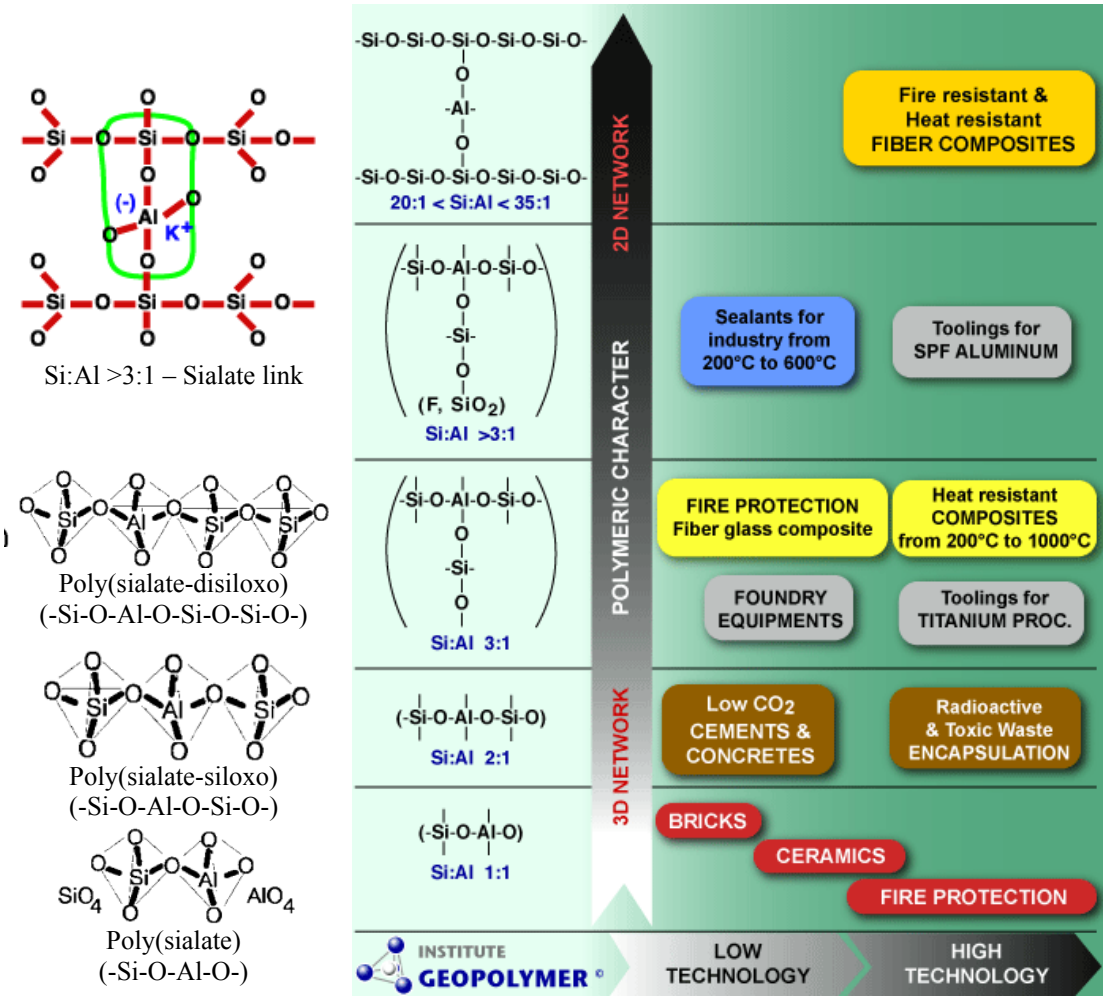

Fig 2.16 Geopolymers and potential applications [7, 8, 30, 68].

The current commercial use of geopolymers alone, compared to plastics, is limited because of the complexity of large scale processing, high density and problems with machining and molding, and most importantly, their brittleness [78].

3. EXPERIMENTAL AND RESEARCH METHODOLOGIES

Provided information in this chapter is a general overview of experimental methodologies, systhesis, conditions and equipments used, measurement and calculation methods. Some more detailed description of experiments will be accompanied with each section where appropriate. In this study, experimental methodologies can be divided into four main parts: (i) The geopolymers are synthesised by mixing an amorphous silicate-rich solid, thermal silica and an alumino-rich solid, such as metakaolin or kaolin with an activating alkaline-silicate solution which is from potassium hydroxide; some functional additives such as boric acid (H_3BO_3) or phosphoric acid (H_3PO_4) be added. (ii) Popular commercial fibers, including Carbon HTS 5631 800tex 12K and 1600tex 24K, Nippon Alkali resistance glass for pultrusion (AR-G 2500tex), Saint-Gobain alkali resistance glass (ARG 2400tex), Advanced Basalt fiber BCF13-2520-KV12 Int., Saint-Gobain Electrical grade glass (E-glass) for pultrusion and Ceramic 3M-312 fiber are evaluated in accordance with Japanese Industrial Standard (JIS R 7601) at ambient conditions before and after treatment at various high temperatures. (iii) Procedure of composite fabrication with assisting of home-made system machine which is designed based on simulating the real pultrusion or filament winding technique, Pre-pregs are set into silicon rubber molds and curing at different conditions. (iv) Mechanical properties of the resulting composites are determined on a universal testing machine under three-point bending mode in accordance with norms of composites based on polymer or ceramic matrices; adjusted “new size-independent method” is utilized. Moreover microstructures of the pure matrices and geocomposites are investigated appropriately by Scanning Electron Microscope (SEM) and Energy Dispersive X-ray Analysis (EDX) as well.

3.1 RAW MATERIALS

Geopolymer composites are fabricated based on thermal silica-based geopolymers and high stiffness reinforcement. Geopolymers as matrices, cured at room conditions or at

elevated temperature lower than 100 ^{o}C, are used not only to combine and transfer load to the reinforcements but also protect fibers from working environment, especially for carbon fibers from oxidation.

3.1.1 GEOPOLYMER RESIN

In the synthesis of geopolymer resins, there are essentially two types of raw materials, the aluminosilicate-containing solids and alkaline-silicate solutions. The aluminosilicate solids function as sols in the alkaline-silicate medium. The sol-liquid will turn into a sol-gel matrix, as a usually done in the sol-gel methodology. Aluminosilicate sources include here a silicate-rich solid, thermal silica and alumino-rich solid, such as metakaolin or kaolin. Activating alkaline-silicate solution are potassium hydroxide.

Three geopolymer resin systems, utilized in our work and abbreviated as M0, M1 and M2, are prepared according to the simplified procedure described in the patent of title Inorganic matrix compositions, composites and process of making the same [90]. As a silica source, thermal silica from Saint-Gobain - France with fine size-particle (D_{50} 0.62 μm, D_{90} 3.24 μm) containing 93.8 wt.% of SiO_2 and 2.9 wt. % of Al_2O_3 is used**.** Thermal silica is blended with 48.5 wt.% KOH and mixed for 30 minutes (used for M0), and then additional network formers, such as boric acid (H_3BO_3 for M1) and phosphoric acid (H_3PO_4 for M2), is diluted with water 1:1 by weight is admixed. Finally an alumina source, chosen from metakaolin (D_{50} 4.06 μm, D_{90} 10.36 μm, calcined shale, Czech Kaolin Company, Inc.) for M0 and M1 systems or kaolin (D_{50} 8.00 μm, D_{90} 17.26 μm, KKAF, LB MINERALS, Ltd.) for M2 system, is added and mixed untill homogeneous mixture is achieved. Details of approximate chemical composition of three used geopolymer matrices as principle elements molar ratios are showed in Table 3.1.

Table 3.1 Chemical composition of geopolymer matrices M0, M1 and M2 expressed as main principle elements atomic ratios

Matrix	**Si/Al**	**K/Al**	**K/Si**	**K/P**	**Si/P**	**K/B**	**Si/B**	**H_2O/K**
M0	11.3	3.1	0.27	-	-	-	-	5.2
M1	11.3	3.1	0.27	-	-	4.9	18.7	5.2
M2	9.7	2.5	0.24	4.2	17.5	-	-	5.2

For rough estimating of mechanical properties of bare matrix, the bars approximately 10 × 10 × 100 mm are prepared by molding, cured for 1 hour at room conditions (temperature about 20 ± 2°C and relative humidity 65%), and then cured at 85 °C for 10 hours. The sample bars are tested under three-point bending at 120, 80 and 40 mm of span; the rest samples are properly cut and tested for compression. The deflection rate of 2 mm/min is used for both tests. The microstructure of pure matrix is analyzed by means of Scanning Electron Microscope (SEM) and Energy Dispersive X-ray Analysis (EDX) as well.

3.1.2 REINFORCEMENT

Many kinds of reinforcements are now available, some special ones designed for a particular matrix system and application. In general all have high stiffness, Young's modulus as high as 450 GPa of SiC fiber; relative low density varying from 1.0 for Cellulose (flax) to 3.9 $Mg.m^{-3}$ for FP™ fiber; tensile strength ranging over 2.0 GPa for many fibers to 5.5 GPa for SiC whisker. In polymer matrix composites, carbon, glass and aramid fibers are now used extensively. Carbon fibers are also important for carbon/carbon composites. Ceramic fibers, whiskers and particles recommended for reinforcing metal and ceramic matrices [91].

3.1.2.1 UNIDIRECTIONAL FIBERS

In the first stage of research and development of new material systems, geopolymer composites, in order to research the effects of curing conditions on properties of geocomposites, unidirectional fibers (rovings) are used to offer the opportunity to test various combinations of fibres and geopolymer matrices, in addition, the results are not affected by the way of how fabrics are weaved [72]; and continuous fibers are used popularly for reinforcing structural composites [92].

Seven popular commercial fibers, such as Carbon HTS 5631 800tex 12K and HTS 5631 1600tex 24K, Nippon Alkali resistance glass for pultrusion (AR-G 2500tex), Saint-Gobain alkali resistance glass (ARG 2400tex), Advanced Basalt fiber BCF13-2520-KV12 Int., Saint-Gobain Electrical grade glass (E-glass) for pultrusion and Ceramic 3M-312 fiber are evaluated in accordance with Japanese Industrial Standard

(JIS R 7601) [93] at ambient condition before and after treatment at various high temperatures.

In order to display potential applications at high temperature, the investigation on the strength retention of the fibers is carried out. All kinds of fibers were put into the furnace at 200, 400, 700 and 1000 ^{o}C for 3 hours with a gradient of 10K/min, and then fibers were cooled in the furnace by opening the gate.

Single filament of each kind of fiber was separated with a magnifier and prepared on a punched mounting tab. The single filament test piece was bonded by adhesive so as to let the length specified gauge length under the condition to make the filament straight along the center line of the mounting tab (Fig. 3.1). This was evaluated in accordance with Japanese Industrial Standard (JIS R 7601) [93]. Tensile strength and Young's modulus were calculated from the load-elongation records and the cross-sectional area measurements.

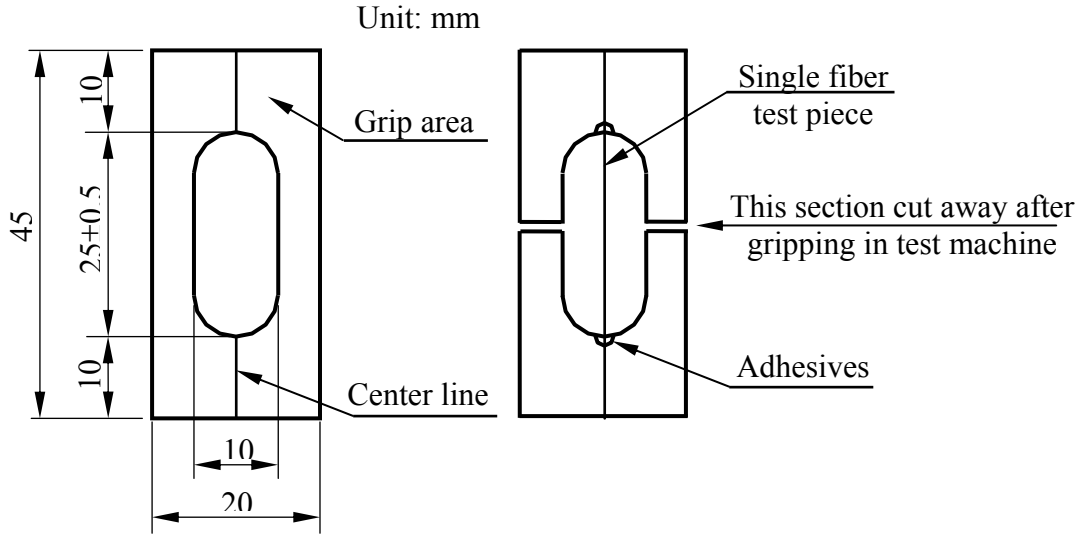

Fig. 3.1 Mounting tab for single filament fiber testing [93]

At least 10 samples were tested by the machine Instron LaborTech 2.050 (maximum load of sensor: 5 N), velocity of testing: 5 mm/min (Fig. 3.2).

Only three kinds of unidirectional fibers are chosen for reinforcing geopolymer composites: carbon HTS 5631 1600tex 24K is expected to apply at high temperature,

due to the ability of geopolymer to protect the fiber from oxidation; basalt BCF13 - 2520tex - KV12 Int. because of chemical compatibility with geopolymer, moreover basalt fiber can be consider an alternation to glass fiber [94]; and Saint-Gobain - Vetrotex E-glass E2400P192 fiber in order to achieve low cost of products.

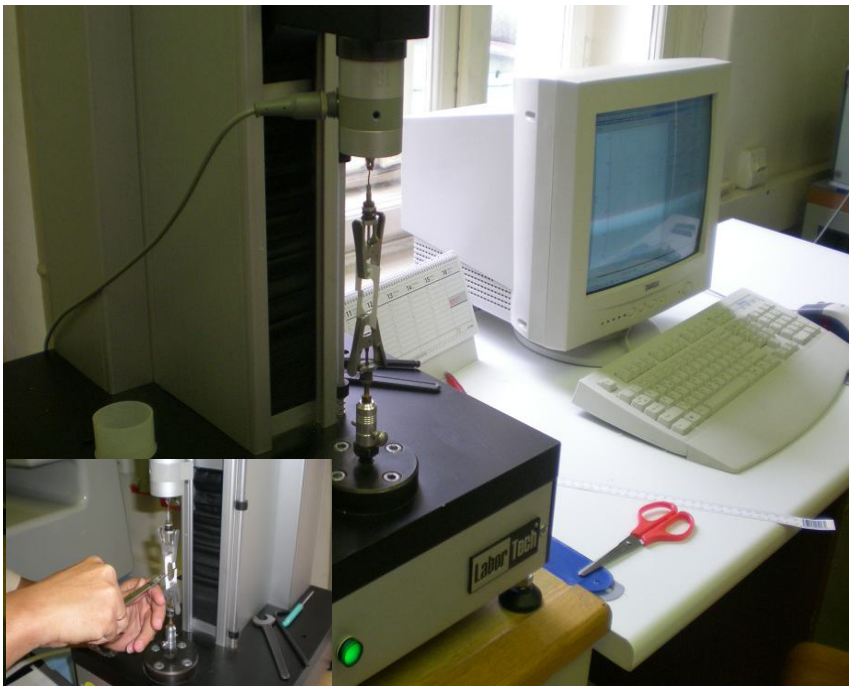

Fig. 3.2 Tensile testing machine Instron LaborTech 2.050, TUL.

3.1.2.2 FABRIC FIBERS

In order to approach more potential industry applications, some kinds of fabrics are used as the preliminary combinations of geopolymeric matrices with fabrics to form laminates of geocomposites.

Table 3.2 Kinds of used fabric fibers

Number	Fiber type	Weaving	Density [g/m^2]
F1	Carbon HTS fiber (type 442 - Tenax)	twill	160
F2	Spaceglass 280 (Tenax)	twill	280

3.2 FABRICATION OF GEOPOLYMER COMPOSITES

3.2.1 PULTRUSION TECHNIQUE

Uniderectional fibers are selected to reinforce geopolymer matrix systems and according to Davidovits the manufacture of geopolymer composites could be follows the well developed process and methods for organic matrices, namely: hand lay-up impregnation; prepregs; vacuum bagging; resin transfer molding (RTM); injection (infusion) molding; chopped fiber and pultrusion or filament winding [8]. The pultrusion or filament winding is selected method, in this work, for impregnating nearly constant amount of geopolymer resin into a same kind of roving fibers, in other words, the proportion of fiber and matrix in the same composite is unchanged.

Pultrusion is a well known technique for forming composite structures. In general, pultrusion involves the steps of unwinding a plurality of nearly all endless reinforcements, collating the reinforcements into a layered arrangement, wetting and/or saturating the reinforcements with a sufficient pot life resin, and transporting the layered arrangement through a pultrusion die wherein the cross-sectional shape is formed and the resin cured. Pultrusion technique is also known in the art to involve forming a laminate comprising a multiplicity of reinforcements, introducing a resin to the multiplicity of reinforcements, forming the laminate into a desired shape and curing, also known as converting, the resin thereby creating a cured laminate structure [95, 96].

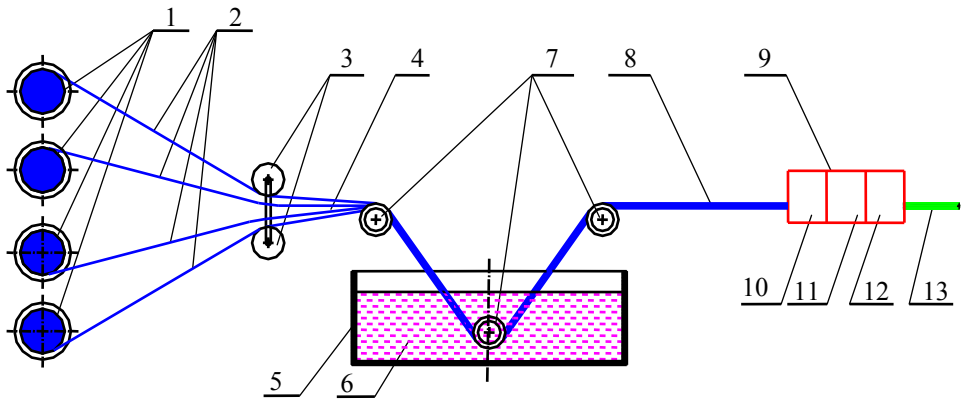

Fig. 3.3 Schematic representation of a pultrusion machine [96]

Pultrusion method is described in more detail with reference to Fig 3.3, including:

1 – roving spools
2 – multiplicity of reinforcements
3 – comprises bars or guides
4 – formed bundle
5 – resin chamber
6 – resin
7 – guide bars
8 – wetted elongated bundle
9 – pultrusion die
10 – forming die
11 – curing section
12 – optional cooling section
13 – composite structure

To simplify the procedure for laboratory scale of composite investigation, we introduced the illustration of pre-preg manufacturing process as Fig. 3.4 and from this schematic representation the home-made impregnation machine is designed and manufactured by ourselves, see Fig. 3.5.

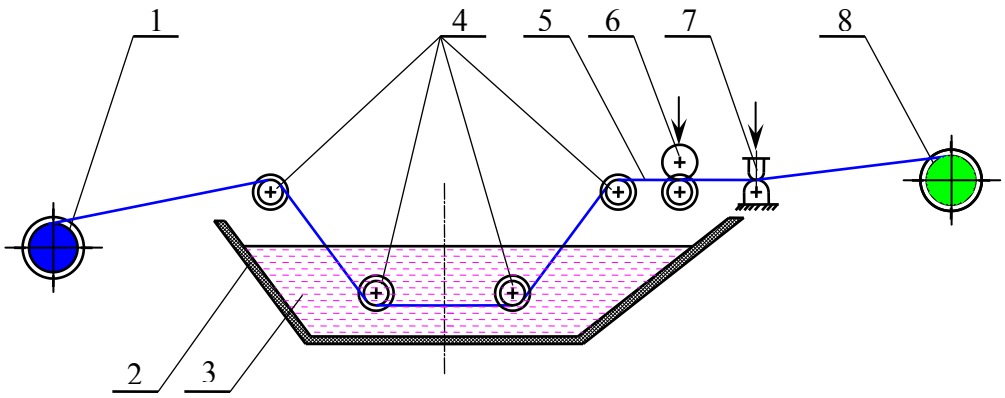

Fig. 3.4 Simplified illustration of a pultrusion machine.

1 – roving spool of fiber reinforcement
2 – resin chamber
3 – geopolymer resin
4 – guide bars
5 – wetted elongated bundle
6 – guide and spare resin discarded rollers
7 – guide and spare resin discarded bars
8 – collected reel of saturated fibers

The collected reel of saturated fibers was designed with diameter of 48 mm to ensure that the circumference of it is approximately 150 mm. This roller is driven by a controlled electric motor inverter with 10 velocity grades, which means the velocity of fiber through resin bath or resin chamber can be adjusted from about 10 to 40 meter

per hour. This designation permits us to choose the velocity for good impregnation of resin into the fibers.

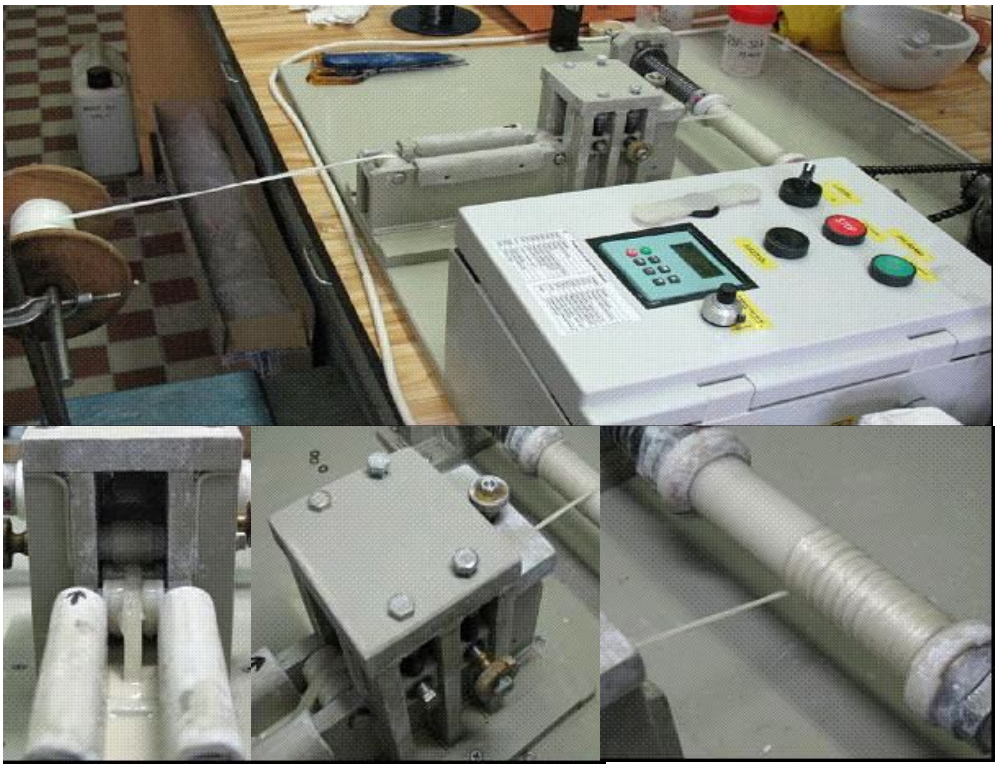

Fig. 3.5 Home-made pultrusion machine, TUL-KMT.

3.2.2 PREPARATION OF GEOCOMPOSITE SAMPLES

Geopolymer composites reinforced by unidirectional fibers were prepared by a three-stage procedure. At first, a roving was impregnated with geopolymer resin in a lab-scale home-made pultrusion or impregnation machine showed on Fig. 3.5. This equipment was designed based on simulating the real pultrusion or filament winding technique. The velocity of the fibers during impregnation process is chosen based on the best penetration of geopolymer resin into the fibers, this value is around 34 m/h. Roving fibers are wetted with resin in the bath, then the rest of the resin removed between two rotated rollers, and finally with a rubber scratcher as spare resin discarded bars. Impregnated fibers with suitable resin content are taken up on the collected reel. By finally cutting the coil to the reel length, approx. 20 pieces of pre-pregs with the same length are obtained.

Secondly, the impregnated fibers (pre-pregs) are rolled manually to achieve the desired width, and stratified layer by layer into a silicon rubber mould (Fig. 3.6). In the case of carbon roving HTS 5631 1600tex 24K, 16 layers of pre-pregs are utilized to prepare a sample; 18 layers of pre-pregs of basalt roving BCF13 - 2520tex - KV12 Int. or 20 layers of Saint-Gobain - Vetrotex E-glass E2400P192 for a sample with dimensions approximately 3x9x150 mm, respectively.

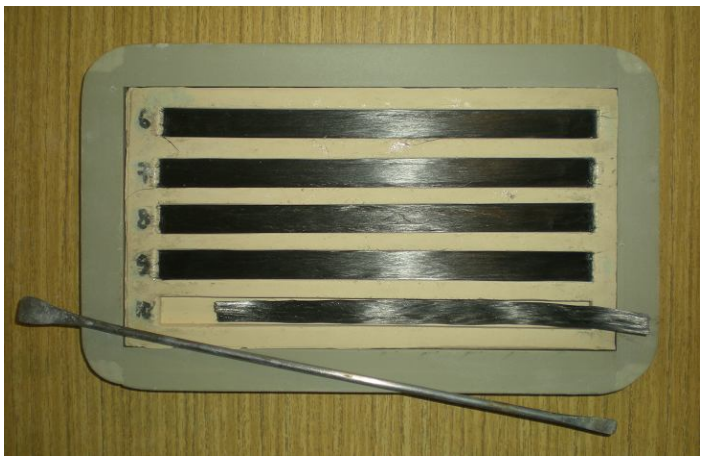

Fig. 3.6 Rubber silicon mould for sample making.

The mould with pre-pregs is covered by a peel ply fabric and suction tissue then installed into a sealed polyethylene bag under vacuum bagging technique [4] (Fig. 3.7), and left at room temperature for 1 hour, followed by desired curing time at desired elevated temperature in a oven. Most of our experiments, a membrane vacuum pump N810.3FT.18 (KNF) with capacity: 10 litter/min. and low vacuum pressure: 100 kPa (also called rough vacuum or coarse vacuum) is used.

In the third stage, after cooling, the composite coupons are dried for 5 hours more with open air in the oven at the same temperature of previous step.

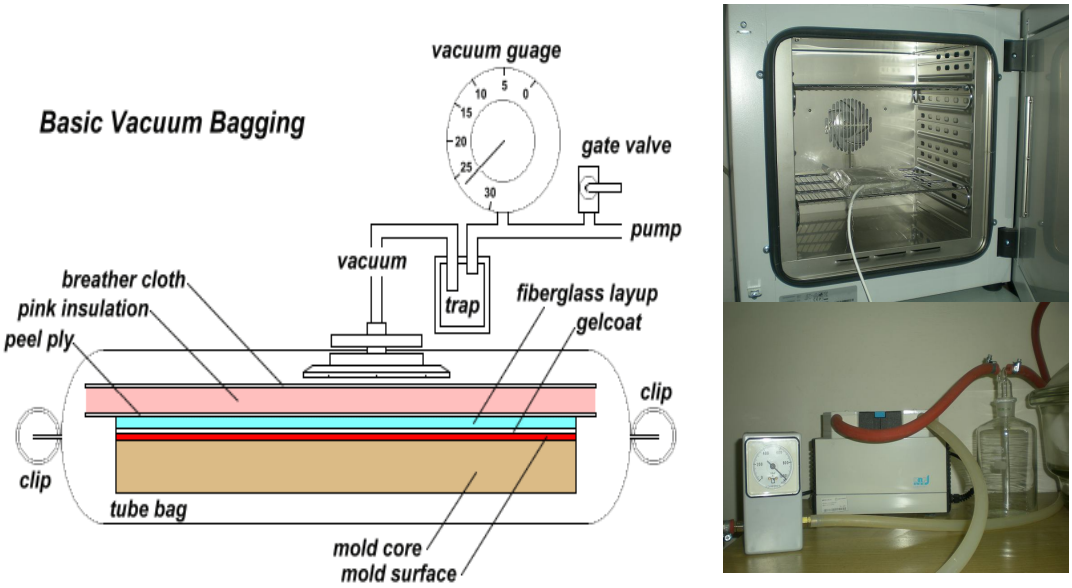

Fig. 3.7 Vacuum bagging technique [4, 97].

In case of curing the composites at ambient condition, the samples are took out of vacuum bag after 1 hour and kept in room conditions for desired time.

During all preparing and curing process the samples were weighted to calculate the weight percentage of fibers content in impregnated, uncured, cured and dried composites.

3.3 CHARACTERIZATION OF GEOPOLYMER COMPOSITES

3.3.1 TESTING OF MECHANICAL PROPERTIES

All samples prepared for mechanical properties are tested on Universal Testing Machine INSTRON Model 4202 (maximum load of the sensor: 10 kN) (Fig. 3.8) at ambient condition temperature about 20 ±2^{o}C and relative humidity 65%.

Generally, a series of five samples for flexural tests are prepared and conducted over at least at 2 or 3 outer support span-to-depth ratios L/H = 16 to 1, 20 to 1 and 40 to 1, equivalent to three simply supported span of 50, 64 and 120 mm in accordance with Standard Test Method for Flexural Properties of Continuous Fiber-Reinforced Advanced Ceramic Composites – ASTM C 1341 – 06 or DIN V ENV 658-3:1993-02: Advanced Technical Ceramics – Mechanical properties of ceramic composites at room temperature – Part 3: Determination of flexural strength (nearly the same as British

Standard for Fiber-reinforced plastic composites – Determination of flexural properties - BS EN ISO 14125:1998, for glass-fiber systems L/H = 20 to 1 and for carbon-fiber systems L/H = 40 to 1). The resulted composites possess, however, different and better properties than traditional composites; use of standards organic-matrix or ceramic matrix fiber composites are inefficient, therefore geopolymer composite materials require a more exact description of their mechanical properties [98].

Fig. 3.8 Universal Testing Machine - Instron Model 4202, TUL-KMT.

3.3.2 EVALUATION METHOD

Geocomposites are novel construction materials, which combine excellent mechanical properties of reinforcing fibers with appreciable stiffness of geopolymer matrix (resin). The composites are distinguished by comparably low density and appreciable fire-safety. Testing segments of these materials can be manufactured, similarly to most common ones with plastic matrix, by pultrusion technique: pulling fibers through a bath of liquid geopolymer matrix, and by final hardening (curing).

Elasticity and strength are the most relevant mechanical properties of these high-tech construction materials. These properties are generally tested in all types of composites by applying bending load. This is typical because of a common manner of construction loading. In comparison with tensile testing more generally with brittle matrix, it also eliminates specific difficulties with gripping of test specimens. It is much more important, especially for research and development, to confront with the existing standards of testing, proposed for ceramic composites, with the phenomena really observed with this type of geopolymer matrix. For this comparison we have exploited the American norm: Standard Test Method for Flexural Properties of Continuous Fiber-Reinforced Advanced Ceramic Composites – ASTM C 1341 – 06 [99]; the European norm from the ceramic group: Advanced Technical Ceramics – Mechanical properties of ceramic composites at room temperature – Part 3: Determination of flexural strength DIN V ENV 658-3:1993-02 [100], and the European standards from the plastic group Fiber-reinforced plastic composites - Determination of flexural properties, BS IN ISO 14125:1998 [101]. The results of testing are always presented with standard deviations denoted by error abscises.

Because geopolymer composites possess like-ceramic properties, so it would seem natural if the tests would be conducted and evaluated according to the ceramic standards. Experimental findings show, however, that these standards cannot be applied with this type of material indiscriminately. In most cases, the specific properties of brittle geopolymer matrix in connection with strong fibers, together with a characteristic high volume content of the fibers round 50 %, lead to such a failure of tested specimen, where the outer layers of fibers do rarely break. The testing bar fails rather by delamination accompanied with creating kink - swerving out in the compression part of the profile. The American standard ASTM C 1341 – 06 turns

down testing of any materials that do not break or fail by tension or compression in the outer fibers, the European standard claims a similar restriction. Note that none of these "ceramic" standards considers explicitly the calculation of elasticity modulus, nor allows using the flexural strength, as being found, for design purposes. In addition, the resulted composites possess different and better properties than traditional composites, use of standards organic-matrix or ceramic matrix fiber composites may be inefficient, therefore geopolymer composite materials require a more exact description of their mechanical properties [98].

Both of these standards require sufficiently long rectangular beams as specimens. For three-point tests, outer support span-to-height ratio ≥16 or 20 should be used. The proclaimed target is eliminating shear as an influential factor; other methods are recommended for the evaluation of the latter. The ASTM C 1341 – 06 takes such a complex behavior into consideration, and higher ratios (as proposed 32, 40, or 60) should be chosen to avoid typical shear failure patterns. The last guideline indicates of DIN V ENV 658-3:1993-02, however, that in testing of ceramic composites the influence of shear should never be indiscriminately neglected. In fact, one cannot easily forecast when shear comes into effect.

It appeared in our work on testing of unidirectional fiber reinforced geocomposites that the influence of shear was never insignificant. Conversely, full evaluation similar to that applied for plastic composites may provide better scope over the tested material.

3.3.2.1 THEORY OF NEW OPTIONAL CALCULATION METHOD

(1) Elasticity

The European standard BS EN ISO 14125 is aimed at testing of plastic composite material as such, so the rectangular beams of recommended dimensions are required. The test results are not declared as physical definitions but only effective quantities, applicable for comparison under invariant test conditions. An effective modulus E (originally written as E_f) is considered as a measure of elasticity. It is evaluated from force-deflexion curve, for three-point bending in terms of Equation (3-1) that is fully valid only for isotropic materials (with high shear modulus)

$$E = \frac{L^3}{4.B.H^3} \times \frac{\Delta F}{\Delta s} \qquad (3\text{-}1)$$

where L is the span of supports, B is width, and H is height of the profile. F is the force that loads rectangular beam specimen in the center of span; s is deflection. Modulus E should be generally lower than the classical Young's modulus E^*, because a simple evaluation does not allow for tangential strain caused by shear stress. As the force-deflection curve may not be linear over the whole extent, the boundaries of deflections are appointed, wherein the slope $\Delta s/\Delta F$ is evaluated, as s/L = 1/200 and s/L = 1/500. On the contrary, in the standard Plastic composites reinforced with fibers – Determination of effective interlaminar shear strength by short beam method EN ISO 14130, tangent of the steepest straight-line portion of a force-deflection curve is used instead of $\Delta F/\Delta s$ in Equation (3-1) [102].

The obtained E values can be further treated. With plastic composites, correction has been introduced by the normative part of standard Reinforced plastics composites - Specifications for pultruded profiles - Method of test and general requirements [103] that should purge resulting effective elasticity modulus E^* from the influence of shear. The correction factor k having a constant value k = 0.05 appears in the equation

$$E^* = (1+k)\cdot E \tag{3-2}$$

where E is calculated by Equation (3-1). Only the informative part of the standard EN 13706-2 2002 extends the evaluation to shear property, where shear modulus (under tangential component of stress in the plane perpendicular to load direction) is defined. The proposed calculation is based theoretically on the works of Tarnopolsky [104-106] which are presented a thorough survey in the field of plastic composites. The basic assumption is the additivity of effective deflection s that is composed from two contributions, s_{Rmo} caused by normal stress, and s_τ caused by tangential stress. The theory provides formulas for the superposition

$$s = s_{Rmo} + s_\tau = \frac{F\cdot L^3}{4\cdot E^*\cdot B\cdot H^3} + \frac{\alpha\cdot F\cdot L}{G\cdot B\cdot H} = \frac{F\cdot L^3}{4\cdot E^*\cdot B\cdot H^3}\left[1+\alpha\cdot\left(\frac{H}{L}\right)^2\frac{E^*}{G}\right] \tag{3-3}$$

Here E^* is a virtual elasticity modulus; α is another correction factor depended on the specimen profile. In the monograph [106], a ratio of virtual to effective modules E^*/E is presented as a function of coefficient of anisotropy κ, which is further defined as

$$\kappa = \frac{\pi}{2}\frac{H}{L}\left(\frac{E^*}{G}\right)^{1/2} \tag{3-4}$$

Based on theoretical considerations of Tarnopolsky [105], the mentioned ratio acquires the resulting shape for rectangular profiles

$$\frac{E^*}{E} = \frac{\kappa^2}{3}\left(\frac{\tanh(\kappa)}{\kappa - \tanh(\kappa)} + \frac{\pi^2}{8}\right) \tag{3-5}$$

The expression on the right side of (3-5) is almost linear function of κ^2, which for $\kappa^2 < 4.5$ gives

$$\frac{E^*}{E} \cong 1 + 0.4761 \cdot \kappa^2 \tag{3-6}$$

within an error max 1 %. From Equations (3-1), (3-2) and (3-5) follows $\alpha = 0.4761 \times \pi^2/4 = 1.1747$. In another practically aimed publication, Tarnopolsky (1969) rounds up to $\alpha = 1.2$ [105]. The difference plays a very small role; we have kept to 1.175 in all of our evaluations.

The correction factor k in (3-2) can then be expressed as

$$k = \alpha\left(\frac{H}{L}\right)^2 \frac{E^*}{G} \tag{3-7}$$

which means that it is in fact both size and material dependent. The method using a constant correction factor *k,* recommended in the normative part of the standard EN 13706-2, cannot be therefore generally applied.

Virtual modulus E^* can be evaluated easily by a test arrangement recommended further in the informative part of EN 13706-2 [103]. It is necessary to use two or better several specimen sizes, differentiated by height-to-span ratios H/L. The effective values E are evaluated on the base of Equation (3-1), but they are now plotted as 1/E vs. $(H/L)^2$. The values of the virtual modulus E^* can be obtained by linear regression, where

$$E^* \cong 1/(1/E)_{(H/L)^2 \to 0} \tag{3-8}$$

The standard EN ISO 14125 defines “interlamellar shear modulus”, but does not bring in any method for its evaluation or interpretation [107]. The standard already does,

though the resulting value of shear modulus is again called effective [103]. From the differentiated theoretical expression (3-3) it is obvious that virtual shear modulus G is easily obtainable from the slope of the same linear regression as described above

$$G \cong \alpha \Big/ \frac{d(1/E)}{d(H/L)^2} \tag{3-9}$$

The ratio of the virtual and effective values of G is expressed just by the coefficient α. The introduction of this coefficient for calculation of genuine values of G according to Equation (3-9) is, in our opinion, fully qualified even for ceramic composites, and we have used it regularly.

Closer examination of the value of correction factor $k = 0.05$ in the standard EN 13706-2 shows that it is acceptable only for specifically coordinated composite properties and specimens dimensions [103]. From Equation (3-6) we find out that for keeping normative value 0.05 in accordance with theory, it is necessary that the complex $(H/L)^2 \times E^*/G$ should amount to 0.0426. With $L/H = 20$ it is fulfilled if $E^*/G=17$, which can be approximately correct for Class III in standard EN ISO 14125 (plastics reinforced, for example, with unidirectional glass fibers) and For the Class IV (plastics reinforced for example with such carbon fibers) with recommended $L/H = 40$ for this class it corresponds to $E^*/G = 68$ [107]. These values seem about at the lower end of actual values with geopolymer unidirectional fiber composites, as it will be documented later.

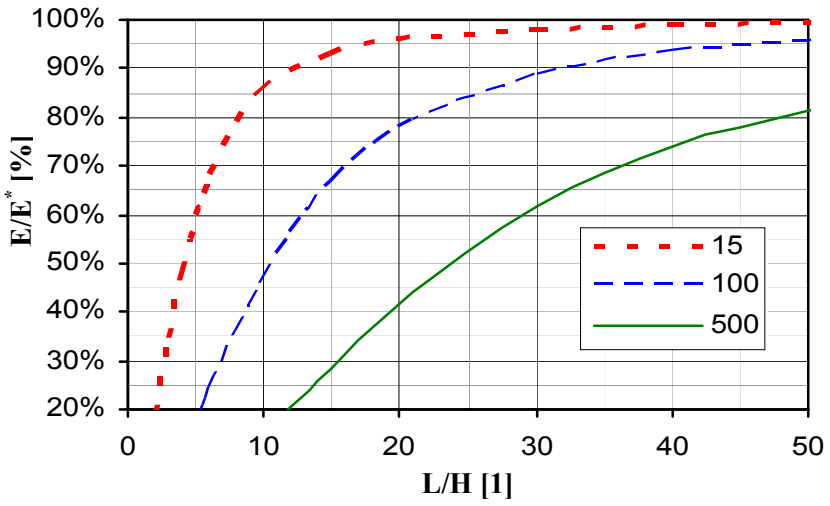

Fig. 3.9 Ratio of the effective value E to the virtual value E^*; ratios E^*/G in the legend.

Fig. 3.9 shows that the effective values E in geopolymer composites can be significantly lower then virtual modules E^* even at long specimens; the impact is the greater the higher is E^*/G value.

An analogical plot in the standard EN 13706-2 has been proposed as exemplary. Unfortunately, without mentioning the fact of having been constructed for specific E^*/G and L/H, it evokes the idea of general validity. Still worse would be mere application of Equation (3-2); in Fig. 3.9 it would be represented by a single 95% value of E/E^*.

(2) Strength

Similar to elasticity, flexural strength in composites is also generally influenced by shear stress. Ratio between normal and tangential stresses controls the mode of the specimen failure, and therefore determines the measured maximum force F_m. Theoretical analysis shows a more complicated pattern of stress dislocation across the specimen composed of typically non-isotropic material. The inhomogeneity of geopolymer composites is further largely influenced by minor irregularities in the preparation process, which causes considerable scatter of results.

All of the standards [99, 100, 102, 103, 107] describe the primary evaluation of effective flexural strength R_{mo}, as calculated from the maximum force F_m according to the relation valid for isotropic materials. For rectangular profiles and three-point bending, the basic formula reads

$$R_{mo} = \frac{3}{2}\frac{F_m \cdot L}{B \cdot H^2} \tag{3-10}$$

Tarnopolsky's work presented an analysis of the strength parameters of plastic composites in the quoted publications. With a certain analogy to the formulation of the influence of shear on elasticity, he defined also effective shear strength τ_m that is, however, fully bonded to flexural strength

$$\tau_m = \frac{3}{4}\frac{F_m}{B \cdot H} = \frac{1}{2}\frac{H}{L}R_{mo} \tag{3-11}$$

Just like with elastic phenomena, the strength analysis reflects the influence of the specimen sizes on R_{mo}. In order to find virtual flexural strength R^*_{mo} as a maximum normal stress, Tarnopolsky (1969) derived the relations analogical to Equation (3-5),

in terms of which these stresses R^*_{mo} (and τ^*_m) can be calculated from effective values as a function of anisotropy coefficient κ. Theoretically based Equations (3-12) and (3-13) were proposed as the first three terms of power expansions

$$\frac{R^*_{mo}}{R_{mo}} = 1 + \frac{1}{15}\kappa^2 - \frac{1}{525}\kappa^4 \tag{3-12}$$

and $$\frac{\tau^*_m}{\tau_m} = 1 - \frac{1}{60}\kappa^2 + \frac{1}{12600}\kappa^4 \tag{3-13}$$

The first of these equations has primary significance, because it justifies the method of extraction of virtual flexural strength R^*_{mo} as a size independent quantity. After substituting κ from Equation (3-4), Equation (3-12) acquires the form

$$\frac{1}{R_{mo}} = \frac{1}{R^*_{mo}} + \frac{\pi^2}{60}\frac{E^*}{G}\frac{1}{R^*_{mo}}\left(\frac{H}{L}\right)^2 - \frac{\pi^4}{8400}\left(\frac{E^*}{G}\right)^4 \frac{1}{R^*_{mo}}\left(\frac{H}{L}\right)^4 \tag{3-14}$$

The dependence R^*_{mo}/R_{mo} ratio vs. $(H/L)^2$ according to Equation (3-14) is illustrated in Fig. 3.10.

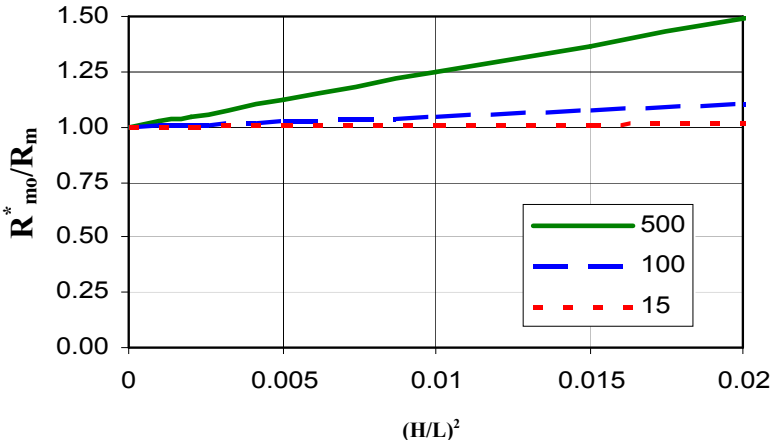

Fig. 3.10 Dependences of R*mo/Rmo ratios at different E*/G (in the legend).

Generally, a non-linear regression $1/R_{mo}$ vs. $(H/L)^2$ over the test data would provide parameters R^*_{mo} and E^*/G. The last term of expansion Equation (3-14) is, however, relatively small at not too big $(H/L)^2$ values; declination from linearity not exceeding 5% for $L/H = 4.5$ at $E^*/G = 15$, for $L/H = 12$ at $E^*/G = 1100$, resp. for $L/H = 20$ at $E^*/G = 1300$. Even those declinations could have been lower if further terms (with

alternating sign) would be included. Considering additionally natural scatter, the curvature of regression line could be in the first approximation neglected. The analysis thus shows that the application of the same pattern of straight-line regression as applied for elasticity is elementary justified even for strength. Reciprocal regression intercept

$$R_{mo}^{*} \cong 1/\left(1/R_{mo}\right)_{(H/L)^2 \to 0} \tag{3-15}$$

should be similarly independent of size.

The way, described above, to evaluate the mechanical properties of geocomposites is contemporarily called “size-independent method” for future presentation.

3.3.3 MICROSTRUCTURE OF GEOCOMPOSITES

In order to estimate not only the adhesion between geopolymer matrices and fiber reinforcement but also the microstructure of the composites, the sections perpendicular to fibers and surfaces of composite of the composites are inspected by scanning electron microscope (SEM) and Energy Dispersive X-ray Analysis (EDX) by the author on TESCAN VEGA 3XM microscope (Fig. 3.11). The failure patterns in samples and stress vs strain curves are investigated to study about behaviour of the composites at bending conditions as well.

Fig. 3.11 TESCAN VEGA 3XM Microscope, TUL.

4. PROPERTIES OF INITIAL MATERIALS OF GEOCOMPOSITES

4.1 INTROCDUCTION

In this chapter, essential properties of thermal silica based geopolymer matrices and fiber reinforcements which considered as initial materials for geocomposites are presented. The pure geopolymers based on thermal silica possess quite homogeneous microstructure with good distribution of chemical elements. With SEM images, many micro-cracks are determined in cured matrices as natural defects of inorganic matrix and unreacted particles. However, they show relative low density and good mechanical properties around at the top of the results of previous studies, while making procedures seem easier. In addition, the properties of commercial fibers evaluated at real conditions and after high temperature exposing are exhibited as well.

4.2 PROPERTIES OF GEOPOLYMER MATRIX

4.2.1 MICROSTRUCTURE OF GEOPOLYMER

Scanning Electron Microscope (SEM) images of geopolymer matrices and EDX mapping of individual elements are depicted on Fig. 4.1, 4.2 and on Appendix A, Fig. A.1 and A.2. There is obvious evidence of spherical, unreacted particles of thermal silica presented. This phenomenon was determined in the previous studies [108]. Moreover, it can be seen from Fig. 4.1b and Fig. 4.2 that there are a lot of micro-cracks in side the geopolymer matrix with the maximal width ranging around 5 μm of M1 matrix and that of approximately 2 μm of M2 system. The length of the micro-cracks may sketch for hundreds of micrometers. The micro-cracks are determined as inborn defects of inorganic matrix.

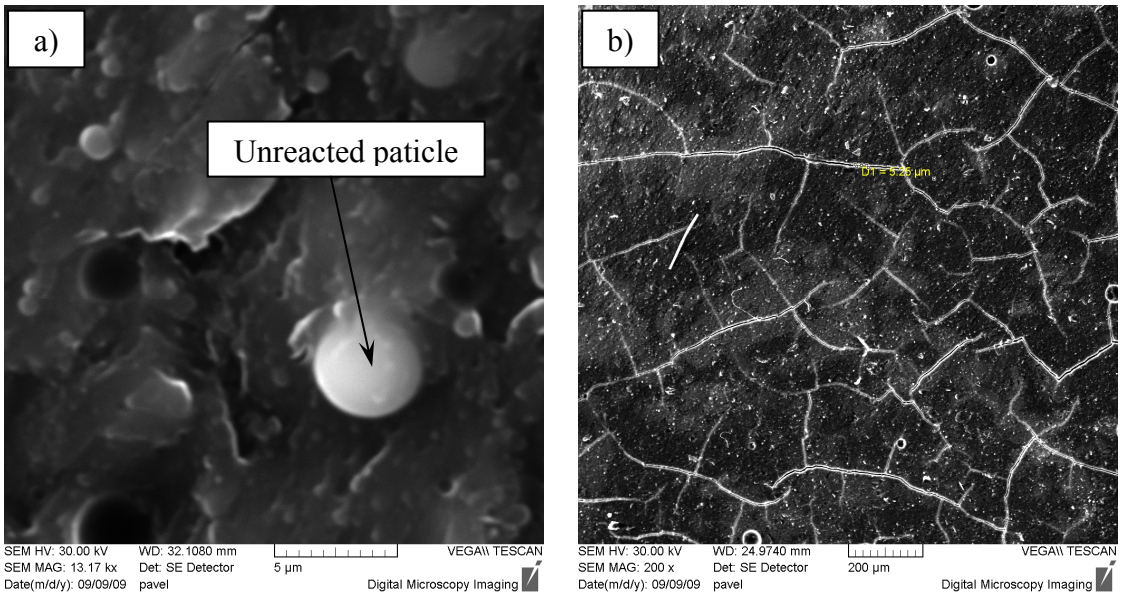

Fig. 4.1 SEM images of unpolished surface of geopolymer composite matrix M1 at magnification a) 13170x and b) 200x.

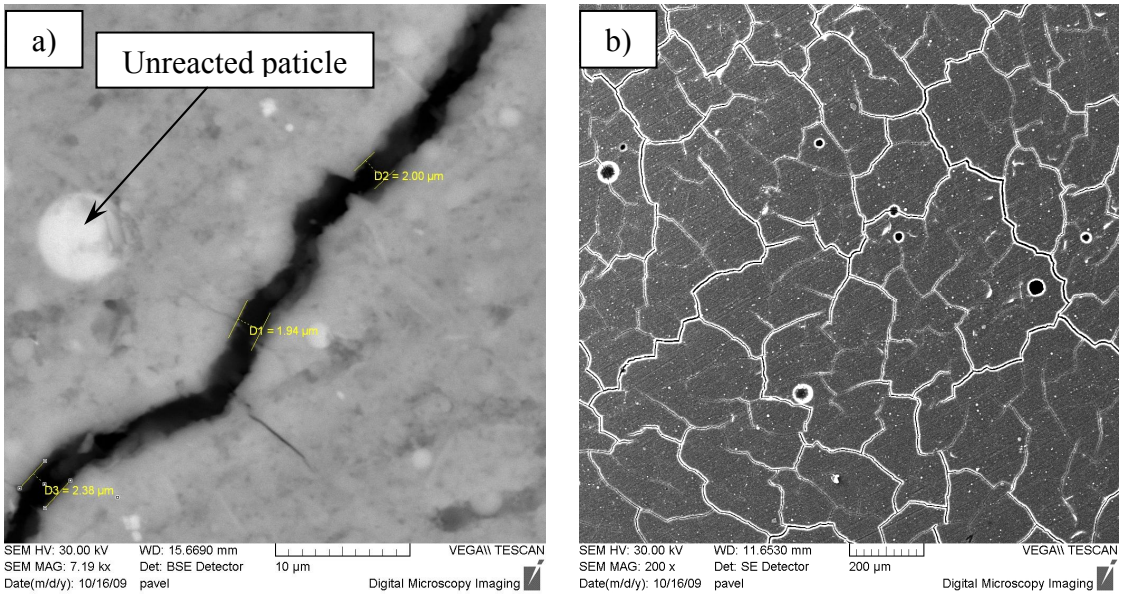

Fig. 4.2 SEM images of polished surface of geopolymer composite matrix M2 at magnification a) 7190x, b) 200x.

From the Energy Dispersive X-ray Analysis (EDX) measurement in a area approximately 512 x 512 μm, it can be seen that the distribution of all main elements is rather homogeneous in this area. However, there are high inhomogeneity of the matrix in size up to tens of micrometers surrounding the area of unreacted particles of thermal silica, especially for M2 system (see Appendix A, Fig A.1 and Fig A.2).

4.2.2 MECHANICAL PROPERTIES

As can be seen from Table 4.1 that after one hour cured at room conditions, approximately 0.3 wt.% of water is removed out and after curing and drying the weight shrinkage of all geopolymer matrices varies in a narrow range of about 8 and 10 wt.%. These materials present quite low density, ranging approximately around 2.20 Mg m^{-3}, in comparision with traditional materials. However, without aggregates or reinforcements the bulk volume shrinkage of pure geopolymer matrix is quite hight, from about from 15 % for thermal silica based geopolymer with aluminum source of kaolin (M2) to 17 % for the matrix with aluminum source of metakaolin. High volume shrinkage usually accompany with micro-crack generation, this is a quite considerable factor should be concerned when utilizing the bare matrices as thin layers.

Table 4.1 Some physical properties of pure geopolymer matrix

Matrix	**Removed water [wt.%]**		**Density [Mg m^{-3}]**	**Bulk volume shrinkage [%]**
	After 1 hour	**After drying**		
M0	0.3	10	2.20 ±0.05	18.5 ±0.7
M1	0.3	10	2.18 ±0.05	16.6 ±1.5
M2	0.3	8	2.14 ±0.05	15.5 ±0.8

Table 4.2 presents the flexural properties of geopolymer in accordance with different spans of testing. We can see that the properties are dependent on the used span for testing. Because there are a lot of micro-cracks in side the matrices, so when testing at high span it seem there are more changes for fracture, some samples are not broken at the middle. At lower spans, the matrices show nearly the same strength but very different modulus (see Table 4.2).

Table 4.2 Flexural properties of pure geopolymer matrix at different spans

Matrix	Span of testing								
	40 mm			80 mm			120 mm		
	R_{mo} [MPa]	E [GPa]	ε_{mo} [%]	R_{mo} [MPa]	E [GPa]	ε_{mo} [%]	R_{mo} [MPa]	E [GPa]	ε_{mo} [%]
M1	26.3	5.4	0.84	27.8	18.5	0.44	16.6	25.7	0.16
M2	16.6	9.0	0.19	17.6	18.8	0.35	-	-	-

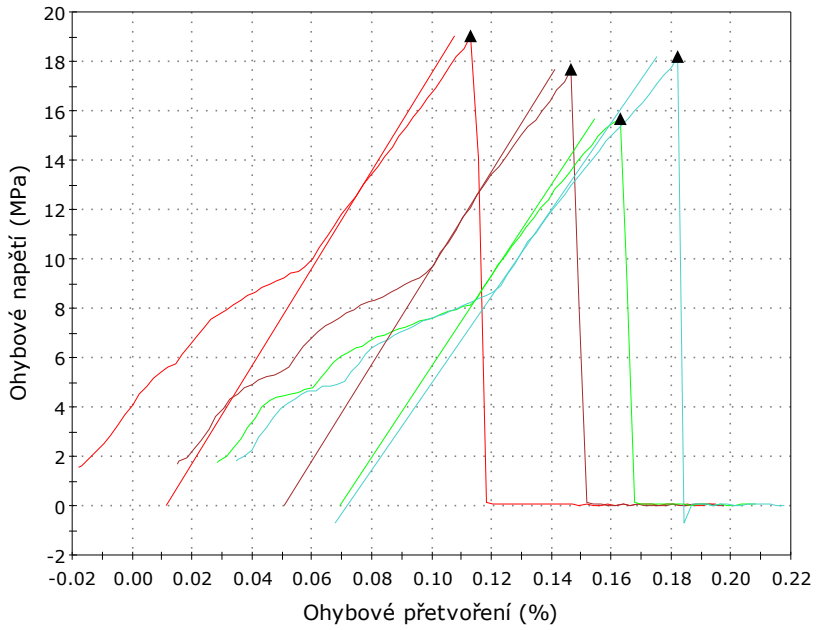

Fig. 4.3 Typical stress vs strain curve in flexure of M2 system at span 80 mm.

The compressive properties of bare matrices are shown in Table 4.3. It can be seen obviously that, the mechanical properties of the pure geopolymer matrices based on thermal silica are much better than these of previous study results which are presented in Chapter 2. From the point of view of flexure, Bortnovsky et, al. (2005) stated that the strength of geopolymer based on metakaolin with chosen optimal chemical composition is about 10-16 MPa when cured at 60 ^{o}C for 20 hours and maturated at room conditions for 28 days [48]. The geopolymer based on fly-ash, cured at room temperature for 7 days, after that dried for each 3 hours in a oven at 60, 100 and 200 ^{o}C respectively, shows 6 – 8 MPa of flexure [61] and while Miller's study presents the flexural strength varies from 2 to 14 MPa due to curing temperature of 55 – 95 ^{o}C and curing time of 8 – 96 hours [65]. Concerning about compressive properties, the former studies show a wide range of 10 – 100 MPa of strength, most of them ranging

lower 50 MPa for both metakaolin or fly-ash based geopolymers [24, 33, 48, 57-62, 64, 109]. These mean the compressive properties of thermal silica based geopolymers are ranged in the top of these values, even bettter for M2 (approximately 111 MPa).

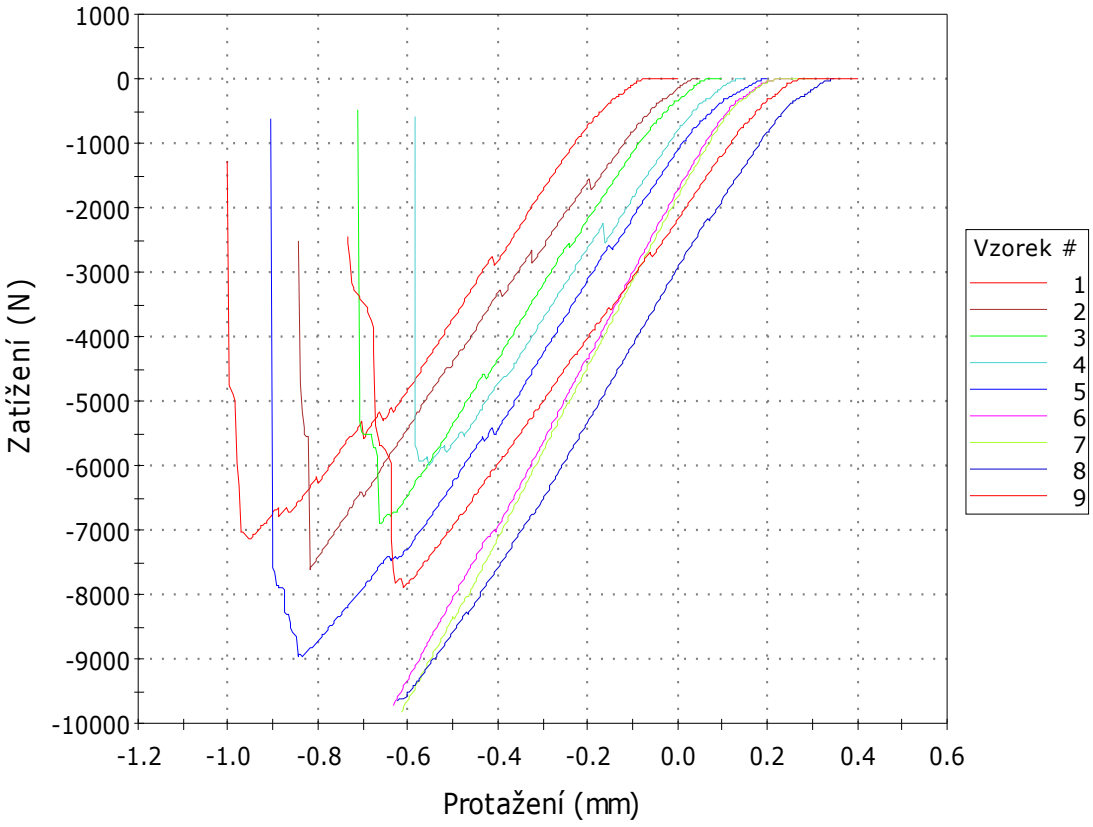

Fig. 4.4 Typical load vs displacement curve of comperessive test of M1 system.

Table 4.3 Compressive properties of geopolymer matrix

Matrix	R_{mc} [MPa]	E_{mc} [GPa]	ε_{mc} [%]
M1	88.9 ±11.5	116.8 ±10.4	3.23
M2	111.8 ±13.1	194.1 ±10.7	5.24

Typical diagrams of flexural and compressive tests of pure geopolymer matrices are shown on Fig. 4.3 and Fig. 4.4. As can be seen from these figures that there is a quite wide region at the begining of loading where the materials behave as fitting solid structure and can be called “toe” regions [99]. The linear parts of the cures seem very short, especially for bending tests. There are a lot of partial fractures during the test

and they present very typical behavior of brittle materials when non plastic, hardening, or creep regions are determined.

In order to understand the mechanical behavior of geopolymer matrix when outer support span-to-depth ratio L/H → ∞; by testing the samples at different spans with flexure and utilizing the theory that is described in previous chapter, linear regression of a fictitious Young's modulus E and a fictitious flexural strength R_{mo} against $(H/L)^2$ (reciprocal span: height ration) value are exhibited on Fig. 4.5. From the linear regression, Virtual modulus (E^*), shear modulus (G), and flexural strength (R^*_{mo}) are estimated and sumerized in Table 4.4.

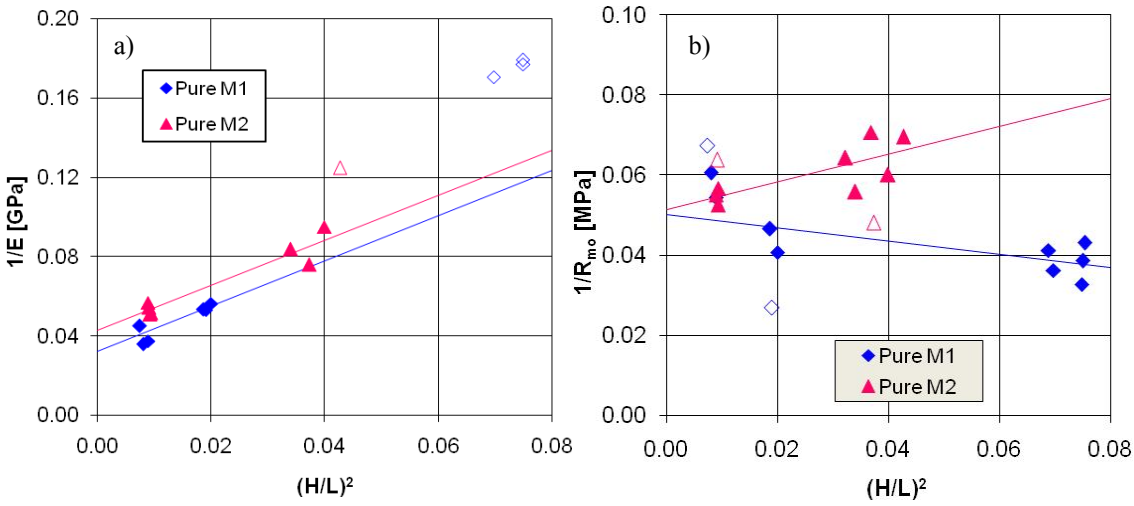

Fig. 4.5 Reciprocal effective flexural properties vs. $(H/L)^2$ ratio a) elasticity modulus, b) flexural strength.

Table 4.4 Flexural properties of pure matrix M1 and M2 when $(H/L)^2 \rightarrow 0$

Matrix	Young's module E^*			Shear module G	E^*/G	Flexural strength R^*_{mo}		
	[GPa]			[GPa]	[1]	[MPa]		
M1	**34.7**	±5.3	±15.4%	**1.0**	**33.6**	**19.9**	±1.4	±7.1%
M2	**23.4**	±2.2	±9.3%	**1.0**	**22.5**	**19.5**	±1.4	±7.4%

It can be seen from the Table 4.2 and Fig 4.4 that two main bending properties of geopolymer matrices, flexural strength and flexural modulus, are dependent on the

distance of outer support span. The elasticity displays positive trend with the ratio of test speciment thickness (H) and testing span (L) for both matrix systems M1 and M2. Meanwhile there are two different trends of flexural strength when the ratio H/L changes; negative tendency for M1 system and in reverse order for M2 system. In addition, from the slope of the linear regression line, we can estimate the dependent intensity of flexural modulus and strength of H/L ratio.

Athough, non fire resitance investigation of pure geopolymer matrices is carried out in this study, however we believe that the pure matrices possess the all similar important properties of fire as materials based on minerals, such as time to flashover lasts to infinitive, non toxic fumes, very low heat release rate and so on [12, 110].

4.3 PROPERTIES OF FIBER REINFORCEMENT

Seven types of popular commercial fibers, Table 4.5, are selected for evaluating their mechanical properties at real ambient conditions and the retention of these properties after exposing up to high temperature in oxidation environment.

Table 4.5 Main properties of selected fibers from producers or suppliers

Fiber	tex [g/km]	d_0 [μm]	ρ [$Mg.m^{-3}$]	R_{mt} [MPa]	E [GPa]	ε_{mt} [%]	Producer/Dealer
Carbon HTS 5631 800tex 12K	800	7	1.77	4300	240	1.8	Toho Tenax Europe GmbH, www.tohotenax-eu.com
Carbon HTS 5631 1600tex 24K	1600	7	1.77	4300	240	1.8	
AR-glass 2400 tex	2400	27	2.6	1400	72	2.4	Saint-Gobain Vetrotex, http://www.vetrotextextiles.com
ARG 2500 tex	2500	14	2.8	1700	74	2.0	Nippon Electric Glass Co., Ltd., http://www.neg.co.jp/EN/
Basalt BCF13 - 2520tex - KV12 Int	2520	13	2.67	2600~ 2800	85-90	x	Basfiber®, Kamenny Vek, Russia, www.basfiber.com
E-glass	2400	24	2.6	1548	76	4.5	Saint-Gobain Vetrotex, http://www.vetrotextextiles.com
3M™ Nextel™ 312 Ceramic Fiber	1800	10	2.7	1700	150	1.5	3M in Europe, http://solutions.3m.com/wps/portal/3M/en_EU/World/Wide/

tex - Nominal linear density [g/km]
d_0 - Average diameter of fiber filament [μm]
ρ - Density [$Mg.m^{-3}$]
R_{mt} - Tensile strength [MPa]
E - Tensile module [GPa]
ε_{mt} - Failure strain [%]

Mechanical properties of commercial single fiber filaments of origin and after exposing to high temperature tested at real ambient conditions, in accordance with JIS R 7601 at gause length 25 mm, are summed up in the Table 4.6 and Fig. 4.6.

Table 4.6. Mechanical properties of filaments in accordance with Japanese Industrial Standard (JIS R 7601)

Fiber	d_0	**20 °C**			**200 °C**			**400 °C**			**700 °C**			**1000 °C**		
		ε	**R_{mt}**	**E**	**ε_{mt}**	**R_{mt}**	**E**	**ε_{mt}**	**R_{mt}**	**E**	**ε_{mt}**	**R_{mt}**	**E**	**ε_{mt}**	**R_{mt}**	**E**
	[μm]	[%]	[MPa]	[GPa]	[%]	[MPa]	[GPa]	[%]	[MPa]	[GPa]	[%]	[MPa]	[GPa]	[%]	[MPa]	[GPa]
Carbon HTS 5631 800tex 12K	7	1.75	3120	178	1.72	3120	181	2.24	3640	163	Fibers were destroyed totally (nearly disappeared)					
Carbon HTS 5631 1600tex 24K	7	1.84	3120	170	1.33	2340	176	1.66	2861	172						
ARG 2400tex	27	3.32	1293	39	3.22	1241	39	1.63	769	47	The fibers still remained in the furnace, but too brittle (*)					
ARG 2500tex	14	2.68	1560	58	2.24	1820	81	0.63	390	62						
Basalt BCF13 - 2520tex - KV12 Int	13	3.98	2563	64	3.44	2111	61	1.7	1281	75						
E-glass	24	4.72	1504	32	3.26	1106	34	2.08	995	48	1.03	575	56	(*)		
Ceramic 3M-312 fiber	10	1.48	1995	140	2.06	2378	128	1.36	1745	117	1.39	1818	123	0.82	1161	99.7

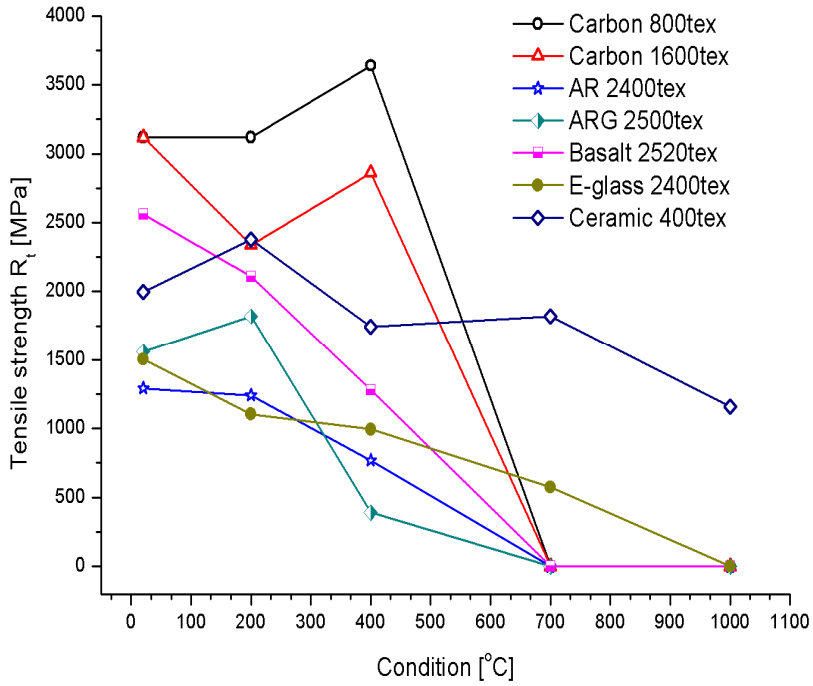

Fig. 4.6 Effect of temperature on tensile strength of commercial fibers.

It is obvious that at ambient conditions, the mechanical properties of all fibers are lower than the original values from the manufacturers, especially for carbon fiber. In real conditions, for both carbon fibers approximately 73% and 74% of tensile strength and modulus are determined (3120 MPa and 178 GPa in contrast with 4300 MPa and 240 GPa). For other fibers we can get around 95% of original strength at ideal conditions of testing from the producers; however, in case of tensile modulus, only 54% and 42% of origins for ARG 2400tex and E-glass are evaluated (39 GPa and 32 GPa in comparision with 72 and 76 GPa) (see more from Table 4.5 and 4.6).

The Table 4.6 shows that the carbon HTS 5631 800tex 24K, HTS 5631 1600tex 24K have the best tensile strength of 3120 MPa, only 20% and 53% higher than that of basalt BCF13 - 2520tex - KV12 Int. and ceramic 3M-312 fibers (3120 MPa compared to 2563 and 1995 MPa respectively); in comparison with modulus, the basalt fiber shows only about 35% and 79% of value of carbon fiber for the basalt and ceramic fibers respectively. Meanwhile carbon fibers show tensile strength nearly two times higher than that the strength of ARG 2500tex and E-glass fiber, and three times higher than tensile strength of AR 2400tex fiber strength at 20 °C of testing conditions.

After 3 hours sustaining at 200 °C, the strength, elongation and Young‘s modulus of all kinds of fibers are approximately the same before, the only exception being E-glass

fiber, which exhibited nearly 73% strength (1106 MPa compared to 1504 MPa) and elongation of this fiber reduced from 4.72% to 3.26% that of at room condition.

For carbon fibers, the strength, elongation and Young modulus are nearly constant after 3 hours exposing up to 400 ^{o}C in a furnace, on the contrary, the properties of the other kinds of fibers go down considerably and they became a little brittle. After 3 hours in the furnace at 700 ^{o}C, there are only E-glass and caramic 3M-312 fibers remained ability for testing elasticity and the strength. About 575 MPa of tensile strength (about 38%) and elongation was 1.03% whereas, other fibers were destroyed totally (carbon) or become too brittle to carry out the mechanical test (glass and basalt). However, for the caramic fiber, the properties remain nearly constant up to 700 ^{o}C and after exposing up to 1000 ^{o}C about 50% of the properties are remained.

Based on preliminary investigation of ability to combine with geopolymer to form geocomposites, only three kinds of unidirectional fibers are chosen for reinforcing geocomposites: carbon HTS 5631 1600tex 24K which is expected to apply at high temperature, due to the matrix ability to protect the fiber from oxidation; Saint-Gobain - Vetrotex E-glass E2400P192 fiber in order to achieve low cost of products and the fiber even retains strength after exposing up to 700 ^{o}C. The last fiber for our investigation is basalt BCF13 - 2520tex - KV12 Int. because of chemical compatibility with geopolymer, moreover basalt fiber can be consider an alternation to glass fiber [94].

5. EFFECTS OF CURING TEMPERATURE ON MECHANICAL PROPERTIES

5.1 INTRODUCTION

Geopolymerization is an important process that determines the microstructure of geopolymer materials and their mechanical properties finally. There are many factors that affect the geopolymerization procedure, such as source materials including solid raw materials, chemical and mineral additives, alkali activators, and plasticizers together with processing conditions, as drainage of surplus matrix gel, pressure, temperature and time of curing [8, 43, 111, 112]. The curing temperature is considered as an unrestricted factor when researching compressive properties of geopolymer concretes [113, 114], geopolymer cement [33, 115] and fly ash-based geopolymer materials in general [56, 116, 117].

In this chapter we try to verify the statement of effects of curing temperature on the mechanical properties of reinforced geocomposites containing 45, 53 and 60 vol.% of unidirectional fibers of carbon HTS 5631 1600tex 24K, basalt BCF13 - 2520tex - KV12 Int. and Saint-Gobain - Vetrotex E-glass E2400P192 fiber respectively. In addition, the porosity of resulting samples is investigated to explain the dependence of flexural properties on curing temperature and SEM images of geocomposites are studies as well.

5.2 EXPERIMENTAL

5.2.1 PREPARATION OF COMPOSITE SPECIMENS

The procedure of settling samples are described in details in Chapter 3, continuous fibres (rovings) are impregnated (“wetted-out”) with geopolymeric resin on the home-made impregnation machine (Fig 3.5) at optimal velocity of 34 m/h for achieving the best penetration of the geopolymer resin into the fibers. Impregnated cutting-up rovings are laid manually into a silicon rubber mould 3×9×150 mm, layer by layer. Series of five samples are prepared from a batch, 16 bunches of impregnated carbon fibers, 18 bunches of pre-preg basalt fibers or 20 bunches of geopolymer saturated

E-glass fibers are needed for each specimen. The mould with pre-pregs is then covered by a peel ply fabric and suction tissue for good distribution of pressure on the samples, removing air bubble and surplus geopolymer resin. Finally, the mould is placed into a good sealed plastic bag.

The specimens are cured for 3 stages by help of currently used technique of vacuum bagging (Fig 3.7). In the first stage at room temperature for 1 hour, the purpose of this is to remove air bubble and superfluous resin, we expect that until at the end of the first stage the resin remains uncured. In the second stage of processing, the samples are cured at elevated temperature in a oven, we assume that this is one most important factor which not only affects the properties of resulting materials but also determines the cost of final products because of most consuming energy. Seven different elevated temperatures 55, 65, 75, 85, 95, 105 and 115 °C are applied for curing the material in the second stage for 5 hours, in the oven. Finally, the specimens are released from bags, dried open in the oven at the same temperature for other 5 hours more. Resulting samples are cut-up to suit the planned outer support span-to depth ratios of testing. Only rough surface treatment with emery paper was applied.

5.2.2 TESTING OF FLEXURAL PROPERTIES AND DATA TREATMENT

The mechanical properties are tested and evaluated in three-point bending mode under center-point load at three outer support span-to-depth ratios of L/H = 16 to 1, L/H = 20 to 1 and L/H = 40 to 1 in proportion to support spans L = 50, 64 and 120 mm respectively on Universal Testing Machine, Model Type: INSTRON Model 4202 in ambient conditions. The ratio L/H = 20 to 1 is recommended by DIN V ENV 658-3:1993-02 [100], L/H = 16 to 1 and L/H = 40 to 1 are introduced by ASTM C 1341 – 06 [99]. Meanwhile the British Standard for BS EN ISO 14125:1998 advised L/H = 20 to 1 for Class III (unidirectional glass fiber systems) and L/H = 40 to 1 for the Class IV (plastics reinforced with carbon fibers) [107]. The displacement rate of crosshead is 2 mm/min. Experimental findings show that, however, both flexural strength and modulus are strongly dependent on the spans of testing. Utilizing the Tarnopolsky's theory (Chapter 3 for details) by enabled reliable linear regression from 8 samples for each kind of resin and fiber, between reciprocal values of effective flexural module E or of effective flexural (maximal) strength R_{mo}, and the squared ratio $(H/L)^2$ at 3 series

of testing, the virtual flexural module E^* and virtual flexural strength R^*_{mo} is presented as optional results.

5.2.3 POROSITY OF COMPOSITES

With intention to discover the source of significantly changing composite properties under altering cure conditions, porosity is determined in intact specimens. Liquid saturation method under vacuum is applied, using n-heptane as an inert imbibition medium that prevents dissolution of inorganic species. By weighing a specimen dry, soaked, and dipped on hinge, open porosity (total volume fraction of pores) is estimated.

5.2.4 MICROSTRUCTURE AND VOLUME FRACTION OF FIBERS

The sections perpendicular to fibers and surfaces of the composites are inspected in scanning electron microscope (SEM) to estimate not only the adhesion between geopolymer matrices and fiber reinforcements but also the microstructure of the composites. In addition, volume fraction is determined via dying the fibers and matrix on the cross-section of SEM image of composites under assistance of the microscope.

5.3 RESULTS AND DISCUSSION

5.3.1 GENERAL PICTURE

Geopolymer M0 system without adding of functional additives is reinforced by only the carbon fibers and tested at outer support span-to-depth ratio L/H = 20 to 1. These series of samples are used as a control experiment and flexural mechanical properties are presented in Table 5.1 and Fig. 5.1.

Table 5.1 Flexural properties of geocomposite with matrix M0 and the carbon fibers at different temperature of curing at L/H = 20 to 1

Temp. of curing [°C]	R_{mo} [MPa]	E [GPa]	Strain in the outer surface (ε_{mo}) [%]	Density of composite [Mg.m^{-3}]
55	386.4 ±30.6	45.0 ±3.0	1.49	1.82
65	425.3 ±41.2	49.1 ±2.0	1.43	1.85
75	570.7 ±58.5	64.3 ±3.7	0.98	1.86
85	504.7 ±1.90	62.6 ±3.3	0.88	1.79
95	511.9 ±15.7	69.1 ±4.1	0.90	1.78
105	361.5 ±13.2	65.2 ±1.7	0.82	1.65
115	98.6 ±25.3	20.2 ±6.5	0.78	1.32

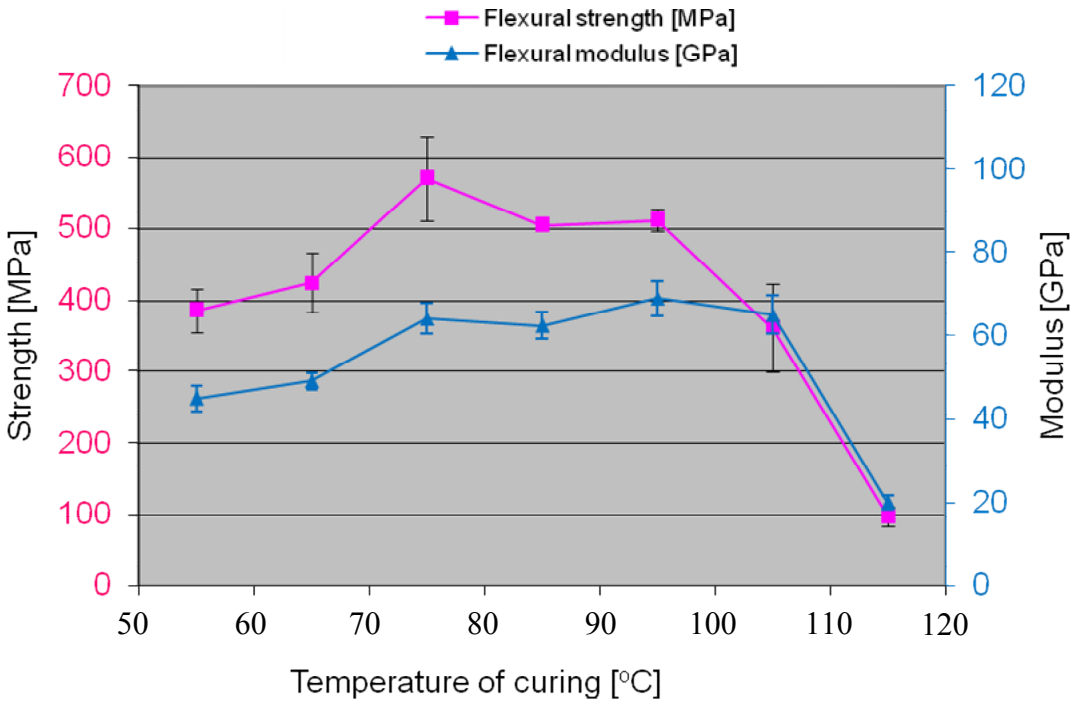

Fig. 5.1 Effects of temperature of curing on flexural strength and modulus of geopolymer composite M0-Carbon.

Table 5.2, 5.3, B.1, B.2 in Appendix B and Fig. 5.2 to 5.5 show the effects of main flexural parameters of geocomposites based on M1 or M2 matrix and reinforced by three selected unidirectional fibers. The properties are measured and evaluated in accordance with popular standards for ceramic matrix composite reinforced by fiber, including ASTM C1341 – 06 and DIN V ENV 658-3:1993-02.

Table 5.2 Flexural properties of geopolymer composites M1 system at outer support span-to-depth ration L/H = 20 to 1.

Temp of curing [^{o}C]	Reinforced geocomposites								
	M1-Carbon			M1-Basalt			M1-Eglass		
	R_{mo} [MPa]	E [GPa]	ε_{mo} [%]	R_{mo} [MPa]	E [GPa]	ε_{mo} [%]	R_{mo} [MPa]	E [GPa]	ε_{mo} [%]
55	405.8 ±29.4	76.2 ±5.8	0.68	277.2 ±12.9	44.5 ±3.5	1.14	176.3 ±29.6	44.5 ±1.1	0.51
65	386.6 ±38.3	80.4 ±4.9	0.65	272.6 ±27.4	39.7 ±1.7	0.90	133.6 ±21.1	35.8 ±7.0	0.53
75	448.6 ±27.6	94.3 ±1.9	0.74	283.6 ±11.3	35.5 ±1.7	1.02	90.0 ±11.6	18.3 ±5.7	0.76
85	383.8 ±44.7	75.1 ±7.2	0.73	285.2 ±16.7	35.2 ±4.5	1.01	78.1 ±8.5	22.2 ±5.5	0.58
95	304.8 ±21.0	58.3 ±2.6	0.78	258.0 ±4.3	35.6 ±3.6	1.03	63.0 ±5.8	18.5 ±3.8	0.70
105	169.6 ±45.8	47.4 ±9.0	0.79	210.8 ±3.3	33.8 ±1.3	0.81	60.7 ±9.1	23.0 ±1.8	0.37
115	121.5 ±20.5	38.0 ±1.9	1.17	112.1 ±15.8	32.5 ±2.4	0.50	68.6 ±12.8	30.8 ±3.8	0.30

R_{mo} – flexural strength [MPa]
E – Young's modulus [GPa]
ε_{mo} - Strain in the outer surface of the specimen [%]

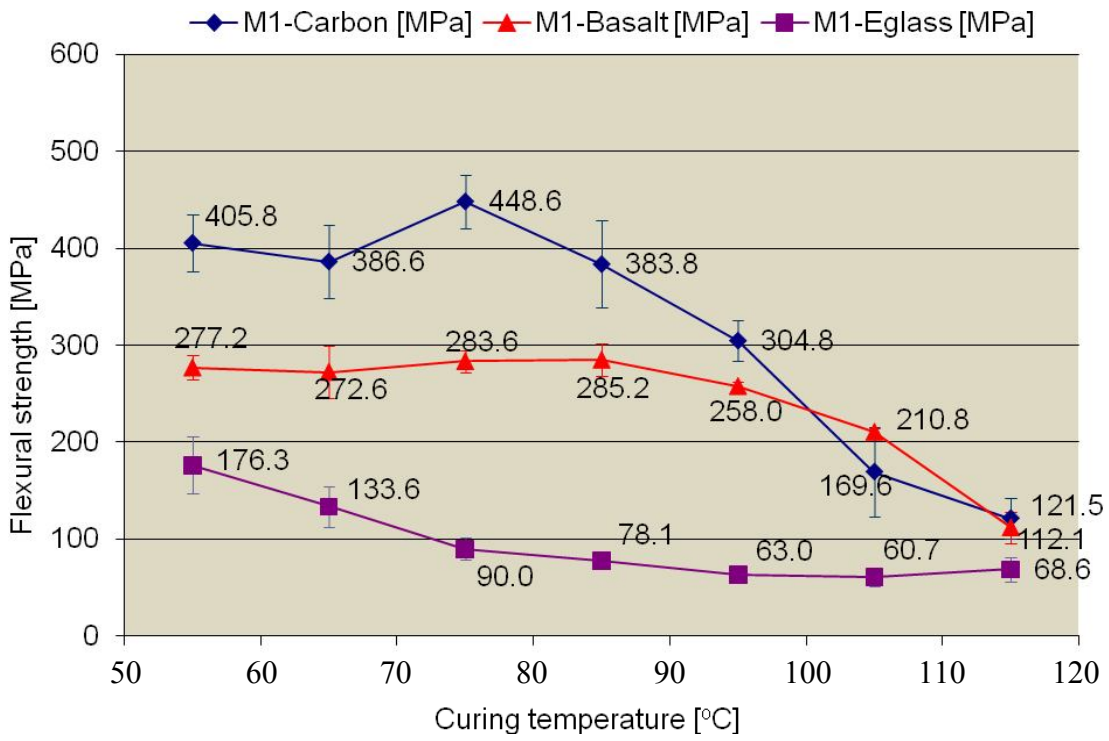

Fig. 5.2 Effects of temperature of curing on flexural strength of geopolymer composite M1 system at outer support span-to-depth ration L/H = 20 to 1.

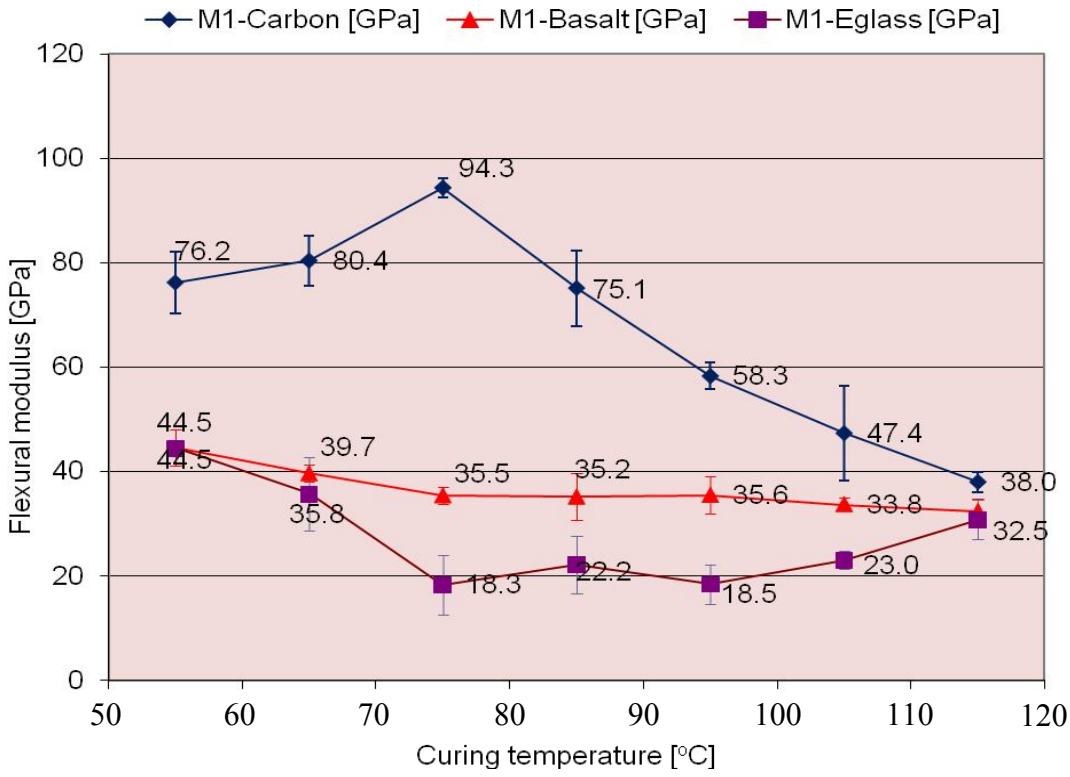

Fig. 5.3 Effects of temperature of curing on flexural modulus of geopolymer composite M1 system at outer support span-to-depth ration L/H = 20 to 1.

Table 5.3 Flexural properties of geopolymer com posites M2 system at outer support span-to-depth ration L/H = 20 to 1.

Temp of curing [^{o}C]	**Reinforced geocomposites**								
	M2-Carbon			**M2-Basalt**			**M2-Eglass**		
	R_{mo} [MPa]	**E [GPa]**	**ε_{mo} [%]**	**R_{mo} [MPa]**	**E [GPa]**	**ε_{mo} [%]**	**R_{mo} [MPa]**	**E [GPa]**	**ε_{mo} [%]**
55	173.3 ±22.7	61.5 ±9.8	0.53	126.4 ±22.5	42.4 ±1.0	0.39	104.3 ±11.5	39.9 ±1.5	0.42
65	180.3 ±13.4	54.9 ±4.3	0.62	152.0 ±15.6	39.5 ±2.3	0.44	142.2 ±20.1	37.7 ±8.4	0.59
75	225.2 ±4.3	72.8 ±8.9	0.47	198.0 ±13.2	48.2 ±1.8	0.76	169.0 ±20.3	49.6 ±1.6	0.56
85	323.2 ±28.2	75.5 ±4.5	0.62	172.3 ±19.1	40.7 ±2.1	0.60	138.1 ±20.6	42.7 ±1.3	0.50
95	324.9 ±14.1	106.9 ±2.7	0.45	164.4 ±7.0	45.8 ±2.3	0.50	132.7 ±16.7	42.7 ±3.4	0.34
105	252.0 ±19.3	75.0 ±12.7	0.47	123.4 ±17.5	43.4 ±0.1	0.40	78.3 ±13.3	30.9 ±7.3	0.46
115	211.2 ±19.6	73.5 ±3.6	0.33	124.6 ±18.1	42.4 ±1.9	0.39	102.9 ±8.0	39.8 ±5.3	0.33

R_{mo} – flexural strength [MPa]
E – Young's modulus [GPa]
ε - Strain in the outer surface of the specimen [%]

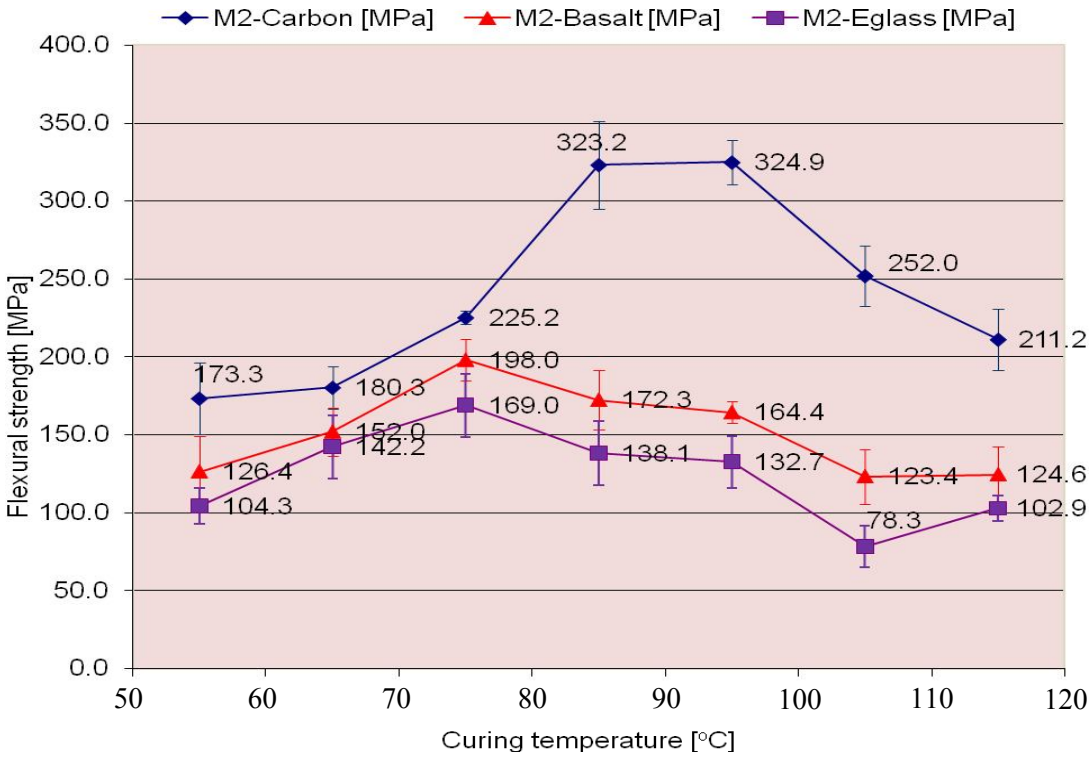

Fig. 5.4 Effects of temperature of curing on flexural strength of geopolymer composite M2 system at outer support span-to-depth ration L/H = 20 to 1.

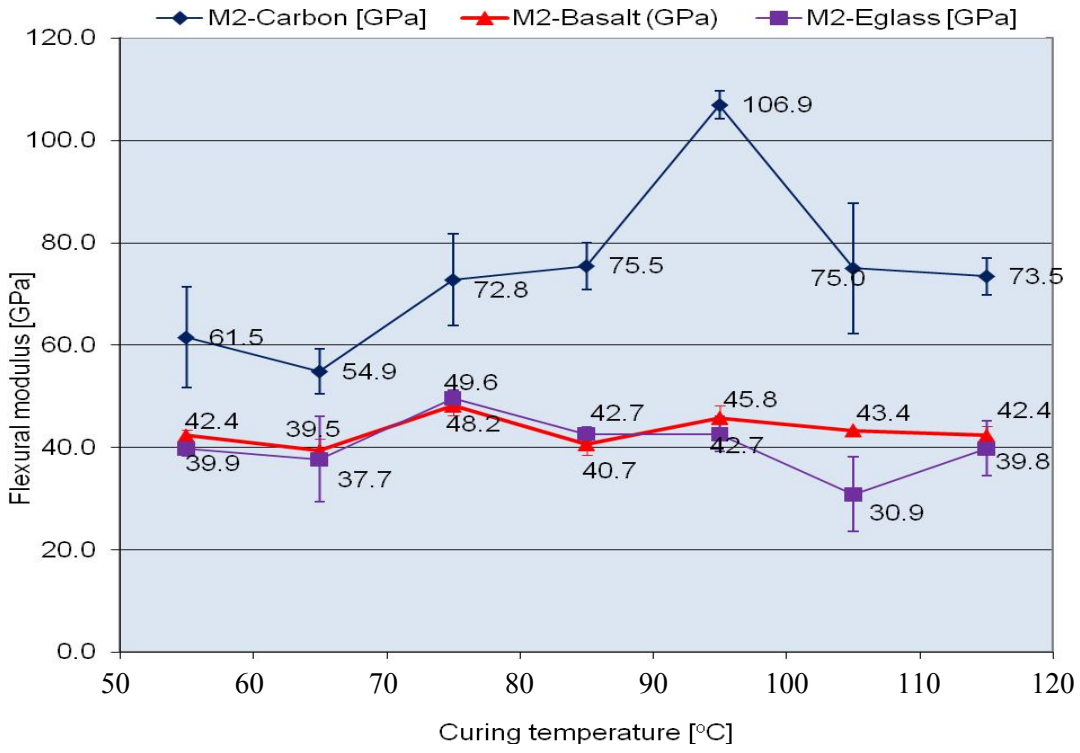

Fig. 5.5 Effects of temperature of curing on flexural modulus of geopolymer composite M2 system at outer support span-to-depth ration L/H = 20 to 1.

As can be seen from Table 5.2, 5.3 and Table B.1, B2, when the geocomposites are tested at different testing spans with recommended standards, their important parameters, flexure and modulus, are shown different values. For examples, at elevated curing temperature 75 ^{o}C, geocomposite M1-carbon exhibited approximately 486 MPa of flexural strength and 94 GPa of flexural modulus when tested at L/H = 20 to 1, meanwhile these values are 298 MPa and 51 GPa of bending strength and modulus respectively when the composites were tested at L/H = 16 to 1.

From Table 5.1, 5.2 and Fig. 5.1 to 5.3, in comparison of geocomposite M0 without functional additive and M1 with boric acid (H_3BO_3) reinforced by the carbon fibers, we can find that the functional additive does not affect the curing temperature at which the composites achieve the best mechanical properties, around 75 °C. The additive, however, do affect the maximum value of flexural strength, nearly 20% of this value is off when the boric acid is added into M1 (448.6 MPa of M1/Carbon in comparison with 570.7 MPa of M0/Carbon).

In order to utilize the theory and equations are described in Chapter 3, for each kind of geopolymer, reinforcement and elevated temperature, two more samples are tested at span 120 mm. In general, a series of 8 tests on 3 different levels of L/H ratio of span 50, 64 and 120 mm are used for regression. This method is called “size-independent method” contemporarily for easier presentation of the results. Fig 5.6 demonstrated example patterns of basic linear regressions of effective mechanical properties**Error! Reference source not found.**. It is evident that linear dependences are regular, revealing no abrupt shifts to another possible deformation mode.

The basic set of results is presented in Table 5.4. The average values of virtual modulus E^* and flexural strength R^*_{mo} are completed with standard deviations, marked with ± sign. As failure properties were at higher curing temperatures extraordinary scattered.

Collective results of effects of curing temperature on flexural strength and modulus of the geocomposites are presented on Fig. 5.7. Each marker represents an extrapolated, size independent value of E^* or R^*_{mo}; standard deviations are denoted by error abscises. Several points distinguished by a smaller marker were added from preceding measurements that are not included in Table 5.4.

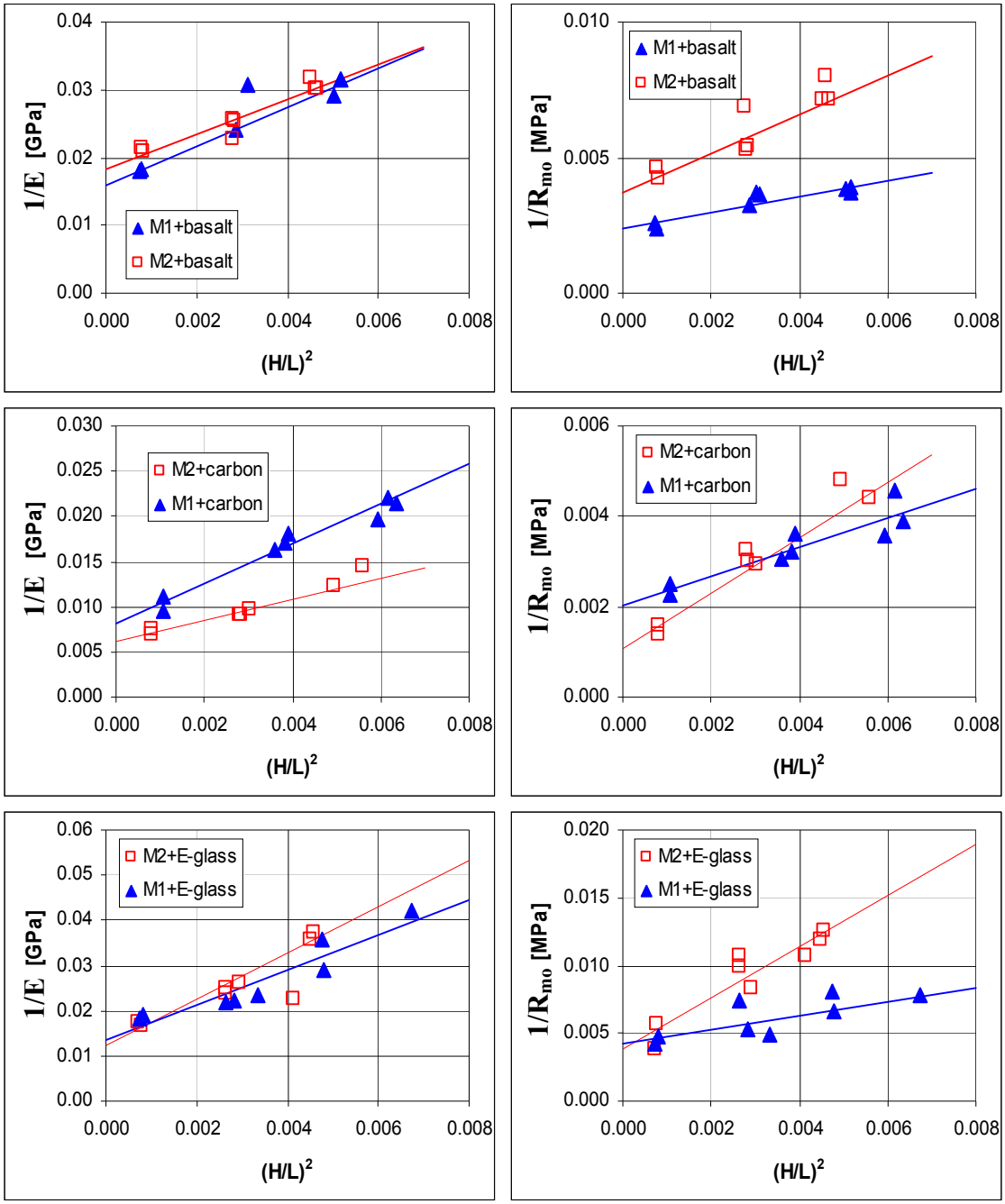

Fig. 5.6 Examples of elementary treatment of results by means of linear regression (curing temperatures: basalt 85 °C, carbon 95 °C, E-glass 55 °C).

Table 5.4 Survey of estimation of basic virtual flexural properties of geocomposites reinforced with unidirectional fibers at different curing temperature

matrix/ fiber	curing temperature	flexural module (E^*)	shear module (G)	E^*/G	flexural strength (R^*_{mo})
	[°C]	[GPa]	[GPa]	[1]	[MPa]
M1/basalt	55	**46.0** ± 4.3	0.76	61	**331** ± 58
	65	**71.1** ± 4.8	0.31	232	**431** ± 48
	75	**49.2** ± 1.9	0.61	80	**377** ± 26
	85	**63.1** ± 2.7	0.41	155	**415** ± 33
	95	**49.1** ± 2.9	0.47	104	**376** ± 9
	105	**45.0** ± 3.1	0.63	72	**215** ± 11
	115	**44.8** ± 3.7	0.69	65	**155** ± 17
M1/carbon	55	**178.1** ± 36.0	0.42	429	**615** ± 75
	65	**212.1** ± 35.5	0.44	482	**754** ± 102
	75	**188.0** ± 28.4	0.48	393	**722** ± 35
	85	**201.3** ± 26.7	0.41	492	**722** ± 74
	95	**116.4** ± 9.1	0.56	207	**490** ± 62
	105	**126.5** ± 30.2	0.39	327	**364** ± 31
	115	**98.8** ± 21.6	0.39	254	**214** ± 18
M1/E-glass	55	**74.2** ± 12.2	0.30	245	**233** ± 37
	65	**70.7** ± 23.5	0.14	501	**195** ± 15
	75	**64.4** ± 7.8	0.16	403	**147** ± 11
	85	**54.1** ± 11.9	0.18	308	**130** ± 12
	95	**55.0** ± 3.3	0.15	359	**107** ± 17
	105	**44.8** ± 9.5	0.29	154	**59** ± 8
	115	**42.3** ± 2.4	0.50	85	**78** ± 17
M2/basalt	55	**56.2** ± 3.6	0.55	103	**346** ± 39
	65	**63.4** ± 4.1	0.45	141	**358** ± 33
	75	**60.9** ± 3.8	0.63	97	**323** ± 31
	85	**54.4** ± 3.4	0.46	119	**271** ± 20
	95	**65.4** ± 4.9	0.46	141	**272** ± 27
	105	**76.8** ± 3.8	0.30	253	**222** ± 14
	115	**62.9** ± 3.7	0.42	149	**241** ± 26
M2/carbon	55	**101.6** ± 9.7	0.87	117	**373** ± 29
	65	**120.9** ± 12.9	0.69	176	**391** ± 52
	75	**129.5** ± 5.5	0.89	145	**491** ± 47
	85	**141.4** ± 16.7	0.66	214	**776** ± 85
	95	**162.2** ± 7.8	1.00	162	**936** ± 115
	105	**150.5** ± 7.1	0.72	210	**453** ± 57
	115	**111.0** ± 7.2	0.94	118	**411** ± 94
M2/E-glass	55	**80.3** ± 7.3	0.23	347	**258** ± 66
	65	**51.3** ± 4.4	0.45	115	**230** ± 33
	75	**60.9** ± 3.1	0.68	90	**321** ± 66
	85	**88.3** ± 7.5	0.26	341	**368** ± 88
	95	**59.7** ± 5.6	0.45	134	**185** ± 13
	105	**57.2** ± 4.7	0.44	129	**278** ± 26
	115	**52.1** ± 4.4	0.50	104	**213** ± 20

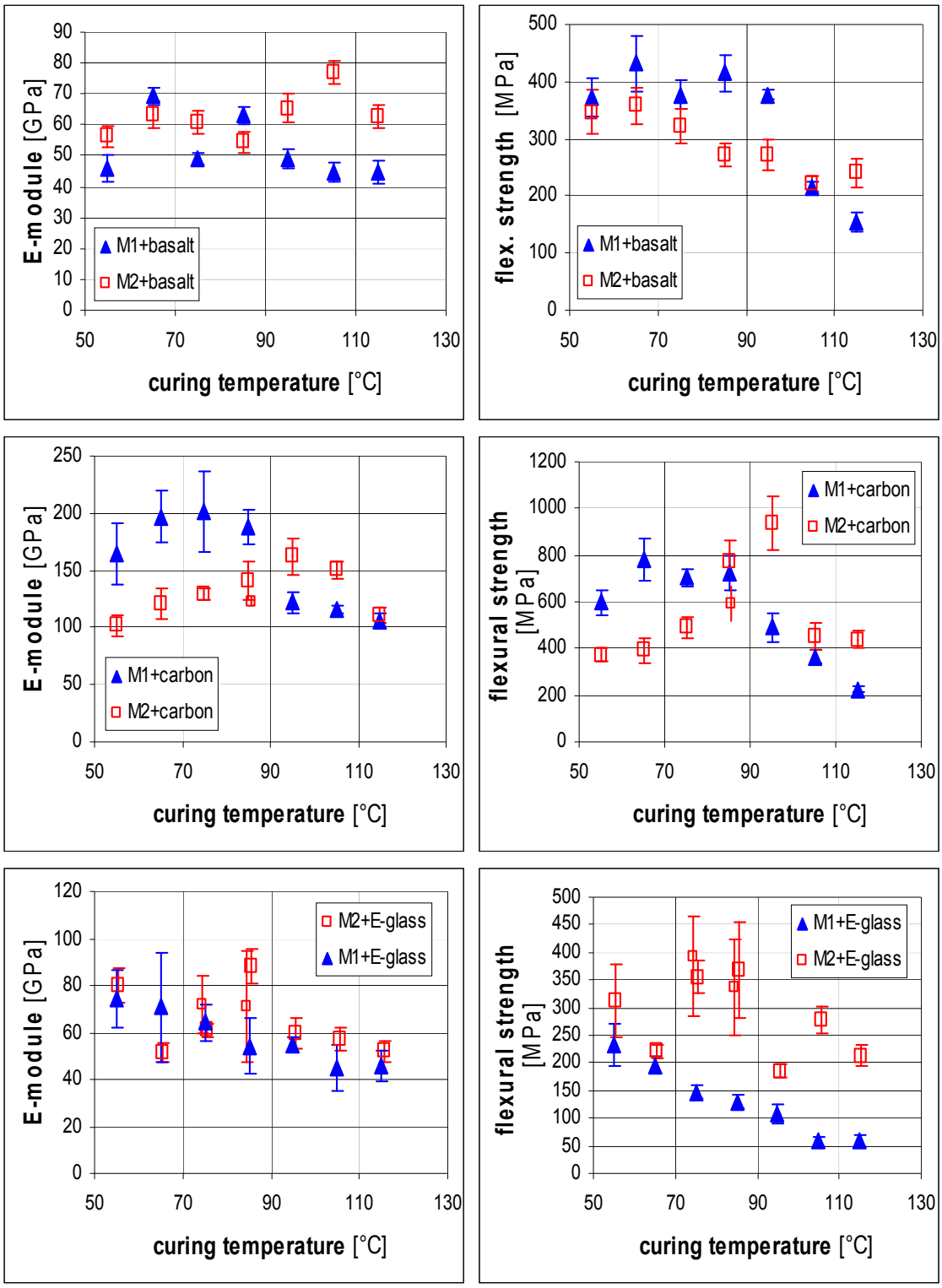

Fig. 5.7 Survey on dependences of main mechanical properties on curing temperature in accordance with size-independent method.

From the practical point of view, even using the standards which are used in ceramic matrix composites or size-independent method, the temperature interval from 65 to 85 °C has been generally recommended for curing geocomposites with basalt and carbon fibers. At lower temperatures there is a danger of unsatisfactorily created bonds between matrix and fiber, and the rate of hardening can be unacceptable from technical standpoint. As described in Chapter 2, a mount of water is repelled during the geopolymerization process. So, at higher temperatures the heating can cause quick evolution of water vapor that cannot adequately escape, so that it enlarges voids. In both cases the lower mechanical properties are determined.

Concerning about geopolymer reinforced by E-glass, generally, The monotonous descending trend in strength of these composites can be deteriorated by acting of alkaline matrix of the type M1 on E-glass fiber at higher temperatures, as Davidovits and Mazany et, al. [90, 118] already explained by chemical embrittlement of E-glass due to the alkaline pH of geopolymer resin, the glass fibers are not dissolved but become fragile. This conclusion will be confirmed when looking the cross-section of the composites under SEM images and when the composites are cured at ambient conditions in Chapter 6.

Table 5.5 Flexural properties of geocomposites cured in optimal range of elevated temperature from 65 to 85 ^{o}C in accordance with size-independent testing method

Matrix /fibre	**Young's module**	**shear module**		**flexural strength**
	E^*	G	E^*/G	R^*_{mo}
	[GPa]	[GPa]	[1]	[MPa]
M1/Basalt	60.5 ± 2.4	0.45	149	407.6 ± 35.6
M2/Basalt	64.4 ± 3.7	0.51	119	317.3 ± 27.8
M1/Carbon	195.6 ± 24.4	0.45	433	735.1 ± 66.9
M2/Carbon	130.6 ± 11.7	0.75	179	552.8 ± 61.3
M1/E-glass	63.1 ± 14.4	0.16	404	157.4 ± 12.7
M2/E-glass	66.8 ± 5.0	0.46	182	314.9 ± 43.3

We can find form the Fig. 5.2 to 5.5 and Appendix B that there are some points at which the experimental values are lower than these of the neighbor one, though they

are sometimes carefully repeated. The roots of the difference are to be sought rather in inadvertent changes in the process of sample preparation and further treatment.

Table 5.5 presents the statistical results of the only those series are selected, which are obtained within the selected interval of curing temperatures 65 to 85°C from the data of original source (Table 5.4).

5.3.2 ROLE OF POROSITY

The course of the dependences of mechanical properties on curing temperature aroused a question, what was the mechanism that mediated this relationship. As there was a suspicion of disturbing effect of escaping water vapor, especially at high temperature of curing, we tried to estimate the dependence of porosity of composites on curing temperature. For estimation of porosity in basic geopolymers, mainly mercury intrusion [77, 119] or gas adsorption [119, 120] had been used. Both methods do not capture porosity in the region of macropores from tenths of millimeter up successfully; only about 0.6 vol.% within 1 to 10 μm in a cured geopolymer was detected [77]; an abrupt rise of pore volume had not been mapped before 0.01-0.05 μm, where in the mesopore region the porosity grew up to 25 to 35 vol.%, as had been estimated by the both methods. In our research, the investigation was carried out by means of n-heptane imbibition into intact samples. Soaking overnight with and without vacuum was tested in parallel; the latter values were by 0.5 to 2 vol.% lower, so for sake of certainty, the vacuum results were chosen and the results are presented on Table 5.6 and Fig. 5.8 with the uncertainty of found porosities was about 1.5 vol.%. The similar method had been applied by Perera and his colleagues to geopolymers of analogous composition by means of imbibition of water in vacuum for 15 minutes to prevent dissolution; porosity 29.5 % had been found in samples cured at 80 °C [120].

A quite large range of scale of porosities, approximately from 9 to 23 vol.%, is determined. Generally, measured porosities were found not to follow ascending trend with curing temperatures closely as Fig. 5.8 shows. However, in range of curing temperature of 65 to 85 °C, when the composites exhibit good mechanical properties, the geocomposites present the low range of the porosities as well, especially for geocomposites reinforced by carbon fibers.

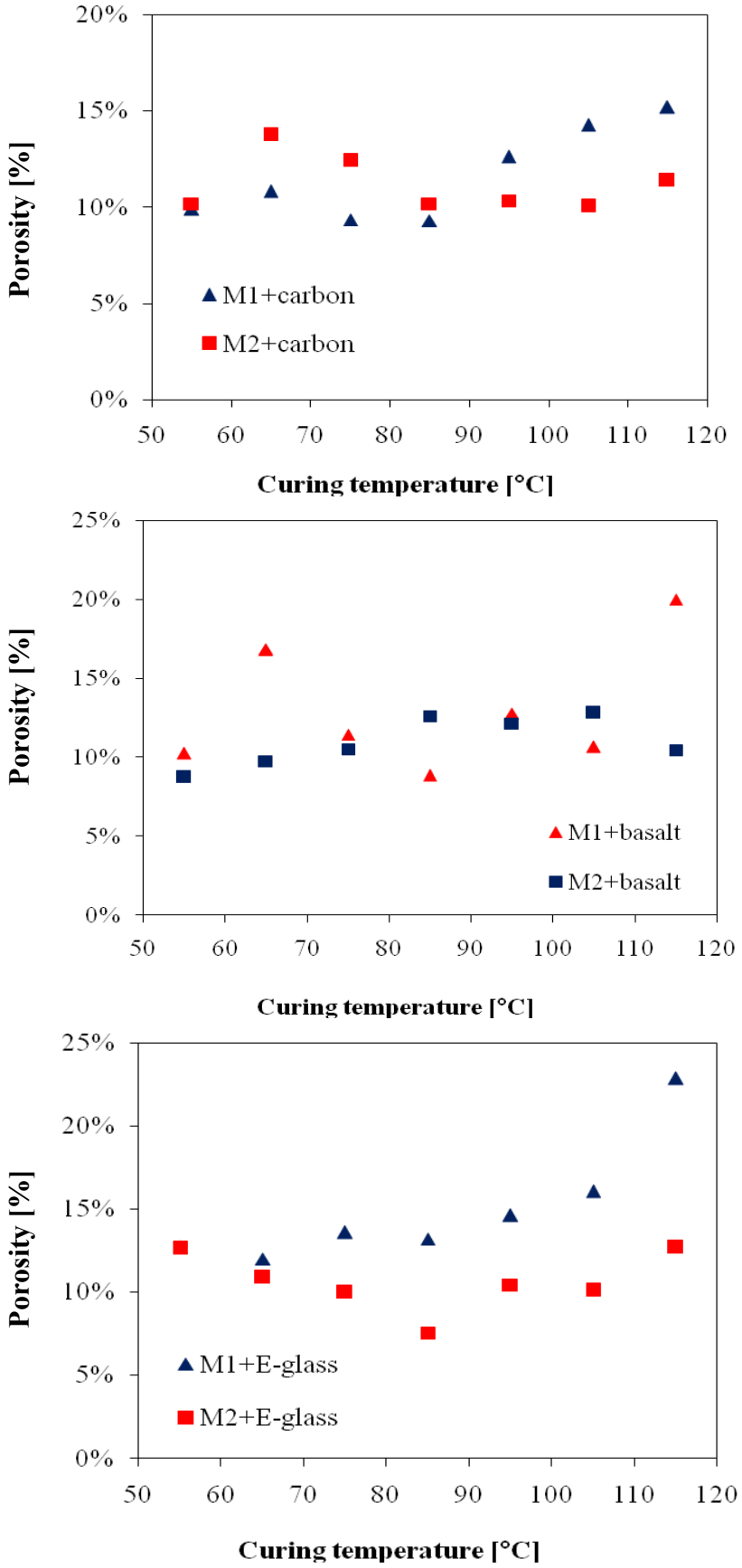

Fig. 5.8 Effects of curing temperature on porosities of geocomposites.

Table 5.6 Effects of porosities (vol.%) of geocomposites on curing temperature

Temp of curing [^{o}C]	Geocomposite system					
	Carbon		Basalt		E-glass	
	M1	M2	M1	M2	M1	M2
55	9.9	10.2	10.3	8.7	12.7	12.6
65	10.8	13.8	16.9	9.8	12.0	10.9
75	9.3	12.4	16.8	10.5	13.6	10.0
85	9.3	10.2	11.5	12.6	13.2	7.6
95	12.6	10.3	8.9	12.1	14.6	10.4
105	14.3	10.1	12.8	12.8	16.0	10.1
115	15.2	11.4	10.6	10.5	22.9	12.7

By the same technique, the porosity of pure matrix is determined as approximately 19.1 vol.% of geopolymer M1 and 12.6 vol.% of M2 system. Generally, considering volume fraction around 50 vol.% of nonporous fiber in actual composites, the total composite porosity would be established only from 6 to 9.5 vol.%, however, which is slightly lower than actual values in comparison with values from Table 5.6. This means that bare geopolymer matrix can possess a structure different from that pasted in composite, due to the non parallelism of the fibers, not very well penetration of resin into reinforcements and last but never least is the hindrance of fibers on the escaping ways of water in the course of hot curing.

In order to study the relationship between the curing temperature, porosities and main flexural parameters (from Table 5.4), the diagrams of these are presented on Fig. 5.9. As can be seen from this figure, measured porosities are found generally not to follow ascending trend with curing temperatures, moreover flexural strength and modulus are not actually decreased when the porosities go up. At low temperature of curing, such as 55 ^{o}C, low porosities are evaluated and low mechanical properties are determined as well. However, the optimal range of curing temperature from 65 to 85 ^{o}C for good mechanical properties and at temperature higher than 100 ^{o}C the outer layers of composite are cured so quickly and prevented water from chemical reaction during the

curing and further drying periods from escaping. This water boiled out at this temperature and enlarges the porosities and even forms cavities in the composites (see Fig. 5.11).

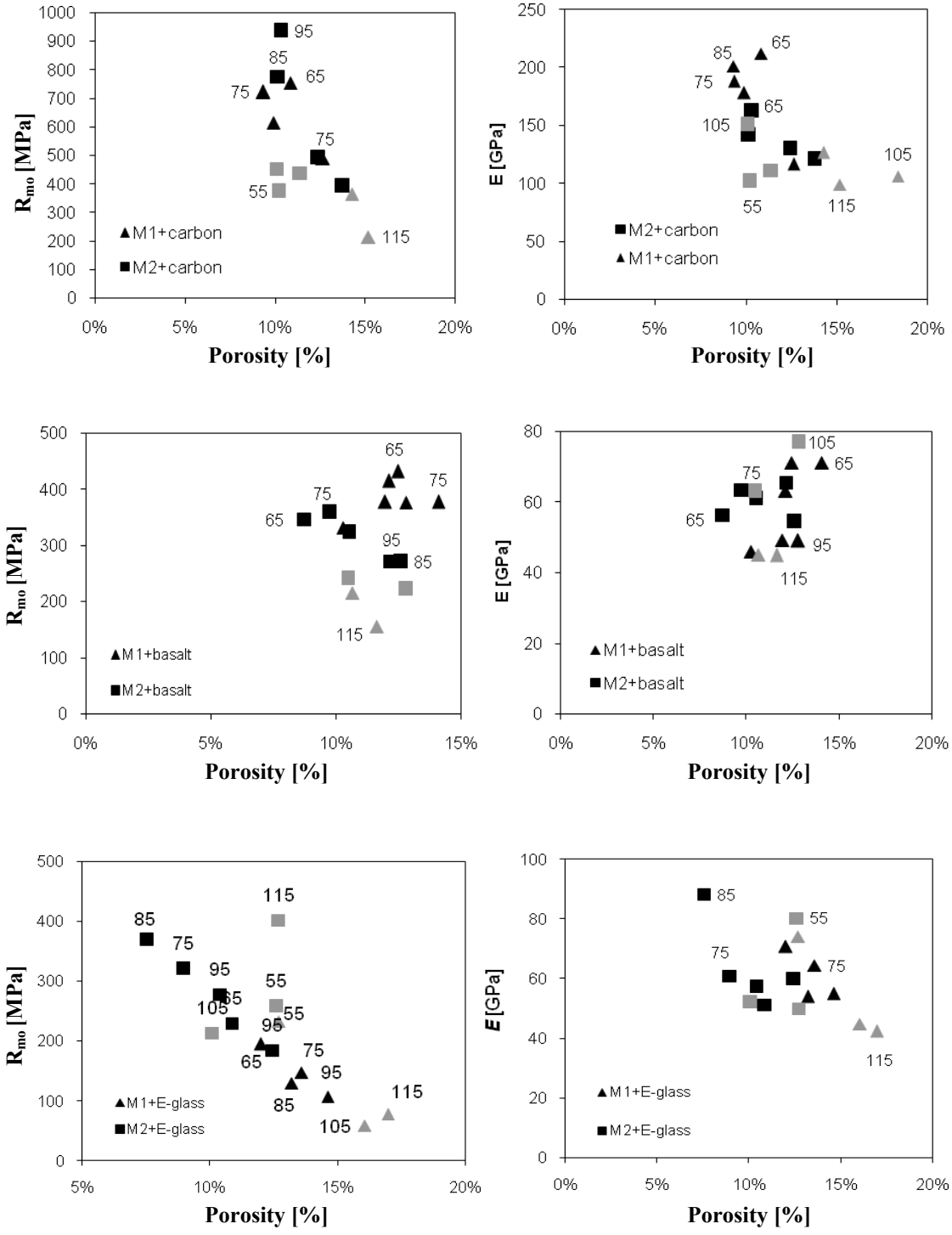

Fig. 5.9 Relationship between flexural strength, modulus and porosity; grey points: temperature of curing >100 °C or < 60 °C.

5.3.3 MICROSTRUCTURE AND VOLUME FRACTION OF FIBERS

Fig. 5.10 shows the SEM images of geocomposite based on geopolymer matrix M0 and reinforced by carbon fiber on the polishing sections perpendicular to the fibers. From the pictures at large magnification we can see that the adhesion between the fibers and geopolymer matrix are very good and it was difficult to recognize the differences between the Fig. 5.10 a, b and c when the composites are cured at different elevated temperature. This means that no conclusion can be drawn about which temperature of curing is the best for the interaction between fibers and matrix.

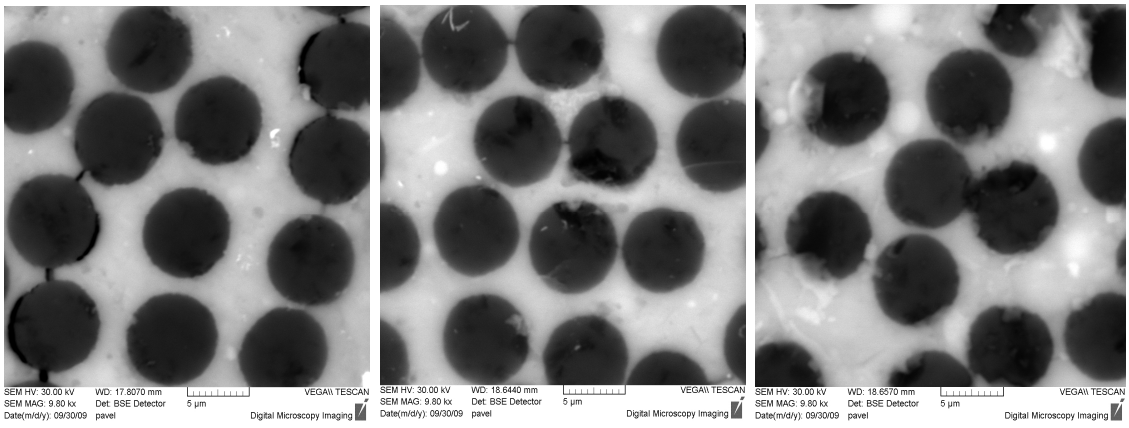

(a) (b) (c)

Fig. 5.10 SEM of geopolymer composite M0/Carbon (a) at 55 ^{o}C, (b) at 75 ^{o}C and (c) at 115 ^{o}C curing temperature with magnification 9800x.

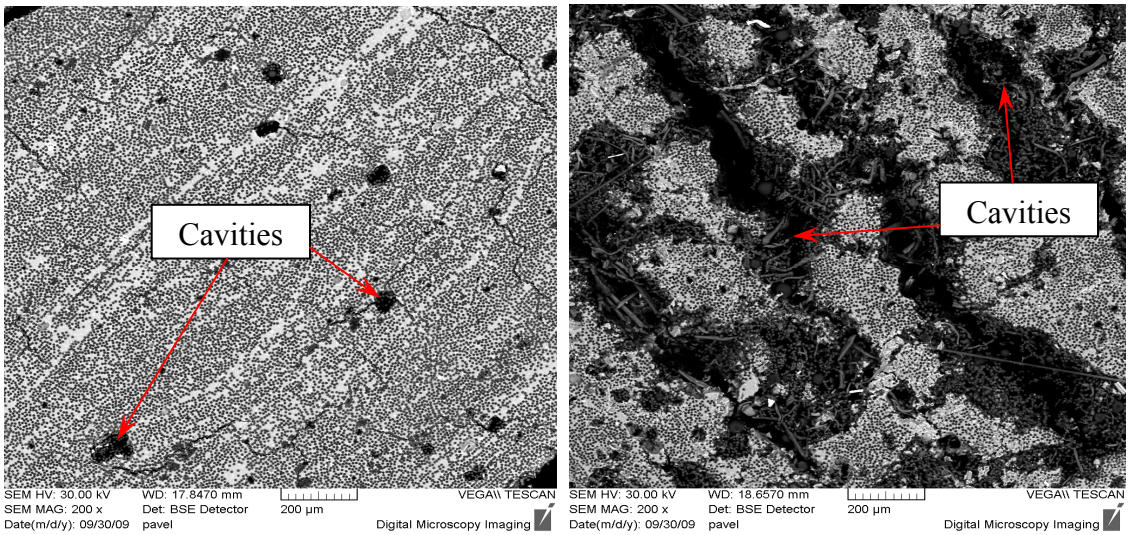

Fig. 5.11 SEM of geopolymer composite M0/Carbon (a) at 75 ^{o}C and (b) at 115 ^{o}C curing temperature with magnification 200x.

On the contrary, however, with lower magnification 200x (Fig. 5.11), we can see that when the composite was cured at temperature higher than 100 ^{o}C, the internal structure of the composites is deteriorated, many cavities are formed during geopolymerization; that made the density of composite decreased and the strength went down significantly (see Table 5.1). Cavities forming can be explained by boiling water which released by chemical reaction of geopolymerization process and could not go out by quickly cured outer layers of composite.

From Fig. 5.12 and Appendix A, Fig. A.3 to A.7 exhibit the SEM images on the sections perpendicular to fibers and surfaces of the geocomposites based on geopolymer matrices M1, M2 and reinforced by carbon HTS 5631 1600tex 24K, basalt BCF13 - 2520tex - KV12 Int. and Saint-Gobain - Vetrotex E-glass E2400P192 fibers respectively. In general, the pictures show that the adhesion between this gopolymer matrix and carbon, basalt or E-glass fiber seems quite good. With higher magnification, however, the micro-cracks are determined as the typical micro-cracks of gepolymer composites. Typically, geopolymer matrices are considered like a kind of inorganic matrices, so the existing of micro-cracks can be considered as inborn defects of inorganic matrix composite materials [8].

The volume fraction of fiber in composite is determined via counting fibers on a SEM image of a composite in cross-section. Fig 5.13 presents the typical SEM images which are used to calculate the volume percentage of fibers in appropriate geocomposites. The results of calculation of volume fraction of fibers are summarized in Table 5.7.

Table 5.7 volume percentage of fibers [vol.%] in geocomposites via SEM images

Matrix	**Reinforcement**		
	Carbon	**Basalt**	**E-glass**
M1	45.8 ±1.1	52.1 ±1.5	61.3 ±1.4
M2	46.3 ±2.3	53.9 ±1.9	59.6 ±1.7

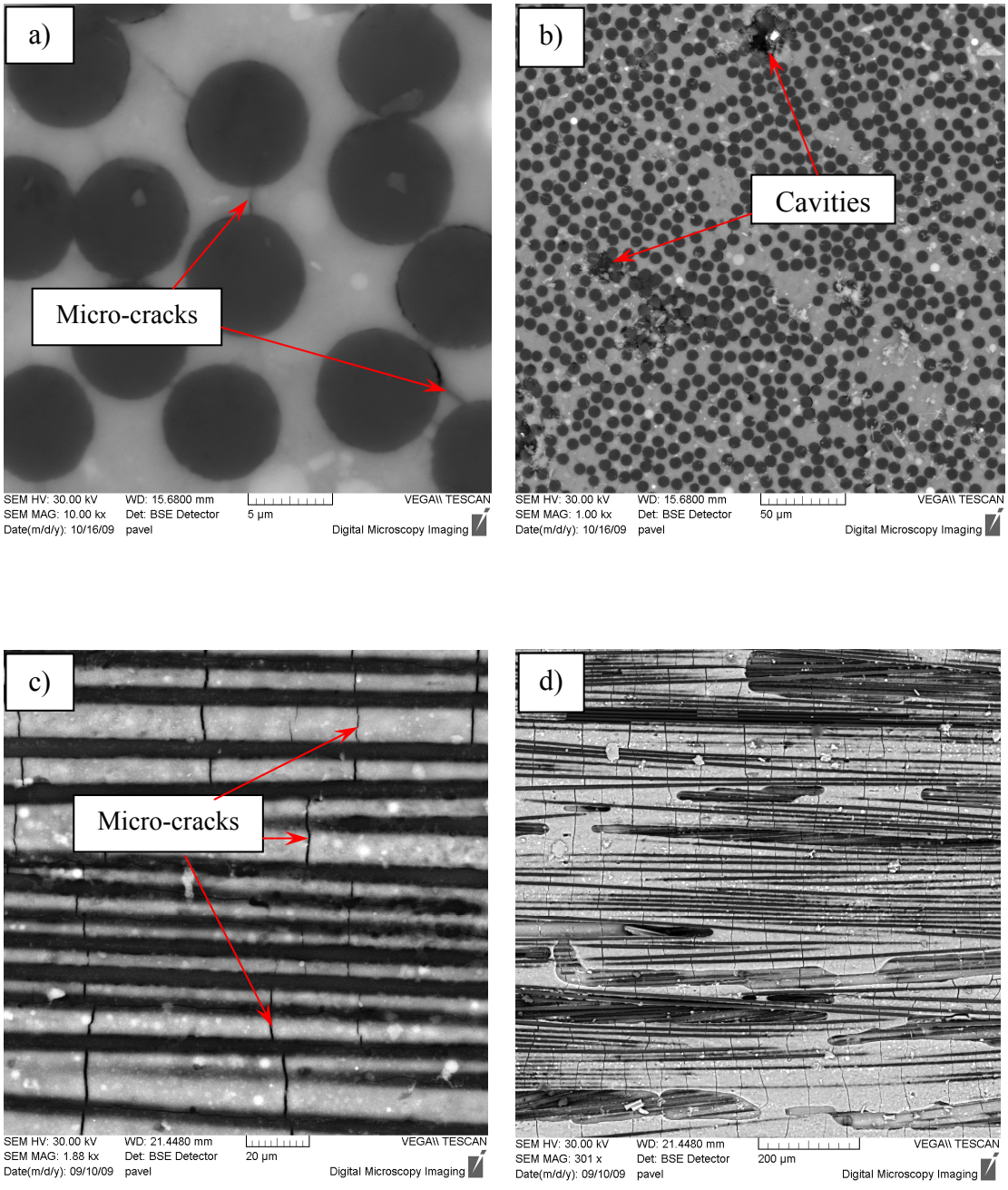

Fig. 5.12 Typical SEM images of M1/Carbon curing at 65 ^{o}C on sections perpendicular to fibers a) 10000x, b) 1000x and surfaces of composite c) 1880x and d) 301x.

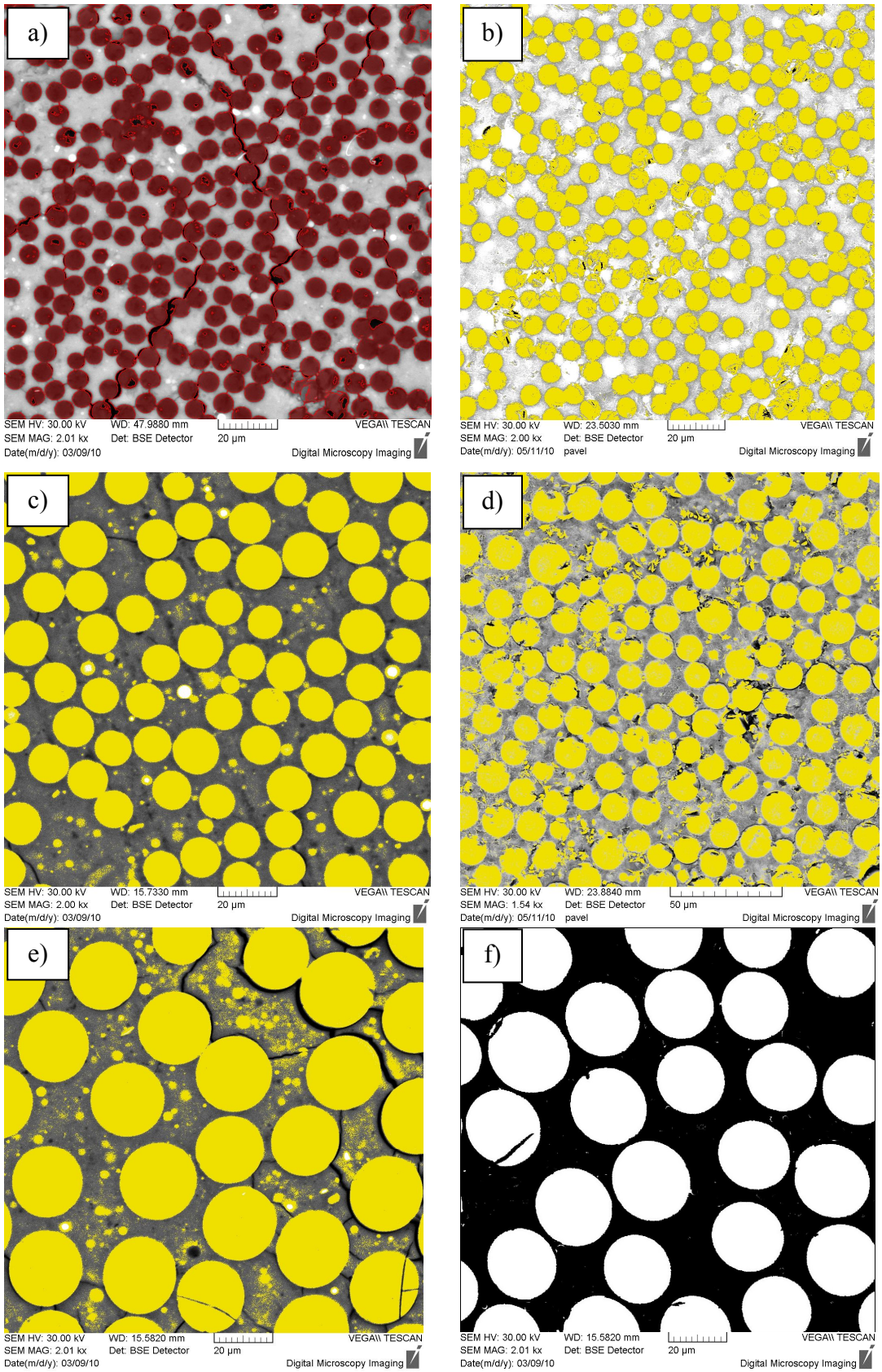

Fig. 5.13 Typical SEM images for volume fraction of fibers a) M1-C, b) M2-C, c) M1-B, d) M2-B, e) M1-E glass and f) M2-E glass with magnation around 2000x.

5.4 CONCLUSIONS

The main mechanical properties of geocomposites based on geopolymer matrices M0, M1 and M2 reinforced by approximately 45, 53 and 60 vol.% of unidirectional fibers of carbon HTS 5631 1600tex 24K, basalt BCF13 - 2520tex - KV12 Int. and Saint-Gobain - Vetrotex E-glass E2400P192 fibers respectively are strongly dependent on the curing temperature. In addition, the mechanical parameters are different when utilizing each span of testing with popular standards for ceramic matrix composites reinforced by continuous fibers, such as ASTM C 1341 – 06 and/or DIN V ENV 658-3:1993-02.

From the practical point of view, even using the standards which are used in ceramic matrix composites or "size-independent method", the temperature interval from 60 to 90 °C has been generally recommended for curing the geocomposites. At lower temperatures there is a danger of unsatisfactorily created bonds between matrix and fiber, and the rate of hardening can be unacceptable from technical standpoint. At higher temperatures the heating can enlarge voids and total porosities. In both cases the lower mechanical properties are determined.

Gopolymer matrices possess a high pH generally, which can frequently damage glass fibers by both chemical and physical means, severely degrading its strength. Even the cured matrices still exhibit a high pH in a solid form, which continues to promote glass fiber degradation. So, the physical performance of E-glass fibers geocomposite usually is extremely poor. Especially when these geocomposites are cured at higher temperature for M1/E-glass.

Because carbon fibers are electrically and thermally conductive, which eliminates many important dielectric and thermal insulating applications. In addition, carbon fibers are several times more expensive than glass fibers and carbon fibers severely oxidize at 450 ^{o}C., which eliminates many important high temperature applications. Also, when carbon fibers are combined with the alkali silicate matrix they have two different thermal expansion coefficients, which can lead to microcracking during thermal cycling [8, 90]. All these factors should carefully take into account for future applications.

6. EFFECTS OF CURING TIME ON MECHANICAL PROPERTIES

6.1 INTRODUCTION

Time of curing is determined as one of two deciding important factors of curing procedure to properties of geopolymer composite systems [8, 43, 111-113]. In addition, the curing time must be highly relevant to labor productivity and finally is the energy of fabrication process and cost of the productions.

In this chapter we try to determine the effects of curing time at optimal elevated temperature and at ambient conditions on the mechanical properties of reinforced geocomposites containing the same volume fraction of as the composites which are tested in the Chapter 5, approximately 45, 53 and 60 vol.% of unidirectional fibers of carbon HTS 5631 1600tex 24K, basalt BCF13 - 2520tex - KV12 Int. and Saint-Gobain - Vetrotex E-glass E2400P192 fibers respectively. From these results, the optimal procedure for curing geocomposites based on thermal silica geopolymer matrices is recommended.

6.2 EXPERIMENTAL

6.2.1 PREPARATION OF COMPOSITE SPECIMENS

The procedure of settling samples, which is utilized here, is the same as method that is described in details in Chapter 3 and used widely in previous Chapter 5. After the resin saturated fibers are set into the mold and covered by a peel ply fabric and suction tissue, the mold is placed into a good sealed plastic bag.

For curing materials, three stages with help of currently used technique of vacuum bagging are recommended again. In the first stage at room temperature for 1 hour, the purpose of this is to remove air bubble and superfluous resin. In the second stage of processing, the samples are cured at elevated temperature in a oven with technique called “hot vacuum bagging” in interval optimal temperature range of curing. As considering in the previous chapter, the second stage of curing is supposed that is strongly effect mechanical properties of composites and the most consuming energy of

the composite fabrication with vacuum bagging and elevated temperature of the oven. Based on the results of the Chapter 5, we used 80 ^{o}C for M1 composite system and 85 ^{o}C for M2 composite system, for 1, 3, 4, 6 and 7 hours in the oven to cure the samples. Finally, the specimens are released from bags, dried open in the oven at the same temperature for other 5 hours more. The time of curing with three stages are abbreviated as 1:01:05, 1:03:05 and so on for the curing time (hour) of the first, the second and the third stage of curing process respectively.

Assuming that open porosities of composites decrease when the composites are cured at lower temperature and the less effects of alkaline medium on fiber reinforcements, especially for E-glass fiber, investigation of mechanical properties of geocomposites cured at ambient conditions is carried out. For fabrication of specimens, the same technique is used. After samples are cured under a technique called “vacuum bagging” at first at room temperature for 1 hour in order to remove air bubble and superfluous geopolymeric resin by a peel ply fabric and suction tissue, however, they are continued to cure at the ambient conditions with temperature about 20 ±2 ^{o}C and relative humidity 65% in 1, 2, 4, 7, 14 and 30 days for geocomposite M1 system and in 4, 7, 14 and 30 days for geopolymer composite M2 system.

All resulting samples are cut-up to suit the planned spans of testing. Only rough surface treatment with emery paper is applied.

6.2.2 MECHANICAL TESTING SETUP AND DATA TREATMENT

The mechanical properties are tested and evaluated by three-point bending under center-point load at various outer support span-to-depth ratios L/H = 16 to 1, 20 to 1 for composites cured at elevated temperatue and ambient conditions and 40 to 1 for only composites cured at ambient conditions (in proportion to support spans L = 50, 64 and 120 mm respectively) on Universal Testing Machine, Model Type: INSTRON Model 4202 in ambient conditions. The displacement rate of crosshead is 2 mm/min.

The results are presented in accordance with DIN V ENV 658-3:1993-02 (L/H = 20 to 1) and ASTM C 1341 – 06 (L/H = 16 to 1). Experimental findings even show that, however, both flexural strength and modulus are dependent on the spans of

testing. New method based on the Tarnopolsky's theory (Chapter 3) is utilized to valuate the virtual flexural module E^* and virtual flexural strength $R^*_{mo.}$

The microstructure and interaction between fibers and geopolymer matrix are also study via the SEM images on the polishing sections perpendicular to fibers and surfaces of the composites.

6.3 RESULTS AND DISCUSSION

6.3.1 EFFECTS OF CURING TIME AT ELEVATED TEMPERATURE

The results of effects of curing time on two main flexural parameters, strength and modulus, are summed up from six samples for both and presented in Table 6.1, 6.2, Apendix B, Table B.3 and B.4 in both standards and ASTM C1341 – 06. However for visual estimation, only results in accordance with DIN EN 658-3:2002 (L/H = 20 to 1) are presented on Fig. 6.1, 6.2, 6.3 and 6.4.

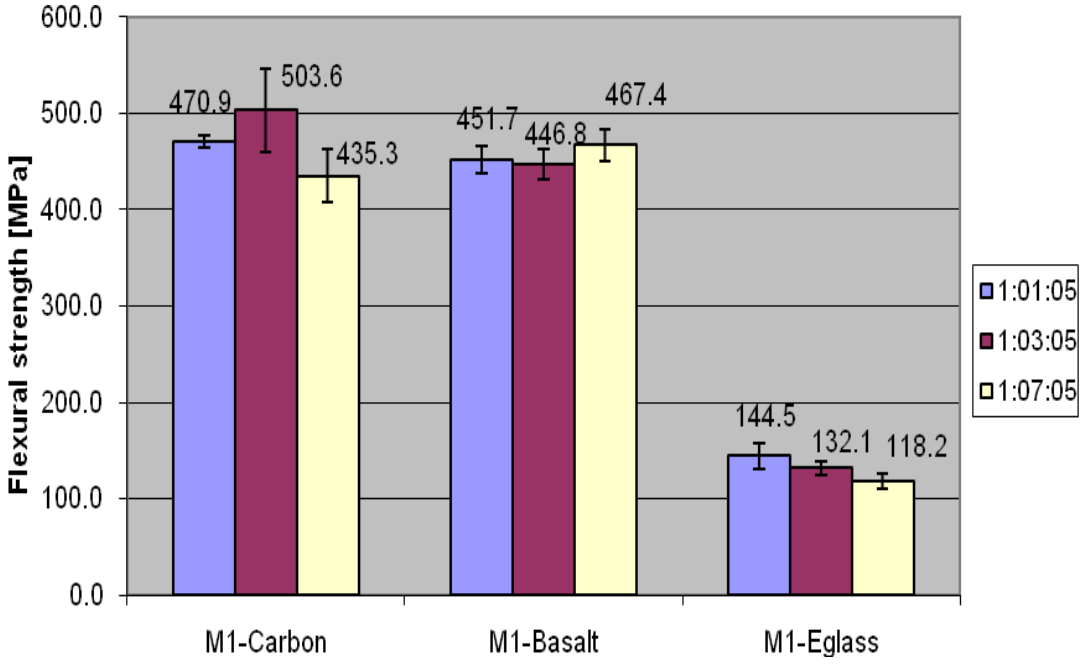

Fig. 6.1 Effects of curing time on flexural strength of geopolymer composite M1 system in accordance with DIN EN 658-3:2002 (L/H = 20 to 1).

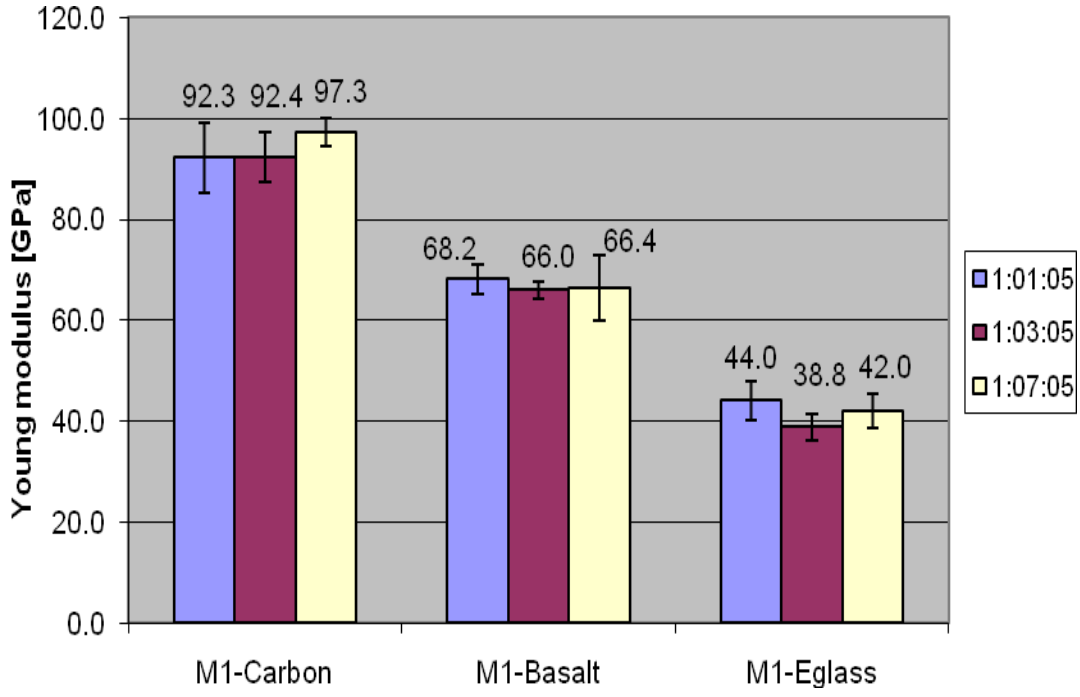

Fig. 6.2 Effects of curing time on flexural modulus of geopolymer composite M1 system in accordance with DIN EN 658-3:2002 (L/H = 20 to 1).

From Table 6.1, 6.2, B.3, B.4 and Fig. 6.1 to 6.4 we can see that the mechanical properties of geopolymer composites are nearly constant when they are cured at room temperature under vacuum bagging for 1 hour as the first stage and for 1, 3, 4, 6 or 7 hours in the oven at optimal elevated temperature under hot vacuum bagging as the second stage of curing process. From these results, one important conclusion can be drawn that is the time for curing these composites at the second stage under hot vacuum bagging technique is not necessary to last longer than 1 hour. Extra experiments show that no shorter time in this stage of process, however, could be used because of limited time for the composites hardening enough to remove from the mold.

Utilizing Tarnopolsky's theory, from linear regression of a fictitious Young's modulus E and a fictitious flexural strength R_{mo} against $(H/L)^2$ (reciprocal span: height ration) value of composites cured at time 1:01:05 hour, the virtual mechanical properties of composites including virtual modulus (E^*), shear modulus (G), and virtual flexural strength (R^*_{mo}) are estimated. The results are presented on Fig. 6.5, C.1 and Table 6.3. However, the large error must be involved in extrapolation.

Table 6.1 Flexural properties of geocomposites M1 system at L/H = 20 to 1.

Composites	Curing time						Average	
	1:1:5		1:3:5		1:7:5			
	R_{mo} [MPa]	E [GPa]	R_{mo} [MPa]	E [GPa]	R_{mo} [MPa]	E [GPa]	R_{mo} [MPa]	E [GPa]
M1-Carbon	470.9	92.3	503.6	92.4	435.3	97.3	**469.9 ±27.9**	**94.0±2.4**
M1-Basalt	451.7	68.2	446.8	66.0	467.4	66.4	**455.3 ±8.8**	**66.8±1.0**
M1-Eglass	144.5	44.0	132.1	38.8	118.2	42.0	**131.6 ±10.8**	**41.6±2.2**

Table 6.2 Flexural properties of geocomposites M2 system at different curing time at outer support span-to-depth ratios L/H = 20 to 1.

Composites	Curing time										Average	
	1:01:05		1:03:05		1:04:05		1:06:05		1:07:05			
	R_{mo} [MPa]	E [GPa]	R_{mo} [MPa]	E [GPa]	R_{mo} [MPa]	E [GPa]	R_{mo} [MPa]	E [GPa]	R_{mo} [MPa]	E [GPa]	R_{mo} [MPa]	E [GPa]
M2-Carbon	355.7	106.6	325.4	109.1	319.5	109.3	318.4	97.8	322.4	103.6	**328.3 ±13.9**	**105.3 ±4.3**
M2-Basalt	273.1	65.9	220.9	59.9	273.5	63.8	219.9	53.7	224.9	54.5	**242.5 ±25.2**	**59.5 ±4.8**
M2-Eglass	202.0	56.6	179.0	62.3	191.8	62.7	177.4	60.2	182.3	59.5	**186.5 ±9.2**	**60.3 ±2.2**

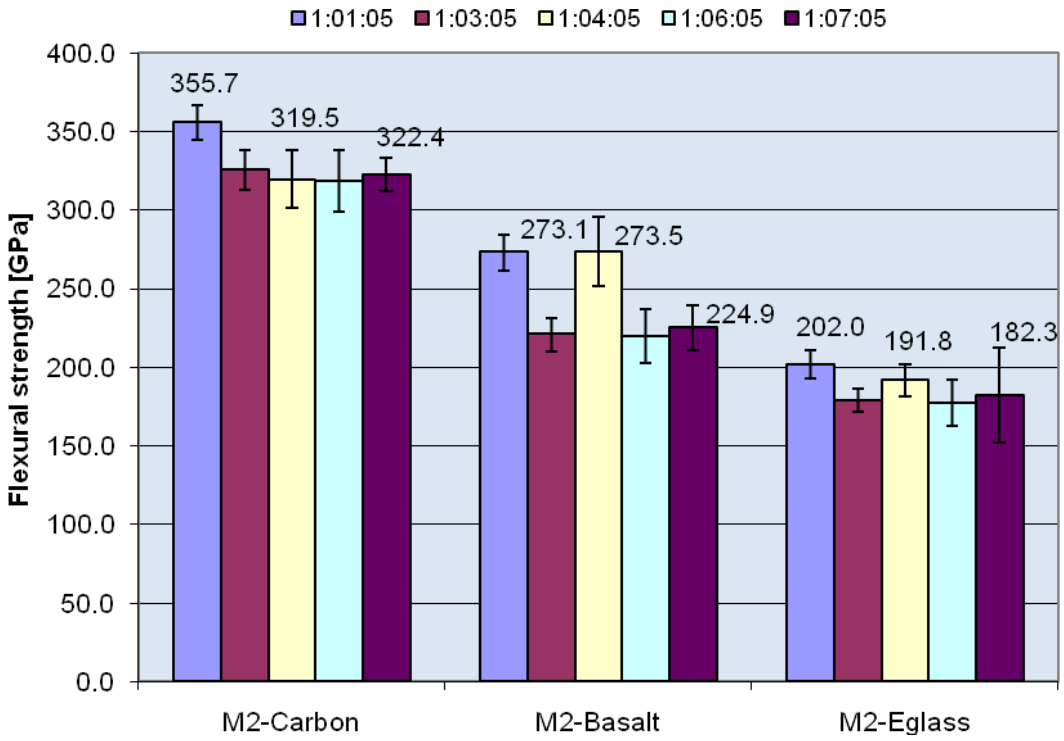

Fig. 6.3 Effects of curing time on flexural strength of geopolymer composite M2 system at ratio L/H = 20 to 1.

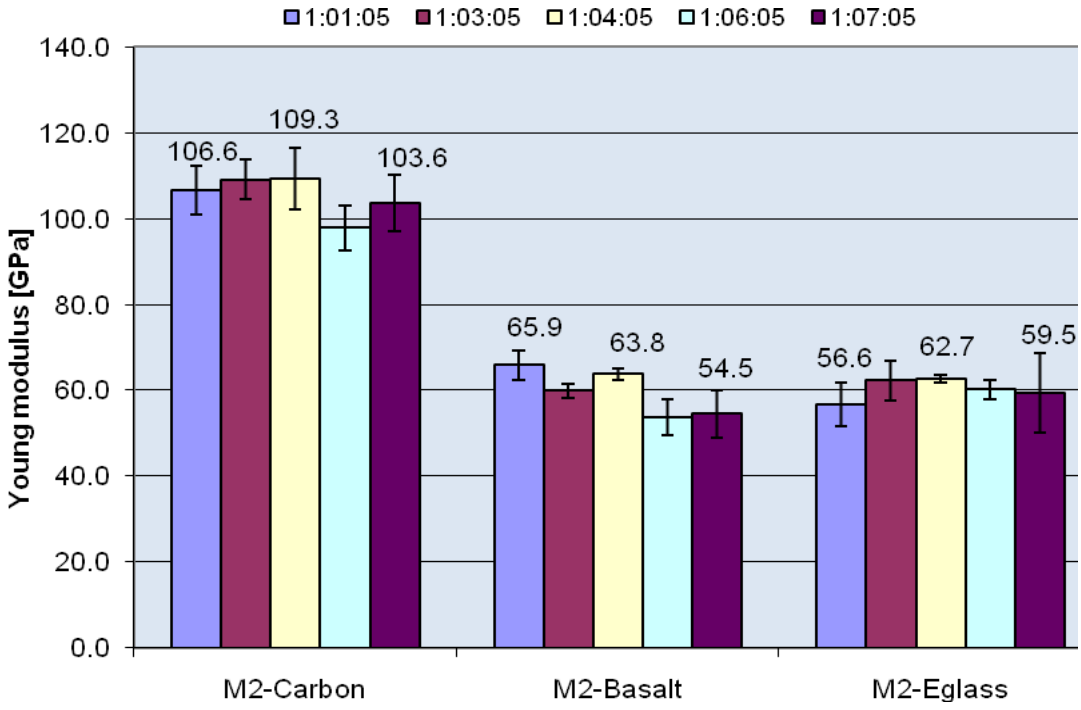

Fig. 6.4 Effects of curing time on flexural modulus of geopolymer composite M2 system at ratio L/H = 20 to 1.

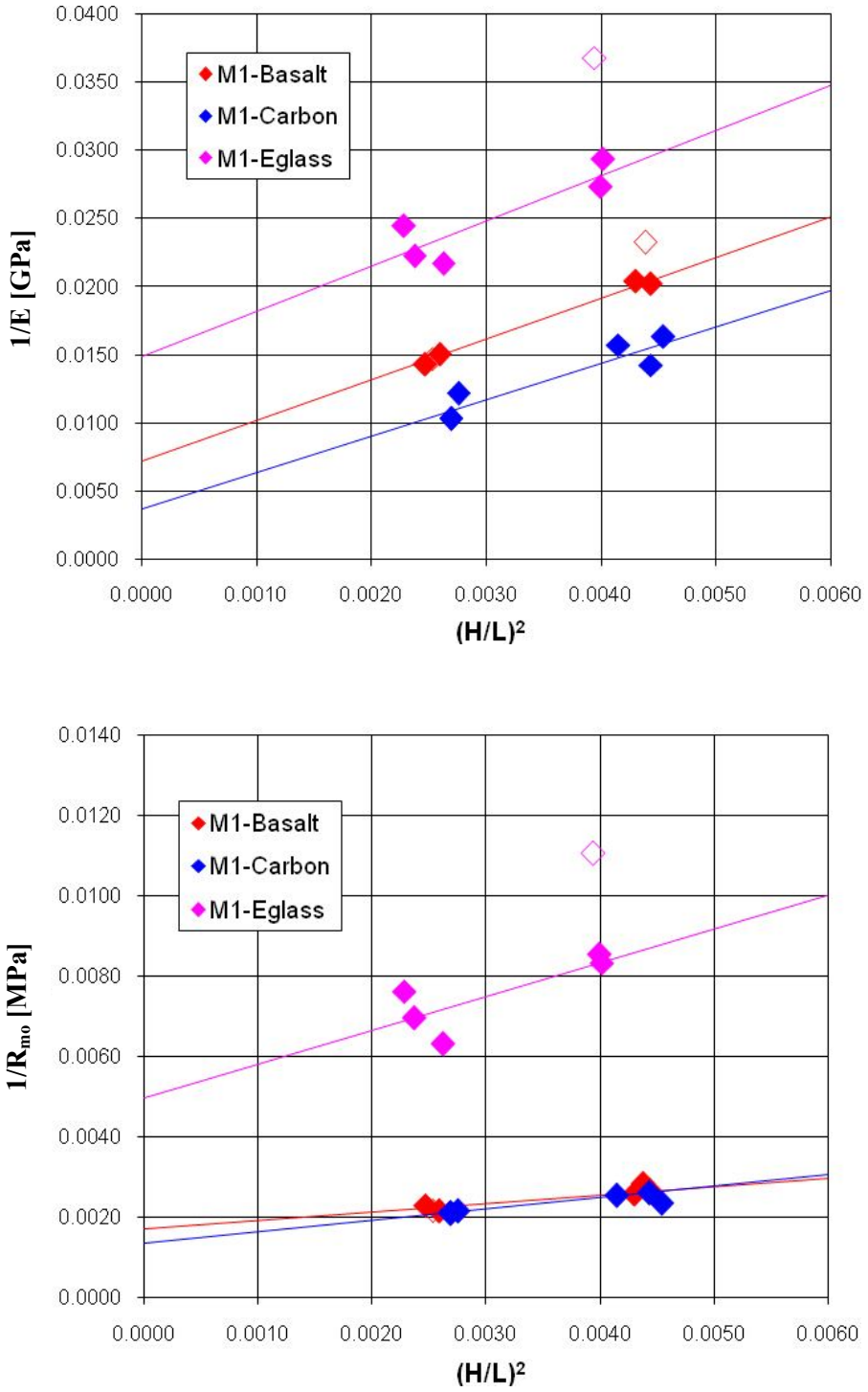

Fig. 6.5 Linear regression of reciprocal effective values 1/E and $1/R_{mo}$ vs $(H/L)^2$ of geocomposites M1 system for curing time 1:01:05 at 80 ^{o}C.

Table 6.3 Virtual flexural properties of geopolymer composites cured at time 1:01:05 hours in accordance with size-independent method

Composites	Young's module			Shear module	E^*/G	Strength		
	E^*			G		R^*_{mo}		
	[GPa]			[GP]	[1]	[MPa]		
M1-basalt	139.0	±10.7	7.7%	0.4	352.7	583.5	±51.3	8.8%
M2-basalt	91.7	±7.7	8.4%	0.7	125.0	424.4	±74.1	17.5%
M1-carbon	271.8	±14.1	5.2%	0.4	616.5	739.9	±29.2	4.0%
M2-carbon	171.5	±17.9	10.4%	1.0	168.4	602.3	±89.0	14.8%
M1-E-glass	67.4	±15.1	22.3%	0.4	190.2	200.9	±48.7	24.3%
M2-E-glass	72.7	±18.2	25.0%	0.7	98.6	300.0	±32.5	10.8%

6.3.2 EFFECTS OF CURING TIME AT AMBIENT CONDITIONS

The flexural properties of composites are determined under three-point bending mode in accordance with DIN EN 658-3:2002. The flexural tests are conducted over a simply supported span of 64 mm with a center-point load by Universal Testing Machine INSTRON Model 4202 (maximum load of the sensor: 10 kN); The deflection control with a mid-span deflection rate of 2 mm/min, at ambient conditions.

The dependence of mechanical properties of geocomposites on days of curing at ambient condition is summarized on Table 6.4 and 6.5, accompanying with visual presentation on Fig. 6.6.

It is easy to be seen form Table 6.4 and Fig. 6.5 that the properties of geopolymer M1, high molar ratio Si/Al = 11.3 and boric acid as functional additive, reinforced by the carbon, basalt or E-glass fibers are approximately constant after 14 days of curing at ambient conditions, which means that the geopolymerization process seems completed after this period of curing time. The flexural properties of geocomposite M2 system with lower molar ratio Si/Al = 10 and addition of phosphoric acid, however, still possessed an increase trend although after curing 30 days at ambient conditions (see Table 6.5 and Fig. 6.6).

Table 6.4 Flexural properties of composites based on M1 system at ratio L/H = 20 to 1

Days of ambient curing	Carbon fiber			Basalt fiber			E glass fiber		
	R_{mo} [MPa]	E [GPa]	ε_{mo} [%]	R_{mo} [MPa]	E [GPa]	ε_{mo} [%]	R_{mo} [MPa]	E [GPa]	ε_{mo} [%]
1	372.8	60.1	0.92	410.3	40.9	1.92	300.1	43.7	0.91
2	450.0	76.2	0.74	429.2	44.5	1.41	357.1	48.7	0.87
4	500.4	77.2	0.75	464.4	40.9	1.34	369.5	49.6	0.82
7	557.0	74.2	0.90	484.8	47.4	1.30	372.1	46.6	0.96
14	674.6	97.7	0.78	529.5	50.1	1.09	389.4	47.3	0.75
30	667.6	98.6	0.86	532.4	56.6	1.11	388.6	50.6	0.78

Table 6.5 Flexural properties of composites based on M2 system at ratio L/H = 20 to 1

Days of ambient curing	Carbon fiber			Basalt fiber			E glass fiber		
	R_{mo} [MPa]	E [GPa]	ε_{mo} [%]	R_{mo} [MPa]	E [GPa]	ε_{mo} [%]	R_{mo} [MPa]	E [GPa]	ε_{mo} [%]
4	105.1	32.4	0.51	98.7	24.0	0.74	101.1	32.8	0.47
7	203.8	68.5	0.38	157.1	31.8	0.62	136.2	39.7	0.44
14	214.4	70.5	0.37	182.5	41.9	0.56	166.0	39.8	0.47
30	352.3	119.7	0.58	182.4	51.5	0.49	153.9	46.8	0.54

For geopolymer matrix M1 system, if we consider that the composites nearly cured after 14 days of curing at ambient conditions with 100% of flexural strength and modulus of M1/Carbon, M1/Basalt, M1/E-glass are 674.6, 532.4, 388.6 MPa and 98.6, 56.6 or 50.6 GPa respectively, in general, we can see that after 24 hours curing at ambient conditions the flexural strength are 56% (372.8 MPa), 77% (410.3 MPa) or 77% (300.1 MPa) and the bending moduli are 61% (60.1 GPa), 72% (40.9 GPa) or 86% (43.7 GPa) in comparison with those of from geocomposites cured over 14 days for composite M1/Carbon, M1/Basalt, M1/E-glass respectively.

On the other hand, composites based on geopolymer matrix M2 system need at least 4 days at ambient conditions of curing to achieve approximately 30% of flexural strength and modulus of composite cured after 30 days for M2/Carbon (105.1 MPa of the strength and 32.4 GPa of modulus compared to 352.2 MPa and 119.7 Gpa respectively). The values for M2/Basalt are 50 % and nearly 70 % for M2/E-glass.

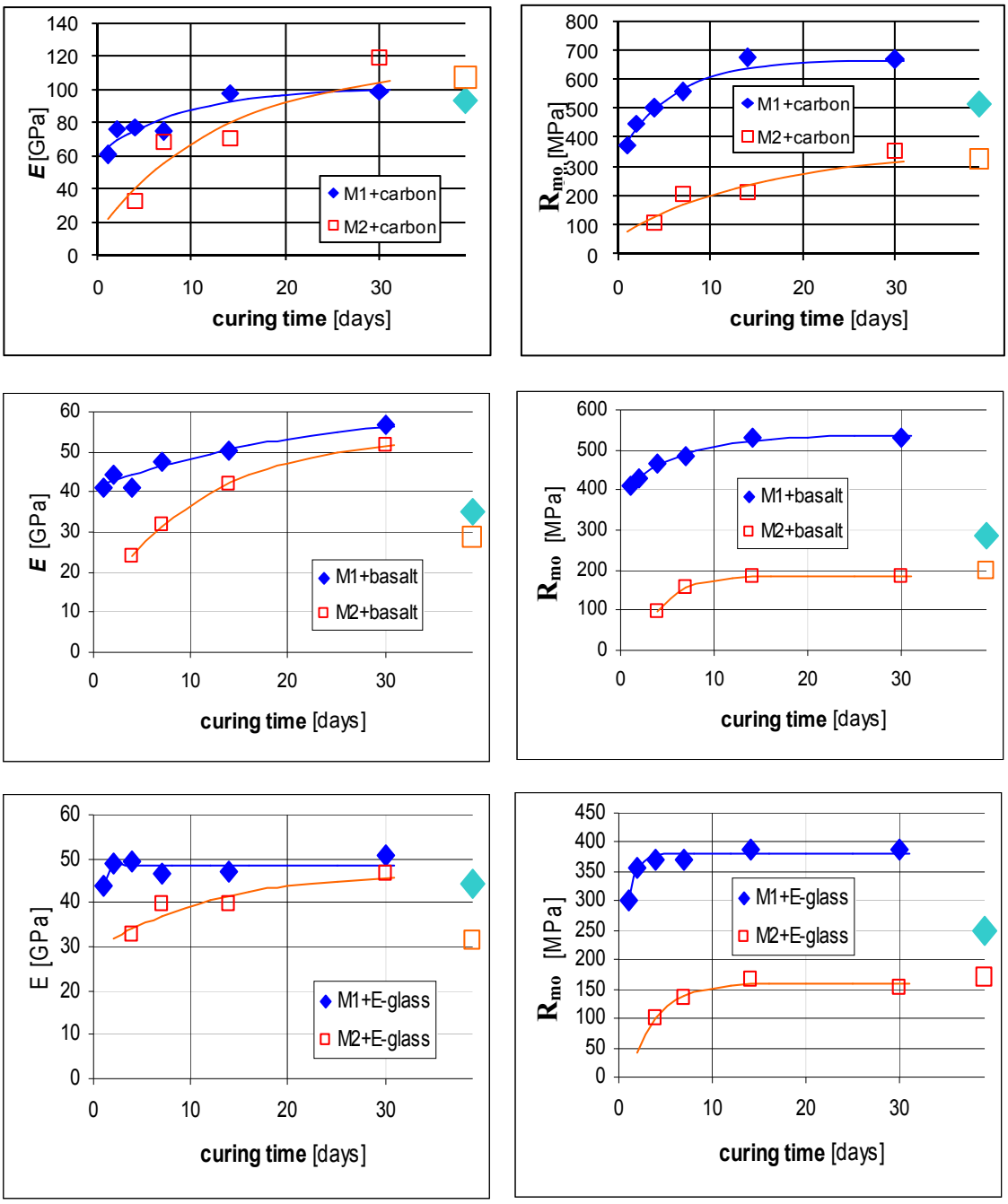

Fig. 6.6 Effects of curing time on mechanical properties of geopolymer composites curing at ambient conditions at ratio L/H = 20 to 1.

In comparison with mechanical properties of geocomposites cured at optimal elevated temperature in Table 6.1 and Table 6.2 (the same conditions of samples and testing), a remarkable difference for M1 composite system. When the composites cured at ambient conditions, the strength can be improved over 40% for M1/carbon (674.6 MPa compared to 469.9 MPa), nearly 17% for M1/Basalt (529.5 MPa in contrast with 455.3 MPa) and specially 195% of strength higher for M1/Eglass (389.4 MPa in comparison with 131.6 MPa). We can see that the higher curing temperature the worse degradation of E-glass is determined and lower strength of the composite. However, there is no difference of the Young's modulus of the composites in both cases of curing.

For the composites based on geopolymer matrix M2, the mechanical properties show nearly the same when the composites cured at optimal elevated temperature and cured at ambient conditions after 30 days (see Table 6.2 and Table 6.5). The functional additive (phosphoric acid) can improve the stability of glass fiber in high alkaline medium in this case.

New rotary oil vacuum pump with **c**apacity: 2.3 m^3/h (38.33 liter/min) and lower vacuum pressure: 20 kPa (Fig. 6.7) is used to prepare composites samples and cured at ambient condition for over 40 days for M1 composite system and over 50 days for M2 composite system. The resulted composites must be more condensable and has brought better mechanical properties.

The resulting composite sampless are cut up appropriate length for testing, mechanical properties of the composites are determined in accordance with ASTM C3141 – 06 and DIN V ENV 658-3: 1993-02 at various outer support span-to-depth ratios. The results are collected in Table 6.6. In this investigation Multi-End Roving S-glass SC 660 with tensile strength over twice higher than that of E-glass is used as more options for further application choice.

Table 6.6 Flexural properties of geocomposites cured at ambient conditions for over 40 days for M1 and 50 days for M2 at various outer support span-to-depth ratios

Matrix/ fiber	Outer support span-to-depth ratio								
	L/H = 16 to 1			L/H = 20 to 1			L/H = 40 to 1		
	R_{mo} [MPa]	E [GPa]	ε_{mo} [%]	R_{mo} [MPa]	E [GPa]	ε_{mo} [%]	R_{mo} [MPa]	E [GPa]	ε_{mo} [%]
M1/Carbon	668.9 ±80.5	111.2 ±2.7	0.74	800.4 ±7.5	125.9 ±4.4	0.74	1149.9 ±104.4	150.0 ±3.9	1.05
M1/Basalt	526.1 ±47.7	51.6 ±2.1	1.28	678.7 ±45.3	62.5 ±4.0	1.35	772.3 ±36.7	77.7 ±1.1	1.24
M1/E-glass	217.5 ±25.0	52.3 ±3.8	0.68	260.2 ±39.1	58.9 ±3.6	0.54	418.2 ±29.6	80.8 ±7.5	0.67
M1/S-glass	762.3 ±27.0	68.5 ±1.6	1.42	812.4 ±30.0	66.9 ±0.4	1.58	800.4 ±3.0	78.2 ±2.9	1.47
M2/Carbon	449.6 ±33.0	92.1 ±1.5	0.65	559.0 ±32.8	110.2 ±3.5	0.60	990.0 ±99.9	126.1 ±3.2	0.89
M2/Basalt	250.6 ±3.3	52.1 ±5.7	0.61	334.8 ±41.3	57.9 ±1.2	0.66	605.2 ±13.1	67.4 ±1.6	1.06
M2/E-glass	206.4 ±13.4	51.1 ±2.9	0.59	267.3 ±25.6	61.6 ±1.4	0.54	428.7 ±93.6	71.3 ±1.9	0.72
M2/S-glass	394.0 ±8.1	58.5 ±3.9	0.82	471.7 ±20.6	63.1 ±1.0	0.85	670.8 ±11.0	70.9 ±1.9	1.06

Fig. 6.7 Rotary oil vacuum pump.

Table 6.6 presents excellent mechanical properties of composites based on thermal silica geopolymer matrices. Utilizing rotary oil vacuum pump (Fig. 6.7) with more power of capacity and lower vacuum pressure in comparison with a membrane vacuum pump (Fig. 3.7) can improve significant mechanical properties of the geocomposites. At the same outer support span-to-depth ratio L/h = 20 to 1 (see Table 6.4 and 6.6), flexural strength of M1/carbon is 20 % higher (800.4 MPa compared to 667.6 MPa) and flexural modulus is about 25% better (125.9 GPa in contrast to 98.6 GPa). For composite M1/Basalt, approximately 27% of the strength and 11% of the modulus are improved (678.7 MPa and 62.5 GPa in comparison with 532.4 MPa and 56.1 GPa respectively). Conversely, for higher compact composites and longer time can cause more effects of chemical and physical degradation on properties of E-glass fibers, the mechanical properties of composites M1/E-glass decreases as a consequence.

Obviously, from Table 6.5 and 6.6, using better vacuum pump and longer time of curing at ambient conditions can enhance the remarkable mechanical properties of all

composites based on geopolymer M2 matrix. Around 58%, 83% and 73% of flexural strength of M2/Carbon, M2/Basalt and M2/E-glass respectively (559.0, 334.8 and 267.3 MPa compared to 352.3, 182.4 and 153.9 MPa). However, the Young's modulus of M2/Carbon keeps nearly constant (119.7 GPa in contrast to 110.2 GPa) and only about 10% and 30% of flexural modulus of M2/Basalt and M2/E-glass are improved respectively (57.9 and 61.6 GPa compared to 51.5 and 46.8 GPa).

As can be seen from Table 6.6 that, the main flexural parameters of geocomposites even show different values at different support span-to-depth ratios, the novel size-independent method is used to evaluate the virtual Young's modulus (E*), shear modulus (G), and flexural strength (R^*_{mo}) when $(H/L)^2 \rightarrow 0$. The regression lines are shown on Fig. 6.8 and Appendix C - Fig. C.2; and the properties are summed up in Table 6.7.

Table 6.7 Virtual flexural properties of geocomposites cured at ambient conditions in accordance with novel size-independent method

Matrix/ fiber	Flexural modulus			Shear modulus	E^*/G	Flexural strength		
	E*			G		R^*_{mo}		
	[GPa]			[GPa]	[1]	[MPa]		
M1/Carbon	**161**	±4	±3%	1.45	111	**1280**	±191	±15%
M1/Basalt	**87**	±5	±5%	0.61	141	**850**	±49	±6%
M1/E-glass	**86**	±6	±7%	0.51	169	**507**	±45	±9%
M1/S-glass	**78**	±4	±5%	2.19	36	**863**	±31	±4%
M2/Carbon	**140**	±6	±4%	1.33	105	**1159**	±177	±15%
M2/Basalt	**72**	±6	±9%	0.77	94	**790**	±126	±16%
M2/E-glass	**77**	±2	±3%	0.78	99	**625**	±169	±27%
M2/S-glass	**74**	±4	±5%	1.25	59	**761**	±49	±6%

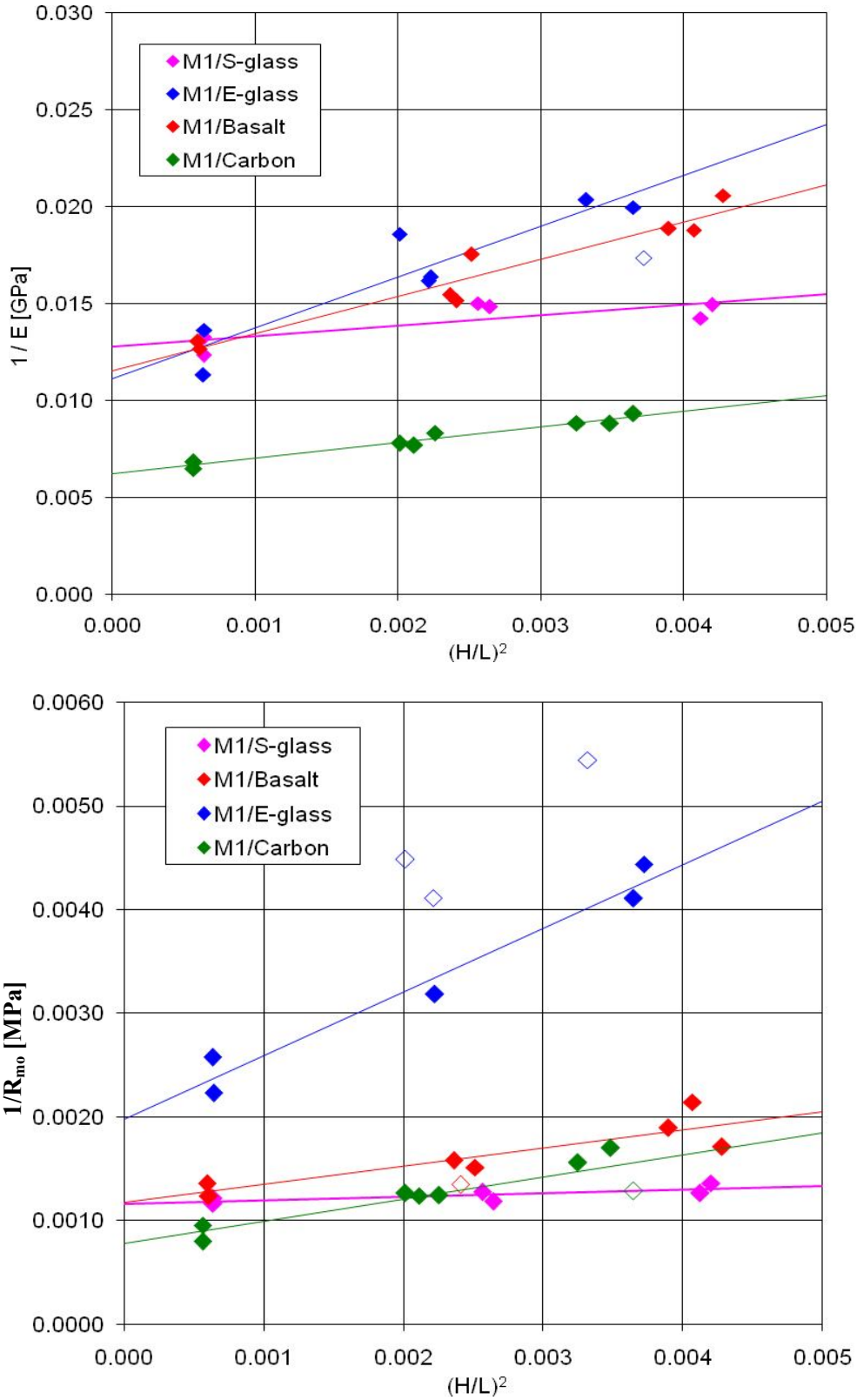

Fig. 6.8 Linear regression of reciprocal effective values 1/E and $1/R_{mo}$ vs $(H/L)^2$ of geocomposites M1 system cured at ambient condition for over 40 days.

6.4 FAILURE BEHAVIOUR OF THE GEOCOMPOSITE

In general, reported data for unidirectional fiber composites tested in flexure are more extensive than in uniaxial tension [14, 15]. Fig. 6.9 and Appendix D.1 present the typical comparison of stress-strain curves for unidirectional fiber reinforced geocomposites of different curing conditions tested in flexure with outer support span-to-depth ratio L/H = 20 to 1 and at room temperature. With a particular observation on these pictures leads to following considerations:

- Most of the composites exhibit seemly bilinear relationships, this behavior is a very typical reaction induced by matrix cracking or cracking of the interface [121].
- At the initial portion of the curve shows nonlinear region of "toe" region (AC) and followed by a linear region (BC) as shown in Fig. 6.19a for example. Generally, toe region may be considered as an artifact of the test specimen or test conditions (for example, straightening of a warped test specimen, or a take up of slack and alignment or seating of test specimen) and thus does not represent the properties of the materials. The correction shall be used for measurements of deflection and strain [99]. In our research, however, the relative comparison is considered as the main objective, therefore the toe correction is overlooked.
- The fact that the matrix composition (M1 and M2) and fabrication conditions play an important role in not only mechanical properties but also fracture manners, these can be seen as well from Fig. 6.9 and D.1. For instant, at the same curing condition, two composites M1/Carbon (Fig. 6.9a) and M2/Carbon (Fig. D.1a) or two same kind composites M1/Basalt composites (Fig. 6.9c and 6.9d) manufactured through different curing processes present entirely different behaviors.

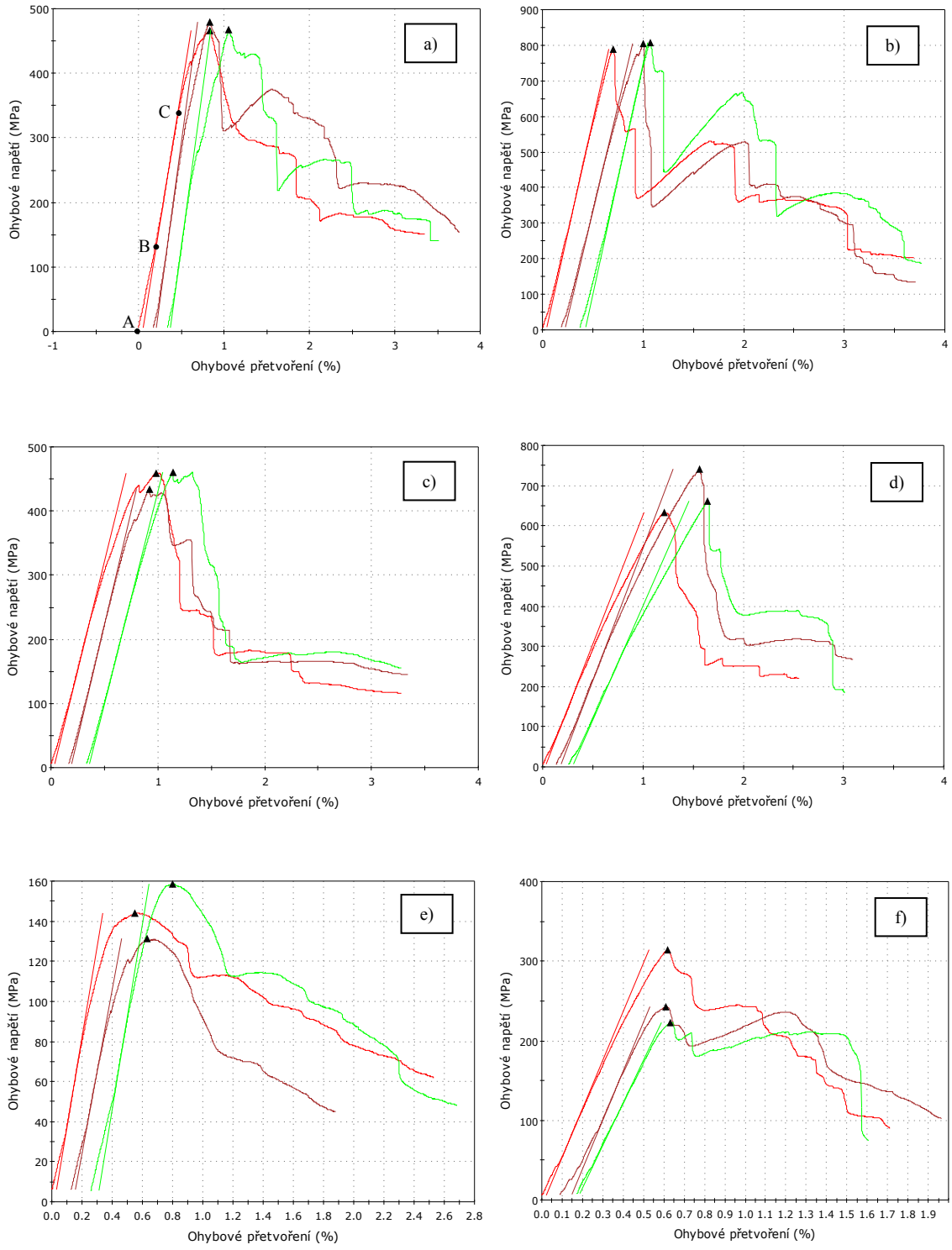

Fig. 6.9 Typical stress – strain relationships of unidirectional geocomposites based on M1 geopolymer matrix tested in flexure at L/H = 20 to 1, a) M1/C, c) M1/B and e) M1/E-glass cured at time 1:1:5 hours at 80 ^{o}C and b) M1/C, d) M1/B and f) M1/E-glass cured at ambient conditions for over 40 days.

Experimental findings show that at span of testing 50 mm or 64 mm (corresponding with ratio L/H = 16 to 1 and L/H = 20 to 1) the main failure pattern of the composite samples are delamination due to shear stress (see Fig. 6.10). At higher outer support span-to-depth ratio L/H = 40 to 1 (testing span 120 mm), however, under the bending moment some kinds of specimens produce compressive failure in the outer fiber surfaces of the composites (Fig. 6.11). These behaviours of the composites seem to meet the demands of standard ASTM C134-06 and the mechanical properties of composites tested at the span get nearly 90 % compared to the virtual values achieved by regression method. For example, when testing the mechanical properties of geocomposite M1/Basalt at L/H = 40 to 1 we can achieve 772.3 MPa of flexural strength and 77.7 GPa of flexural modulus, meanwhile the virtual values are 850 MPa and 87 GPa are determined when using regression of extrapolation theory when $(H/L)^2 \rightarrow 0$. In this case, the typical curve of stress – strain relationship is shown on Fig. 6.12.

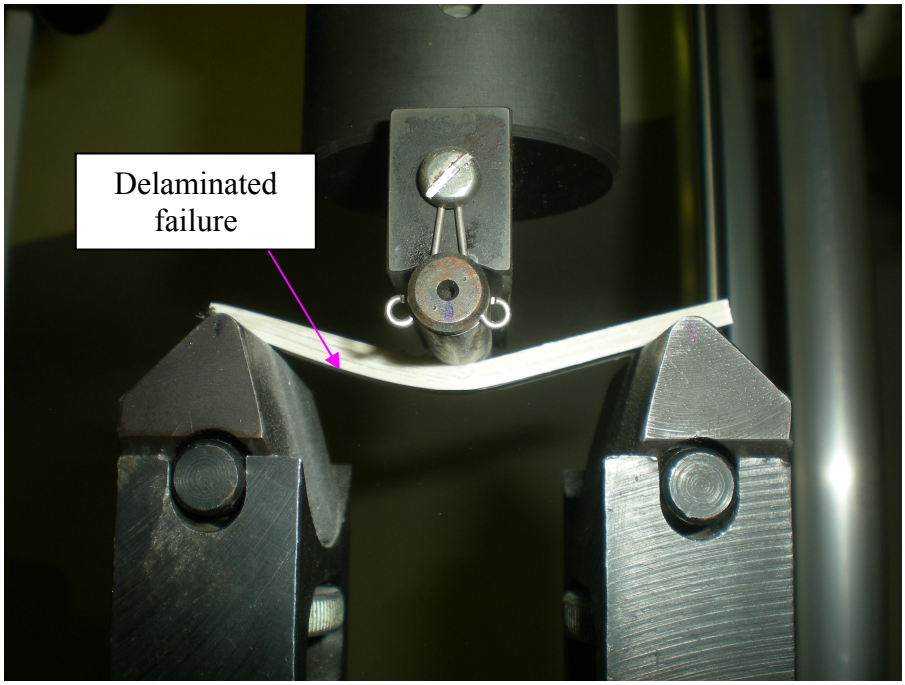

Fig. 6.10 Typical delamination failure pattern of the composite samples.

Fig. 6.11 Typical compressive failure pattern in the outer fiber surfaces of the composite samples.

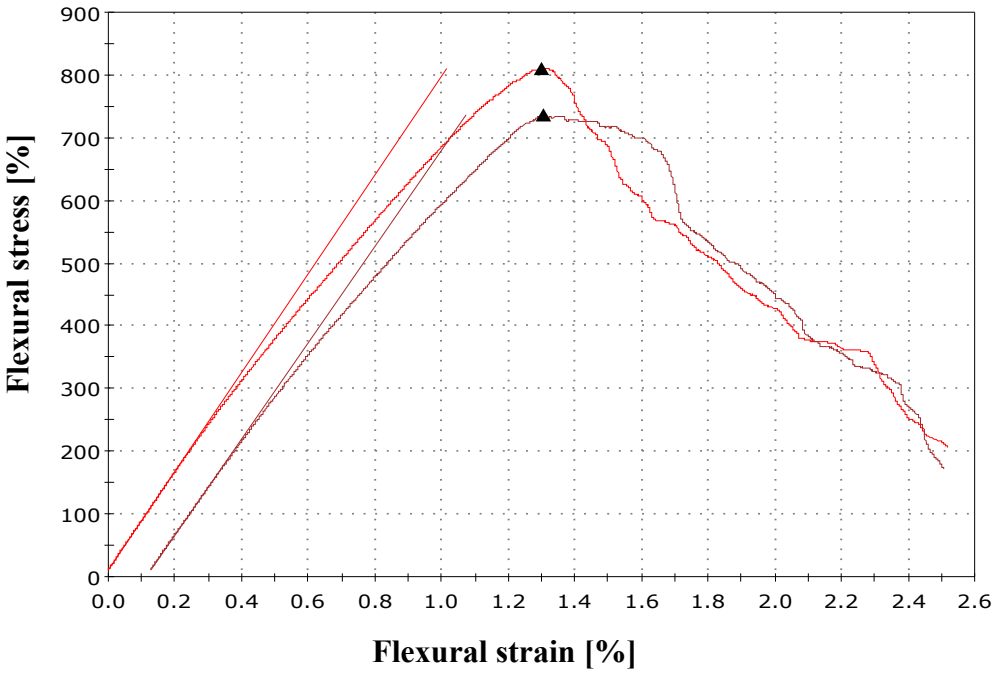

Fig. 6.12 Stress – strain relationships of unidirectional geocomposites M1/Basalt cured at ambient conditions for over 40 days and tested in flexure at L/H = 40 to 1.

6.5 MICROSTRUCTURE OF GEOCOMPOSITE CURED AT AMBIENT CONDITIONS

Scanning Electron Microscopy images are investigated to study the microstructure of geocomposites cured at ambient conditions as well. It is easy to see from Fig. 6.13 and 6.14 that the interaction between fibers and geopolymer matrix seems very well, the micro-cracks on the perpendicular sections and surfaces of the composites still exist as a natural defect of ceramic matrix composites and induce bilinear behavior of composites in flexure tests.

Fig 6.14d shows the microstructure on the surface of geocomposite M1/carbon cured at room temperature for 1 hour and then 5 hours at 65 ^{o}C in the oven with vacuum bagging and hot vacuum bagging respectively, and final drying for 5 hours as well. With the same magnification (1880x), it can be seen with the naked eye from Fig. 6.14c and 6.14d that, the micro-cracks in the composite cured at elevated temperature (even at 65 ^{o}C) would be bigger than the micro-cracks in the same kind of geopolymer resin M1 and reinforced by carbon fibers. This conclusion is demonstrated by progress of mechanical properties of geocomposites when cured at ambient conditions in comparison with those of composites cured at elevated temperature as detailed describing in previous sections.

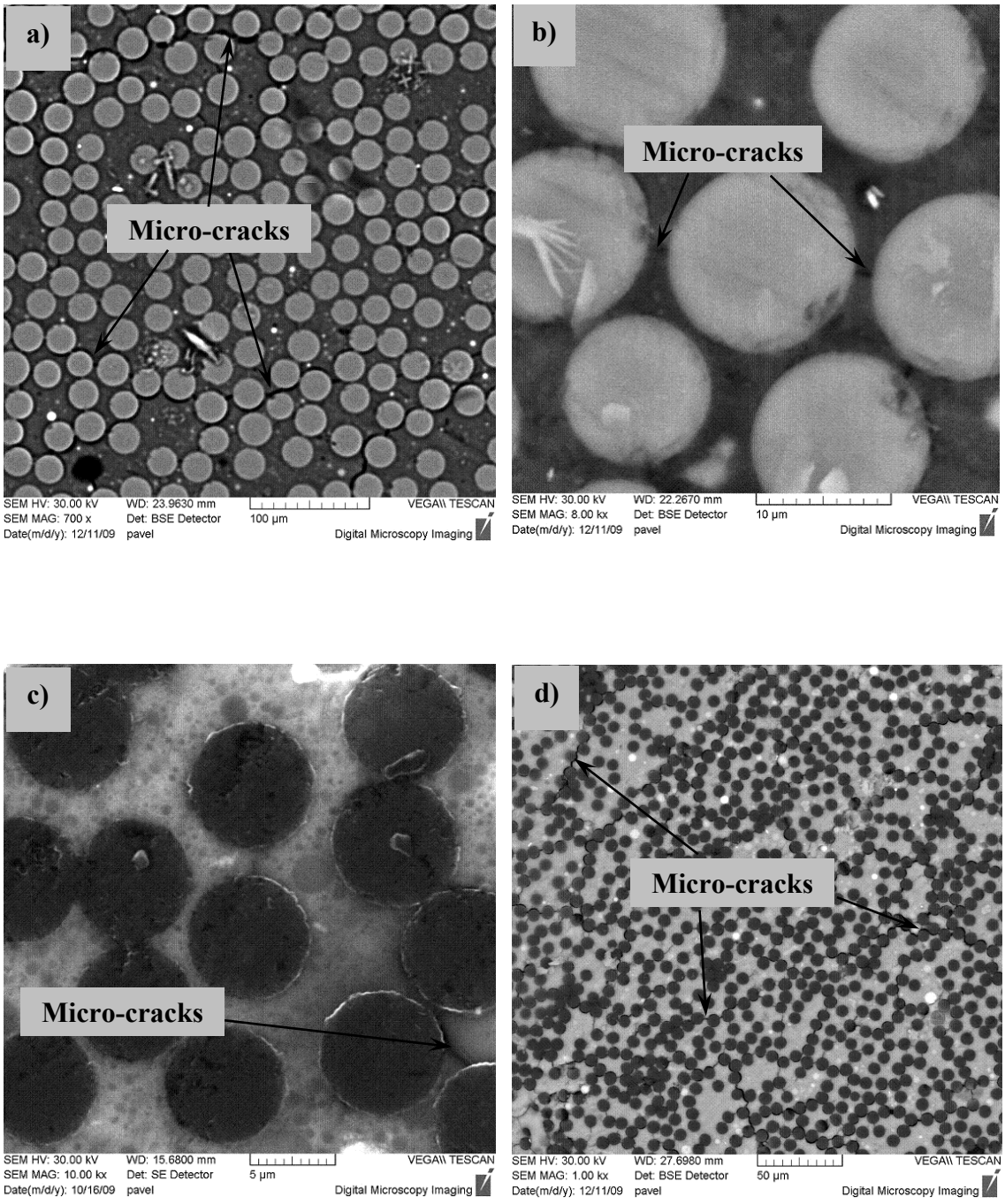

Fig. 6.13 SEM images of perpendicular sections of geopolymer composite matrix M1 with a) E-glass (700x), b) basalt (8.000x), c) carbon (10.000x) and d) carbon (1000x).

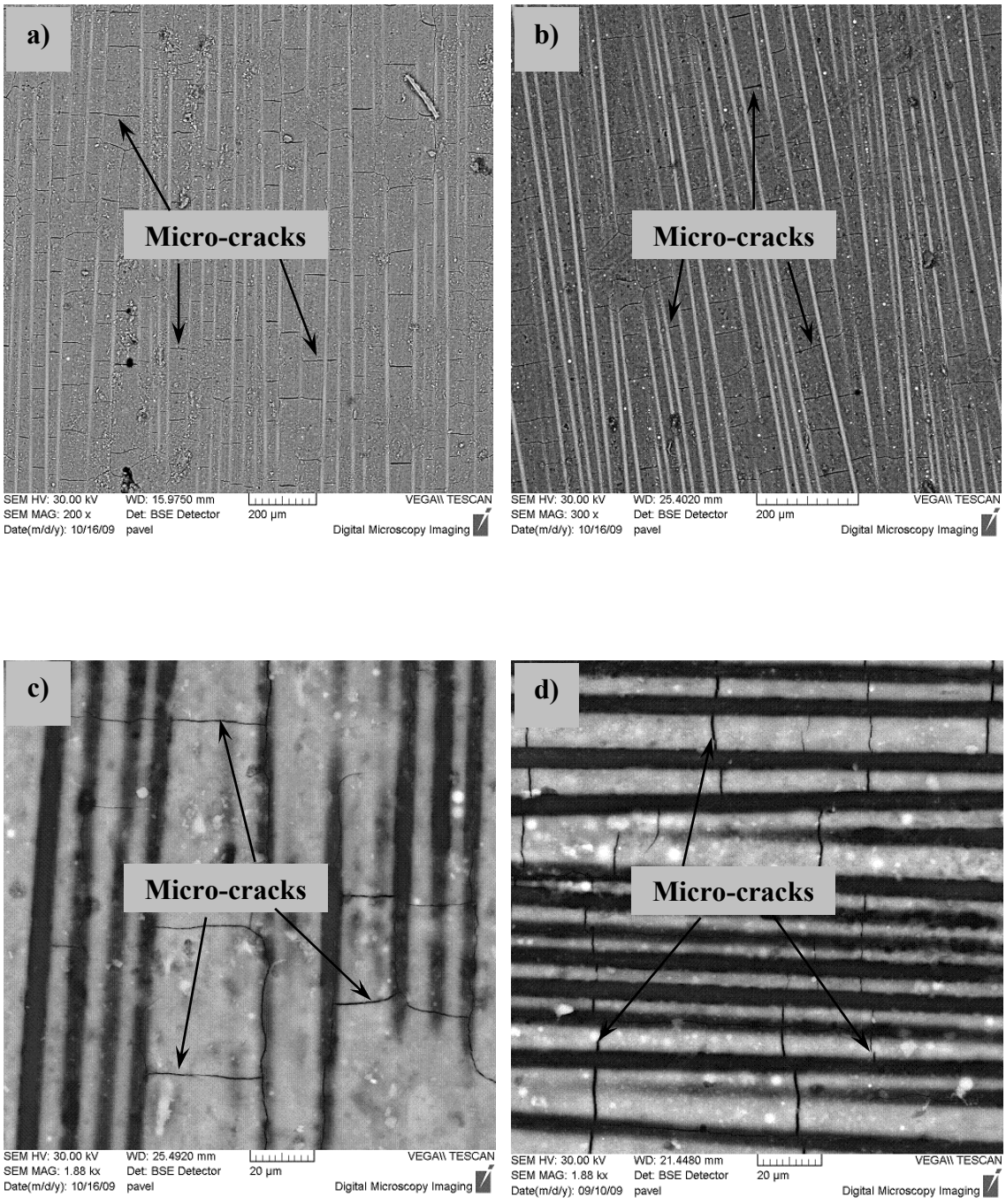

Fig. 6.14 SEM surface images of geopolymer composite matrix M1 and a) E-glass (300x), b) basalt (300x), c) carbon (1.880x) and d) typical micro-crack of M1/C composite curing at elevated temperature 65 ^{o}C for 5 hours (1880x).

6.6 CONCLUSIONS

Generally, fiber reinforced geocomposites based on thermal silica geopolymer matrix can be fabricated and cured in interval optimal temperature range of 60 to 90 ^{o}C with three stages of process, for 1 hour at room temperature and 1 hour at optimal elevated temperature with vacuum bagging technique; finally dried for 5 hours more in a forced air oven at the same temperature as previous stage.

Curing geocomposites at ambient conditions can enhance remarkable mechanical and physical properties of these materials. For geopolymer composites M1 system, the time for curing at these conditions should be over 14 days; while for geocomposites based on M2 system, the time should be over 50 days, even longer is recommended.

At low outer support span-to-depth ratio L/H ≤ 20 to 1, even L/H = 40 to 1, many kinds of the geocomposites possess failure patterns of delamination due to shear stress. Utilizing the regression of extrapolation theory when $(H/L)^2 \rightarrow 0$ we can achieve the virtual flexural strength and modulus of these composites.

The geocomposite M1/E-glass is not recommended for curing at elevated temperature and even should not use E-glass for reinforcing geopolymer M1 matrix, due to chemical and physical degradation in high alkaline medium of this matrix.

7. FIRE-RESISTANT PROPERTIES OF GEOCOMPOSITES

7.1 INTRODUCTION

The most popular matrix used for fiber-reinforced industrial composites is organic polymer. The nature flammability of the organic polymer matrix [122]. However, limits the use of these materials in ground transportation [123], submarine and ships [124], and commercial aircraft [7], where restricted egress of fire hazard is an important design consideration, although traditional fibers, such as carbon and glass fibers or new developed, high temperature, thermal-oxidative stable fibers from boron, silicon carbide and ceramic are inherently fire resistant [14]. In other word, most of organic matrix composites cannot be used in applications that require more than 200 ^{o}C of temperature exposure. In these cases of applications, composites based on carbon matrix or ceramic matrices are being exploited. However, use of these materials is even strongly limited, due to high cost accompany with special and high-thermal processing requirements [14, 15].

Geopolymers are still considered as a new material for coatings and adhesives, a new binder for fiber composites, and a new cement for concrete [110]. They are mineral polymers and the essence of all mineral polymers is never burn [82]. Therefore, we can state that geopolymer materials are ideal for high temperature and fire applications.

In order to study the fire-resistant properties of materials in general and geopolymer composites, three following groups of specifications of materials should be investigated, including: Ignitability, heat release and smoke for the first group; the second group includes flame spread index and the last one is residual flexural strength [12, 125]. Among these parameters, Richard E. Lyon and his colleagues determined that perhaps the most important fire behavior parameter for structure applications is the strength retention of the composite after fire exposure [125].

In this chapter, geopolymer composites based on geopolymer matrices M1 and M2 reinforced by approximately 45, 53 or 60 vol.% of unidirectional carbon HTS 5631 1600tex 24K, basalt roving BCF13 - 2520tex - KV12 Int. or Saint-Gobain - Vetrotex

E-glass E2400P192 fibers are synthesized and fabricated at optimal range of curing conditions, and the effects of calcination in a furnace at high temperatures up to 1000 ^{o}C for 1 hour on the thermal-mechanical properties are studied. The flexural properties of the resulting composites are determined on a universal testing machine under three-point bending mode in accordance with ASTM C 1341 – 06 and DIN V ENV 658-3:1993-02. The microstructure of concerned composites M1/Carbon and M2/Carbon are analyzed by means of Scanning Electron Microscope (SEM). Moreover, Energy Dispersive X-ray Analysis (EDX) is used to determine weather initial reaction layer on the fibers will be presented as well.

7.2 EXPERIMENTAL DESIGN

7.2.1 FABRICATION PROCEDURES

Totally six kinds of geopolymer composites consisting of three different selected unidirectional fibers and based on two classes of geopolymer binders as described in Chapter 3 and 4. The fabrication method of samples used in this investigation is three-stage procedure which is popularly displayed in details in many previous chapters. The specimens are prepared at the optimal cured conditions with the time 1:01:05 hour, that means 1 hour at room temperature under vacuum bagging, 1 hour in oven at optimal temperature, 80 ^{o}C for M1 system and 85 ^{o}C for M2 system, with hot vacuum bagging and finally 5 hours more for drying. One long specimen (3x9x150 mm) is cut into two samples in dimension 3x9x85 mm and 3x9x65 mm.

7.2.2 TESTING SETUP

Specimens are tested for flexural properties before and after the fire exposure up to high temperature to determine the residual properties of the composites. Generally, for testing the residual properties, the specimens are exposed to a 25 kW/m^2 radiant heat source for a duration of 20 minutes according to ASTM E-662 protocol for smoke generation in a flaming mode. After that they are tested in flexure for mechanical properties. Since the geopolymer composites would not burn, they are not subjected to the ASTM E-662 protocol [12]. As a replacement, the samples are tested at room temperature (20 ^{o}C) or subjected to temperatures of 200 ^{o}C, 400 ^{o}C, 600 ^{o}C, 800 ^{o}C and 1000 ^{o}C (1000^{o}C for carbon fiber reinforced geocomposites only) for 60 minutes

of soaking time and at the oxidizing environment in a forced air furnace (Appendix E, Fig. E.1). The ramp of temperature is 10 $K.min^{-1}$ and samples then are cooled in the furnace with opening gate for 24 hours. At 400 ^{o}C of the furnace exposure is comparable to the equilibrium surface temperature of a vertically oriented, unit-emissivity surface exposed to 25 kW/m^2 of radiant energy in quiescent air for the same time period as the ASTM E-662 protocol [126].

7.2.3 MECHANICAL MEASUREMENT

The residual mechanical properties of composites after exposing up to high temperature are measured on Universal Tensile Testing machine Instron Model 4202 (Fig. 3.8) with a mid-span deflection rate of 2 mm/min at two different outer support span-to-depth ratios L/H = 20 to 1 in DIN V ENV 658-3:1993-02 and L/H = 16 to 1 as in accordance with ASTM C 1314 – 06 (a series of six specimens are tested). Virtual flexural values are evaluated in agreement with the size-independent method and presented as a visual presentation as well.

7.3 RESULTS AND DISCUSSION

Mechanical properties of the geocomposites after thermal exposure up to high temperature are evaluated by equations in agreement with DIN EN 658-3:2002 (L/H = 20 to 1) and ASTM C 1314 – 06 (L/H = 16 to 1). The degradation of specimen weight is also concerned. Residual flexural strength (R_{mo}), modulus (E), strain in the outer surface (ε) and weight lost (Δm) are presented in Table 7.1 to 7.6. Visual demonstrations are exhibited on Fig. 7.1 and 7.6 respectively. In order to make the figures clearly, no error of measurements are shown on the figures.

Appendix E, Fig. E.2 and E.3 present photographs illustrating the typical condition of the specimens before and after thermal exposure.

Table 7.1 Flexural properties of geocomposites M1 reinforced by Carbon fibers cured at 80 °C after thermal exposure for 60 minutes at different L/H ratios

M1/Carbon	L/H = 16 to 1			L/H = 20 to 1			Δm
	R_{mo} [MPa]	E [GPa]	ε_{mo} [%]	R_{mo} [MPa]	E [GPa]	ε_{mo} [%]	[%]
20 °C	401.1 ±18.5	65.2 ±3.8	0.90	470.9 ±6.5	92.3 ±6.9	0.74	0.0
200 °C	316.3 ±14.0	62.5 ±1.6	0.77	437.3 ±19.1	88.7 ±5.3	0.72	4.1
400 °C	198.6 ±26.3	39.9 ±6.6	1.00	275.8 ±21.6	49.4 ±2.4	1.06	8.8
600 °C	111.8 ±2.1	11.3 ±1.1	1.43	173.5 ±33.5	19.1 ±3.9	1.69	15.5
800 °C	266.6 ±29.5	38.3 ±4.8	1.35	255.2 ±26.0	37.5 ±2.6	1.04	17.4
1000 °C	154.9 ±21.6	43.4 ±9.2	1.06	222.2 ±57.5	59.4 ±8.5	0.66	18.1

Δm – percentage of weight lost

Table 7.2 Flexural properties of geocomposites M1 reinforced by Basalt fibers cured at 80 °C after thermal exposure for 60 minutes at different L/H ratios

M1/Basalt	L/H = 16 to 1			L/H = 20 to 1			Δm
	R_{mo} [MPa]	E [GPa]	ε_{mo} [%]	R_{mo} [MPa]	E [GPa]	ε_{mo} [%]	[%]
20 °C	371.0 ±14.4	42.7 ±3.0	1.10	451.7 ±12.2	68.2 ±1.3	0.86	0.0
200 °C	291.4 ±20.0	45.9 ±1.8	0.84	307.9 ±7.1	55.5 ±1.4	0.72	5.3
400 °C	222.9 ±4.6	39.0 ±1.0	0.76	257.5 ±27.5	51.2 ±1.5	0.64	4.9
600 °C	94.4 ±8.2	39.9 ±2.3	0.27	84.4 ±1.5	48.1 ±0.7	0.21	5.1
800 °C	52.5 ±6.2	26.2 ±2.9	0.30	45.1 ±5.7	26.8 ±5.6	0.25	4.7

Table 7.3 Flexural properties of geocomposites M1 reinforced by E-glass fibers cured at 80 °C after thermal exposure for 60 minutes at different L/H ratios

M1/E-glass	L/H = 16 to 1			L/H = 20 to 1			Δm
	R_{mo} [MPa]	E [GPa]	ε_{mo} [%]	R_{mo} [MPa]	E [GPa]	ε_{mo} [%]	[%]
20 °C	109.2 ±13.3	32.6 ±4.0	0.59	144.5 ±11.2	44.0 ±2.3	0.53	0.0
200 °C	69.8 ±5.0	21.3 ±2.5	0.64	82.0 ±10.0	30.8 ±1.7	0.50	1.9
400 °C	42.7 ±0.6	9.7 ±2.0	0.71	54.9 ±6.0	18.2 ±4.0	0.52	4.0
600 °C	40.0 ±3.3	10.8 ±1.4	0.58	42.9 ±2.6	20.2 ±1.3	0.29	4.3
800 °C	41.0 ±4.8	11.8 ±1.3	0.75	24.9 ±0.4	6.9 ±1.2	0.48	4.5

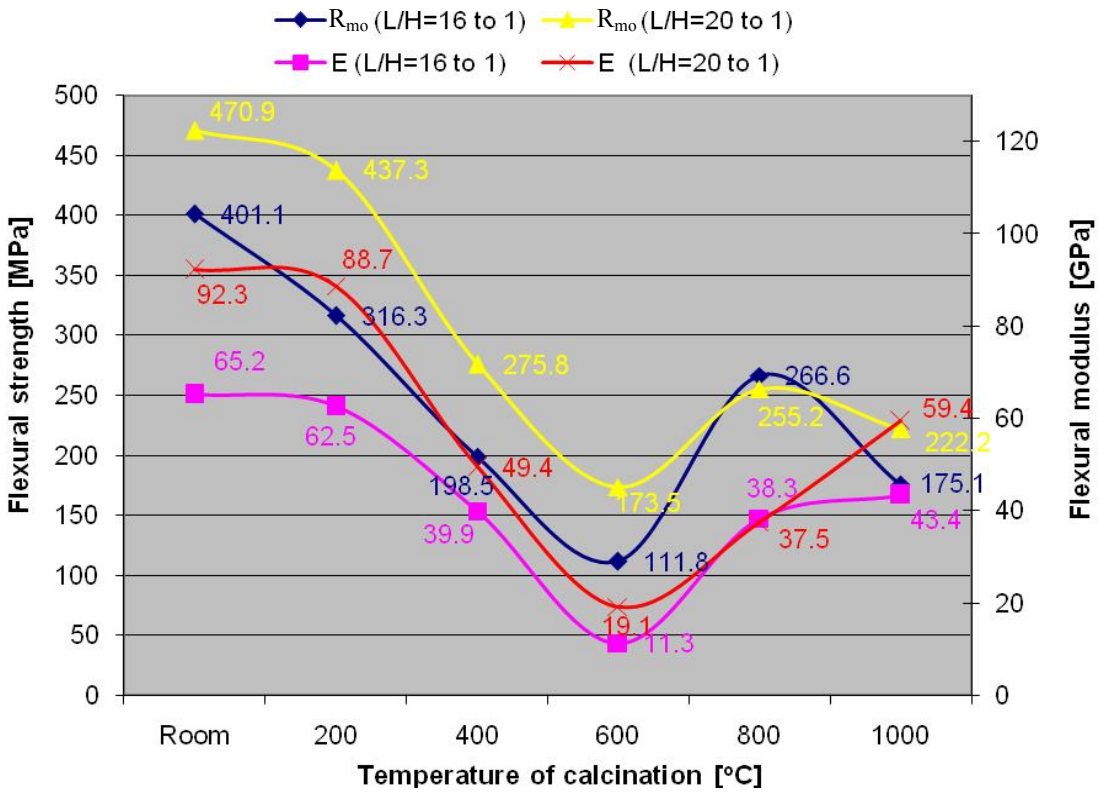

Fig. 7.1 Residual mechanical properties of geocomposites M1/Carbon fibers.

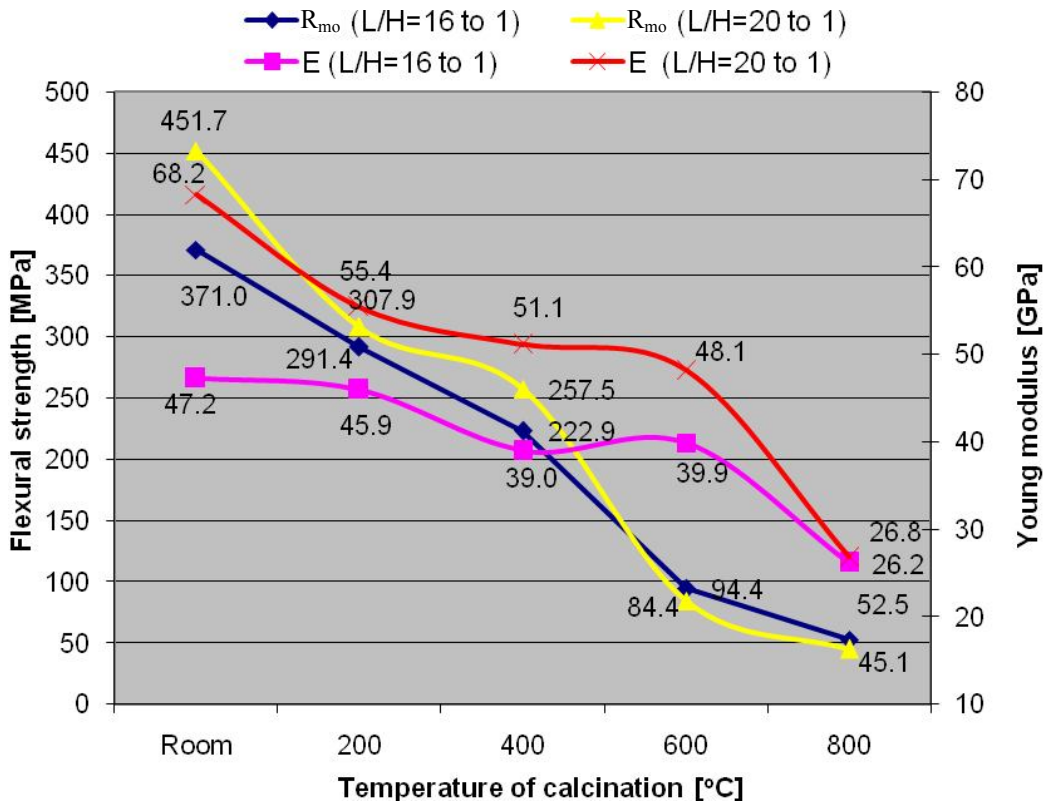

Fig. 7.2 Residual mechanical properties of geocomposites M1/Basalt fibers.

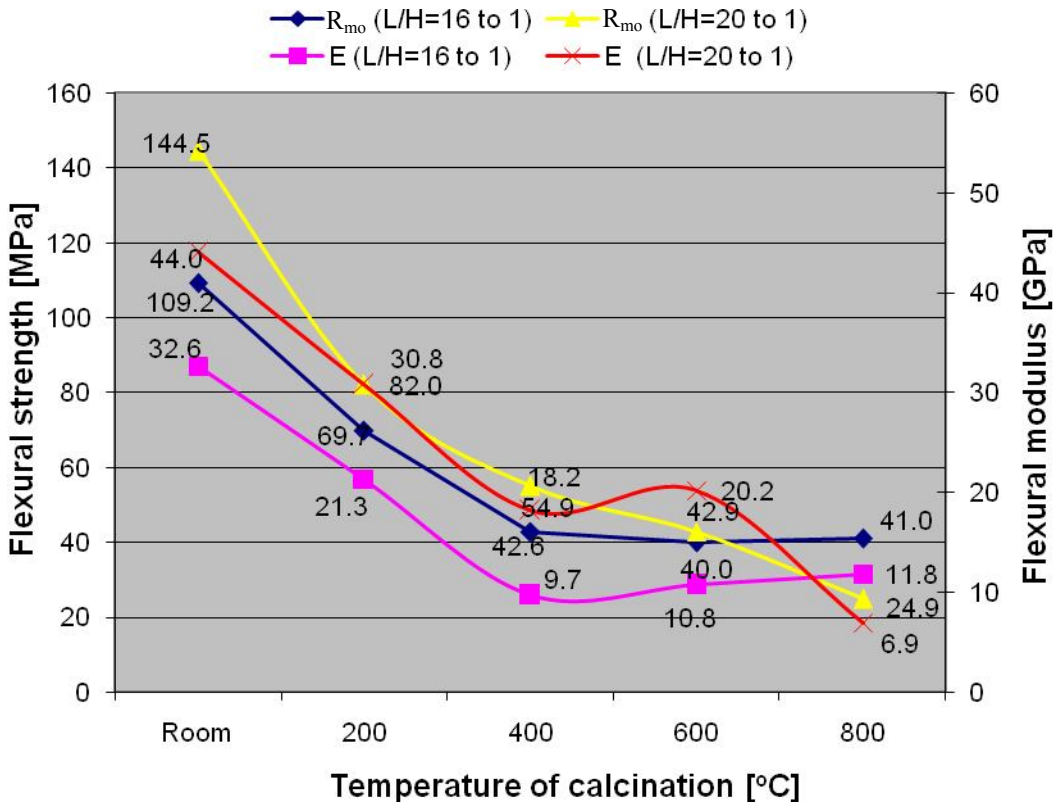

Fig. 7.3 Residual mechanical properties of geocomposites M1/E-glass fiber.

Table 7.4 Flexural properties of geocomposites M2 reinforced by Carbon fibers cured at 85 °C after thermal exposure for 60 minutes at different L/H ratios

M2/Carbon	L/H = 16 to 1			L/H = 20 to 1			Δm
	R_{mo} [MPa]	E [GPa]	ε_{mo} [%]	R_{mo} [MPa]	E [GPa]	ε_{mo} [%]	[%]
20 °C	290.9 ±15.7	85.3 ±1.4	0.49	355.7 ±10.8	106.6 ±5.7	0.40	0.0
200 °C	283.4 ±2.5	69.3 ±7.1	0.84	322.4 ±19.7	99.7 ±13.8	0.56	4.0
400 °C	259.1 ±17.9	64.0 ±1.2	0.86	269.4 ±6.8	77.4 ±4.1	0.87	5.8
600 °C	184.0 ±7.5	36.0 ±1.5	1.11	204.9 ±7.5	47.2 ±1.5	0.80	11.6
800 °C	173.6 ±10.0	28.9 ±1.1	1.25	211.7 ±11.8	35.3 ±3.8	1.24	18.6
1000 °C	190.1 ±13.3	28.9 ±1.1	1.11	206.1 ±8.9	36.6 ±1.5	0.98	18.5

Table 7.5 Flexural properties of geocomposites M2 reinforced by Basalt fibers cured at 85 °C after thermal exposure for 60 minutes at different L/H ratios

M2/Basalt	L/H = 16 to 1			L/H = 20 to 1			Δm
	R_{mo} [MPa]	E [GPa]	ε [%]	R_{mo} [MPa]	E [GPa]	ε [%]	[%]
20 °C	220.5 ±11.4	53.5 ±3.5	0.58	273.1 ±2.0	65.9 ±1.4	0.49	0.0
200 °C	221.3 ±12.4	48.9 ±4.4	0.78	250.3 ±13.5	58.7 ±2.1	0.61	2.3
400 °C	211.8 ±7.0	52.4 ±5.0	0.55	221.0 ±10.5	55.8 ±2.0	0.57	3.0
600 °C	152.6 ±15.1	56.2 ±1.5	0.35	153.6 ±19.7	68.3 ±2.7	0.28	4.4
800 °C	44.9 ±26.3	46.3 ±4.1	0.12	47.0 ±8.6	56.4 ±5.0	0.07	5.0

Table 7.6 Flexural properties of geocomposites M2 reinforced by E-glass fibers cured at 85 °C after thermal exposure for 60 minutes at different L/H ratios

M2/E-glass	L/H = 16 to 1			L/H = 20 to 1			Δm
	R_{mo} [MPa]	E [GPa]	ε [%]	R_{mo} [MPa]	E [GPa]	ε [%]	[%]
20 °C	158.1 ±8.8	51.9 ±5.0	0.46	202.0 ±6.9	56.6 ±4.6	0.40	0.0
200 °C	128.2 ±11.8	42.5 ±4.6	0.42	165.6 ±2.8	57.2 ±0.6	0.40	2.7
400 °C	140.8 ±15.5	51.1 ±8.8	0.35	133.8 ±5.4	64.0 ±2.6	0.23	3.3
600 °C	95.9 ±7.6	46.8 ±8.2	0.37	126.0 ±25.1	66.0 ±3.7	0.28	4.0
800 °C	56.1 ±5.0	51.1 ±5.3	0.14	61.8 ±1.9	63.7 ±3.8	0.07	4.0

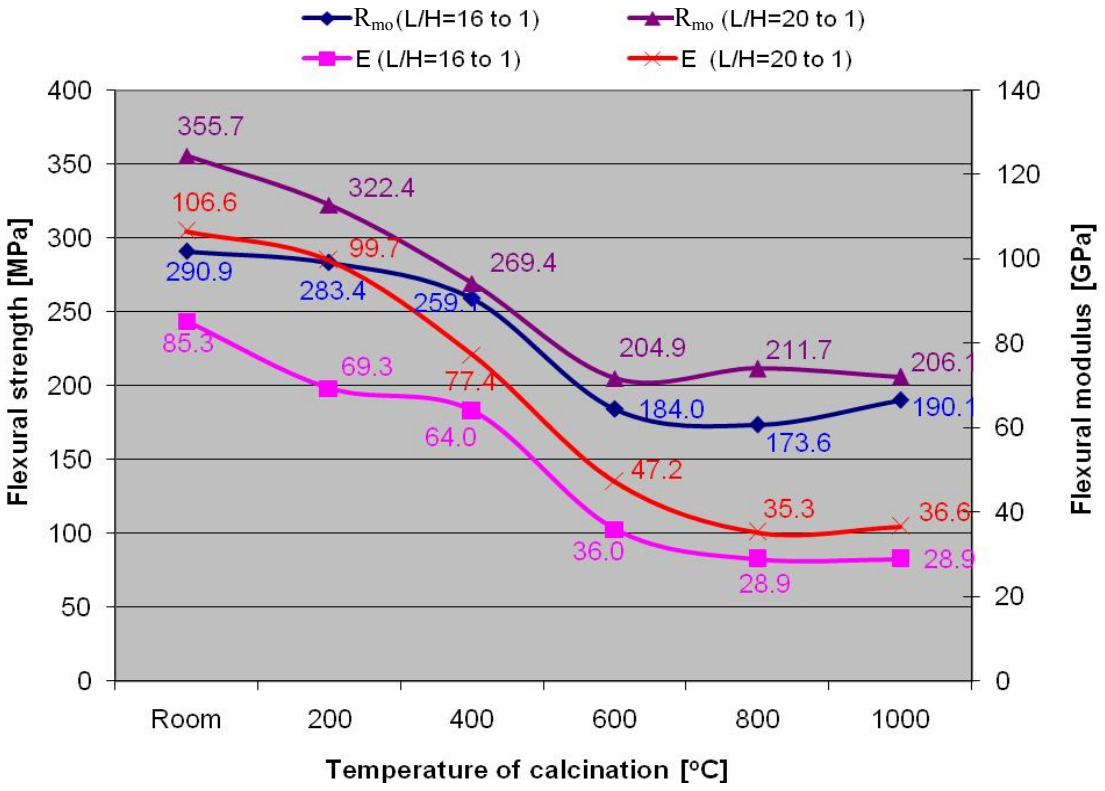

Fig. 7.4 Residual mechanical properties of geocomposites M2/Carbon fiber.

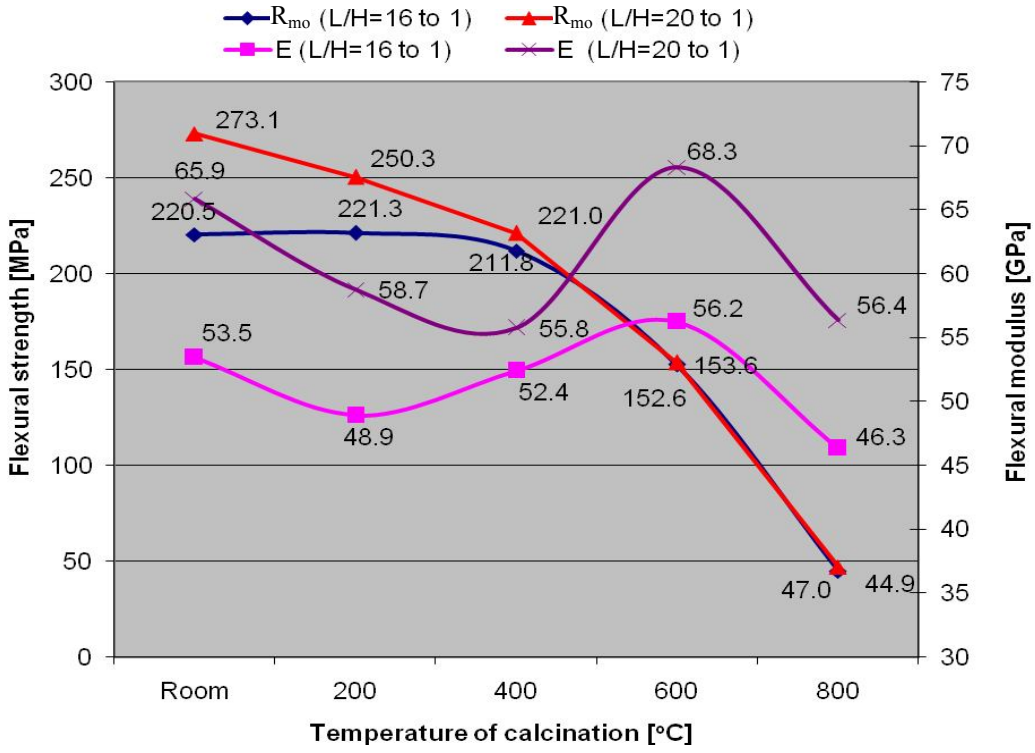

Fig. 7.5 Residual mechanical properties of geocomposites M2/Carbon fiber.

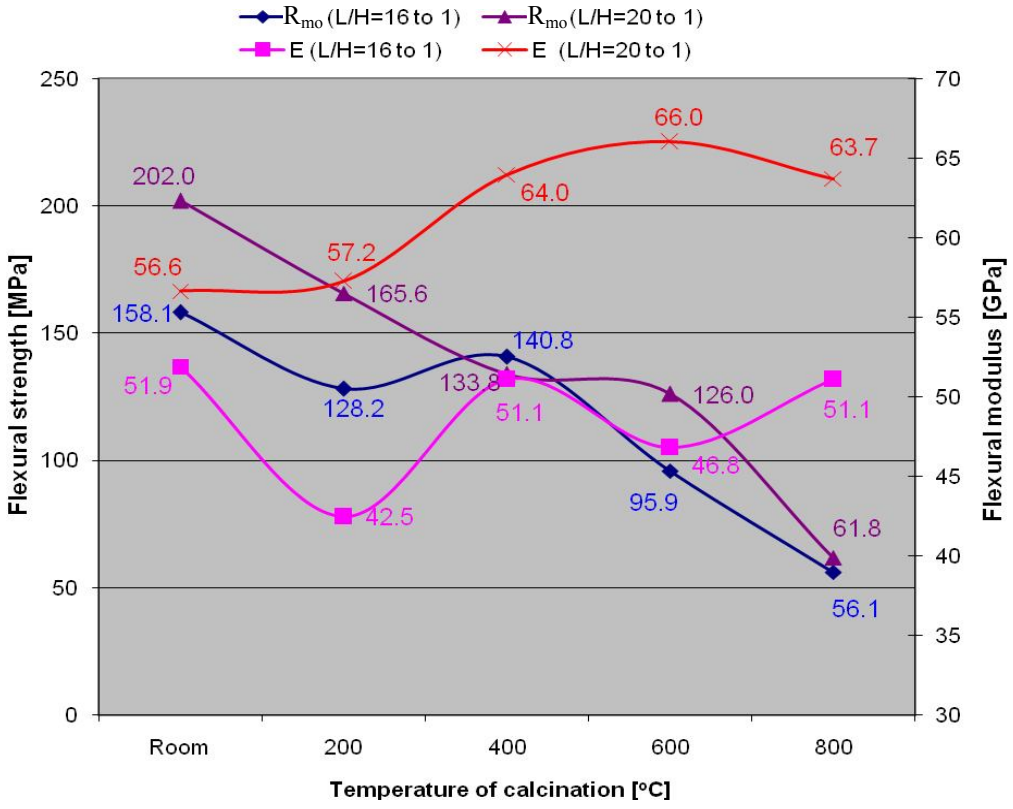

Fig. 7.6 Residual mechanical properties of geocomposites M2/E-glass fiber.

In general, the mechanical properties of geocomposites reinforced by carbon, basalt or E-glass fibers remain approximately around 90% after sustaining up to 400 ^{o}C for 1 hour. Almost all composites remained over 50% of strength after calcination at 600 ^{o}C, for carbon fiber reinforced geocomposites the temperature can be over 1000 ^{o}C; exceptionally, geocomposite M1/E-glass, due to degradation in alkaline medium and by themselves at high temperature.

The shear strength could even take an important role in the failure pattern of fiber reinforced geocomposites after exposing up to high temperature. For both geocomposites reinforced by basalt fibers, however, after calcinating to over 400 ^{o}C their flexural strengths of testing at different L/H ratios are nearly similar (see Fig. 7.2 and 7.5). Some unusual behavior of elastic moduli of geocomposites M2/basalt and M2/E-glass are determined (Fig. 7.5 and 7.6). It may need more experiments for explaining the mechanism of these behaviors.

Meanwhile the major weight lost of geocomposites reinforced by basalt or E-glass during the calcination is assumed that from evaporation of free water of 4.5 to 5.0 wt.%, the value can be reached after the composites are exposed up to over 400 ^{o}C. The value of carbon fiber reinforced geocomposites must be caused by not only free water evaporation but also partial carbon fiber oxidizing of the outer layers at temperature higher 400 ^{o}C, it is estimated that approximately 14 wt.% of carbon fibers is disappeared (see the last columns of Table 7.1 to 7.6 and Table 4.6).

Experimental findings show that composites based on geopolymer matrix M2 are very good at thermal dimensional stability, the composites exhibited no thermal expansion even they are calcinated up to 800 ^{o}C for basalt and E-glass reinforcements and 1000 ^{o}C for carbon fiber reinforcement. On the contrary, the geocomposites based M1 and carbon, basalt and E-glass have different expansion under thermal conditions. Meanwhile dimensional stability is recorded up to 600 ^{o}C for M1/basalt, the temperature for M1/carbon and M1/E-glass remain dimensional stability is 400 ^{o}C and 200 ^{o}C respectively. After exposing up to 600 ^{o}C, the expansion of M1/C and M1/E-glass are 40.7 vol.% and 30.8 vol.% in comparison with values at room temperature. After exposing to 800 ^{o}C, expansion of M1/E-glass is 135.2 vol.% and

M1/basalt is 53.1 vol.%. Moreover, over 800 ^{o}C of thermal exposure, white outer calcinated layer of the composite is formed for M1/C (Fig. 7.7 and Appendix E.2).

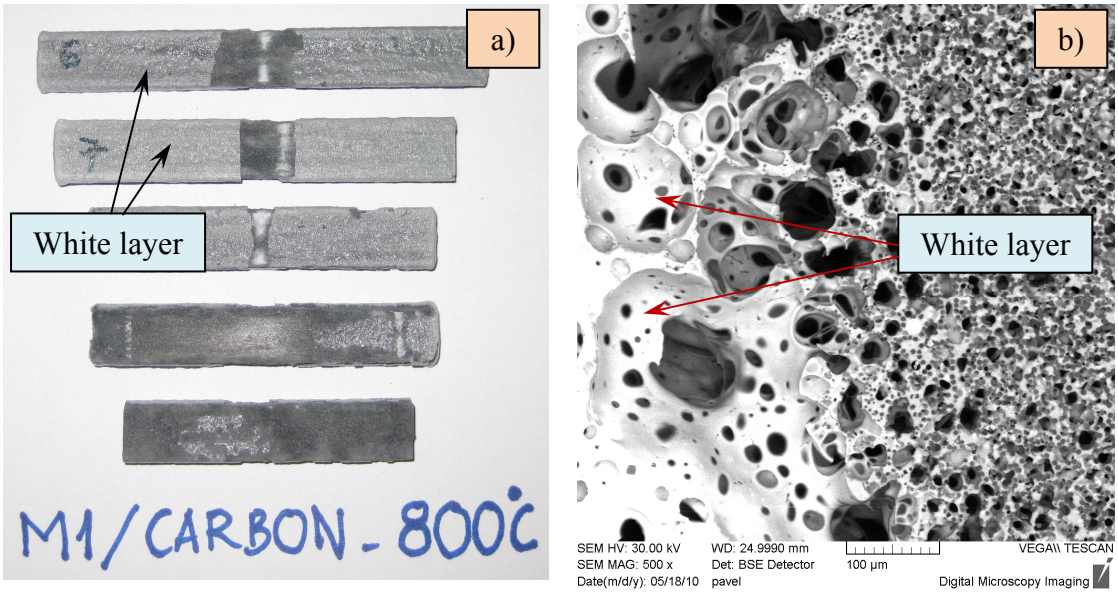

Fig. 7.7 Outer calcinated layer of composite M1 after exposing up to 800 ^{o}C at macro structure (a) and micro-structure (b at 500x).

The most advantages of geopolymer materials are they possess ceramic-liked properties, meanwhile they can be fabricated at room or very low temperature (in our research, 65-85 ^{o}C is recommended) and special ones can protect carbon fiber from oxidation. Among three kinds of commercial selected roving fibers, carbon (HTS 5631 1600tex 24K, TohoTenax), advanced basalt (BCF13-2520tex KV12 Int, Basaltex) or electrical grade glass (E-glass: E2400P192, Saint-Gobain, Vetrotex) which used to reinforce geopolymer composites, the combination between geopolymer and carbon fiber reinforcement attracted much more our attention. The materials have a great expectation for applying into high-tech applications.

Mechanism of mechanical behavior of geocomposite M1/Carbon is very special (Table 7.1 and Fig. 7.1). At support span-to-depth ratios L/H = 20 to 1, the properties of the composites seem to be constant when the samples are exposed up to 200 ^{o}C. It was easy to notice that the properties go down drastically after exposing up to higher than 200 ^{o}C of calcination, when these composites are exposed up to 600 ^{o}C, the flexural strength remains only 37% and elasticity modulus approximately 20% compared to the original ones. It can be seen from Fig. 7.8 that the interaction of the

fiber reinforcement and geopolymer matrix is so loose, it seems no connection between them. The reason is assumed that the difference of relative thermal expansion of these two component parts could be maximum around 600 ^{o}C of calcination, this problem should be next investigations.

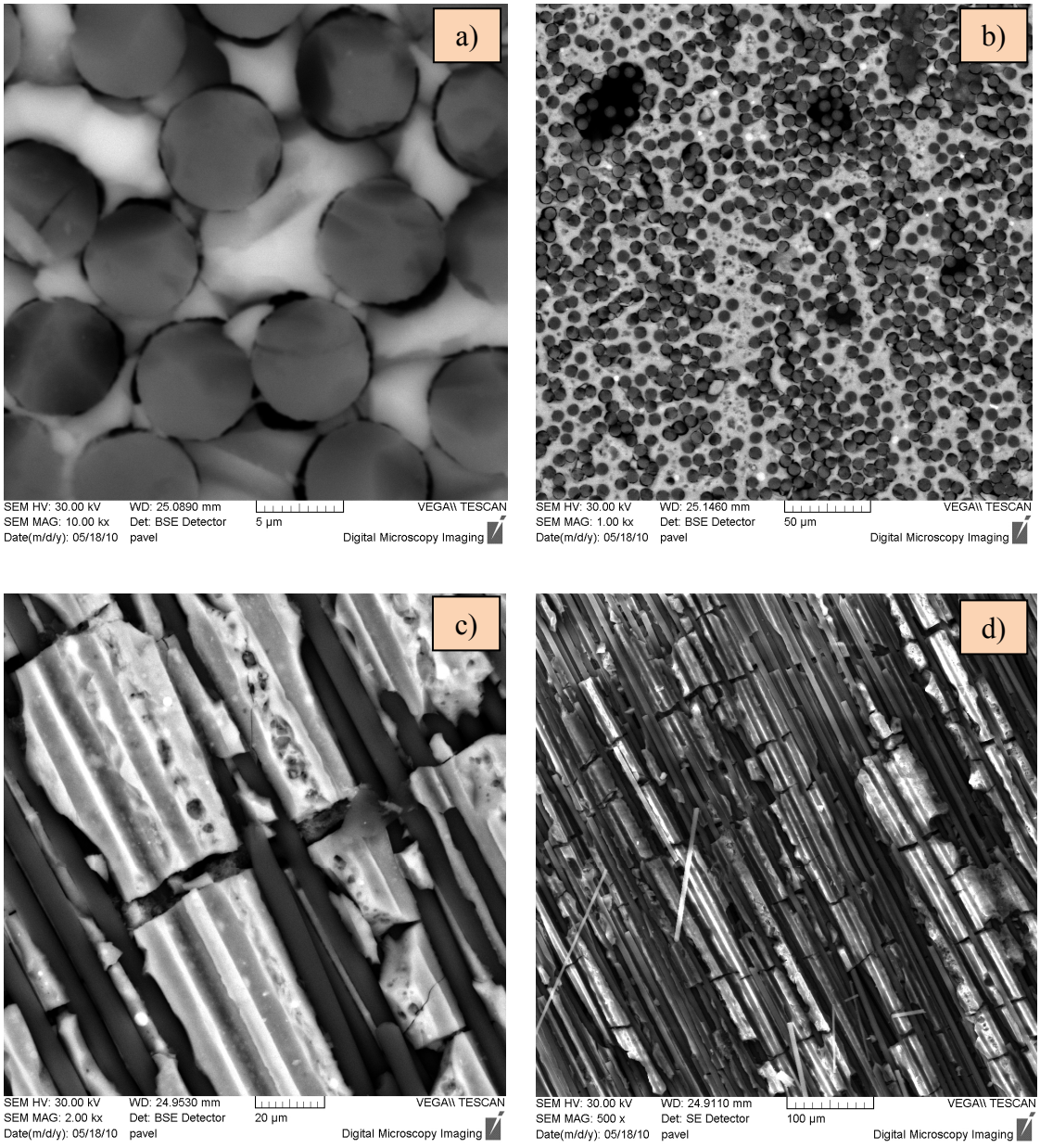

Fig. 7.8 SEM images of M1/carbon after exposing up to 600 ^{o}C on sections perpendicular to fibers a) 10kx and b) 1.0 kx and surfaces of composite c) 2.0 kx and d) 500x.

When the temperature of calciantion is higher than 600 ^{o}C, the mechanical properties of the composites are shown better, because the adhesion is improved and initial

reaction layer might be created, so the flexural strength gained 54% and remained around 50% after calcination up to 800 ^{o}C and 1000 ^{o}C respectively, meanwhile the flexural modulus could be 65 % compared to those of composites at room temperature (Fig. 7.9a and c). In addition, after exposing up to higher 800 ^{o}C, at low magnification 500x (Fig. 7.9b and d), the microstructure of geocomposite looked like foam structure. Fig. 7.10 shows many micro-cracks in the composites M1/Carbon after high temperature exposing.

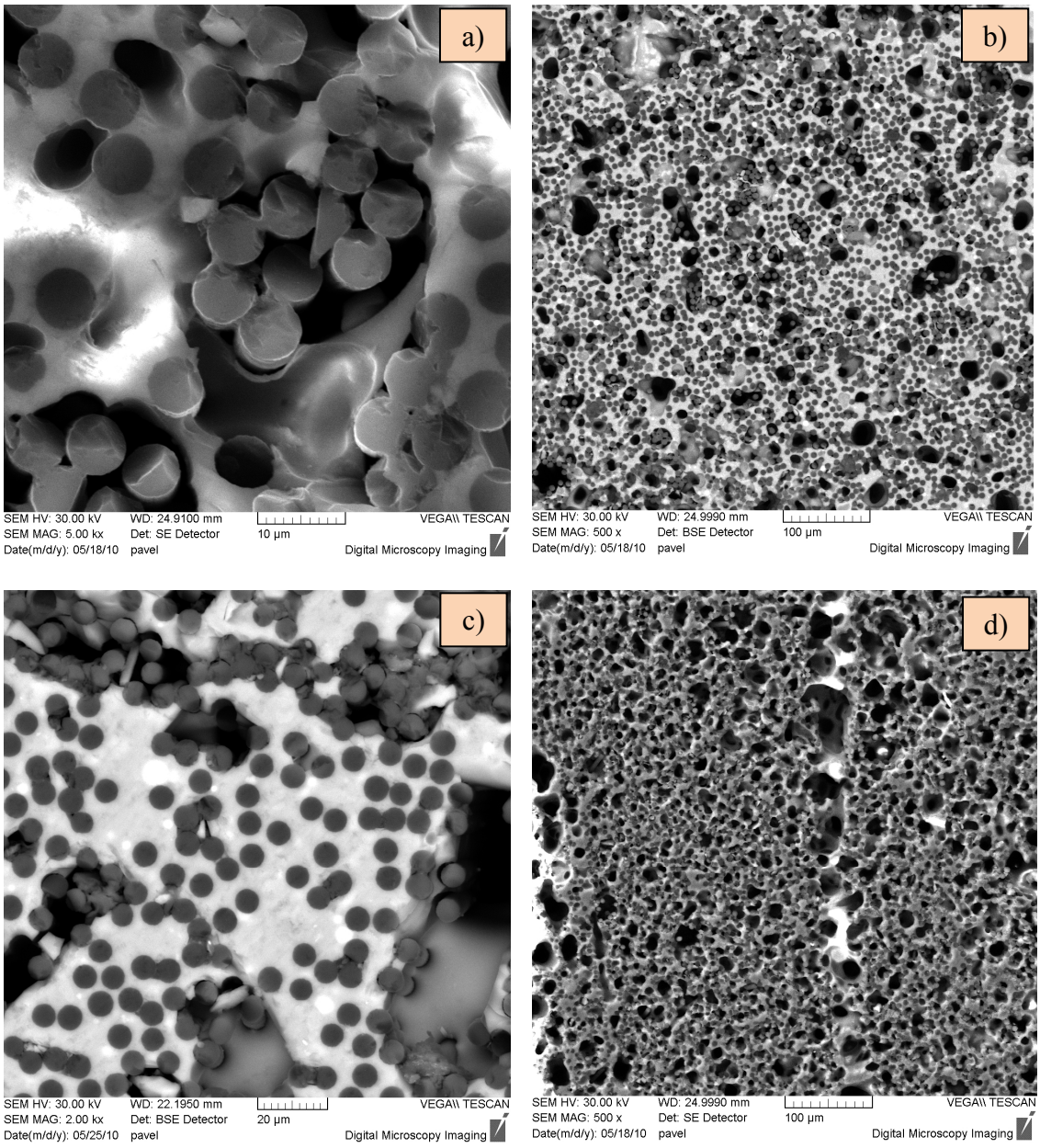

Fig. 7.9 SEM of M1/carbon after exposing up to 800 ^{o}C a) 5.0kx and b) 500x and 1000 ^{o}C c) 2.0kx and d) 500x on sections perpendicular to fibers.

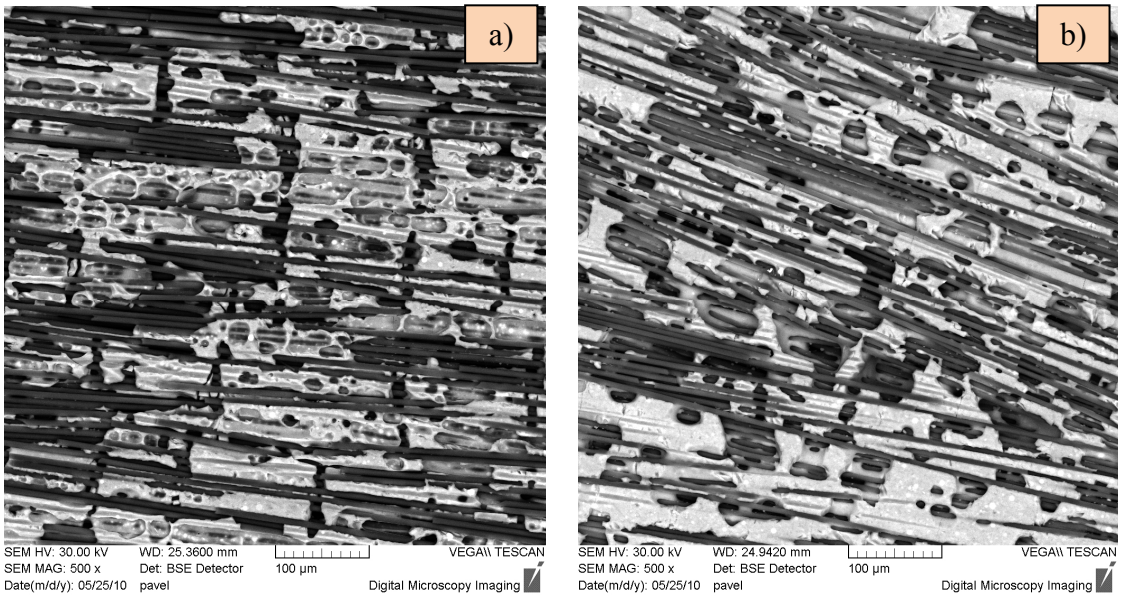

Fig. 7.10 SEM of M1/carbon after exposing up to 800 ^{o}C (a) and 1000 ^{o}C (b) on the surfaces of composite at magnification 500x.

For M2/carbon fiber composites (Table 7.4 and Fig. 7.4), with the span of testing is 64 mm (L/H = 20 to 1), the flexural strength and modulus of elasticity seem to go down quite dramatically when the temperature of calcination increases from 200 to 600 ^{o}C, retain around 57 % of flexural strength (204,9 MPa compared to 355,7 MPa) and 45% of elastic modulus (47,2 MPa in contrast with 106,6 MPa). However, the flexural properties seem constant even when the composites are exposed up to 800 ^{o}C and 1000 ^{o}C. Microstructure of the composites is also presented on Fig. 7.11, as can be seen from this figure that after exposing the composite at 600 ^{o}C, the adhesion between carbon fiber and M2 matrix is also not very good (Fig. 7.11a and b) and show better after 1000 ^{o}C of exposure (Fig. 7.11c and d). The behaviors look like the same as composites M1/carbon. However, for M2/carbon nearly non difference of flexural strength, modulus and dimensional stability are determined in range of 600 to 1000 ^{o}C of thermal exposure. Furthermore, the microstructure of geocomposite M2/carbon after exposing high temperature is exhibited on Fig. 7.12.

It seems quite interesting when both M1/carbon and M2/carbon possess nearly the same flexural strength around 220 MPa after thermal exposing up to 800 ^{o}C and 1000 ^{o}C, although their microstructures are presented differently on Fig. 7.10 and Fig 7.12. For

composite M2/carbon (Fig. 7.12), it is visible to the naked eye that not so many cracks and porosities are determined in comparison with composites M1/carbon. This means that the composites based on geopolymer matrix M2 with phosphoric acid as functional additive, the chemical and physical properties of this matrix are stable at high temperature and the thermal dimensional stability is determined as unavoidable results.

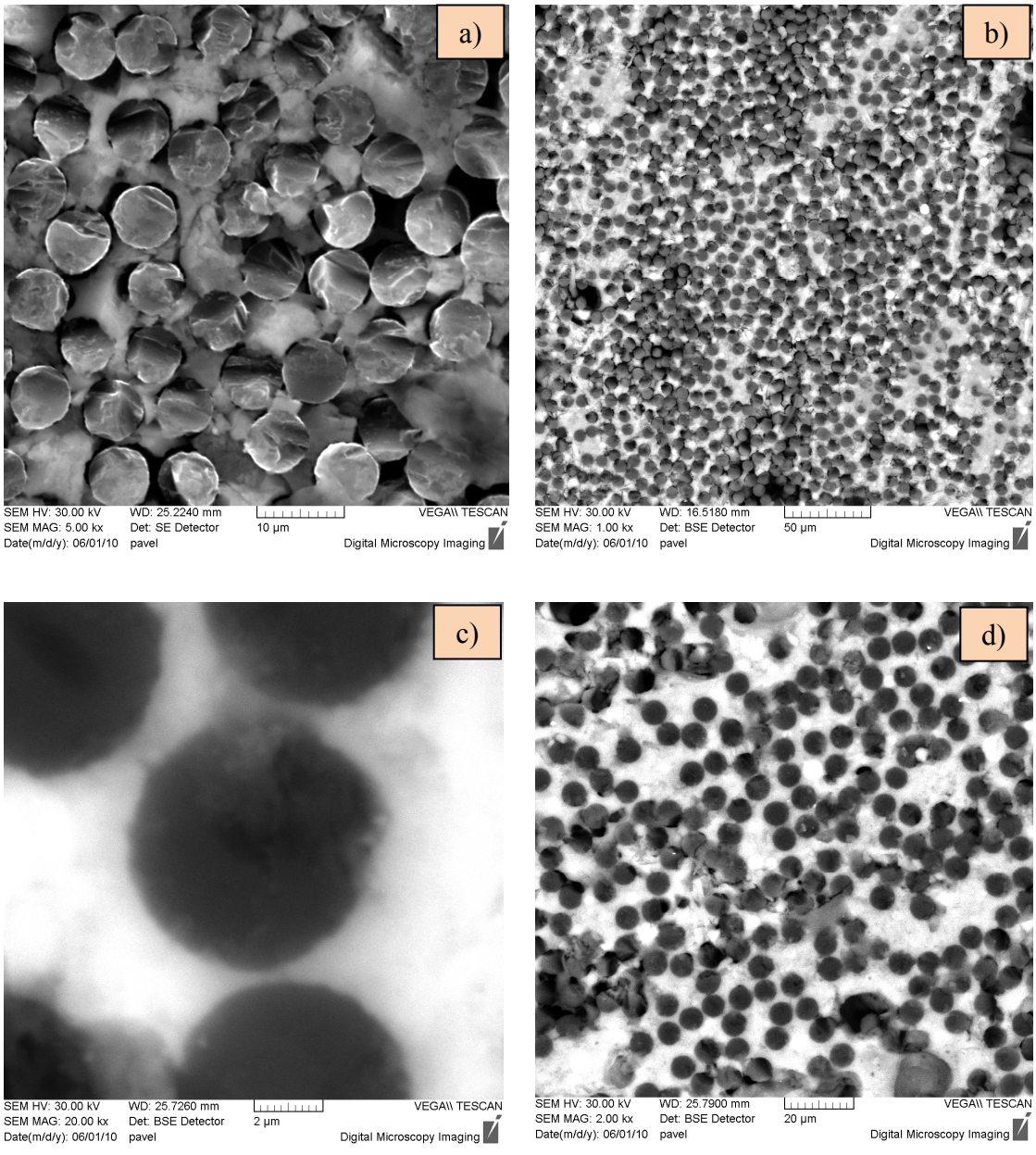

Fig. 7.11 SEM of M2/carbon after exposing up to 600 ^{o}C a) 5.0kx and b) 1.0kx and 1000 ^{o}C c) 20.0kx and d) 200x on sections perpendicular to fibers and surfaces of composite.

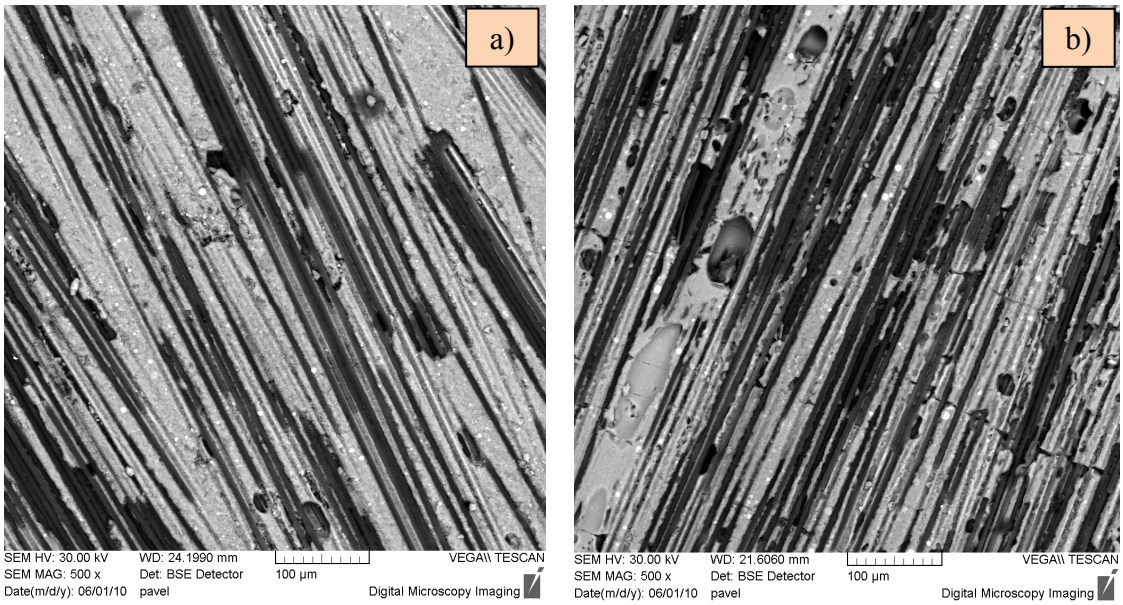

Fig. 7.12 SEM of M2/carbon after exposing up to 600 ^{o}C (a) and 1000 ^{o}C (b) on the surfaces of composite at 500x.

With the hypothesis that at high temperature a chemical reaction between interface of carbon fiber and derivative silicon of geopolymer matrix might be taken place to generate SiC which could prevent carbon fiber from oxidation in turn, the Energy Dispersive X-ray Analysis (EDX) is used. Fig. 7.13b and 7.13c show minor change of silicon and carbon atoms on the interface of fiber and matrix when compared with original one shows on Fig. 7.13a. These results show that it is very difficult to confirm at temperature higher than 800 ^{o}C the carbon fiber could be protected from oxidization by the initial reaction layer on the fiber (Fig. 7.13d). Until now the mechanism of geopolymer for protection carbon fiber from oxidation is not identified clearly. The mechanism would be assumed that at high temperature the slowly continuous free water evaporation could create a vapor that can protect carbon fiber and with an special medium the SiC would be create at lower temperature instead of over 1400 ^{o}C as usual. Many investigations must be taken place to explain these assumptions.

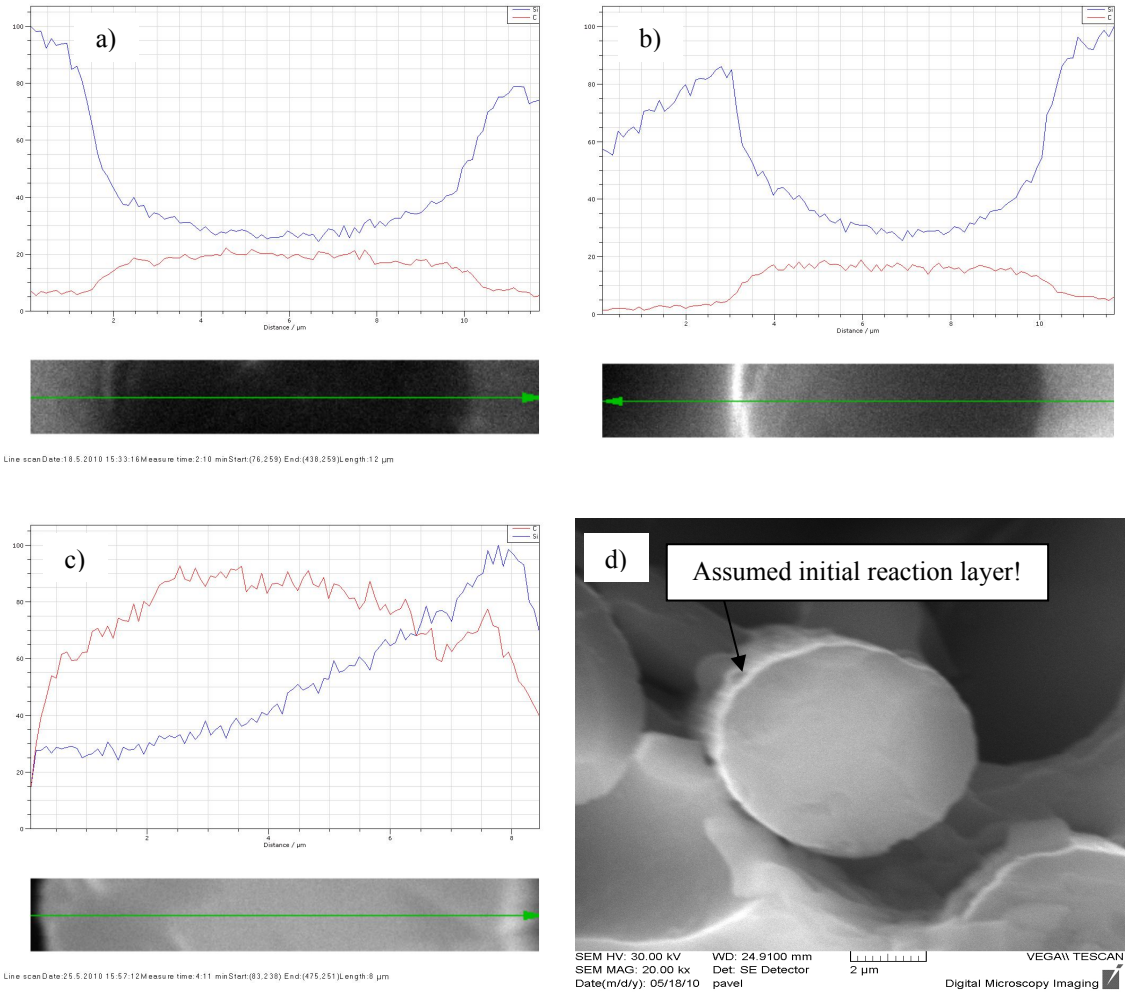

Fig. 7.13 EDX of line profiles through cross-section of filament fiber in the composite M1-carbon after calcination at a) room temperature, b) 800 ^{o}C , c) 1000 ^{o}C and d) SEM after exposing up to 800 ^{o}C (at 20kx).

Comparison of the composite resin categories on the basis of percent residual flexural strength retained after the fire exposure is shown in Fig. 7.14. They are exhibited a combined average for the thermoset (vinyleste, epoxy), advanced thermoset (BMI, PI), phenolic, and engineering thermoplastic (PPS, PEEK) [12, 125]. A big notice should be taken into account is the values here just evaluated after the materials are exposed to a 25 kW/m^2 radiant heat source (equivalent to thermal exposure at 400 ^{o}C) for 20 minutes according to ASTM E-662 protocol. In our case of study all the geocomposites are subjected to a much more severe thermal condition (example 800 ^{o}C equivalent to 75 kW/m^2) but geocomposites retain 50 to 60% of their original

strength at room temperature after exposing up to 600 ^{o}C for one hour for M2/basalt and M2/E-glass. Especially the temperature for M1/carbon and M2/carbon can be higher than 1000 ^{o}C.

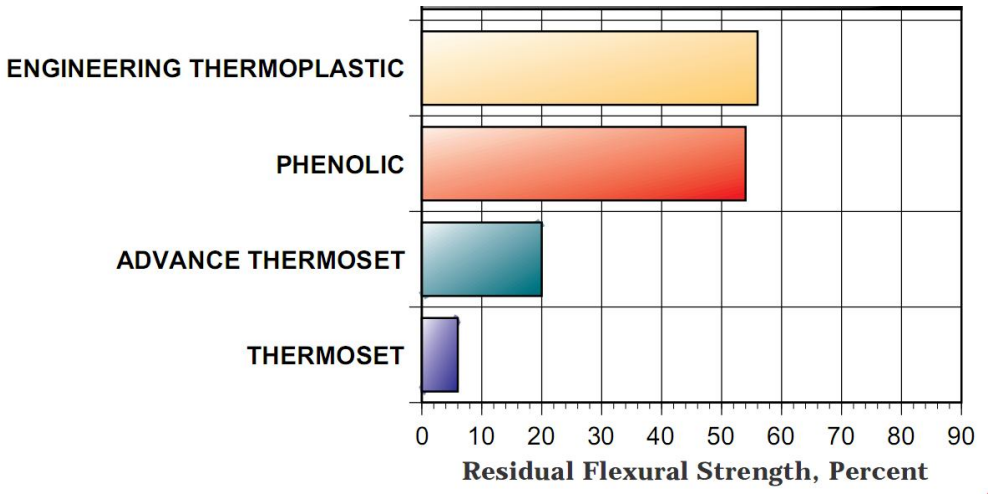

Fig. 7.14 Residual flexural strength of some commercial composites after fire exposure at a 25 kW/m^2 radiant heat source for 20 minutes [12, 125].

In comparison with the fiber reinforced ceramic matrix composites, the residual flexural strength of SiC/SiC composite retains about 80% of the room temperature at 800 ^{o}C and drops almost linearly to 55% at 1200 ^{o}C [121]. For alumina/glass and alumina/tin/glass composites behave comparably well up to 400 ^{o}C, and retaining almost 75% of their strength, but at 600 ^{o}C the glass matrix softens [14]. Meanwhile in oxidizing environments, typical carbon/carbon composites oxidize at 400 ^{o}C [75]; at 1000 ^{o}C the carbon/carbon composites retain only 20% of the room temperature strength and even optimal anti-oxidative fillers ($MoSi_2$) is added, the strength of the composites can increase up to only 41% of origins at room temperature [76].

Table 7.7 presents the thermomechanical properties of fiber reinforced concrete, structural steel, a 7000-series alminium used in aircraft structures, a phenolic - carbon fabric laminate, a phenolic – E-glass fabric laminate [125] and fiber reinforced geocomposites based on thermal silica geopolymer matrices M1 and M2. Maximum temperature capacity is defined as the temperature in air at which the nominal tensile or flexural strength falls to one-half of its room temperature value. The results show

that the composites based on geopolymer matrices and fiber reinforcements are much better in both specific flexural strength and maximum temperature capacity.

Table 7.7 Typical properties of structural materials [125]

Material	Density	Tensile Modulus	Specific Modulus	Flexural Strength	Specific Flexural Strength	T_{MC}
	[kg/m^3]	[GPa]	[MPa.m^3/kg]	[MPa]	[MPa.m^3/kg]	[^{o}C]
Fiber-Reinforced Concrete	2300	30	13.0	14	0.006	400
Structural Steel	7860	200	25.4	400	0.053	500
7000 Series Aluminium	2700	70	25.9	275	0.102	300
Phenolic-Carbon Fabric Laminate	1550	49	31.6	290	0.187	200
Phenolic-E-glass Fabric Laminate	1900	21	11.0	150	0.074	200
M1/Carbon	2000	x	x	471	0.236	≥1000
M1/Basalt	2400	x	x	452	0.188	≥400
M2/Carbon	2000	x	x	356	0.178	≥1000
M2/Basalt	2400	x	x	273	0.114	≥600
M2/E-glass	2400	x	x	202	0.084	≥600

T_{MC} - Maximum Temperature Capacity

In order to estimate the virtual flexural strength (R^*_{mo}) and modulus (E^*) of the geocomposites when support span-to-depth ratios L/H → ∞ to 1. The novel size-independent method is utilized and the typical of reciprocal effective flexural properties vs. $(H/L)^2$ ratio of geocomposites M1/Carbon after thermal exposure are presented on Fig. 7.15. However, the linear regressions are created on two series of H/L ratios so large error could be involved in extrapolation. In some cases, the error can reach nearly 100%, it is supposed that the results from these calculation are not enough accurate and no detailed presentation in our works.

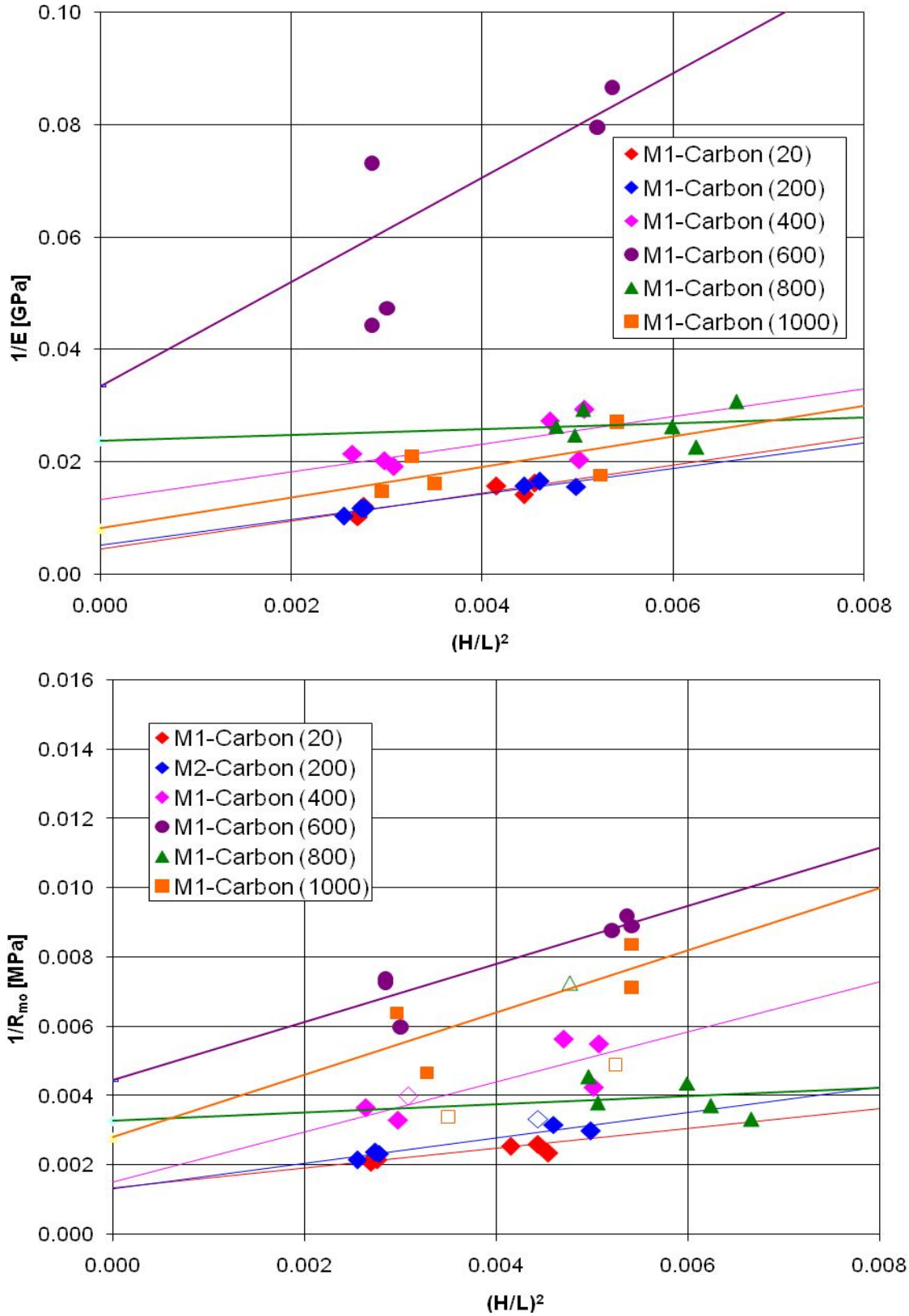

Fig. 7.15 Reciprocal effective flexural properties vs. $(H/L)^2$ ratio a) elasticity modulus, b) flexural strength of M1/Carbon after thermal exposure.

7.4 CONCLUSIONS

Thermal silica-based geopolymer reinforced composites possessing ceramic-like properties can be fabricated with simple process (using pultrusion technique, 1 hour at room temperature and 1 hour in oven at only 80 ^{o}C for M1 and 85 ^{o}C for M2 under vacuum-bagging technique and post-cured by drying at the same temperature for 5 hours more).

Generally, all the geocomposites reinforced by 45, 53 or 60 vol.% of unidirectional carbon fiber HTS 5631 1600tex 24K, basalt roving BCF13 - 2520tex - KV12 Int. or Saint-Gobain - Vetrotex E-glass E2400P192 exhibit very good thermal-mechanical properties, retain nearly 50% of flexural strength even after severe thermal exposure up to 600 ^{o}C for basalt and E-glass fiber reinforced geocomposites and 1000 ^{o}C for geocomposites with carbon fiber reinforcement for 1 hour in oxidation environment. The geopolymer resins can protect carbon fibers from oxidation; however, approximately 14 wt.% of carbon fibers is oxidized after the composites are exposed higher 800^{o}C. In addition, experimental findings show that composites based on geopolymers are very good at thermal dimensional stability, especially for matrix M2, the composites exhibit no thermal expansion even they are calcinated up to 800 ^{o}C for basalt and E-glass reinforcements and 1000 ^{o}C for carbon fiber reinforcement.

The adhesion between geopolymers and carbon fibers shows very good after curing and even exposing up to over 800 ^{o}C, after calcination at higher temparature the morphology of composite look like foam and initial reaction layer of SiC may be created as well. Around 600 ^{o}C, however, the loose interaction of fiber and matrix is detected, that causes low mechanical properties. In addition, non toxic fumes and smokes are generated during thermal exposure.

8. FABRIC REINFORCED GEOCOMPOSITES AND REAL PULTRUDED GEOCOMPOSITE RODS

In order to approach the industrial applications, the preliminary study about woven fabric reinforced geopolymers and experiments of real pultruded composite rods are carried out. In this chapter we will present the mechanical properties of based on geopolymer matrix M1 and M2 reinforced by twill carbon HTS fiber 160 g/m^2 (type 442 - Tenax) and Spaceglass 280 g/m^2 (S-glass - Tenax)**.** The procedures to fabricate unidirectional basalt fiber reinforced composites rods and their mechanical properties are displayed as well.

8.1 GEOCOMPOSITES REINFORCED BY WOVEN FABRICS

8.1.1 FLEXURAL PROPERTIES OF WOVEN FABRIC GEOCOMPOSITES

The preliminary study of four kinds of woven fabric reinforced geopolymers based on geopolymer matrices M1, M2 and two types of fabrics twill carbon HTS fiber (160 g/m^2) and twill Spaceglass 280 (280 g/m^2) (Table 3.2) are carried out in this investigation. The geocomposites are fabricated by wet hand lay-up technique, the samples are simply done by placing a woven fabric on a mold (in this case on a flat), the geopolymer is then rolled or squeegeed into the fabric layer by layer until desire thickness. Then the saturated fabrics are covered by a peel ply fabric and suction tissue then placed into a sealed plastic bag. The fabric laminate is then cured at optimal condition with 3 stages, one hour at room temperature and one hour at elevated temperature in the oven under vacuum bagging and hot vacuum bagging respectively, finally the laminate is dried for five hours more in the oven at the same temperature of the previous stage. The temperature is used for the second and third step of curing material is 80 ^{o}C for M1 system and 85 ^{o}C for M2 system. The resulting laminate having dimension about 120 x 120 x 2 mm are then cut into samples having 12 x 2 mm and suitable length for flexural testing.

Table 8.1 Flexural properties of geocomposites reinforced by woven fabrics at various outer support span-to-depth ratios

Matrix/fiber	**Fiber content**	**Outer support span-to-depth ratio**								
		L/H = 20 to 1			**L/H = 32 to 1**			**L/H = 40 to 1**		
	[vol.%]	**R_{mo}** [MPa]	**E** [GPa]	**ε_{mo}** [%]	**R_{mo}** [MPa]	**E** [GPa]	**ε_{mo}** [%]	**R_{mo}** [MPa]	**E** [GPa]	**ε_{mo}** [%]
M1/Carbon HTS twill	39	229.0 ±27.7	43.6 ±0.0	0.65	159.2 ±29.5	44.6 ±0.6	0.40	153.8 ±29.6	45.5 ±0.7	0.37
M1/S-glass twill	48	142.1 ±9.9	18.7 ±1.8	1.01	129.7 ±4.8	19.7 ±1.7	0.75	117.0 ±16.6	22.6 ±0.4	0.65
M2/Carbon HTS twill	40	213.7 ±16.6	41.2 ±1.3	0.64	226.8 ±12.4	45.1 ±0.5	0.58	189.0 ±11.3	48.8 ±0.4	0.40
M2/S-glass twill	48	113.8 ±4.1	20.9 ±1.0	0.65	103.9 ±6.4	25.4 ±1.5	0.49	113.0 ±4.2	26.6 ±0.0	0.48

Samples are tested on the universal testing machine, Instron Model 4202 (Fig. 3.8) at various outer support span-to-depth ratios L/H = 20 to 1, L/H = 32 to 1 and L/H = 40 to 1 in agreement with test spans of DIN V ENV 658:1993-02 and ASTM C1341-06. The flexural properties of resulted composites are presented in Table 8.1.

Using linear regression of a fictitious Young's modulus E and a fictitious flexural strength R_{mo} against $(H/L)^2$ value for M1 and M2 reinforced by fabric F1 and F2 (Fig. 8.1), the bending properties are summed up in Table 8.2.

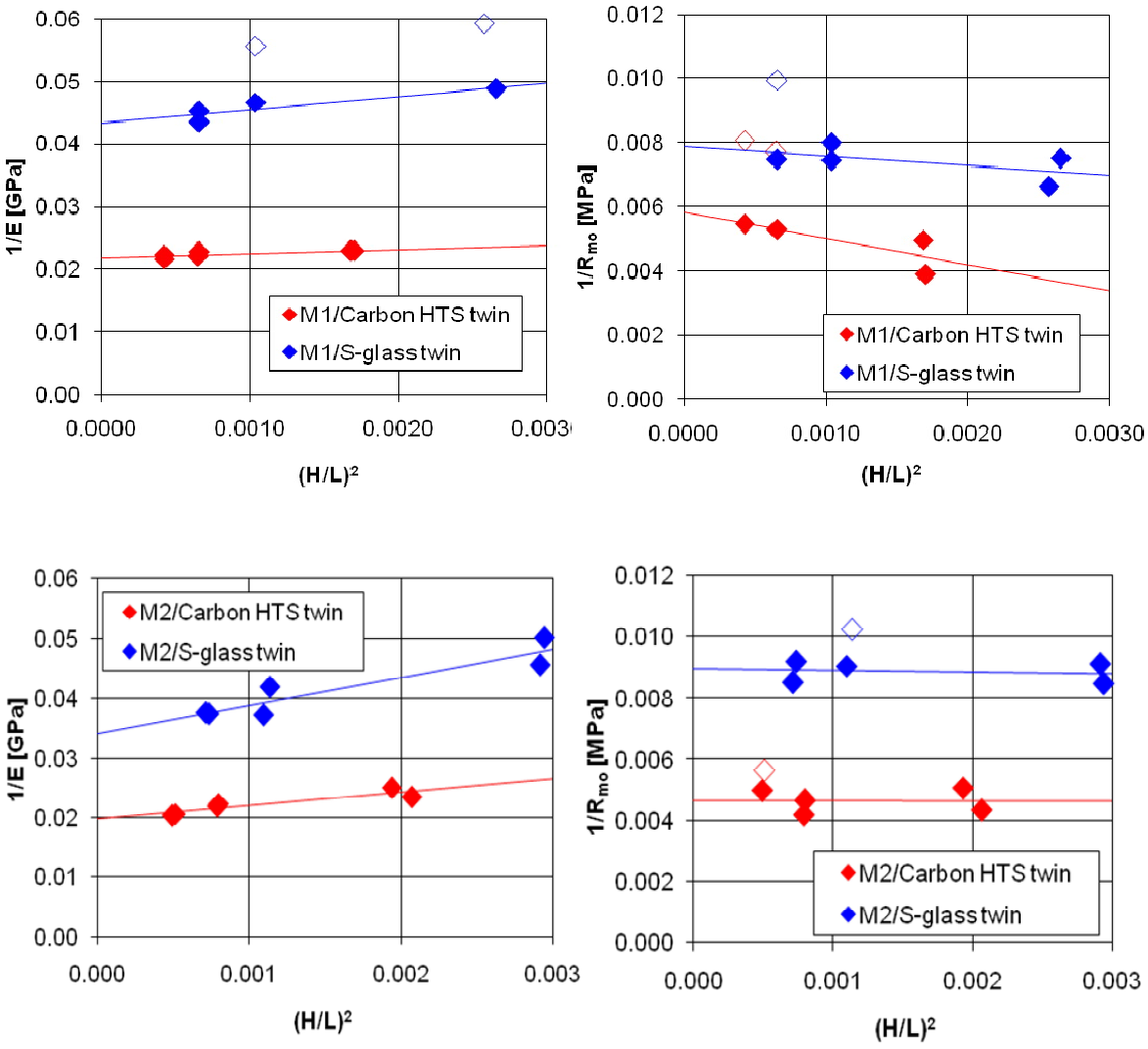

Fig. 8.1 Reciprocal effective flexural properties of M1 and M2 reinforced by F1 and F2 vs. $(H/L)^2$ ratio.

Table 8.2 Flexural strength of M1 and M2 reinforced by F1 and F2 in accordance with Size-independent method

Matrix/fabric fiber	Young's module		Shear module		Flexural strength	
	E^*		G	E^*/G	R^*_{mo}	
	[GPa]		[GPa]	[1]	[MPa]	
M1/Carbon HTS twill	**45.8** ±0.6	±1.3%	**1.7**	**26.4**	**179.3** ±1.8	±1.0%
M1/S-glass twill	**23.0** ±0.6	±2.6%	**0.6**	**41.5**	**131.1** ±8.6	±6.5%
M2/Carbon HTS twill	**50.3** ±1.7	±3.5%	**0.5**	**95.8**	**214.8** ±19.7	±9.2%
M2/S-glass twill	**29.2** ±1.5	±5.1%	**0.3**	**115.5**	**114.5** ±5.7	±5.0%

It can be seen from Table 8.1 and Fig. 8.1 that the mechanical properties of the woven fabric reinforced geocomposites are not much dependent on the outer support span-to-depth ratio. For geocomposites based on M1 system, however, the negative trend between flexural strength and modulus and H/L ratios are determined.

8.2.2 MICROSTRUCTURE OF FABRIC REINFORCED GEOCOMPOSITES

The microstructure of these geopolymer matrix composites are studied by assistance of Scanning Electron Microscopy. Generally, from the SEM images (Fig. 8.2 and 8.3) of polished sections we can see that the adhesion between geopolymer matrices and the fabric fibers seem quite good and geopolymer resins are well penetrated into the fibers although no compression technique is used. However, the micro-cracks are determined and many defects such as voidage and lacked resin zones are detected as well. Futher investigation should be carried out to improve the fiber content, reduce the voidage and finally enhance the mechanical properties of the composites.

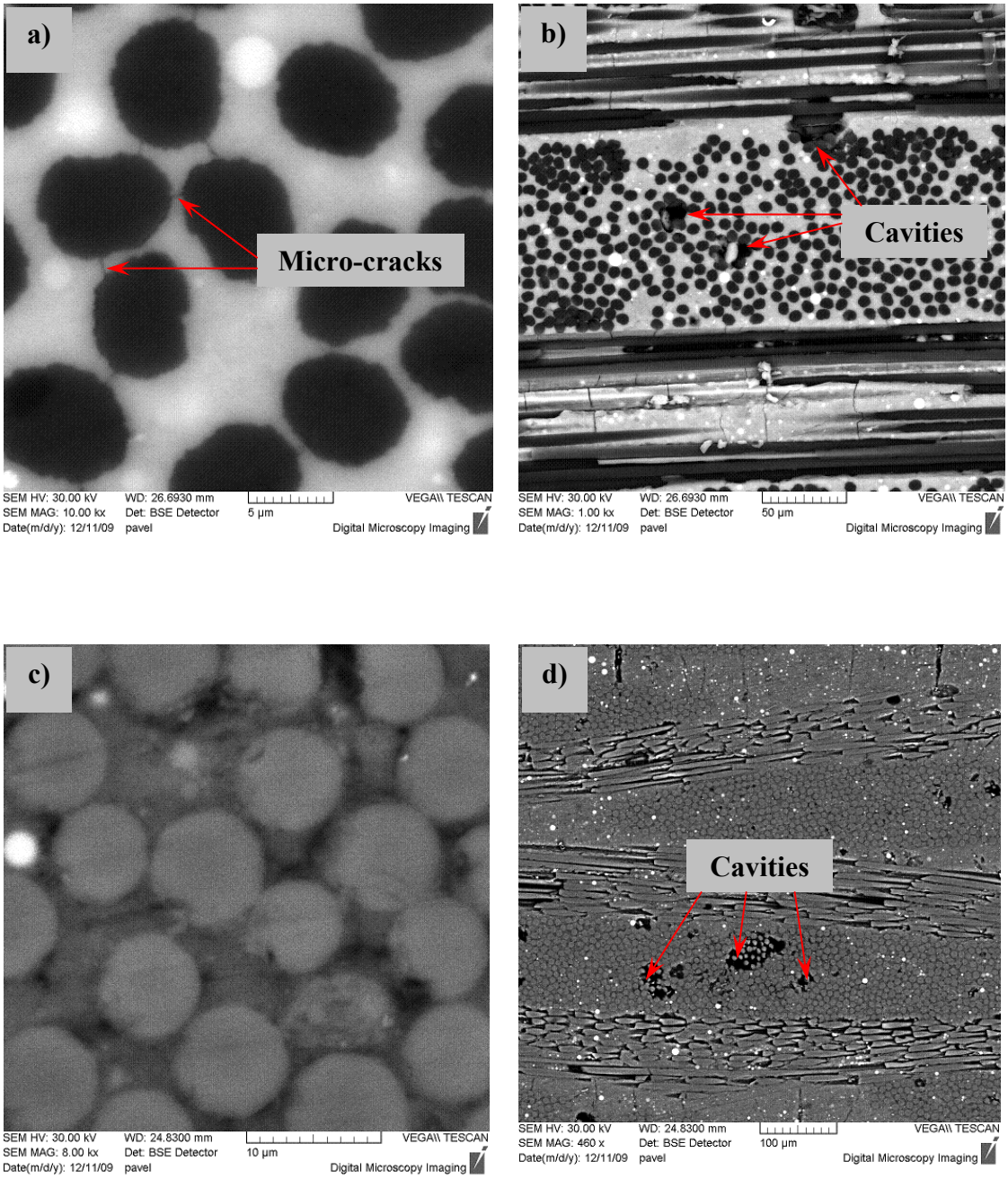

Fig. 8.2 SEM images on polished sections of geopolymer composite matrix M1 and carbon HTS twill a) 10.0kx and b) 1.0kx and S-glass twill c) 8.0kx and d) 400x.

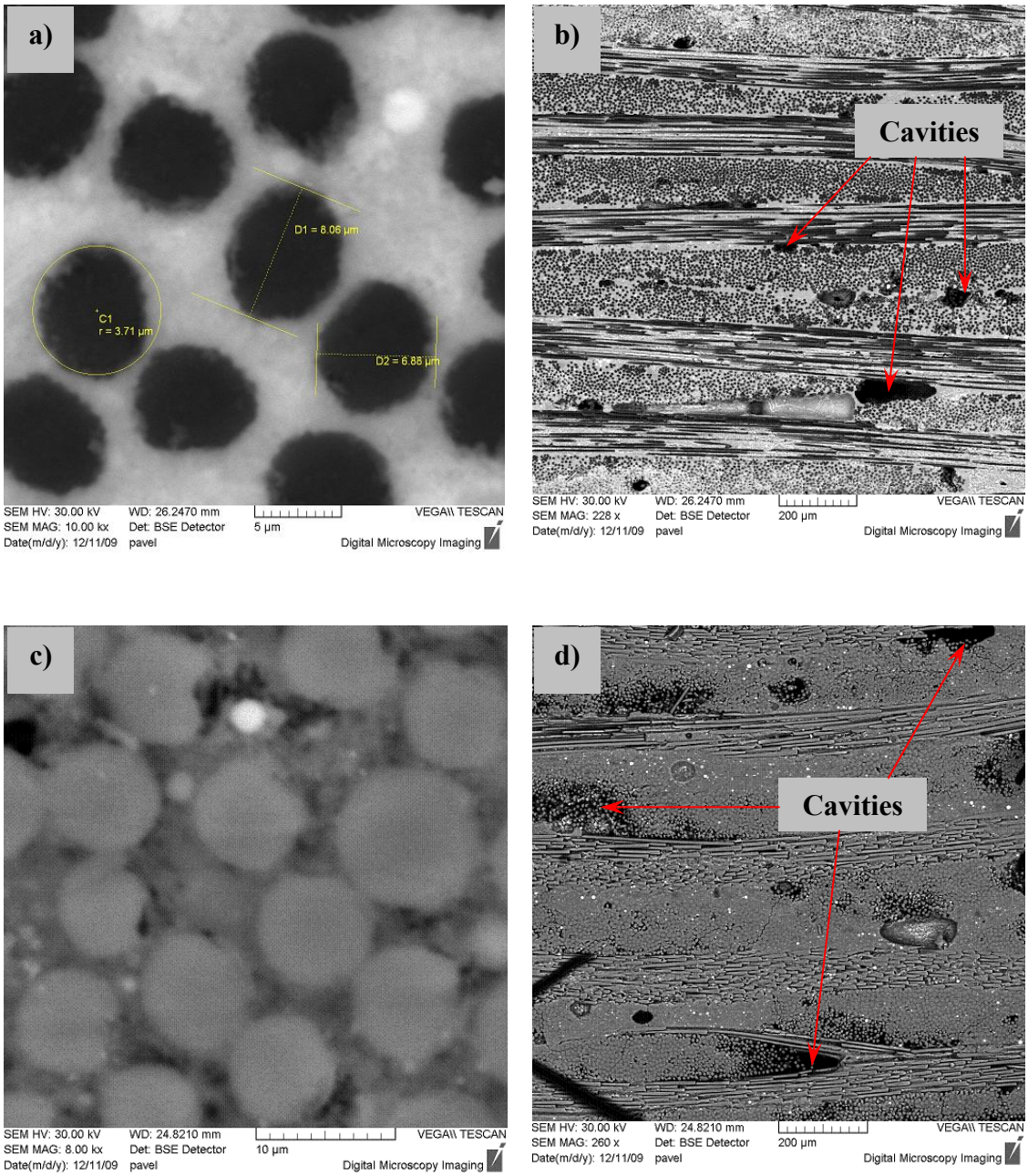

Fig. 8.3 SEM images on polished sections of geopolymer composite matrix M2 and carbon HTS twill a) 10.0kx and b) 228x and S-glass twill c) 8.0kx and d) 200x.

8.2 MECHANICAL PROPERTIES OF GEOCOMPOSITE RODS

Fig. 8.4 presents schematic representation of real pultrusion machine used for fabricating the unidirectional basalt fiber reinforced composite rods. Fourteen roving pools (1) of advanced basalt fiber BCF13-2520-KV12 Int. are used. The multiplicity of reinforcements (2) with the assistance of comprises and guide bar (3 and 6) are pulled through resin bath (4) containing geopolymer resin M1 (5). All saturated bundles (7)

are pulled continuously through 500 mm of hot forming die (8) with cross-section of form 8 x 4 mm^2, the temperature of forming die is maintained approximately 60 ^oC by a metal mat heater. The uncured formed geopolymer rod is continued pulling through approximately 5 meter of controlled hot curing chamber with temperature of 80 ^oC guaranteed by two heat guns. Linear velocity of the sample moving is 8 cm/min, therefore the material is cured totally about 70 minutes.

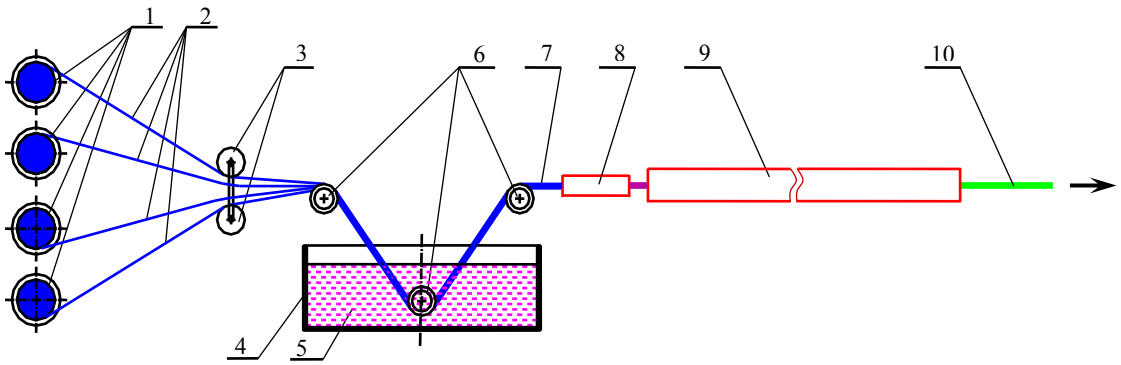

Fig. 8.4 Schematic representation of machine for basalt fiber composite rod.

1 – roving spools
2 – multiplicity of reinforcements
3 – comprises bars or guides
4 – resin chamber
5 – geopolymer resin (M1)
6 – guide bars
7 – saturated bundles
8 – controlled hot forming die
9 – controlled hot curing chamber
10 – composite rod

Generally, the samples are not completely cured after being taken from the pultrusion machine. They are kept in room temperature for over 5 days more and cut up appropriate length for flexural test. In our research, we used two recommended outer support span-to-depth ratios L/H = 32 to 1 and L/H = 40 to 1 (corresponding with span L = 120 and L = 155 mm respectively) for testing and evaluating mechanical properties of the composite rods.

The mechanical properties of geocomposite rods based on geopolymer M1 and continuous basalt fibers with density around 2.4 Mg m^{-3} are presented in Table 8.3. As can be seen from the table that the pultruded basalt reinforced composite rods show quite good mechanical properties when they are fabricated by real pultrusion machine, although the composites presents lower percentage of fiber content (around 47 vol.% in comparison with 53 vol.% for composites made in laboratory scale) and fortunately,

at high outer support span-to-depth ratios L/H ≥ 32 to 1 we can achieve the same mechanical properties at different testing spans for pultruded unidirectional basalt BCF13-2520tex-KV12 Int. fiber reinforced geopolymer rods.

Table 8.3 Flexural properties of unidirectional basalt fiber reinforced geocomposite rod by real pultruded machine at various outer support span-to-depth ratios

Outer support span-to-depth ratio	**Fiber content**		**Flexural properties**		
	[wt.%]	[vol.%]	$\mathbf{R_{mo}}$ [MPa]	**E** [GPa]	$\boldsymbol{\varepsilon_{mo}}$ [%]
L/H = 32 to 1	53.6	47.2	439.4 ±26.6	43.4 ±2.1	1.10
L/H = 40 to 1			472.1 ±12.4	42.3 ±1.2	1.31

8.3 CONCLUSIONS

Utilizing a very simple wet hand lay-up technique we can manufacture woven fabric reinforce geocomposites with quite good distribution of geopolymer resin in the composites. This means that geopolymers based on thermal silica with fine particles can overcome obstacles and difficulties of very high pressure must be applied to penetrate the resin into the spaces between single filament fibers from the geopolymers based on classical raw materials such as kaoline, metakaoline, fly-ash, furnace blast slag and so on [18].

The geopolymer resins show good preliminary properties when real pultrusion technique are applied to manufacture fiber reinforced geocomposites for potential industrial applications as constructional materials.

9. CONCLUSIONS AND RECOMMENDATIONS

9.1 REMARKABLE CONCLUSIONS

The key outcome of the thesis is to develop geopolymers based on thermal silica, use them as matrices for fiber reinforced composites and finally to recommend potential applications.

Two formulations of geopolymer matrices, abbreviated as 'M1' and 'M2', based on thermal silica with fine size-particle, potassium hydroxide solution and further minor admixtures for improving application features, such as boric and phosphoric acid, are created and synthesized. The pure geopolymers, with the density around 2.2 Mg m^{-3} and rather homogeneous distribution of all main elements, present very good mechanical properties, almost at the top of the results of previous studies. Generally, about 20 MPa of flexural strength for both M1 and M2; 35 and 23 GPa of flexural modulus for M1 and M2 respectively. Compressive properties of the bare matrices are outstanding, approximately 89 and 119 MPa of compressive strength, 117 and 194 GPa of compressive modulus for geopolymer M1 and M2 system respectively. However, many micro-cracks with the maximum width ranging around 5 μm of M1 and 2 μm of M2 are detected.

For first stage of research and development of new material systems, geopolymer composites, unidirectional fibers (rovings) are used to offer the opportunity to test various combinations of fibres and geopolymer matrices, in addition, the results are not affected by the way of how fabrics are weaved [72]; and continuous fibers are used popularly for reinforcing structural composites [92]. Seven popular commercial unidirectional fibers, including Carbon HTS 5631 800tex 12K and HTS 5631 1600tex 24K, Nippon Alkali resistance glass for pultrusion (AR-G 2500tex), Saint-Gobain alkali resistance glass (ARG 2400tex), Advanced Basalt fiber BCF13-2520-KV12 Int., Saint-Gobain Electrical grade glass (E-glass) for pultrusion and Ceramic 3M-312 fiber are evaluated in accordance with Japanese Industrial Standard (JIS R 7601) [93] at ambient condition before and after treatment at 200 ^{o}C, 400 ^{o}C, 700 ^{o}C and 1000 ^{o}C for 3 hours with a gradient of 10K.min^{-1} in oxidation environment. Results show that at

ambient conditions, the mechanical properties of all fibers are lower than the original values from the manufacturers, especially for carbon fiber. In real conditions, for both carbon fibers approximately 73% and 74% of tensile strength and modulus are determined. For other fibers we can get around 95% of original strength at ideal conditions of testing from the producers; however, in case of tensile modulus, only 54% and 42% of origins for ARG 2400tex and E-glass are evaluated. Exceptionally carbon fibers which shown that strength, elongation and Young's modulus are nearly constant after 3 hours sustaining at 400 ^{o}C in a furnace, the other kinds of fibers present considerable lower values in comparison with the origins from ambient condition, the strength of basalt and E-glass are about 50% retention after exposing to this temperature and they seem to become a little brittle. After thermal exposure up to 700 ^{o}C, only E-glass and ceramic 3M-132 fibers show residual strength, for E-glass about 37% of strength remain. Based on preliminary investigation of ability to combine with geopolymer to form geopolymer composites, only three kinds of unidirectional fibers are chosen for reinforcing geopolymer composites: carbon HTS 5631 1600tex 24K is expected to apply at high temperature, due to the matrix ability to protect the fiber from oxidation; Saint-Gobain - Vetrotex E-glass E2400P192 fiber in order to achieve low cost of products and E-glass fiber even retains strength after exposing up to 700 ^{o}C. The last fiber for our investigation is basalt BCF13 - 2520tex - KV12 Int. because of chemical compatibility with geopolymer, 80% of strength of carbon fibers, moreover basalt fiber can be consider an alternation to glass fiber [94].

Unidirectional fiber reinforced geocomposites containing 45, 53 and 60 vol.% of unidirectional fibers of carbon HTS 5631 1600tex 24K, basalt BCF13 - 2520tex - KV12 Int. and Saint-Gobain - Vetrotex E-glass E2400P192 respectively are fabricated. In laboratory scale, simplified home-made impregnation machine is designed based on the simulation of real pultrusion technology; the machine permits us to choose the optimal impregnated velocity (around 34 m/h) with well resin penetration into the bundle of fibers and nearly constant proportion of fibers and resin are controlled. The materials are cured at three stage process with vacuum bagging technique. Generally, experimental findings show that in terms of good mechanical properties, the optimal temperature is recommended to cure these geocomposites ranging from 60 to 90 ^{o}C at the second stage of curing, the stage contains two deciding important factors of curing

procedure to properties of geopolymer composite systems and determines labor productivity and finally is the energy of fabrication process and cost of the productions. At lower temperatures there is a danger of unsatisfactorily created bonds between matrix and fiber, and the rate of hardening can be unacceptable from technical standpoint; at higher temperatures the heating can enlarge voids and total porosities. In both cases the lower mechanical properties are determined.

By measuring the mechanical properties of geocomposites at different curing time at the second stage of curing process, the optimal curing time for unidirectional fiber reinforced geocomposites is one hour at room temperature and one hour at elevated temperature in a oven (80 ^{o}C for M1 system and 85 ^{o}C for M2 system) under vacuum bagging and hot vacuum bagging technique respectively, finally the geocomposites are dried for 5 hours at the same temperature as that of previous stage and time curing is abbreviated as 1:01:05.

The effects of curing time at ambient conditions on mechanical properties of the fiber reinforced composites are studied. For the composites based on geopolymer M1 system, the composites seem completely cured after approximately 14 days of curing and in general, we can see that after 24 hours curing at ambient conditions the flexural strength and modulus are nearly 60% of values of composites after cured 14 days for all geocomposites M1/Carbon, M1/Basalt, M1/Eglass. Meanwhile, for geopolymer M2 composites, the time for curing must be longer than 30 days and after 4 days of ambient conditions of curing, approximately 30% of flexural strength and modulus of composites cured after 30 days for M2/Carbon, the value for M2/Basalt is 50% and nearly 70% for M2/E-glass.

Utilizing better vacuum pump, a rotary oil vacuum pump with more power of capacity and lower vacuum pressure instead of a membrane vacuum pump, and longer time for curing at ambient conditions the geocomposites show excellent mechanical properties. After curing 40 days for M1 system, in comparison with the mechanical properties when the composites are cured at optimal time and elevated temperature and at the same outer support span-to-depth ratio L/H = 20 to 1, we have flexural strength of M1/carbon is 70% higher (800.4 MPa compared to 470.9 MPa) and flexural modulus is about 36% better (125.9 GPa in contrast to 92.3 GPa). For composite M1/Basalt,

approximately 50% of the strength is improved but 9% of modulus is determined lower (678.7 MPa and 62.5 GPa in comparison with 451.7 MPa and 68.2 GPa respectively). And for geocomposite M1/E-glass fibers, the mechanical properties present 80% and 34% of better flexural strength and modulus are evaluated (260.2 MPa and 58.9 GPa compared to 144.5 MPa and 44.0 GPa). For more details, see Table 6.1 and 6.6.

For M2 system, after curing at ambient condition for over 50 days, remarkable better mechanical properties of all composites are determined. Around 57%, 23% and 32% of flexural strength of M2/Carbon, M2/Basalt and M2/E-glass respectively (559.0, 334.8 and 267.3 MPa compared to 355.7, 273.1 and 202.0 MPa). However, the Young's modulus of M2/Carbon and M2/E-glass increases only 12% and 9% (119.7 GPa and 61.6 GPa in contrast to 106.6 GPa and 56.6 GPa); on the contrary, about 14% of flexural modulus of M2/Basalt are lower than that of when curing at optimal condition at elevated temperature (57.9 compared to 65.9). More information are shown from Table 6.2 and 6.6.

Geopolymer matrices possess a high pH generally, which can frequently damage glass fibers by both chemical and physical means, severely degrading its strength. Even the cured matrices still exhibit a high pH in a solid form, which continues to promote glass fiber degradation. So, the physical performance of E-glass fibers geocomposite usually is extremely poor, especially, when these geocomposites are cured at higher temperature and longer time (M1/E-glass). However, when phosphoric acid is added (M2) the problems are improved.

Because carbon fibers are electrically and thermally conductive, which eliminates many important dielectric and thermal insulating applications. In addition, carbon fibers are several times more expensive than glass fibers and carbon fibers severely oxidize at 450 ^{o}C, which eliminates many important high temperature applications. Also, when carbon fibers are combined with the alkali silicate matrix they have two different thermal expansion coefficients, which can lead to micro-cracks during thermal cycling [8, 90]. All these factors should carefully take into account for future applications.

Thermal silica-based geopolymer reinforced composites possessing ceramic-like properties can be fabricated with simple process at low temperature. Generally, all the geocomposites exhibit very good thermal-mechanical properties, retain nearly 50% of

flexural strength even after severe thermal exposure up to 600 ^{o}C for basalt and E-glass fiber reinforced geocomposites and 1000 ^{o}C for geocomposites with carbon fiber reinforcement for 1 hour in oxidation environment. The geopolymer resins can protect carbon fibers from oxidation; however, approximately 14 wt.% of carbon fibers is oxidized after the composites are exposed higher 800 ^{o}C. In addition, experimental findings show that composites based on the geopolymers are very good at thermal dimensional stability, especially for matrix M2, the composites exhibit no thermal expansion even they are exposed up to 800 ^{o}C for basalt and E-glass reinforcements and 1000 ^{o}C for carbon fiber reinforcement.

The adhesion between geopolymers and carbon fibers shows very good after curing and even exposing up to over 800^{o}C, after calcination at higher temparature the morphology of composites look like foam and initial reaction layer of SiC may be created as well. Around 600^{o}C, however, the loose interaction of fiber and matrix is detected, that causes low mechanical properties. In addition, non toxic fumes and smokes are generated during thermal exposure.

With the fine size-particle (D_{50} 0.62 μm, D_{90} 3.24 μm), thermal silica based geopolymers present good penetration of resins into reinforcements just with a very simple wet hand lay-up technique, fine distribution of geopolymer binders are determined in twill woven fabric carbon HTS fiber 160 g/m^2 and Spaceglass 280 g/m^2 with the diameter of single filament around 7 and 10 μm without high pressure for penetrating the resin into the spaces between single filament fibers.

The success of preliminary study of pultruded unidirectional fiber reinforced geocomposites rods which are fabricated by real pultrusion technique and machine exhibits that geopolymer resins possess good workability with pultruded fabrication and open a nice view of geocomposites for potential industrial applications as constructional materials.

In summary, two new kinds of thermal silica based geopolymer materials (Si/Al ≈ 10; fine size-particle, compatible with fabrics) are developed with very good properties ranging in the top of the results of previous studies. Seven popular commercial fibers are evaluated at real ambient conditions before and after heat treatment, which are not only necessary for our investigation but for any researches that prefer the real abbilities

of fibers than the manufacurers' values in nearly ideal conditions. Simplified home-made impregnation machine can be used to study the combination of any new binders and unidirectional fibers. Five kinds of fiber reinforced geocomposites possess ceramic-like properties: light-weight, high strength, fire-resistance, low-thermal conductivity, dimensional stability, non toxic fumes and smokes, protect carbon fibers from oxidation ect, meanwhile the composites can be made with simple process at very low temperature (even at room temperature). Last but never least, the price of geopolymer materials is relative cheap.

9.2 LIMITATIONS AND RECOMMENDATIONS

Although we tried our best to study wide knowledge from literatures and organize our best experiments for solving and explaining the planned aims of the dissertation. However, many limitations appear during the time and in order to apply these materials in to industries, further experiments should be carried out.

- Based on mechanical properties, microstructures and total porosities, the optimal curing conditions are determined. However, the chemical mechanism of the procedures is not explained.
- Geopolymers do possess high pH even after solidification (pH = 10 to 11), due to the fiber degradation in this medium, long-term mechanical properties of composites cured at ambient conditions for longer time must be carried out.
- Residual mechanical properties of geocomposites are measured after one cycle thermal exposure, but in constructional applications the properties as soon as high temperature or repeated thermal or even long-term exposure must be more important. Therefore, further investigation of these should be taken place.
- The mechanical properties just defined under static load. In real applications, the load could be impact or repetitive or both. So, the impact test and fatigue properties should be taken into account.
- The relative thermal expansion of two component part of composites should be investigated together to know their behavior at elevated temperature, these may explain why at 600 ^{o}C the mechanical properties of M1/carbon degreases remarkably.

- Thermal properties, such as thermal conductivity, heat capacity should be studied carefully for each kind of composites.
- In order to widen the potential applications of geocomposites, their properties should be determined at minus temperature.
- From the literature, high-press or even high-hot-press could be used to improve mechanical properties of fabric reinforced composites. This matter should be considered in case we would like to improve mechanical properties of our composites ect.
- In addition, the geopolymer could be developed based on fly-ash, in this case geopolymers and composites thereof is considered as a new trend of green ecological materials.

Based on our preliminary results, we recommend to use our materials for further research to apply into building industries as fire and insulation barriers, fiber geocomposite rods for reinforcing concretes; or anywhere restricted egress of fire hazard is an important design consideration such as ground transportations, submarine and ship industries and even aircraft.

REFERENCES

[1] Brent Strong, A. (2002) *History Of Composite Materials -- Opportunities And Necessities*. **Brigham Young University**.

[2] Chung, D.D.L., *Composite Materials - Science and Applications*. 2010, Springer: Springer London Dordrecht Heidelberg NewYork.

[3] Kakani, S.L. and A. Kakani, *Material Science*. 2004: New Age International (P) Ltd., Publishers. 657.

[4] Advanced Composites Group, A. *Introduction to Advanced Composites and Prepreg Technology*. 2010 [cited 2010 1 September]; Available from: http://www.advanced-composites.co.uk/intro%20to%20advanced%20composites/prepregs%20and%20introduction%20to%20advanced%20composites.html.

[5] Davidovits, J. *Chemistry of Geopolymeric Systems, Terminology*. in *Geopolymere '99 International Conference*. 1999. Saint-Quentin, France.

[6] Davidovits, J. and J.L. Sawyer, *Early high-strength mineral polymer* U.S. Patent 4,509,985, 1985: United States.

[7] Davidovits, J., *Geopolymers: Inorganic Polymeric New Materials.* Thermal Analysis, 1991. **37**: p. 1633-1656.

[8] Davidovits, J., *Geopolymer Chemistry & Applications*. 2008a, France: Institute Géopolymèr. 587.

[9] Davidovits, N., M. Davidovics, and J. Davidovits, *Ceramic-ceramic composite material and production method*, U.S. Patent 4,888,311, 1989: United States.

[10] Davidovits, J. *30 Years of Successes and Failures in Geopolymer Applications - Market trends and Potential breakthroughs*. in *Geopolymer 2002 Conference*. 2002. Melbourne, Australia: Geopolymer Institute.

[11] Davidovits, J. *Geopolymer chemistry and sustainable Development - The Poly(sialate) terminology : a very useful and simple model for the promotion and understanding of green-chemistry*. in *Geopolymer 2005 World Congress*. 2005. Saint-Quentin (North of Paris), France: Geopolymer Institute.

[12] Lyon, R.E., et al., *Fire-resistant aluminosilicate composites.* Fire and Materials, 1997. **21**(2): p. 67-73.

[13] Duxson, P., et al., *Geopolymer technology: the current state of the art.* Journal of Materials Science, 2007. **42**(9): p. 2917-2933.

[14] Papakonstantinou, C.G., P. Balaguru, and R.E. Lyon, *Comparative study of high temperature composites.* Composites Part B: Engineering, 2001. **32**(8): p. 637-649.

[15] Papakonstantinou, C.G. and P.N. Balaguru, *Use of geopolymer matrix for high temperature resistant hybrid laminates and sandwich panels*, in *Geopolymer 2005 World Congress*, J. Davidovits, Editor. 2005, Geopolymer Institute: Saint-Quentin (North of Paris), France. p. 201-207.

[16] Sheppar, L.M. *Geopolymer Composites: A Ceramics Alternative to Polymer Matrices*. The 105th Annual Meeting and Exposition of the American Ceramic Society 2007 [cited 2009 30 September]; Available from: http://composite.about.com/library/weekly/aa030529.htm.

[17] Bortnovsky, O., et al., *Properties of Phosphorus-Containing Geopolymer Matrix and Fiber-Reinforced Composite.* Mechanical Properties and Performance of Engineering Ceramics and Composites IV, 2009: p. 283-299.

[18] J.L. Bell, D.C.C., M. Gordon, and W.M. Kriven. *Graphite Fiber Reinforced Geopolymer Molds for Near Net Shape Casting of Molten Diferrous Silicide*. in *GGC 2005: International Workshop On Geopolymers And Geopolymer Concrete*. 2005. Perth, Australia: Curtin University of Technology.
[19] Malhotra, V.M., *High-Performance High-Volume Fly Ash Concrete.* ACI Concrete International, 2002. **24**(7): p. 1-5.
[20] Malhotra, V.M. and P.K. Mehta, *High-Performance, High-Volume Fly Ash Concrete: Materials, Mixture Proportioning, Properties, Construction Practice, and Case Histories.* 2002, Suppementary Cementing Materials for Sustainable Development Inc.: Ottawa, Canada.
[21] van Jaarsveld, J.G.S., J.S.J. van Deventer, and G.C. Lukey, *The effect of composition and temperature on the properties of fly ash- and kaolinite-based geopolymers.* Chemical Engineering Journal, 2002. **89**(1-3): p. 63-73
[22] Davidovits, J. *Solid phase synthesis of a mineral blockpolymer by low temperature polycondensation of aluminosilicate polymer*. in *IUPAC International Symposium on Macromolecules*. 1976. Stockholm.
[23] Tossell, J.A., *A theoretical study of the molecular basis of the Al avoidance rule and of the spectral characteristics of Al-O-Al linkages.* American Mineralogist, 1993. **78**: p. 911-920.
[24] Duxson, P., et al. *Structural Ordering in Geopolymers Derived from Metakaolin*. in *Geopolymer: Green Chemistrty and Sustainable Development Solutions*. 2005a.
[25] Davidovits, J. *Soft Mineralurgy and Geopolymers*. in *Geopolymer '88, First European Conference on Soft Mineralurgy*. 1988a. Compiegne, France.
[26] Davidovits, J. *Geopolymer Chemistry and Properties*. in *Geopolymer '88, First European Conference on Soft Mineralurgy*. 1988b. Compiegne, France.
[27] Davidovits, J. *Properties of Geopolymer Cerments*. in *First International Conference on Alkaline Cements and Concretes*. 1994. Kiev, Ukraine.
[28] Davidovits, J., *Mineral polymers and methods of making them* U.S. Patent 4,349,386, 1982: United States.
[29] Van Jaarsveld, J.G.S., J.S.J. Van Deventer, and L. Lorenzen, *The potential use of geopolymeric materials to immobilise toxic metals: Part I. Theory and applications.* Minerals Engineering, 1997. **10**(7): p. 659-669.
[30] Davidovits, J. 2008b [cited 2008 15 March]; Available from: http://www.geopolymer.org.
[31] Krivenko, P.V. *Alkaline cements*. in *First International Conference on Alkaline Cements and Concretes*. 1994. Kiev, Ukraine.
[32] Rahier, H., et al., *Low-temperature synthesized aluminosilicate glasses.* Journal of Materials Science, 1996. **31**(1): p. 71-79.
[33] Palomo, A., M.W. Grutzeck, and M.T. Blanco, *Alkali-activated fly ashes: A cement for the future.* Cement and Concrete Research, 1999. **29**(8): p. 1323-1329.
[34] Fernández-Jiménez, A., A. Palomo, and M. Criado, *Microstructure development of alkali-activated fly ash cement: a descriptive model.* Cement and Concrete Research, 2005. **35**(6): p. 1204-1209.
[35] Bao, Y., M.W. Grutzeck, and C.M. Jantzen, *Preparation and Properties of Hydroceramic Waste Forms Made with Simulated Hanford Low-Activity Waste.* Journal of the American Ceramic Society, 2005. **88**(12): p. 3287-3302.

[36] Mallicoat, S., B. Sarin, and W.M. Kriven. *Novel, Alkali-bonded, Ceramic Filtration Membranes*. in *Developments in Advanced Ceramics and Composites: A Collection of Papers Presented at the 29th International Conference on Advanced Ceramics and Composites*. 2005. Cocoa Beach, Florida: Wiley.
[37] Sofi, M., et al., *Bond performance of reinforcing bars in inorganic polymer concrete (IPC).* Journal of Materials Science, 2007. **42**(9): p. 3107-3116.
[38] García-Lodeiro, I., et al., *Effect of Calcium Additions on N–A–S–H Cementitious Gels.* Journal of the American Ceramic Society, 2010. **93**(7): p. 1934-1940.
[39] Hermann E., et al. *Solidification of various radioactive residues by Geopolymere with special emphasis on long-term stability*. in *Geopolymer International Conference: GÉOPOLYMÈRE '99*. 1999. Saint-Quentin.
[40] Xu, H. and J.S.J. Van Deventer, *The geopolymerisation of alumino-silicate minerals.* International Journal of Mineral Processing, 2000. **59**(3): p. 247-266.
[41] Hos, J.P., P.G. McCormick, and L.T. Byrne, *Investigation of a synthetic aluminosilicate inorganic polymer.* Journal of Materials Science, 2002. **37**(11): p. 2311-2316.
[42] Duxson, P., et al., *Effect of Alkali Cations on Aluminum Incorporation in Geopolymeric Gels.* Industrial & Engineering Chemistry Research, 2005. **44**(4): p. 832-839.
[43] Xu, H. and J.S.J. van Deventer, *Effect of Source Materials on Geopolymerization.* Industrial & Engineering Chemistry Research, 2003. **42**(8): p. 1698-1706.
[44] Blum, L.A., *Role of surface speciation in the low-temperature dissolution of minerals.* Nature, 1988. **331**(6155): p. 431-433.
[45] Walther, J.V., *Relation between rates of aluminosilicate mineral dissolution, pH, temperature, and surface charge.* American Journal of Science, 1996. **296**: p. 693-728.
[46] Oelkers, E.H., *General kinetic description of multioxide silicate mineral and glass dissolution.* Geochimica et Cosmochimica Acta, 2001. **65**(21): p. 3703-3719.
[47] Madani, A., et al., *Silicon-29 and aluminum-27 NMR study of zeolite formation from alkali-leached kaolinites: influence of thermal preactivation.* The Journal of Physical Chemistry, 1990. **94**(2): p. 760-765.
[48] Bortnovsky, O., et al. *Structure and stability of geopolymers synthesized from kaolinitic and shale clay residues*. in *Geopolymer, green chemistry and sustainable development solutions, The World Congress Geopolymer 2005, Sain-Quentin*. 2005. Sain-Quentin, France: Geopolymer Institute.
[49] Amândio, T.-P. and V. Eduardo, *Optimised Conditions for the Obtaining of Metakaolin.* Materials Science Forum, 2006. **514 - 516**: p. 1536-1540.
[50] Giancaspro, J., C. Papakonstantinou, and P. Balaguru, *Fire resistance of inorganic sawdust biocomposite.* Composites Science and Technology, 2008. **68**(7-8): p. 1895-1902.
[51] Van Jaarsveld, J.G.S., J.S.J. Van Deventer, and L. Lorenzen, *Factors Affecting the Immobilization of Metals in Geopolymerized Flyash.* Metallurgical and Materials Transactions B, 1998. **29**(1): p. 283-291.
[52] Rangan, B.V. *Fly Ash-Based Geopolymer Concrete*. 2008 [cited 2010 25 July]; Available from: http://www.yourbuilding.org/Article/NewsDetail.aspx?p=83&id=1570.
[53] Duxson, P., et al., *Understanding the relationship between geopolymer composition, microstructure and mechanical properties.* Colloids and Surfaces A: Physicochemical and Engineering Aspects, 2005b. **269**(1-3): p. 47-58.

[54] Kriven, W.M. and J.L. Bell, *Effect of Alkali Choice on Geopolymer Properties.* Ceramic Engineering and Science Proceedings, 2004: p. 99-104.
[55] Singh, P.S., T. Bastow, and M. Trigg, *Outstanding problems posed by nonpolymeric particulates in the synthesis of a well-structured geopolymeric material.* Cement and Concrete Research, 2004. **34**(10): p. 1943-1947.
[56] Sindhunata, et al., *Effect of Curing Temperature and Silicate Concentration on Fly-Ash-Based Geopolymerization.* Industrial & Engineering Chemistry Research, 2006. **45**(10): p. 3559-3568.
[57] Wang, H., H. Li, and F. Yan, *Synthesis and mechanical properties of metakaolinite-based geopolymer.* Colloids and Surfaces A: Physicochemical and Engineering Aspects, 2005. **268**(1-3): p. 1-6.
[58] Weng, L., et al., *Effects of aluminates on the formation of geopolymers.* Materials Science and Engineering B, 2005. **117**(2): p. 163-168.
[59] Mehta, P.K. *High-Performance, High-Volume Fly Ash Concrete for Sustainable Development*. in *International Workshop on Sustainable Development and Concrete Technology*. 2004. Beijing, China.
[60] Duxson, P., et al., *The effect of alkali and Si/Al ratio on the development of mechanical properties of metakaolin-based geopolymers.* Colloids and Surfaces A: Physicochemical and Engineering Aspects, 2007. **292**(1): p. 8-20.
[61] Jirasit, F. and L. Lohaus. *Effects of High Silica-Content Materials on Fly Ash-Based*. in *Geopolymer : Green Chemistrty and Sustainable Development Solutions, The World Congress Geopolymer 2005*. 2005. Sain-Quentin, France: Geopolymer Institute.
[62] Van Jaarsveld, J.G.S., J.S.J. Van Deventer, and A. Schwartzman, *The potential use of geopolymeric materials to immobilise toxic metals: Part II. Material and leaching characteristics.* Minerals Engineering, 1999. **12**(1): p. 75-91.
[63] Pacheco Torgal F., Castro Gomes J. P., and J. S. *Geopolymeric Binder Using Tungsten Mine Waste: Preliminary Investigation*. in *Geopolymer : Green Chemistrty and Sustainable Development Solutions, The World Congress Geopolymer 2005*. 2005. Sain-Quentin, France.
[64] Nugteren, H.W., V.C.L. Butselaar-orthlieb, and M. Izquierdo, *High Strength Geopolymers Produced from Coal Combustion Fly Ash.* Global NEST Journal, 2009. **11**(2): p. 155-161.
[65] Miller, N.A., C.D. Stirling, and C.I. Nicholson. *The relationship between cure conditions and flexural properties in flyash-based geopolymers*. in *Geopolymer, green chemistry and sustainable development solutions, the World Congress Geopolymer 2005*. 2005. Sain-Quentin, France.
[66] Davidovits, J., *Synthetic mineral polymer compound of the silicoaluminates family and preparation process*, U.S. Patent 4,472,199, 1984: United States.
[67] Laney Bill, E., et al., *Advanced geopolymer composites*, U.S. Patent, Editor. 1993.
[68] Davidovits, J. and M. Davidovics, *Geopolymer: Ultra-High temperature Tooling Material for the Manufacture of Advanced composites.* 36th SAMPE Symposium, 1991. **36**(2): p. 1939-1949.
[69] Davidovits, J., M. Davidovics, and N. Davidovits, *Process for obtaining a geopolymeric alumino-silicate and products thus obtained*, in *United States Patent*, 5,342,595, 1994: United States.

[70] Davidovits, J., M. Davidovics, and N. Davidovits, *Geopolymeric fluoro-alumino-silicate binder and process for obtaining it*, in *United States Patent*, 5,352,427, 1994: United States.
[71] Hammell, J., P. Balaguru, and R. Lyon, *Influence of reinforcement types on the flexural properties of Geopolymer composites.* International SAMPE Symposium and Exhibition, 1998. **43**: p. 1600-1608.
[72] Hammell, J., P. Balaguru, and R. Lyon. *Influence of reinforcement types on the flexural properties of Geopolymer composites*. in *the 2nd International Conference, Géopolymère '99*. 1999.
[73] Hammell, J.A., P.N. Balaguru, and R.E. Lyon, *Strength retention of fire resistant aluminosilicate-carbon composites under wet-dry conditions.* Composites Part B: Engineering, 2000. **31**(2): p. 107-111.
[74] Davies, I.J. and R.D. Rawlings, *Mechanical properties in compression of CVI-densified porous carbon/carbon composite.* Composites Science and Technology, 1999. **59**(1): p. 97-104.
[75] Luo, R., Z. Yang, and L. Li, *Effect of additives on mechanical properties of oxidation-resistant carbon/carbon composite fabricated by rapid CVD method.* Carbon, 2000. **38**(15): p. 2109-2115.
[76] Park, S.-J. and M.-S. Cho, *Effect of anti-oxidative filler on the interfacial mechanical properties of carbon-carbon composites measured at high temperature.* Carbon, 2000. **38**(7): p. 1053-1058.
[77] Kriven, W.M., Bell, L.J., Gordon, M., *Microstructure and microchemistry of fully-rected geopolymers and geopolymer matrix composites.* Ceramic Transactions, 2003. **153**: p. 227-252.
[78] Hussain, M., et al., *Investigation of thermal and fire performance of novel hybrid geopolymer composites.* Journal of Materials Science, 2004. **39**(14): p. 4721-4726.
[79] Zhao, Q., et al., *Novel geopolymer based composites with enhanced ductility.* Journal of Materials Science, 2007. **42**(9): p. 3131-3137.
[80] Papakonstantinou, C.G., J.W. Giancaspro, and P.N. Balaguru, *Fire response and mechanical behavior of polysialate syntactic foams.* Composites Part A: Applied Science and Manufacturing, 2008. **39**(1): p. 75-84.
[81] Giancaspro, J., C. Papakonstantinou, and P. Balaguru, *Mechanical behavior of fire-resistant biocomposite.* Composites Part B: Engineering, 2009. **40**(3): p. 206-211.
[82] Davidovits, J., *Geopolymer - fiber composites*, in *Geopolymer Chemistry & Applications*, D. Joseph, Editor. 2008, Geopolymer Institute: Saint-Quentin, France.
[83] Duxson, P., et al., *The role of inorganic polymer technology in the development of 'green concrete'.* Cement and Concrete Research, 2007. **37**(12): p. 1590-1597.
[84] Davidovits, J., *Global Warming Impact on the Cement and Aggregates Industries.* World Resource Review, 1994. **6**(2): p. 263-278.
[85] Davidovits, J., *Geopolymer Cements to minimize Carbon-dioxide greenhouse-warming.* CERAMIC TRANSACTIONS, 1993. **37**: p. 165-182.
[86] Davidovits, J. *Environmentally Driven Geopolymer Cement Applications*. in *Geopolymer 2002 Conference*. 2002. Melbourne, Australia.
[87] Davidovits, J., *Waste solidification and disposal method*, U.S. Patent 4,859,367, 1989: United States.
[88] Li, L., S. Wang, and Z. Zhu, *Geopolymeric adsorbents from fly ash for dye removal from aqueous solution.* Journal of Colloid and Interface Science, 2006. **300**(1): p. 52-59.

[89] Tomas Hanzlicek, et al., *Reinforcement of the terracotta sculpture by geopolymer composite.* Materials and Design, 2009. **30**: p. 3229-3234.
[90] Mazany Anthony, M., W. Robinson John, and L. Cartwright Craig, *Inorganic matrix compositions, composites and process of making the same*, U.S. Patent, Editor. 2005.
[91] Hull, D. and T.W. Clyne, *An Introduction to Composite Materials*, ed. S.S. D. R Clarke, I. M. Ward FRS. 2002: Cambridge University Press.
[92] Walton, J.M. and Y.C.T. Yeung, *The Fatigue Performance of Structural Strands of Pultruded Composite Rods* Mechanical Engineering Publications Ltd, 1986. **C286/86**: p. 315-320.
[93] Japanese Standards Association, J., *JIS R 7601 - Japanese Industrial Standard - Testing Methods for Carbon Fibers*. 1986, Japanese Standards Association.
[94] Ross, A. *Basalt Fibers: Alternative To Glass?* 2006 [cited 2010 10 July]; Available from: http://www.compositesworld.com/articles/basalt-fibers-alternative-to-glass.
[95] Kusek Walter, W., *Pultrusion with Plastisal*, U.S. Patent 6,899,837, 2005: United States.
[96] Walter, W.K., *Pultrusion with Plastisal*, U.S. Patent 6,955,735, 2005: United States.
[97] McCrary, P. *Basic Vacuum Bagging*. 2008 05/11/09 [cited 2008 7 July]; Available from: http://www.bertram31.com/proj/tips/vaccuum.htm.
[98] Institute, G. *GeopolymerCamp*. 2009 [cited 2010 7 April]; Available from: http://www.geopolymer.org/camp.
[99] ASTM C 1341 - 06, *Standard test method for flexural properties of continuous fiber-reinforced advanced ceramic composites*. 2006, ASTM.
[100] DIN V ENV 658-3:1993-02, *Advanced Technical Ceramics - Mechanical properties of ceramic composites at room temperature - Part 3: Determination of flexural strength* 1993.
[101] British Standard, *Fiber-reinforced plastic composites - Determination of flexural properties,*. 2003, British Standard Institute.
[102] EN ISO 14130, *Plastic composites reinforced with fibers - Determination of effective interlaminar shear strength by short beam method*. 1997.
[103] EN 13706-2, *Reinforced plastics composites - Specifications for pultruded profiles - Method of test and general requirements*. 2002.
[104] Tarnopolsky, Y.M., A.V. Roze, and V.A. Polyakov, *Shear effects in flexure of oriented glass-fiber laminates (Russian)*. Mechanika polimerov, 1965. **2**: p. 38-46.
[105] Tarnopolsky, Y.M. and A.V. Roze, *Specialties of calculation of reinforced plastics details (Russian)*. Zinatne, Riga, 1969.
[106] Tarnopolsky, Y.M. and T.Y. Kincis, *Methods of static investigation of reinforced plastics (Russian)*. Chimiya, Moscow, 1981.
[107] BS IN ISO 14125:1998, *Fiber-reinforced plastic composites - Determination of flexural properties,*. 2003, British Standard Institute.
[108] Davidovits, J., *Silica-based geopolymer, sialate link and siloxo link in poly(siloxonate) Si:Al>5*, in *Geopolymer Chemistry & Application*, J. Davidovits, Editor. 2008 - C4a, Institute Geopolymer: Saint-Quentin, France. p. 255-273.
[109] Pacheco Torgal, F., J.P. Castro Gomes, and J. S. *Geopolymeric Binder Using Tungsten Mine Waste: Preliminary Investigation*. in *Geopolymer : Green*

Chemistrty and Sustainable Development Solutions, The World Congress Geopolymer 2005. 2005. Sain-Quentin, France.
[110] Davidovits, J., *Polymers and Geopolymers: Introduction*, in *Geopolymer Chemistry & Applications*. 2008, Geopolymer Institut: Saint-Quentin, France. p. 3-17.
[111] Khale, D. and R. Chaudhary, *Mechanism of geopolymerization and factors influencing its development: a review.* Journal of Materials Science, 2007. **42**(3): p. 729-746.
[112] Anurag, M., et al., *Effect of concentration of alkaline liquid and curing time on strength and water absorption of geopolymer concrete.* ARPN Journal of Engineering and Applied Sciences, 2008. **3**(1): p. 14-18.
[113] Brooks, J.J., *Prediction of setting time of fly ash concrete.* ACI Materials Journal 2002. **99**(6): p. 591-597.
[114] Djwantoro, H. and B.V. Rangan, *Develoment and properties of low-calcium fly ash-based geopolymer concrete*, J. Davidovits, Editor. 2005, Faculty of Engineering, Curtin University of Technology: Perth, Australia.
[115] Swanepoel, J.C. and C.A. Strydom, *Utilisation of fly ash in a geopolymeric material.* Applied Geochemistry, 2002. **17**(8): p. 1143-1148.
[116] Wang, K., S.P. Shah, and A. Mishulovich, *Effects of curing temperature and NaOH addition on hydration and strength development of clinker-free CKD-fly ash binders.* Cement and Concrete Research, 2004. **34**(2): p. 299-309.
[117] Palomo, A., et al., *Alkaline activation of fly ashes: NMR study of the reaction products.* Journal of the American Ceramic Society 2004. **87**(6): p. 1141-1145.
[118] Davidovics, J., *Geopolymer - fiber composites*, in *Geopolymer Chemistry & Applications*, D. Joseph, Editor. 2008 (C5), Geopolymer Institute: Saint-Quentin, France.
[119] Bell, J.L., Kriven, W.M., ed. *Preparation of ceramic foams from metakaolin-based geopolymer gels*. Developments in Strategy Materials: Ceramic Engineering and Science Proceedings ed. H.-T.K. Lin, kunihito/ Kriven, Waltraud M./ Norton, David P./ Garcia, Edwin/ Reimanis, Ivar E. Vol. 29. 2009. 97.
[120] Perera, D.S., Rachael, L., Trautman, R.L., *Geopolymers with the potential for use as refractory castables* Advances in Technology of Materials and Materials Processing, 2005. **7**: p. 187-190.
[121] Gomina, M., P. Fourvel, and M.H. Rouillon, *High temperature mechanical behaviour of an uncoated SiC-SiC composite material.* Journal of Materials Science, 1991. **26**(7): p. 1891-1898.
[122] Marsh, G., *Fire-safe composites for mass transit vehicles.* Reinforced Plastics, 2002. **46**(9): p. 26-30.
[123] Hathaway, W.T. *Fire Safety in Mass Transit Vehicle Materials*. in *36th International SAMPE Symposium and Exhibition*. 1991. San Diego Convention Center, San Diego, California.
[124] Demarco, R.A. *Composite applications at Sea: Fire Ralated Issues*. in *Proc. 36th Int'l. SAMPLE Sumposium*. 1991.
[125] Lyon, R.E., et al. *Fire response of geopolymer structural composites*. in *The First International Conference on Composites in Infrastructure (ICCI' 96)*. 1996. Tuscon, Arizona, United States.
[126] Foden, A., et al. *High Temperature Inorganic Resin for Use in Fiber Reinforced Composites* in *the 1st International Conference on Composites in Infrastructure (ICCI'96)*. 1996. Tucson, Arizona; United States.

APPENDIX A - EDX MAPPING AND SEM IMAGES

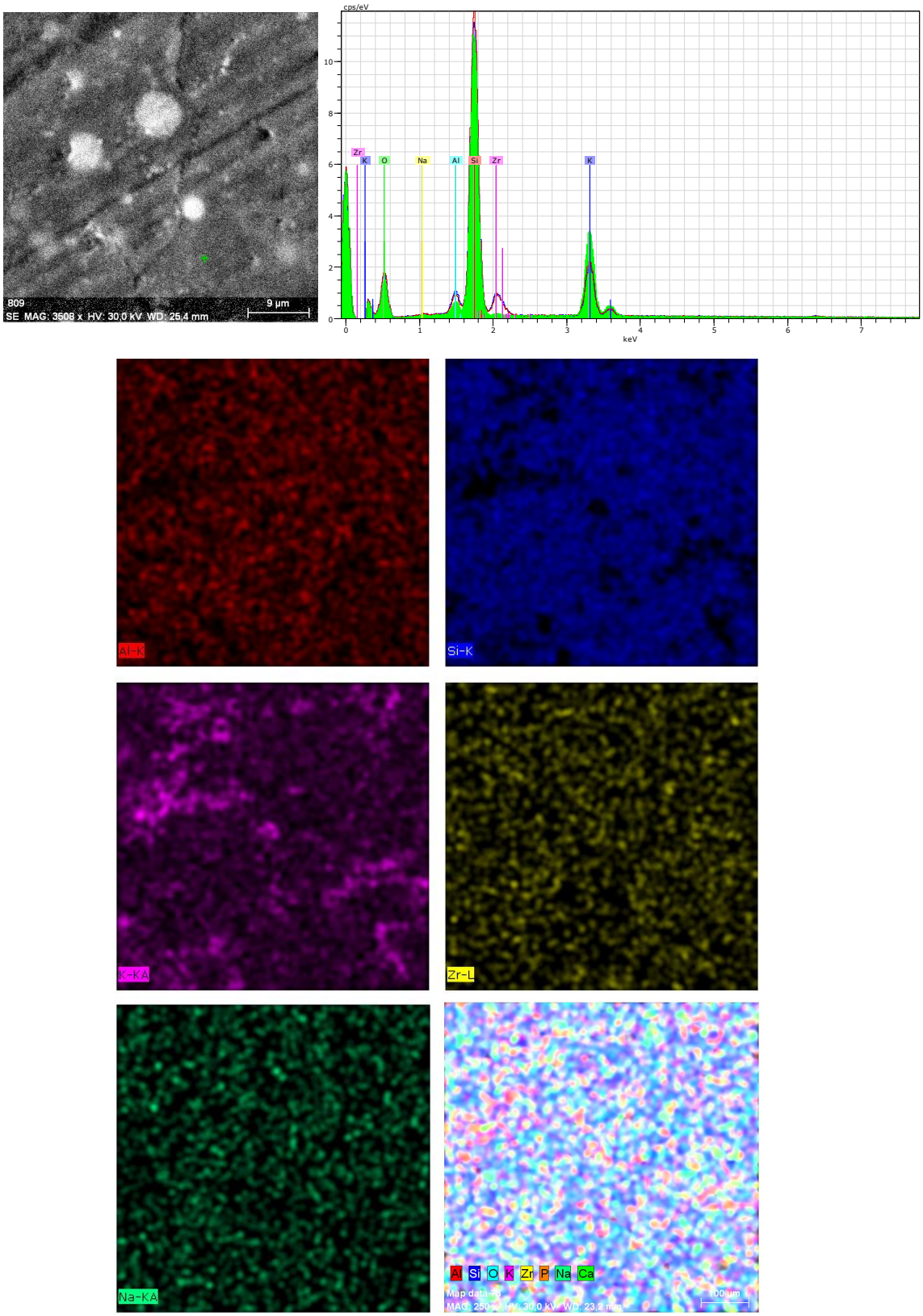

Fig A.1 SEM and EDX mapping of an individual element of M1 matrix.

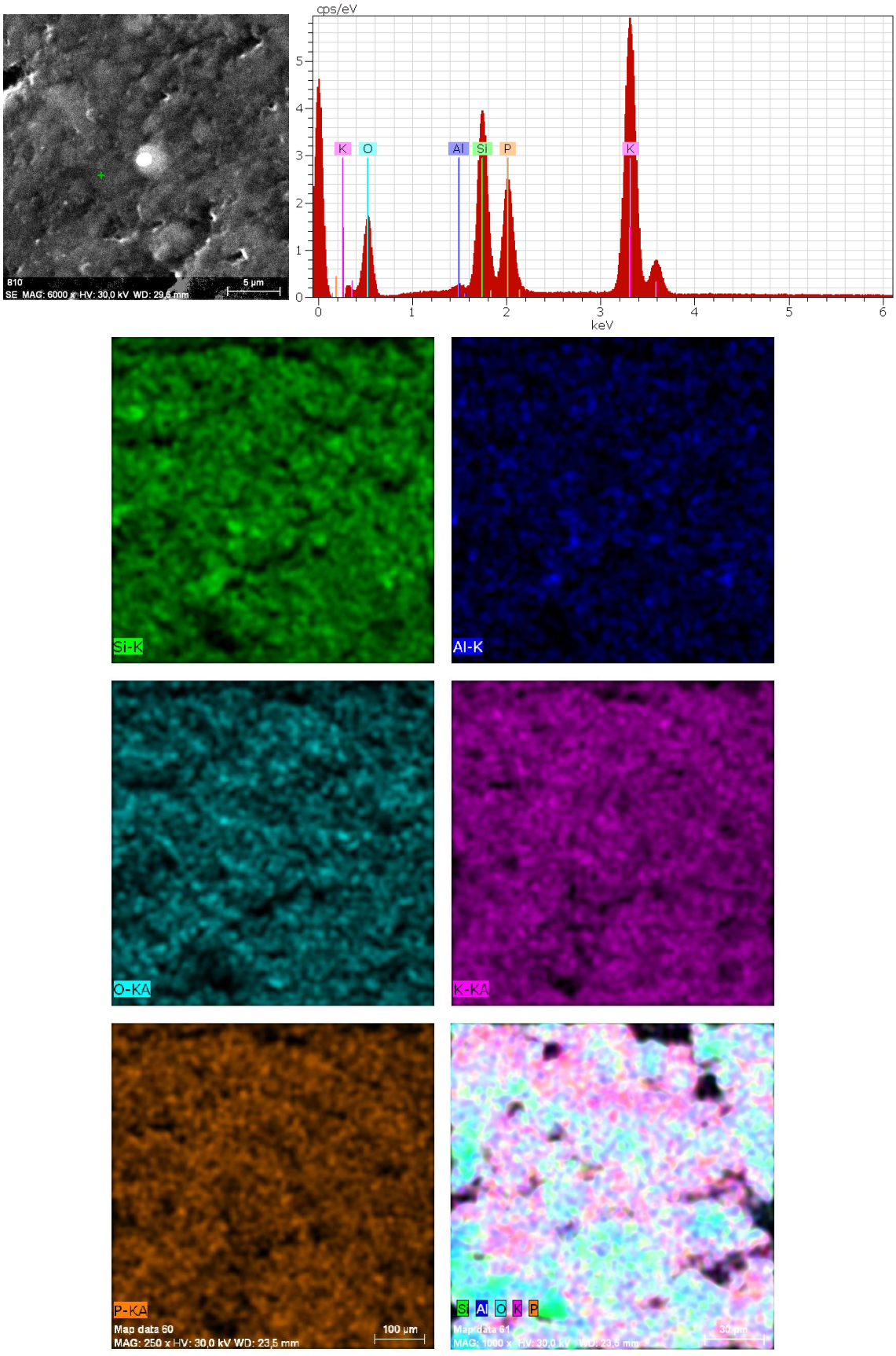

Fig A.2 SEM and EDX mapping of an individual element of M2 matrix.

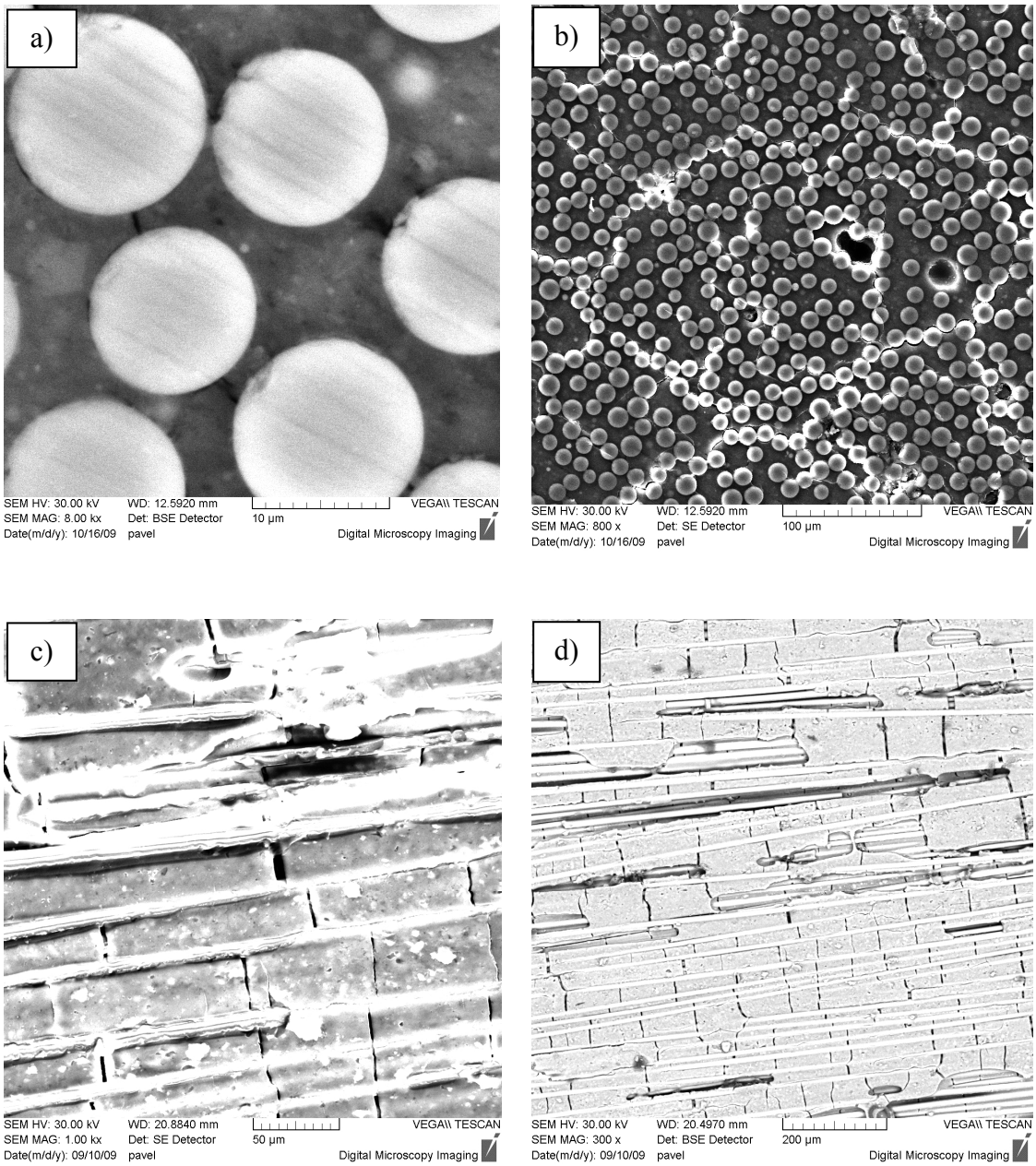

Fig. A.3 SEM of M1/Basalt curing at 65 ^{o}C on sections perpendicular to fibers and surfaces of composite.

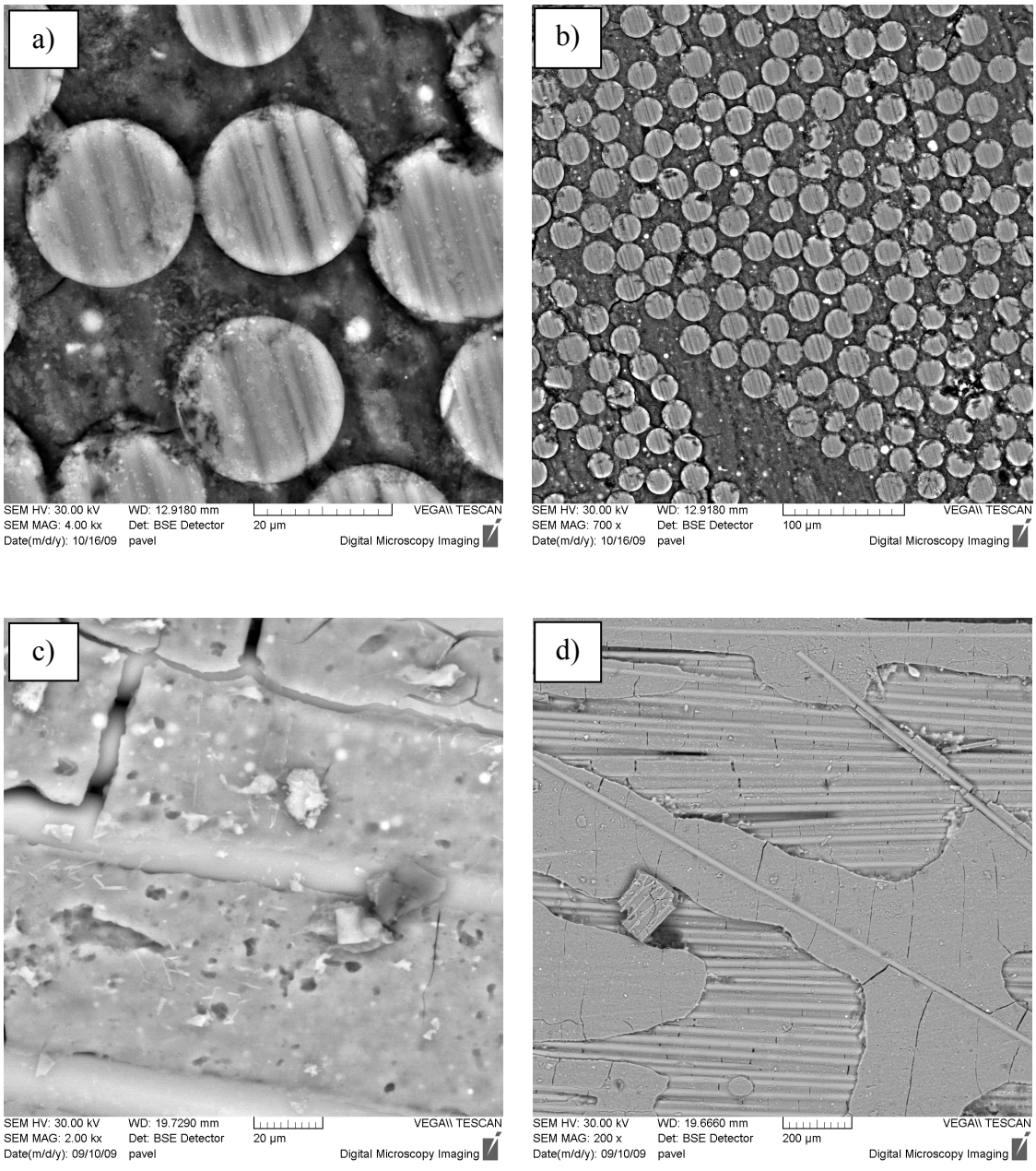

Fig. A.4 SEM of M1/E-glass curing at 65 ^{o}C on sections perpendicular to fibers and surfaces of composite.

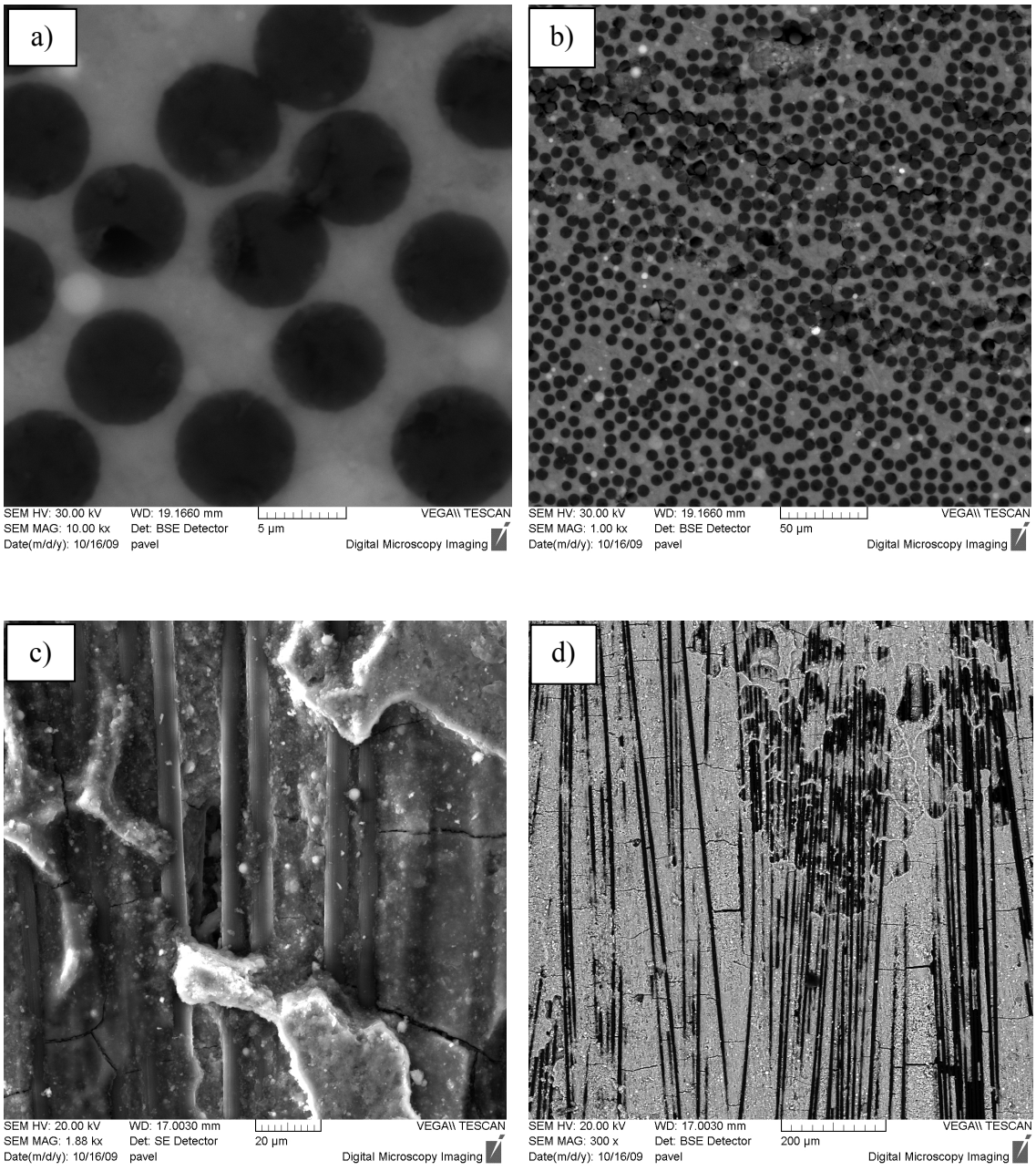

Fig. A.5 SEM of M2/Carbon curing at 85 ^{o}C on sections perpendicular to fibers and surfaces of composite.

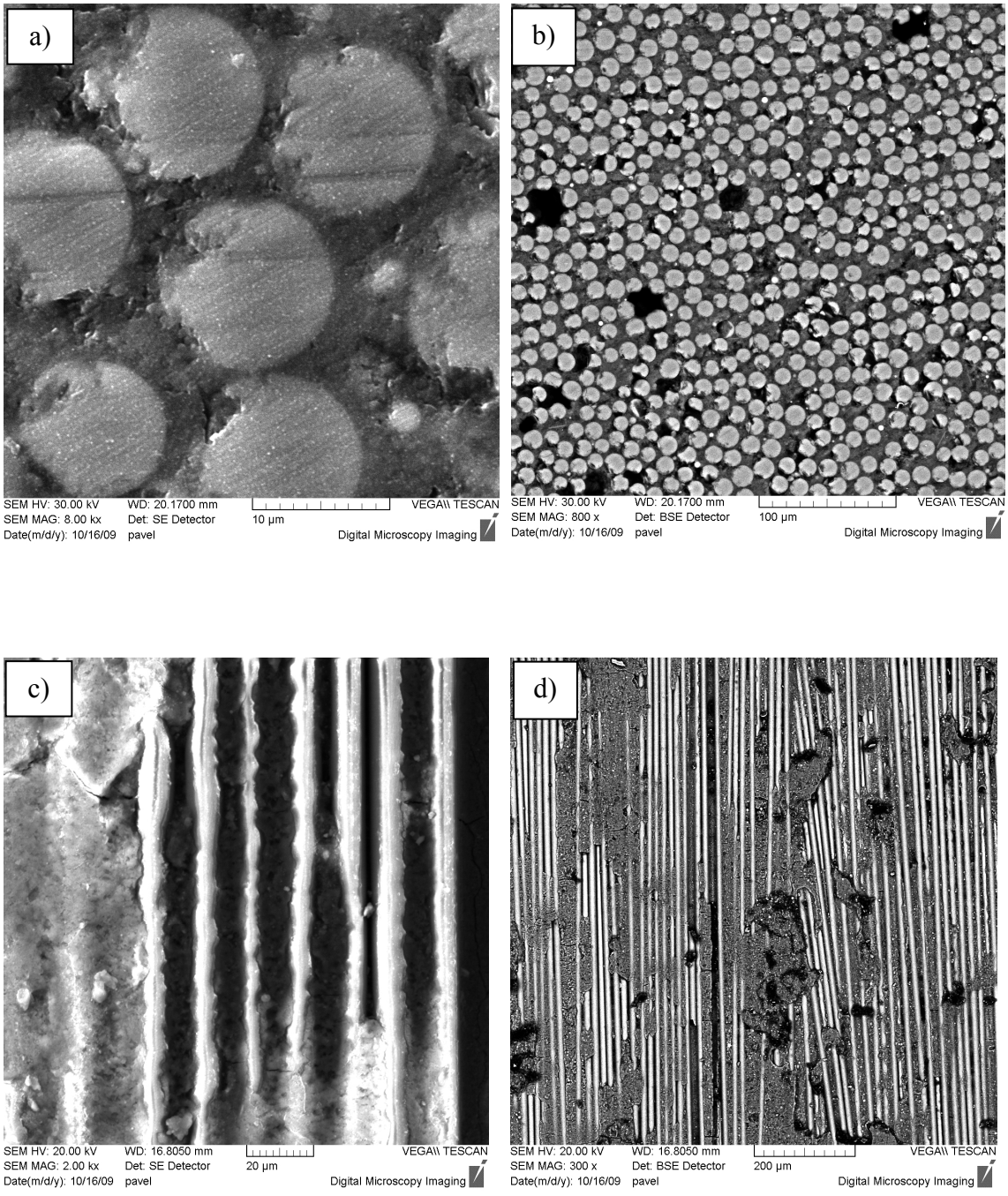

Fig. A.6 SEM of M2/Basalt curing at 85 ^{o}C on sections perpendicular to fibers and surfaces of composite.

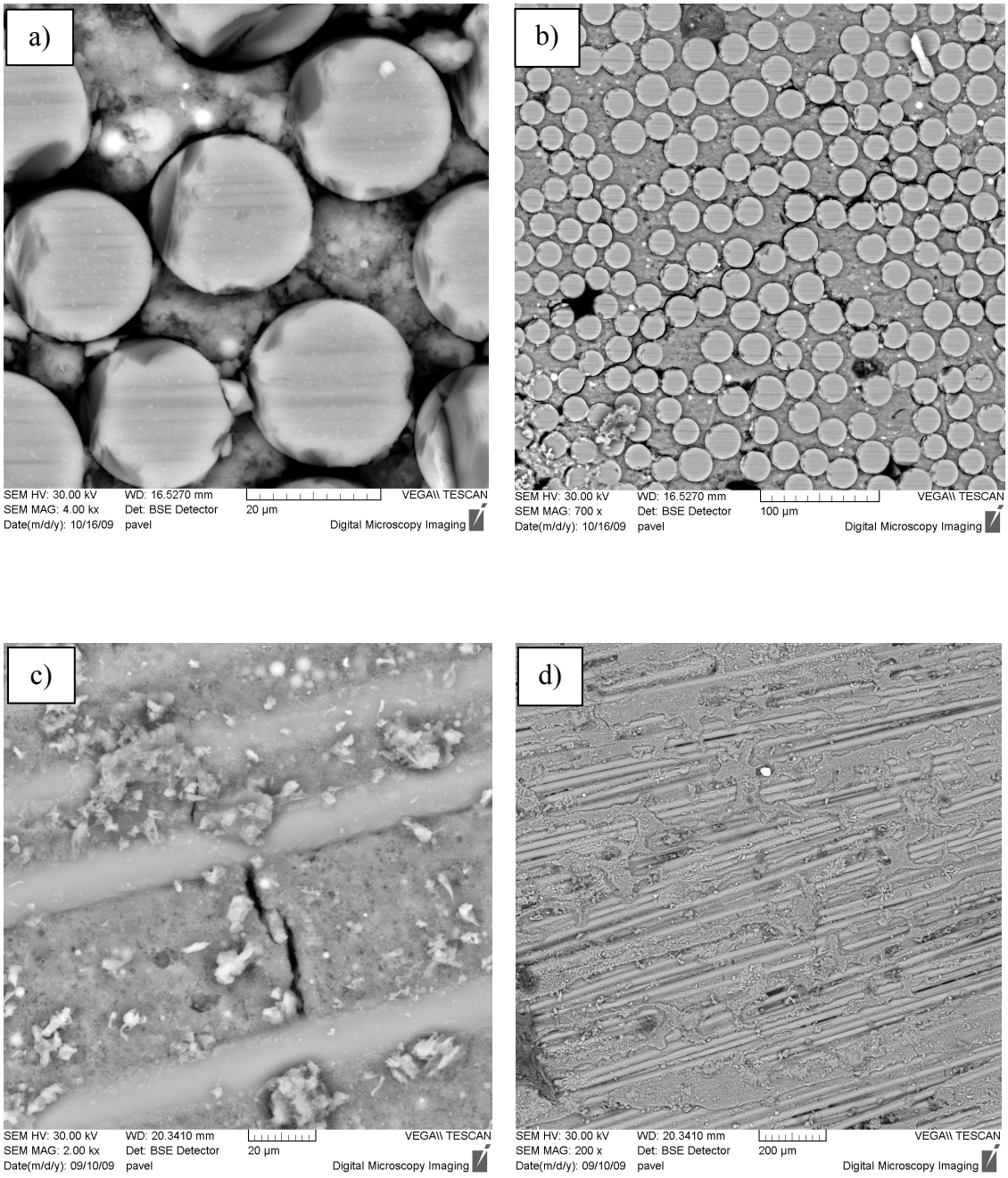

Fig. A.7 SEM of M2/E-glass curing at 85 ^{o}C on sections perpendicular to fibers and surfaces of composite.

APPENDIX B

Table B.1 Flexural properties of geopolymer composites M1 system at outer support span-to-depth ration L/H = 16 to 1

Temp of curing [^{o}C]	Reinforced geocomposites								
	M1-Carbon			M1-Basalt			M1-Eglass		
	R_{mo} [MPa]	E [GPa]	ε_{mo} [%]	R_{mo} [MPa]	E [GPa]	ε_{mo} [%]	R_{mo} [MPa]	E [GPa]	ε_{mo} [%]
55	289.8 ±19.4	45.3 ±0.8	1.18	249.8 ±24.3	31.4 ±2.6	1.14	134.2 ±12.4	28.8 ±4.5	0.81
65	314.9 ±20.3	48.1 ±2.8	1.11	247.7 ±3.60	29.2 ±0.7	1.33	95.0 ±12.9	17.1 ±2.1	0.92
75	298.1 ±20.6	51.0 ±1.3	1.01	253.1 ±15.2	31.4 ±0.7	1.09	71.8 ±2.5	14.7 ±2.4	0.90
85	329.7 ±28.5	48.3 ±4.4	1.26	263.6 ±5.7	32.7 ±1.2	1.22	73.4 ±2.8	16.1 ±1.1	0.93
95	252.7 ±25.1	47.6 ±2.3	0.97	211.7 ±7.2	29.2 ±1.8	1.25	58.8 ±4.9	15.3 ±1.3	0.92
105	174.7 ±6.4	31.9 ±1.8	1.37	199.2 ±11.9	35.9 ±2.0	0.89	73.8 ±14.8	22.5 ±3.9	0.59
115	120.2 ±3.8	28.4 ±2.7	1.82	145.9 ±15.9	31.4 ±3.3	0.81	61.9 ±6.0	25.0 ±2.9	0.35

R_{mo} – flexural strength [MPa]
E – Young's modulus [GPa]
ε - Strain in the outer surface of the specimen [%]

Table B.2 Flexural properties of geopolymer composites M2 system at outer support span-to-depth ration L/H = 16 to 1

Temp of curing [^{o}C]	Reinforced geocomposites								
	M1-Carbon			M1-Basalt			M1-Eglass		
	R_{mo} [MPa]	E [GPa]	ε_{mo} [%]	R_{mo} [MPa]	E [GPa]	ε_{mo} [%]	R_{mo} [MPa]	E [GPa]	ε_{mo} [%]
55	173.5 ±13.2	58.3 ±2.0	0.48	128.2 ±6.9	36.7 ±2.1	0.44	85.3 ±6.0	33.0 ±8.0	0.37
65	126.3 ±16.8	62.6 ±7.8	0.35	130.0 ±7.8	37.5 ±2.2	0.43	106.1 ±9.2	31.3 ±2.5	0.51
75	181.9 ±13.9	69.8 ±3.4	0.48	141.9 ±1.1	39.3 ±0.1	0.45	144.6 ±14.3	42.3 ±3.5	0.43
85	215.3 ±6.4	50.2 ±7.7	0.87	134.9 ±6.8	32.5 ±0.8	0.96	141.4 ±14.0	29.3 ±0.8	0.84
95	217.4 ±9.8	75.1 ±6.4	0.46	135.0 ±4.5	35.8 ±0.8	0.45	109.9 ±14.2	31.3 ±2.8	0.47
105	204.2 ±14.4	56.2 ±8.1	0.61	110.8 ±0.8	28.6 ±1.0	0.55	86.9 ±10.5	31.4 ±3.1	0.41
115	207.8 ±18.0	62.9 ±2.0	0.50	102.0 ±3.9	25.8 ±2.3	0.50	87.2 ±7.3	32.8 ±2.7	0.36

R_{mo} – flexural strength [MPa]
E – Young's modulus [GPa]
ε - Strain in the outer surface of the specimen [%]

Table B.3. Flexural properties of geocomposites M1 system at L/H = 16 to 1

Composites	Curing time						Average	
	1:01:05		1:03:05		1:07:05			
	R_{mo} [MPa]	E [GPa]	R_{mo} [MPa]	E [GPa]	R_{mo} [MPa]	E [GPa]	R_{mo} [MPa]	E [GPa]
M1-Carbon	401.1	65.2	403.1	59.5	395.7	64.0	**400.0 ±3.1**	**62.9±2.5**
M1-Basalt	371.0	47.2	369.9	55.0	392.2	56.1	**377.7 ±10.3**	**52.8±4.0**
M1-Eglass	109.2	32.6	110.7	27.4	86.9	22.8	**102.3 ±10.9**	**27.6 ±4.0**

Table B.4 Flexural properties of geocomposites M2 system at different curing time at outer support span-to-depth ratios L/H = 16 to 1

Composites	Curing time										Average	
	1:01:05		1:03:05		1:04:05		1:06:05		1:07:05			
	R_{mo} [MPa]	E [GPa]	R_{mo} [MPa]	E [GPa]	R_{mo} [MPa]	E [GPa]	R_{mo} [MPa]	E [GPa]	R_{mo} [MPa]	E [GPa]	R_{mo} [MPa]	E [GPa]
M2-Carbon	290.9	85.3	246.4	59.7	254.5	69.0	256.9	76.4	232.2	64.9	**256.2 ±19.4**	**71.0 ±9.0**
M2-Basalt	220.5	53.5	182.7	51.1	256.0	58.3	203.1	49.6	212.3	48.3	**214.9 ±24.1**	**52.2 ±3.5**
M2-Eglass	158.1	51.9	163.0	57.1	151.8	52.8	163.2	48.7	153.8	43.2	**158.0 ±4.7**	**50.7 ±4.6**

APPENDIX C

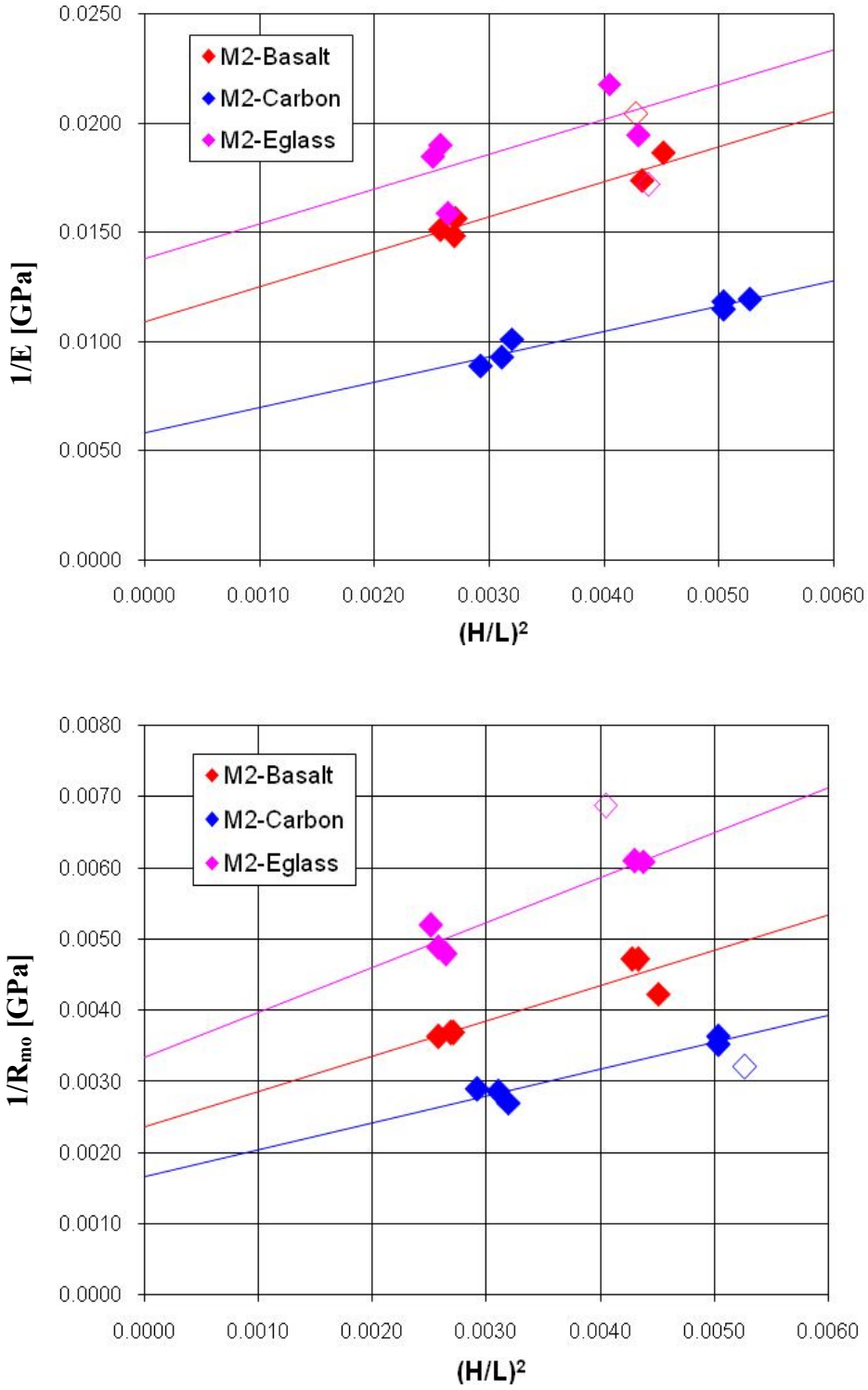

Fig. C.1 Linear regression of reciprocal effective values 1/E and $1/R_{mo}$ vs $(H/L)^2$ of geocomposites M2 system for curing time 1:01:05 at 85 ^{o}C.

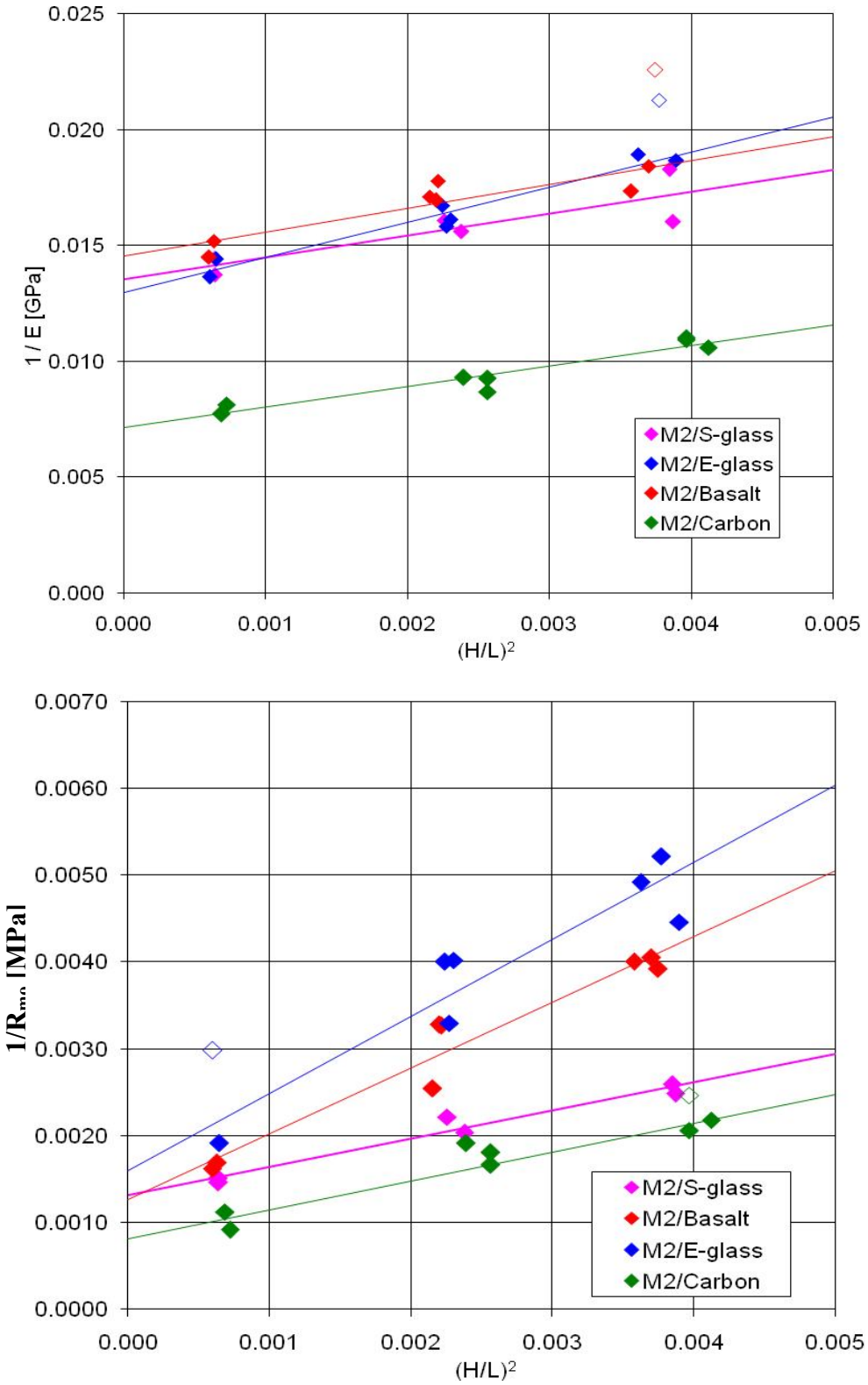

Fig. C.2 Linear regression of reciprocal effective values 1/E and $1/\sigma_m$ vs $(H/L)^2$ of geocomposites M2 system cured at ambient condition for over 50 days.

APPENDIX D

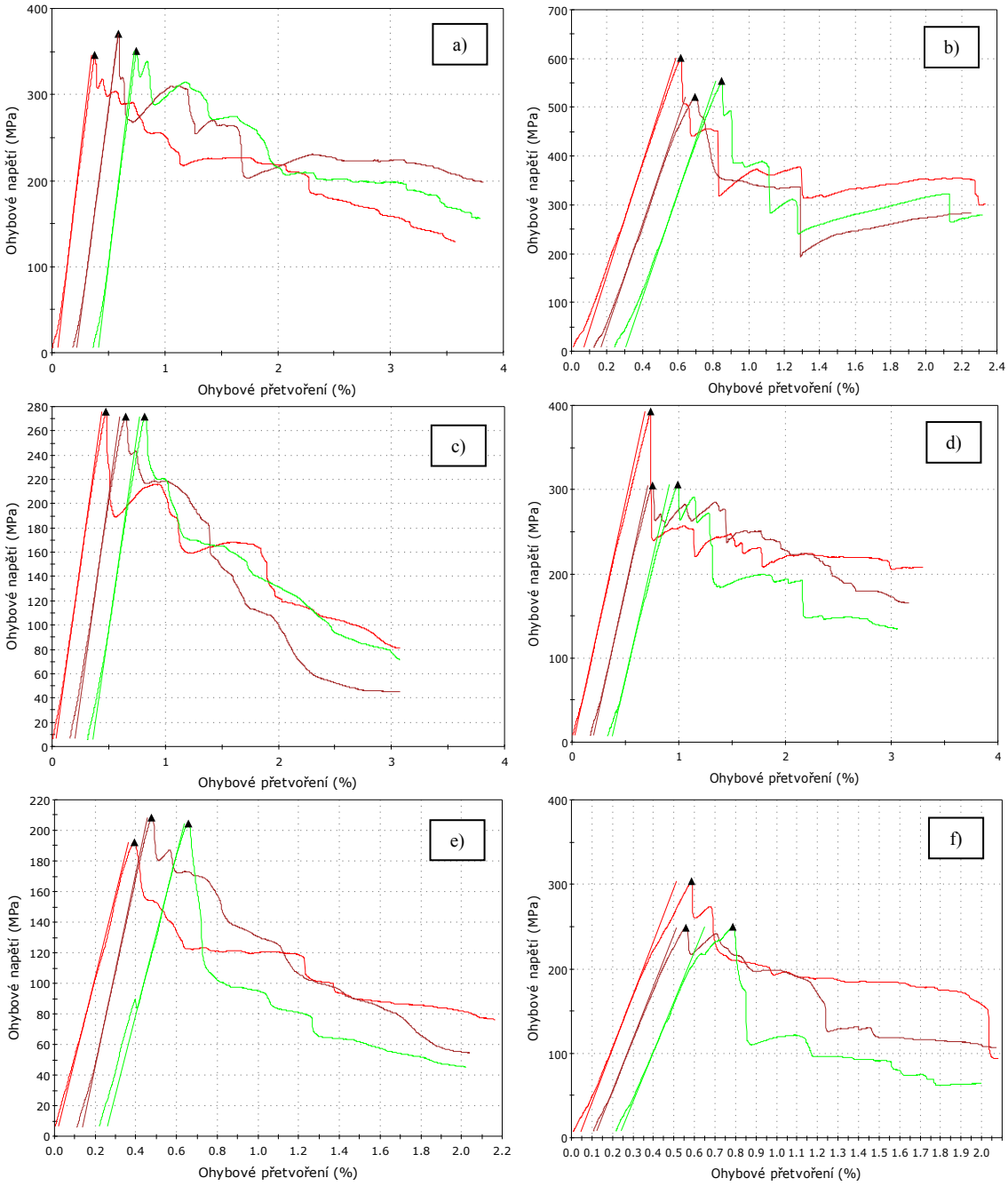

Fig. D.1 Typical stress – strain relationships of unidirectional geocomposites based on M2 geopolymer matrix tested in flexure at L/H = 20 to 1, a) M2/C, c) M2/B and e) M2/E-glass cured at time 1:1:5 hours at 85 ^{o}C and b) M2/C, d) M2/B and f) M2/E-glass cured at ambient conditions for over 50 days.

APPENDIX E

Fig. E.1 Furnace for geocomposite exposure at high temperature, TUL – KMT.

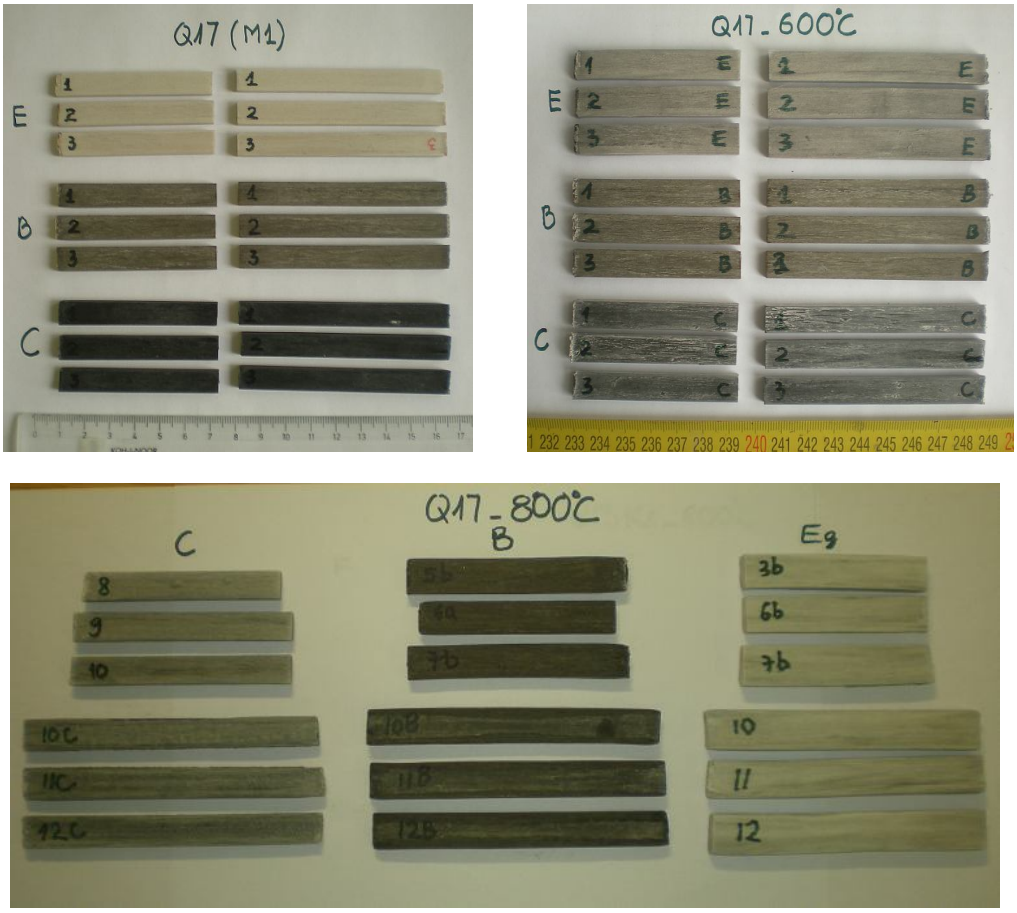

Fig. E.2 Geocomposite specimens (M1 system) before and after thermal exposure.

Fig. E.3 Geocomposite specimens (M2 system) before and after thermal exposure and typical failure pattern of M2-Carbon after calcination at 800 ^{o}C.